frontiers | Research Topics

Holobiont interactions

Edited by
Jennifer L. Matthews, Ty N. F. Roach
and Alexandra Helene Campbell

Published in
Frontiers in Ecology and Evolution

ISSN 1664-8714
ISBN 978-2-8325-4621-5
DOI 10.3389/978-2-8325-4621-5

About Frontiers

Frontiers is more than just an open access publisher of scholarly articles: it is a pioneering approach to the world of academia, radically improving the way scholarly research is managed. The grand vision of Frontiers is a world where all people have an equal opportunity to seek, share and generate knowledge. Frontiers provides immediate and permanent online open access to all its publications, but this alone is not enough to realize our grand goals.

Frontiers journal series

The Frontiers journal series is a multi-tier and interdisciplinary set of open-access, online journals, promising a paradigm shift from the current review, selection and dissemination processes in academic publishing. All Frontiers journals are driven by researchers for researchers; therefore, they constitute a service to the scholarly community. At the same time, the *Frontiers journal series* operates on a revolutionary invention, the tiered publishing system, initially addressing specific communities of scholars, and gradually climbing up to broader public understanding, thus serving the interests of the lay society, too.

Dedication to quality

Each Frontiers article is a landmark of the highest quality, thanks to genuinely collaborative interactions between authors and review editors, who include some of the world's best academicians. Research must be certified by peers before entering a stream of knowledge that may eventually reach the public - and shape society; therefore, Frontiers only applies the most rigorous and unbiased reviews. Frontiers revolutionizes research publishing by freely delivering the most outstanding research, evaluated with no bias from both the academic and social point of view. By applying the most advanced information technologies, Frontiers is catapulting scholarly publishing into a new generation.

What are Frontiers Research Topics?

Frontiers Research Topics are very popular trademarks of the *Frontiers journals series*: they are collections of at least ten articles, all centered on a particular subject. With their unique mix of varied contributions from Original Research to Review Articles, Frontiers Research Topics unify the most influential researchers, the latest key findings and historical advances in a hot research area.

Find out more on how to host your own Frontiers Research Topic or contribute to one as an author by contacting the Frontiers editorial office: frontiersin.org/about/contact

Holobiont interactions

Topic editors

Jennifer L. Matthews — University of Technology Sydney, Australia

Ty N. F. Roach — University of Hawaii at Manoa, United States

Alexandra Helene Campbell — University of New South Wales, Australia

Citation

Matthews, J. L., Roach, T. N. F., Campbell, A. H., eds. (2024). *Holobiont interactions*. Lausanne: Frontiers Media SA. doi: 10.3389/978-2-8325-4621-5

Table of contents

04 Editorial: Holobiont interactions
Jennifer L. Matthews

06 Wheat Rhizosphere Microbiota Respond to Changes in Plant Genotype, Chemical Inputs, and Plant Phenotypic Plasticity
Samuel Jacquiod, Tiffany Raynaud, Eric Pimet, Chantal Ducourtieux, Leonardo Casieri, Daniel Wipf and Manuel Blouin

22 Rapid acquisition of microorganisms and microbial genes can help explain punctuated evolution
Eugene Rosenberg

29 The mesoglea buffers the physico-chemical microenvironment of photosymbionts in the upside-down jellyfish *Cassiopea* sp.
Niclas Heidelberg Lyndby, Margaret Caitlyn Murray, Erik Trampe, Anders Meibom and Michael Kühl

41 Transcriptomic-based selection of reference genes for quantitative real-time PCR in an insect endosymbiotic model
Agnès Valliert, Elisa Dell'Aglio, Mariana Galvão Ferrarini, Ophélie Hurtado, Carole Vincent-Monégat, Abdelaziz Heddi, Rita Rebollo and Anna Zaidman-Rémy

52 Acidification and hypoxia drive physiological trade-offs in oysters and partial loss of nutrient cycling capacity in oyster holobiont
Deevesh Ashley Hemraj, Laura J. Falkenberg, Khan Cheung, Lauren Man, Alessia Carini and Bayden D. Russell

63 Disentangling the impacts of macroalgae on corals via effects on their microbiomes
Cody S. Clements and Mark E. Hay

72 Inoculation with *Roseovarius* increases thermal tolerance of the coral photosymbiont, *Breviolum minutum*
Karla Heric, Justin Maire, Pranali Deore, Alexis Perez-Gonzalez and Madeleine J. H. van Oppen

87 Identification of coral disease within the high-latitude reef, Lord Howe Island Marine Park
Tess Moriarty, Tracy D. Ainsworth and William Leggat

104 Environmental generalism, holobiont interactions, and Pocilloporid corals in the warming oceans of the eastern coast of Australia
Jessica L. Bergman, Zoe T. Richards, Paige Sawyers and Tracy D. Ainsworth

frontiers | Frontiers in Ecology and Evolution

TYPE Editorial
PUBLISHED 07 March 2024
DOI 10.3389/fevo.2024.1382169

OPEN ACCESS

EDITED AND REVIEWED BY
Michael Charleston,
University of Tasmania, Australia

*CORRESPONDENCE
Jennifer L. Matthews
Jennifer.Matthews@uts.edu.au

RECEIVED 05 February 2024
ACCEPTED 01 March 2024
PUBLISHED 07 March 2024

CITATION
Matthews JL (2024) Editorial: Holobiont interactions.
Front. Ecol. Evol. 12:1382169.
doi: 10.3389/fevo.2024.1382169

Editorial: Holobiont interactions

Jennifer L. Matthews*

Climate Change Cluster, University of Technology Sydney, Ultimo, NSW, Australia

KEYWORDS

holobiont, symbiosis, interactions, metabolism, concept

Editorial on the Research Topic
Holobiont interactions

The holobiont concept has emerged as a theoretical and experimental framework to study the interactions between hosts and their associated microbial communities in all types of ecosystems and organisms, providing a paradigm shift from bipartite interactions to a community-based integration of factors that determine the resilience of organisms. The spread of this concept across biological sciences, including aspects of mathematics (bioinformatics, statistics, and modelling), results from a recent realisation of the ubiquitous nature of host-associated microbes and their central role in host biology, ecology, and evolution, particularly regarding adaptation to environmental change. Yet, several challenges in holobiont research remain, including the theoretical and experimental approaches to elucidate the role of microbiota in host adaptation and evolution, and inherent bioinformatics challenges of complex multicomponent datasets. Consequently, the application of holobiont manipulation to enhance host health and ecosystem restoration is extremely limited.

Understanding the intricate role of microbial communities in influencing a host's capacity to adapt to environmental shifts and evolve is a pivotal aspect of holobiont research. But defining the boundaries of the holobiont, determining which organisms are integral parts and which are not, and elucidating the stability and flexibility of these associations over time and space all pose experimental challenges. These challenges include manipulating or isolating intricate microbial communities to establish causative links in holobiont studies, which is not always possible with obligate symbionts. Metabolic or genetic comparisons between symbiotic and artificially acquired aposymbiotic host counterparts can help unravel organism interactions. For example, Vallier et al. employed high throughput transcriptomics at various developmental and symbiotic states to enhance our comprehension of the insect endosymbiotic model involving the cereal weevil *Sitophilus oryzae* and its intracellular bacterium *Sodalis pierantonius*. Nevertheless, numerous methodological hurdles remain, especially for non-model organisms. To address these challenges, microscale technologies can play a crucial role. Lyndby et al., for instance, employed optical and electro-chemical microsensors to investigate how light is modulated at the water-tissue interface of the upside-down jellyfish, Cassiopeia. This technological approach represents a significant advancement, shedding light on microscale interactions within holobionts. In the case of the jellyfish, it unveiled the mesoglea's role in buffering the physio-chemical microenvironment, effectively regulating oxygen and pH dynamics in the dark, while also providing light attenuation in tissues containing symbionts.

The intricacies of host-microbe metabolic interactions are further compounded when considering the influence of neighbouring biotic environments on microbiomes, as expounded by Clements and Hay in the context of corals. The authors underscore the prevalent transition of coral reefs from coral to macroalgal dominance, yet the precise role of macroalgae in coral decline remains insufficiently understood. This challenge echoes across holobiont research, necessitating the development of effective theoretical and experimental approaches. Designing experiments to explore the nuanced dynamics of host-microbe interactions and their impact on holobiont health becomes complex due to the intricate relationships with local and associated microbial communities. Bergman et al., in their examination of environmental generalism and holobiont interactions in high-latitude corals, caution against oversimplification, emphasizing the context-dependent nature of host-microbe interactions across diverse environmental conditions, locations, and temporal changes. Despite these complexities, progress is being made in accessing and unravelling these intricacies, offering rewarding insights. Jacquiod et al., for instance, employed bacterial and fungal amplicon sequencing alongside multifactorial host genotype and environment information, providing an initial assessment of individual (genotype and environment) effects as well as their interactions on holobiont relationships in the field. However, the vast and intricate datasets generated in multifaceted holobiont research present bioinformatics challenges. Analysing and interpreting these complex, interdisciplinary datasets demand advanced computational tools, statistical methods, and bioinformatics expertise. While demanding, this analytical process is crucial, as successful application to one organism can lay the foundation for further methodological advancements in subsequent studies.

Once armed with an expanded knowledge base, technological advances, and ability to control associations, there is potential to craft practical strategies for manipulating the holobiont towards positive outcomes, such as identifying key pathways for integrative pest management strategies (e.g. Vallier et al.). However, delving into the applications of holobiont manipulation for enhancing host health and contributing to ecosystem restoration remains an area of limited exploration. Heric et al. showcase a promising example of this potential for corals, where bacterial probiotics can play a mitigating role in coral bleaching by diminishing reactive oxygen species (ROS) levels within the microalgal partner of corals, Symbiodiniaceae, through the production of bacterial antioxidants. While this intervention has shown efficacy in cultured environments, its applicability to Symbiodiniaceae within the coral holobiont, especially in the context of natural bleaching events, is yet to be tested. This becomes increasingly crucial considering the escalating prevalence of coral diseases during bleaching events, as revealed by Moriarty et al., and the potential protective role of the holobiont microbiome, or alternatively, its role as a source for opportunistically pathogenic bacteria.

Holobiont research, particularly in understanding microbiome interactions, presents a potential, albeit hotly debated, paradigm shift in our comprehension of evolution and ecology. An influential contribution to this discourse within our Research Topic is Rosenberg's article, "*Rapid acquisition of microorganisms and microbial genes can help explain punctuated evolution*," delving into the role of microorganisms in the evolutionary processes of animals and plants. The proposition suggests that the swift incorporation of microorganisms from the environment into host microbiomes, coupled with the subsequent integration of microbial genes into host genomes through horizontal gene transfer, can elucidate instances of punctuated evolution. This hypothesis finds support in evidence from significant evolutionary events driven by microorganisms. However, it's crucial to emphasise that this perspective doesn't diminish the importance of host genetics in steering evolutionary trajectories and determining adaptive capacities. In a case study on oysters, Hemraj et al. illuminate how microbiomes respond to acidic and low oxygen environments, potentially affecting the nutritional status of oysters. Nevertheless, the study underscores that oysters exhibit the ability to regulate their physiological processes, maintaining homeostasis in the short term despite environmental challenges. This dual consideration of microbial influences and host genetics contributes to a more nuanced understanding of the intricate interplay in shaping evolutionary dynamics.

The generalisability of the holobiont concept across diverse organisms and ecosystems remains a challenge. Nevertheless, amidst the aspects requiring refinement, this Research Topic underscores the active efforts of researchers to address gaps by conducting additional studies, applying innovative methodologies, reviewing current status, refining research approaches, and integrating findings from various biological systems. These collective endeavours aim to unravel the intricate dynamics of holobiont interactions and enhance our understanding of this emerging field.

Author contributions

JM: Funding acquisition, Writing – original draft, Writing – review & editing.

Funding

The author(s) declare that financial support was received for the research, authorship, and/or publication of this article. JM was supported by UTS Chancellors Research Fellowship for the research, authorship, and/or publication of this article.

Conflict of interest

The author declares that the research was conducted in the absence of any commercial or financial relationships that could be construed as a potential conflict of interest.

Publisher's note

frontiers | Frontiers in Ecology and Evolution

ORIGINAL RESEARCH
published: 13 July 2022
doi: 10.3389/fevo.2022.903008

Wheat Rhizosphere Microbiota Respond to Changes in Plant Genotype, Chemical Inputs, and Plant Phenotypic Plasticity

*Samuel Jacquiod[1], Tiffany Raynaud[1], Eric Pimet[1], Chantal Ducourtieux[1], Leonardo Casieri[2], Daniel Wipf[2] and Manuel Blouin[1]**

[1] Agroécologie, Institut Agro, INRAE, Université de Bourgogne, University Bourgogne Franche-Comté, Besançon, France, [2] Agroécologie, Institut Agro, CNRS, INRAE, Université de Bourgogne, University Bourgogne Franche-Comté, Besançon, France

Modern wheat varieties that were selected since the Green Revolution are generally grown with synthetic chemical inputs, and ancient varieties released before1960 without. Thus, when changes occur in rhizosphere microbiota structure, it is not possible to distinguish if they are due to (i) changes in wheat genotypes by breeding, (ii) modifications of the environment *via* synthetic chemical inputs, or (iii) phenotypic plasticity, the interaction between wheat genotype and the environment. Using a crossed factorial design in the field, we evaluated the effects of either modern or ancient wheat varieties grown with or without chemical inputs (a N fertilizer, a fungicide, and an herbicide) on "microbiome as a phenotype." We analyzed the rhizosphere microbiota by bacterial and fungal amplicon sequencing, coupled with microscope observations of mycorrhizal associations. We found that plant genotype and phenotypic plasticity had the most influence on rhizosphere microbiota, whereas inputs had only marginal effects. Phenotypic plasticity was particularly important in explaining diversity variations in bacteria and fungi but had no impact on the mycorrhizal association. Our results show an interest in considering the interaction between wheat genotype and the environment in breeding programs, by focusing on genes involved in the phenotypic plasticity of plant-microbe interactions.

Keywords: genotype, environment, phenotypic plasticity, rhizosphere microbiota, mycorrhiza, plant breeding

OPEN ACCESS

Edited by:
Jennifer L. Matthews, University of Technology Sydney, Australia

Reviewed by:
Alessio Mengoni, University of Florence, Italy
Johannes Helder, Wageningen University and Research, Netherlands

***Correspondence:**
Manuel Blouin
manuel.blouin@agrosupdijon.fr

Specialty section:
This article was submitted to Coevolution, a section of the journal Frontiers in Ecology and Evolution

Received: *23 March 2022*
Accepted: *15 June 2022*
Published: *13 July 2022*

Citation:
Jacquiod S, Raynaud T, Pimet E, Ducourtieux C, Casieri L, Wipf D and Blouin M (2022) Wheat Rhizosphere Microbiota Respond to Changes in Plant Genotype, Chemical Inputs, and Plant Phenotypic Plasticity. Front. Ecol. Evol. 10:903008. doi: 10.3389/fevo.2022.903008

INTRODUCTION

Plant genotypes have an influence on the composition of rhizosphere microbiota (Lundberg et al., 2012; Peiffer et al., 2013) and function (Lemanceau et al., 2017), which in turn affects plant growth, development, and immunity (Mendes et al., 2011; Berendsen et al., 2012). The rhizosphere microbiota recruited by plants is sensitive to changes in root exudate composition (Lebeis et al., 2015; Hu et al., 2018), and recently, plant loci correlated with specific subsets of rhizosphere microbiota were identified by genome-wide association (Deng et al., 2021). Understanding factors favoring crop associations with beneficial microbes may help in maintaining high crop yields while decreasing synthetic chemical inputs (e.g., man-made herbicides, fungicides, and mineral fertilizers). To steer beneficial interactions between plants and microbiota, two

strategies are developed: manipulating soil microbial community directly (Jacquiod et al., 2022) and manipulating plant traits involved in microbial interactions (Bakker et al., 2012). In the latter, the goal can be to enhance specific microbial functions (e.g., nitrogen fixation/mineralization) or enhance community intrinsic properties (e.g., diversity, evenness, and composition) associated with beneficial effects on plants (Bakker et al., 2012).

However, plant breeding has changed interactions with soil microorganisms (Milla et al., 2015; Turcotte et al., 2015). An effect of domestication, from wild relatives to cultivated varieties, on rhizosphere microbiota was observed in barley (Bulgarelli et al., 2015), maize (Szoboszlay et al., 2015), foxtail millet (Chaluvadi and Bennetzen, 2018), and common bean (Pérez-Jaramillo et al., 2017), generally leading to microbiota changes between wild relatives and selected varieties (Pérez-Jaramillo et al., 2018). Domestication was also shown to decrease the mycorrhizal associations and yield gain responsiveness of selected wheat varieties (Kapulnik and Kushnir, 1991; Hetrick et al., 1992). A similar effect was observed in relation to a recent selection effort that started with the Green Revolution (Smale, 1997) between varieties released after 1960 (hereafter called "modern") and those released before 1960 (hereafter called "ancient") (Leiser et al., 2016). This recent selection effort was linked with a relaxed selective process of wheat microbiota assembly (Hassani et al., 2020), but the effects are small (Özkurt et al., 2020) and apparently more pronounced for fungi (Spor et al., 2020). However, meta-analyses concluded that agricultural and breeding practices are not responsible for a decrease in mycorrhizal responses in modern varieties (An et al., 2010; Lehmann et al., 2012). The first hypothesis tested in our study is that recent selection has changed wheat rhizosphere microbiota community structure *via* deteriorated ability to maintain high microbial diversity and mycorrhizal levels in modern varieties.

From another perspective, rhizosphere microbiota changes observed since the Green Revolution may be attributed to the field application of synthetic chemical inputs (e.g., fertilizers, herbicides, and fungicides, hereafter called "inputs"). Effects of inputs were linked with decreased microbial diversity while favoring only few taxa (Dunn et al., 2021). Among different inputs, fertilization is often reported in the literature for its impact on soil microbiota. In a meta-analysis, long-term mineral fertilization was linked with increased microbial biomass (Geisseler and Scow, 2014). Fertilization alters soil microbiota composition by promoting copiotroph microorganisms (Ramirez et al., 2010, 2012). Modifications of the bulk soil microbial reservoir instigated by fertilization are associated with altered rhizosphere community assembly in lettuces (Chowdhury et al., 2019), legumes (Weese et al., 2015), and wheat (Ai et al., 2015; Chen et al., 2019). Similarly, fertilization may reduce the diversity (Egerton-Warburton et al., 2007) and cost-benefit balance of arbuscular mycorrhizal fungi (Lambers et al., 2009). Since fertilizers could promote the dominance of copiotrophs and fungicides could prevent fungal diseases, we formulate a second hypothesis: the presence of inputs will decrease the microbial diversity and abundance of arbuscular mycorrhizal fungi in the wheat rhizosphere.

Furthermore, it needs to be emphasized that the recent selection effort and the use of inputs are two interconnected agricultural practices that evolved in parallel: modern varieties were selected and are generally grown with synthetic inputs, whereas ancient varieties have been selected before 1960 at a time where inputs were not used in a systematic way and are generally grown today in organic farming without synthetic inputs. Studies on the effect of recent selection efforts on the wheat rhizosphere microbiota do not explicitly consider inputs (Spor et al., 2020). Likewise, studies focusing on the effect of inputs on the assembly of wheat rhizosphere microbiota do not consider the recent selection efforts between ancient and modern varieties (Chen et al., 2019). This tangled association between genotypes and inputs, even if applied at low doses (e.g., Voss-Fels et al., 2019), prevents the assessment of their relative importance on wheat rhizosphere microbiota assembly. It is thus paramount to assess the interaction between genotypes and inputs, a neglected aspect in rhizosphere microbiota studies. Here, we formulate our third hypothesis: the effect of recent selection efforts on wheat rhizosphere microbiota and mycorrhizal associations is influenced by inputs.

To test our hypotheses, the effects of recent breeding efforts (ancient vs. modern varieties) and inputs (absence vs. presence) on rhizosphere microbiota assembly can be described using the formalism of quantitative genetics "$P = G + E + G \times E$" (Falconer, 1989). Indeed, beyond morphological or physiological traits of plants, rhizosphere microbiota can be considered as an extended phenotype of plants (de la Fuente Cantó et al., 2020) with an important influence on plant fitness (Lemanceau et al., 2017). As such, the structural and functional properties of rhizosphere microbiota can be considered a host phenotype (Oyserman et al., 2021) that contributes to the inclusive fitness of the host (Danchin et al., 2011). Here, we thus consider the diversity of rhizosphere microbiota as a phenotypical trait "P," which can be determined by (i) plant genotype "G" (hereafter called "breeding type" differentiating modern and ancient varieties), (ii) environment "E" (modified by agricultural practices such as application of inputs, here an herbicide, a fungicide, and a nitrogen fertilizer), and (iii) interaction between wheat genotype and inputs "G × E," defined as plant phenotypic plasticity. Phenotypic plasticity denotes the ability of a genotype to exhibit changes in a specific trait across different environments (Laitinen and Nikoloski, 2019), usually visualized as a "norm of reaction" where phenotype changes in each genotype are depicted across environments (Schmalhausen, 1949; Stearns, 1989). Phenotypic plasticity could explain discrepancies between studies regarding the microbial diversity associated with ancient and modern varieties due to environmental differences. It is thus mandatory to evaluate the relative importance of G (hypothesis 1), E (hypothesis 2), and the G × E interaction (hypothesis 3). We thus set an experiment with five ancient and five modern wheat varieties with or without inputs (**Supplementary Figure 1**) and analyzed rhizosphere microbiota with an integrated approach coupling microscopic observations of mycorrhiza with amplicon sequencing of the bacterial (16S rRNA gene) and fungal (ITS2) communities to determine the relative importance of the three terms in explaining variations in wheat rhizosphere microbiota.

MATERIALS AND METHODS

Field Site and Experimental Design

The field experiment was conducted at Institu Agro Dijon (47° 18′32 ″N 5° 04′02″ E, Dijon, France preceding culture: *Vicia faba*). The soil is Calcosol (−22 cm: pH_{H2O} = 8; 34.6% clay, 36.2% loam, and 29.2% sand; 46.2 $g.kg^{-1}$ organic matter, 26.7 $g.kg^{-1}$ organic carbon, and 2.11 $g.kg^{-1}$ total nitrogen; 294 $g.kg^{-1}$ total Ca; 0.02 $g.kg^{-1}$phosphorous pentoxide (P_2O_5); 24.3 $cmol^{+}.kg^{-1}$ CEC). Plots (1 × 1 m^2, separated by 0.8-m-wide paths) were randomized and distributed in three repeated blocks of 20: five plots for ancient varieties without inputs, five plots for ancient varieties with inputs, five plots for modern varieties without inputs, and five plots for modern varieties with inputs for a total of 60 plots across the three blocks, with N = 15 for each breeding type × input modality (**Supplementary Figure 2**). Seeds were sown manually (3 and 4 November 2016). We selected two groups of varieties, one that has not been submitted to the recent selection effort in high input systems and one that has been selected in such systems. Based on the hypothesis of disruption of plant-microbial symbiosis, our rationale was that genotypes continuously grown without synthetic inputs and exposed to local microbial communities should have kept ancestral interactions with microorganisms, whereas genotypes selected in high-input systems could have lost these ancestral plant-microbe interactions because of evolutionary trade-offs between selected traits and symbiosis traits (Porter and Sachs, 2020). In the group of varieties selected in high-input systems, we chose five of the most common modern varieties currently grown in the Burgundy region from a diversity of seed suppliers (**Table 1**). In the group of varieties selected and grown without synthetic inputs, we chose five grown locally among 200 owned by the non-governmental organization "Graines de Noé"[1], which promotes *in situ* conservation of wheat landraces. Information on ancient varieties was retrieved from Jacques Le Gouis and François Balfourier (Centre de Ressources Biologiques « Céréales à paille » of the INRAE Clermont-Ferrand, France). The panel (**Table 1**) is made of two varieties with a name attesting to their local origin (Barbu du Mâconnais and Blé de Saône) and the most commonly grown by organic farmers in Burgundy (Automne Rouge). To avoid a potential bias due to local selection (small population size amplifying stochastic genetic effects or inbreeding), we supplemented the panel with Alauda, a German crossbreed of Probus (1948, Swiss) × Inntaler (< 1960) specifically selected for organic farming (indeed recent but not selected in high-input systems) and einkorn wheat (*Triticum monococcum*), an external taxon that is likely to share ancestral plant-microbes interactions, since it was also not selected in high-input systems. These ancient varieties are not fixed genetically, but the *in situ* conservation method and their phenotypical stability suggested a relative genetic homogeneity. Each variety was grown either (i) with inputs (w) or (ii) without inputs (w/o). Inputs included practices typically applied by local farmers in Burgundy: a fertilizer (ammonium nitrate 27%, Dijon Céréales, Longvic, France) for a total of 150 kg $N.ha^{-1}$, was applied as 50 kg $N.ha^{-1}$ three times, on week 18 after sowing (9 March 2017), week 25 (24 April 2017), and week 30 (30 March 2017); a herbicide (Bofix^{TM}; Dow Agro Science) was supplied once at 0.3 $l.ha^{-1}$ on week 23 (10 April 2017), and a fungicide (Bell Star^{TM}; Dow Agro Science) was applied once at 2.5 $kg.ha^{-1}$ on week 26 (5 May 2017).

[1]http://www.graines-de-noe.org/

Rhizosphere Soil Sampling

Sampling was conducted before wheat heading. In each plot, two plants were sampled in opposed corners (green circles, **Supplementary Figure 2**). All field and laboratory equipment was cleaned with ethanol 70% before each use. Root systems with adhering soil were retrieved by loosening the soil with a fork and immediately transferred to the laboratory. Rhizosphere soil was collected using sterilized brushes. Two rhizosphere soils coming from the same plot were pooled to obtain representative samples and stored at −20 °C. Total DNA was extracted from 250 mg of the rhizosphere soil using a DNeasy PowerSoil-htp 96-well DNA isolation kit (Qiagen, France) based on a combined mechanical and alkaline lysis coupled with chromatography purification, which guarantees the molecular-grade recovery of soil metagenomic DNA.

Microbial Community Sequencing

Bacterial/fungal amplicon sequencing was adapted from previously described methods (Spor et al., 2020). Total bacterial and fungal diversity and composition were obtained by sequencing the V3-V4 hypervariable regions of the bacterial 16S rRNA gene (small subunit of the ribosomal operon, Baker et al., 2003; Herlemann et al., 2011) and the ITS2 region (Internal Transcribed Spacer 2 in the ribosomal operon, White et al., 1990; Ihrmark et al., 2012) by Illumina Miseq 2 × 250-bp paired-end analysis. For consistency, we analyzed both the 16S rRNA and ITS2 sequences using an OTU pipeline instead of Amplicon Sequence Variants (ASV), since the latter is currently not optimal for fungal ITS (Estensmo et al., 2021). Plant contaminations were removed from 16S rRNA gene amplicon sequences by systematically removing OTUs sharing at least 98% identity with a wheat plastid DNA sequence (*Triticum aestivum* chloroplast; accession: NC_002762.1:c123842-122352 and NC_002762.1:91051-92542). A summary of sequenced samples is provided in **Supplementary Table 1**. Raw sequences have been deposited to the SRA (Sequence Read Archive, bacteria: SUB9063594, Fungi: SUB9104701) public repository.

Statistical Analysis

Data analysis was performed with the Rstudio software (R Core Team, 2020). We used the following model: "P ∼ E + G/Variety + G*E + block," where "P" is the rhizosphere microbiota parameter considered (e.g., diversity indices), "G" is the genotype, defined as the breeding type (either modern or ancient varieties), and "E" is the environment, defined as inputs (either with or without). We added a "variety" factor to consider the random variance that could arise from the difference between varieties inside the modern or ancient groups ("G/variety"). The effect of spatial heterogeneity in our experimental site was assessed through the "block" factor with an additive effect. Since

TABLE 1 | Detailed list of modern and ancient wheat varieties used in this study.

Breeding type	Variety name	Identifier	Year of release	Accession	Provider	URL
Modern varieties	Rubisco	R	2012	36680	RAGT Semences	https://ragt-semences.fr/
	Descartes	D	2014	1365	Secobra	https://secobra.fr/bles
	Sherlock	S	2015	36751	Secobra	https://secobra.fr/bles
	Alixan	A	2005	24559	Limagrain	https://www.limagrain.com/
	Tulip	T	2011	36713	Saaten Union	http://www.fiches.arvalis-infos.fr/
Ancient varieties	Barbu du Mâconnais	BM	End of XIX - Early XX centuy	1234	Graines de Noé	http://www.graines-de-noe.org/
	Blé de Saone	BL	< 1960	1440	Graines de Noé	http://www.graines-de-noe.org/
	Automne Rouge	AR	XIX century	1117	Graines de Noé	http://www.graines-de-noe.org/
	Alauda	AL	Probus (1948) x Inntaler (< 1960) crossing (2013)	39379	Graines de Noé	http://www.graines-de-noe.org/
	Einkornwheat	EN	< 1960	26624	URGI - Unité de Recherche Génomique Info	https://urgi.versailles.inra.fr/Projects/Achieved-projects/Siregal

The table features the name, year of release, accession, provider, and URL of each variety.

observations of mycorrhiza were conducted in two batches, we specifically included an additive "batch" factor in the model (refer to the Mycorrhizal colonization section). Normality and homoscedasticity were assessed by Shapiro and Bartlett tests. Normally distributed data were analyzed with ANOVA models, followed by *post hoc* Tukey's honest significant difference test (Tukey's HSD, $p < 0.05$, package '*agricolae,*' de Mendiburu and Yaseen, 2020). Data that were not normally distributed were analyzed with the non-parametric Scheirer-Ray-Hare tests followed by *post hoc* false discovery rate test correction to account for multiple testing (FDR, $p < 0.05$, "*rcompanion*" and "*FSA,*" Sokal and Rohlf, 1995). In the Results section, we present the percentage of variance explained and associated *p*-values from the ANOVA and Scheirer-Ray-Hare models.

Alpha Diversity

Sequencing completeness and quality were verified with rarefaction curves ("*vegan*"; Dixon, 2003; **Supplementary Figure 3**), enabling the identification of eight outlier samples coming from the same plate column harboring significantly higher sequence counts but relatively lower OTU discovery rates than the others ($p < 0.001$). The samples were excluded from further analyses, leaving $N = 11–14$ in each G × E modality, with at least four biological replicates per variety (**Supplementary Table 1**). Sequencing profiles were resampled at 14,000 counts to normalize diversity discoveries (Schöler et al., 2017), and the following indices were used: observed taxon richness (S: the number of OTUs detected), Chao-1 (estimation of real taxon richness based on rare taxon occurrence represented by one sequence in a sample), ACE (abundance-based coverage estimator: estimation of real taxon richness based on rare taxon occurrence represented by 10 sequences in a sample), Simpson Reciprocal index (1/D, D = dominance, the probability of picking the same taxon twice from two random drawings), Shannon index (H: a measure of species diversity and evenness based on the sum of all species contribution in a community), and Pielou's equitability ($J = H/\ln(S)$, an index ranging from 0 to 1 indicating the level of evenness in the community). The models are available in **Supplementary Table 2** (Bacteria) and **Supplementary Table 3** (Fungi). A PERMANOVA was performed on the six diversity indices (**Supplementary Table 4**). The distribution and phylogenetic composition of core OTU fractions were visualized in Venn diagrams (**Supplementary Figure 4**).

Beta Diversity

Resampled sequencing profiles were analyzed by PERMANOVA ("*vegan,*" Bray-Curtis dissimilarity, **Supplementary Table 4**). As only breeding type and block had significant effects, a partial distance-based redundancy analysis (db-RDA) was performed to visualize the profiles with the model: "breeding type + condition (block)" ("*capscale*" function, 10,000 permutations). OTUs whose abundance was significantly altered among breeding types (G), inputs (E), and phenotypic plasticity (G x E) were detected using non-rarefied data by quasi-likelihood *F*-test (QLFT) under negative binomial distributions and generalized linear models (nb-GLM, package "*edgeR,*" Robinson et al., 2009), as recommended in the literature (Schöler et al., 2017; Jacquiod et al., 2020). Only OTUs with abundance fold-change > 2, overall occurrence > 20 times, and FDR-adjusted *p*-value < 0.05 were considered (**Supplementary Table 5**).

Network Analysis

Modern and ancient wheat variety rhizosphere microbiota were visualized as networks using Poisson Log Normal (PLN) models, a performant method for sparse count data that enables control of dependency effects arising from compositional profiles (PLN, package "*PLNmodels,*" Chiquet et al., 2019). Partial correlation matrices integrating both core bacterial and fungal OTUs in the ancient ($N = 26/26$) and modern varieties ($N = 24/24$) were computed using the "Total Sum Scaling" offset criteria (TSS) and the following model: "∼ 1 + block + input + offset." PLN models were validated with the Bayesian Information Criterion (BIC) to set the appropriate sparsifying penalty levels. The complexity of networks was investigated by means of the degree index (average number of edges per node), node betweenness (average shortest node path between node pairs), and edge betweenness (average

shortest edge path between edge pairs). We identified keystone species, i.e., species that have a disproportionate deleterious effect on the community network structure upon their removal (Berry and Widder, 2014), as those having the highest degree, reaching 40% of the total proportion of edges. Edge arithmetic was applied with the "*igraph*" package function (Csardi and Nepusz, 2006; Jacquiod et al., 2020) to intersect the modern and ancient networks. Visualization of the finalized network was performed with the "*Cytoscape*" software (Shannon et al., 2003). Separated networks obtained from the modern and ancient varieties are presented in supporting information (**Supplementary Figure 5**).

Mycorrhizal Colonization

Two root systems per plot were collected and pooled together 29 weeks after sowing (22–24 May 2017). The root material was washed and stained (Vierheilig et al., 1998). Roots were cleared (90 °C, 5–10 min, 10% KOH), dipped in black ink (90 °C, 5 min, 5% in acetic acid), rinsed (with water), dipped in acetic acid (8%, 25 min, room temperature), rinsed (with water), dipped in pure glycerol, and stored (at 4 °C). For microscopic observation, roots were cut (1 cm), and 15 fragments were mounted with glycerol between slides (see pictures in **Supplementary Figure 6**). To avoid discoloration during conservation, the root samples were divided into two staining batches. A significant difference in staining intensity was found between the two batches (**Supplementary Figure 7**). To account for coloration fluctuations, the two batches were identified in the statistical model as a "+ batch" factor. Mycorrhization rates were assessed according to Trouvelot et al. (1986) *via* the following indices: frequency of root fragments with mycorrhizal structures on the root system scale (F), the intensity of mycorrhizal colonization on the root system scale (M) or restricted to mycorrhizal root fragments (m), and arbuscular abundance on the root system scale (A) or restricted to mycorrhizal root fragments (a). Univariate models and the global PERMANOVA model are available in supporting data (**Supplementary Tables 4, 6**).

RESULTS

Sequencing Statistics

From the 60 initial rhizosphere samples, 51 (bacteria) and 50 (fungi) amplicon profiles passed the quality control for downstream analysis. For bacterial profiles, 2,099,307 raw sequences were recovered, averaging 41,163 ± 1,049 sequences per sample (standard error of the mean). For fungal profiles, 3,993,837 raw sequences were recovered, averaging 79,877 ± 2,120 sequences per sample. After assembly and cleaning, the bacterial profiles yielded 1,076,714 raw sequences, averaging 21,112 ± 597 sequences per sample. Clean fungi profiles yielded 1,333,569 raw sequences, averaging 26,671 ± 1,001 sequences per sample. All the bacterial and fungal profiles could be resampled at a minimal depth of 14,000 sequences.

Effects on the Bacterial Community

We first performed a global analysis on all diversity indices to detect main effects by PERMANOVA (**Table 2** and **Supplementary Table 4**), and 63.5% of the variance was explained by our model, with a significant effect of breeding type (7.4%, $p = 0.013$), the G × E interaction (5.7%, $p = 0.034$), and different varieties nested in each breeding type (48.8%, $p = 0.015$). In detail, breeding type (ancient vs. modern varieties) had a significant effect on all the diversity indices: richness (explaining 15.57% of the total variance, $p < 0.001$), Chao-1 (6.89%, $p = 0.025$), ACE (5.87%, $p = 0.044$), Simpson reciprocal (9.18%, $p = 0.032$), Shannon (20.08%, $p = 0.001$), and equitability (13.82%, $p = 0.009$) (**Table 3** and **Supplementary Table 2**). The modern varieties had higher diversity than the ancient varieties (**Figure 1**). The presence of inputs had a significant negative effect on community evenness *via* the Simpson reciprocal (7.83%, $p = 0.048$). The G × E interaction had a significant effect on richness (7.7%, $p = 0.011$), ACE (6.8%, $p = 0.031$), and Shannon (8.64%, $p = 0.038$), as the addition of inputs led to a significant decrease in diversity only for the ancient varieties (**Figure 1**). The different varieties nested in each breeding type was the main source of variation in the richness (46.1%, $p = 0.009$), Chao1 (49.9%, $p = 0.015$), and ACE (47.5%, $p = 0.028$) indices. No effect of spatial heterogeneity was detected (block: $p > 0.05$). The visual distribution of bacterial taxa in Venn diagrams across G × E treatments allowed the detection of distinct OTUs associated with breeding type and inputs and their interaction and covering a broad phylogenetic diversity (**Supplementary Figure 4**). The modern varieties had more unique taxa (61 including unique representatives from Gemmatimonadetes and TM7) than the ancient ones

TABLE 2 | Permutational analysis of variance for bacterial and fungal alpha diversity (based on the six diversity indices: richness, Chao-1, ACE, Simpson reciprocal, Shannon, and equitability), beta diversity (based on Bray-Curtis dissimilarity index), and for parameters describing mycorrhizal colonization (F, M, m, A, and a, refer to Materials and methods for a description).

PERMANOVA	Bacteria (Alpha)	Bacteria (Beta)	Fungi (Alpha)	Fungi (Beta)	Mycorrhization
Breed (G)	7.38%*	2.60%*	0.02%	2.50%*	2.77%**
Inputs (E)	1.43%	1.75%	0.39%	2.24%	0.79%
G x E	5.71%*	1.81%	10.45%*	1.66%	1.09%
Breed/Variety	47.80%*	30.10%	11.82%	34.74%*	18.81%**
Block	1.22%	6.38%***	4.62%	5.38%*	2.8%*
Variance explained	63.53%	42.65%	27.30%	46.52%	26.26%

*Percentages of explained variance are given with asterisks indicating the significance of effects. *p < 0.05; **p < 0.01; ***p < 0.001.*

TABLE 3 | Analysis of variance for bacterial alpha diversity indices.

Statistical test		ANOVA (F)			Scheirer-Ray-Hare (H)		
Alpha diversity indices		**Richness**	**Chao-1**	**ACE**	**Simpson reciprocal**	**Shannon**	**Equitability**
Breed (G)		15.57%***	6.89%*	5.87%*	9.18%*	20.08%**	13.82%**
Inputs (E)		0.06%	2.08%	0.27%	7.83%*	2.56%	7.24%·
G x E		7.74%*	4.21%·	6.81%*	4.65%	8.64%*	3.94%
Variety		46.07%**	49.93%*	47.54%*	20.2%	28.61%	23.28%
Block		0.09%	1.1%	1.16%	11.41%·	3.42%	8.96%
Variance explained		69.52%	64.21	61.65	53.27	63.31	57.24
Direction of effects	Breed (G)	Mod > Anc	Mod > Anc	Mod > Anc	Mod > Anc	Mod > Anc	Mod > Anc
	Inputs (E)	–	–	–	w/o > inputs	–	–
	G x E	Anc: w/o > inputs	–	Anc: w/o > inputs	–	Anc: w/o > inputs	–

*Normally distributed indices were analyzed by ANOVA, while non-parametric indices were analyzed by Scheirer-Ray-Hare test. Percentages of explained variance are given, with asterisks indicating the significance of effects. "Block" is the factor identifying the three replicated blocks in the field. "Variety" is a sub-stratum of variance in the breeding factor, identifying five different wheat varieties inside each breeding type. The directions of significant effects are indicated (Anc = ancient; Mod = modern, and w/o = without inputs), ·p < 0.1; *p < 0.05; **p < 0.01; ***p < 0.001.*

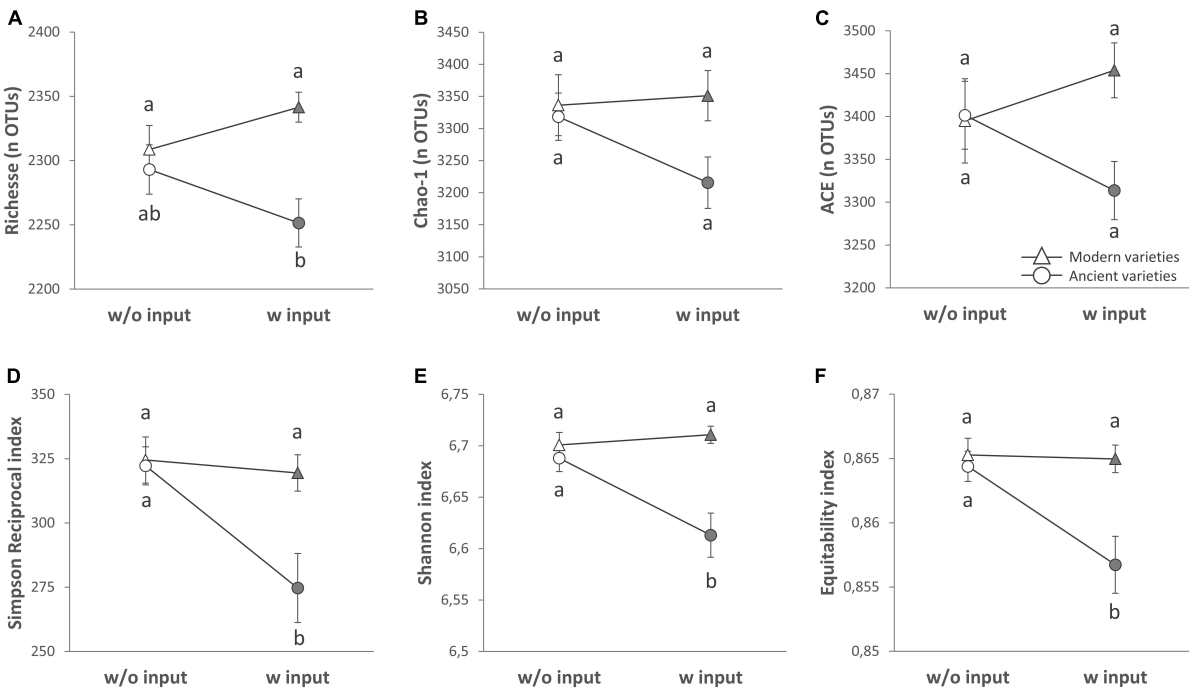

FIGURE 1 | Alpha diversity of the rhizosphere bacterial community (16S rRNA gene amplicon sequencing) presented as reaction norms of ancient and modern wheat genotypes to environment modification by inputs. Panels are respectively showing: the **(A)** richness, **(B)** Chao-1 estimator, **(C)** ACE estimator, **(D)** Simpson Reciprocal index, **(E)** Shannon index, and **(F)** Pielou's equitability. Data are shown as the interaction between breeding type and the presence/absence of inputs (w/o: without inputs; w: with inputs, N = 11–14 per treatment, error bars are standard error of the mean). Significance was inferred with an ANOVA under Tukey's HSD *post hoc* test for normally distributed data (honest significant differences, $p < 0.05$). Data that were not normally distributed were analyzed by Scheirer-Ray-Hare test followed by *post hoc* false discovery rate test correction to account for multiple testing (FDR, $p < 0.05$).

(34 including unique representatives from Planctomycetes). Similar numbers of unique OTUs were detected without (42) and with inputs (46 including unique representatives from Gemmatimonadetes and Planctomycetes). The G × E interaction yielded 98 (without inputs) and 92 (with inputs) unique taxa in the ancient varieties, while 86 (without inputs) and 110 (with inputs) unique taxa with similar phylogenetic signatures in all fractions were observed in the modern varieties.

At the beta diversity level (**Table 2**), the PERMANOVA showed a weak but significant effect on breeding type (2.6%, $p = 0.036$) but not inputs (1.8%, $p = 0.701$). Spatial heterogeneity had a significant effect as well (block: 6.5%, $p < 0.001$). A separation between the modern and the ancient varieties was clearly observed on the constrained axis (CAP1: 2.5%, **Figure 2A**). A total of 23 bacterial OTUs significantly responded to G, E, and G × E and were

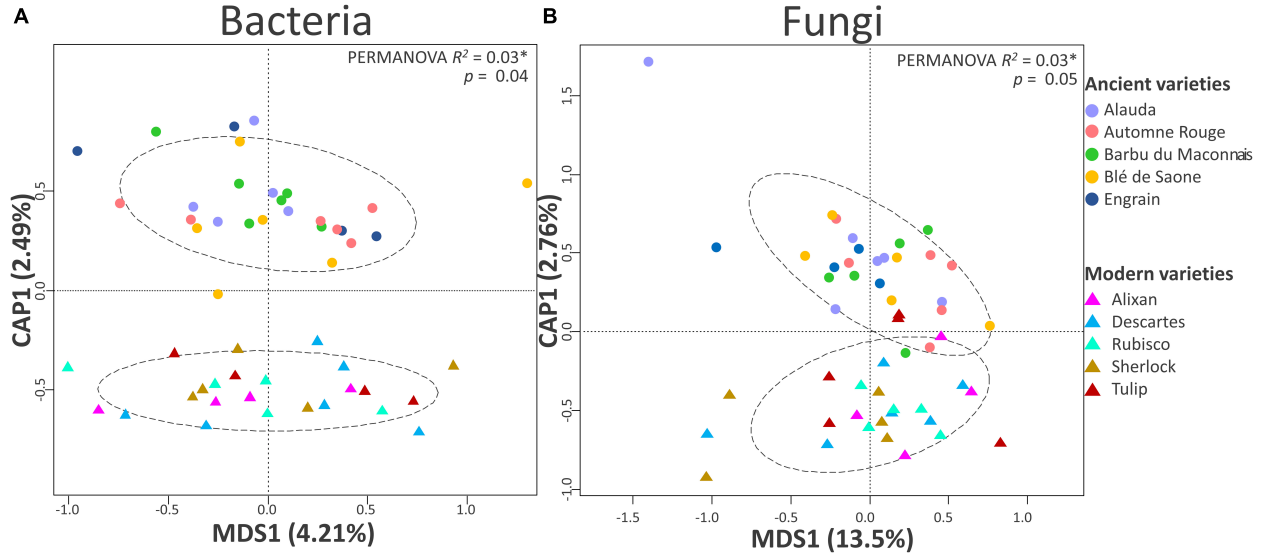

FIGURE 2 | Beta diversity analysis of the **(A)** bacterial and **(B)** fungal communities by partial distance-based redundancy analysis (db-RDA). Partial db-RDAs were conducted to output the following constrained models: breeding type + condition (block) (10,000 permutations, *N* = 24 for modern varieties; *N* = 27 and 26 for ancient varieties in the bacteria and fungi panels, respectively).

mainly from Bacteroidetes, Proteobacteria, Actinobacteria, and Verrucomicrobia (**Supplementary Table 5**). Eleven OTUs mainly from Flavobacteriaceae (*Flavobacterium succinicans*), Cytophagaceae, Cellulomonadaceae, Caulobacteraceae, Hyphomicrobiaceae, and Verrucomicrobiaceae had higher abundance in the ancient varieties, while only one unclassified Gemmatimonadetes OTUs was enriched in the modern varieties. Only one OTU from Cytophagaceae was altered by input addition in all the varieties. Ten OTUs from various families were altered by the G × E interaction, mostly being lowered in the modern varieties (with or without inputs) than in the ancient varieties (with or without inputs). Noteworthy is that a Corynebacteriaceae (OTU_17410, Actinobacteria) and a Haliangiaceae (OTU_41432, Proteobacteria) were decreased 11 folds by inputs in the ancient varieties.

To summarize (**Supplementary Table 7**), the main factor that significantly altered the bacterial component of the rhizosphere microbiota (P) was a breeding type (G), with higher diversity and different community structure in the modern varieties. Phenotypic plasticity (G × E) was the second most structuring factor of the microbiota with (i) lower richness and evenness with inputs in the ancient varieties, (ii) three OTUs altered by the interaction, and (iii) important changes in presence-absence of OTUs in each G × E modality. The effect of input (E) was marginal.

Effects on the Fungal Community

A global analysis of all the diversity indices was performed to detect the main effects by PERMANOVA (**Table 2** and **Supplementary Table 4**), and 27.3% of the variance was explained by our model, enabling the detection of an overall significant effect of the G × E effect (10.5%, $p = 0.053$), whereas breeding type (0.02%, $p = 0.995$), inputs (0.4%, $p = 0.765$), and varieties (11.8%, $p = 1$) had no effect. No effect of spatial heterogeneity was detected (block: 4.6%, $p = 0.444$). In detail, the breeding type had indeed no effect on the fungal diversity indices (**Figure 3**, **Table 4** and **Supplementary Table 3**). Unlike the bacterial profiles, spatial heterogeneity was detected in fungal evenness indices, including the Shannon index (6.57%, $p = 0.005$) and equitability index (17.99%, $p = 0.007$). The presence of inputs had a significant negative effect on the Shannon index (6.7%, $p = 0.044$), mostly driven by the ancient varieties (**Figure 3**). The effect of varieties on each breeding type was not significant despite a relatively high percentage of variance (up to 30.7%). For most of the indices, the G × E interaction induced a decrease in fungal diversity for the ancient varieties with inputs and, conversely, an increase in the modern varieties, as illustrated by the crossing of reaction norms (**Figure 3**) although supported statistically only for the Chao-1 estimator (13.9%, $p = 0.025$, **Table 4**).

The visual distribution of taxa in Venn diagrams across G × E treatments allowed for the detection of distinct OTUs associated with breeding type and inputs and their interaction, showing a clear dominance of Ascomycota (**Supplementary Figure 4**). The ancient varieties had more unique taxa (54, mainly from Chaetomiaceae, Ascobolaceae, Nectriaceae, and Trichocomaceae) than the modern ones (38 mainly from Nectriaceae, Ascobolaceae, and Trebouxiaceae including a unique *Mortierellasarnyensis*). Without inputs, more unique taxa were detected (56 mainly from Chaetomiaceae, Lasiosphaeriaceae, Nectriaceae, and Trebouxiaceae and including unique representatives from Basidiomycota and Chytridiomycota) than with inputs (36 mainly from Helotiales, Nectriaceae, Pyronemataceae, and Trichocomaceae and including unique representatives from Glomeromycota). The

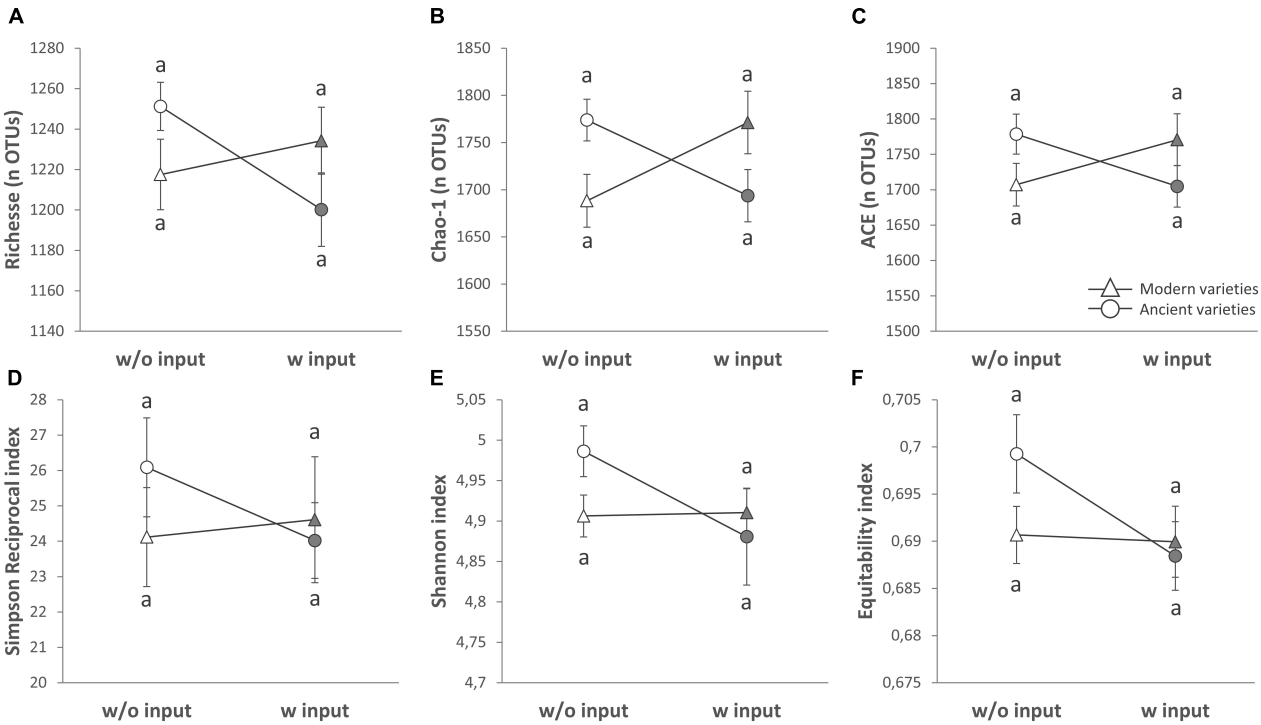

FIGURE 3 | Alpha diversity of the rhizosphere fungal community (ITS2 gene amplicon sequencing) presented as reaction norms of ancient and modern wheat genotypes to environment modification by inputs. Panels are respectively showing: the **(A)** richness, **(B)** Chao-1 estimator, **(C)** ACE estimator, **(D)** Simpson reciprocal index, **(E)** Shannon index, and **(F)** Pielou's equitability. Data are shown as the interaction between breeding type and the presence/absence of inputs (w/o: without inputs; w: with inputs; $N = 11–14$, error bars are standard error of the mean). Significance was inferred with an ANOVA under Tukey's HSD *post hoc* test for normally distributed data (honest significant differences, $p < 0.05$). Data that are not normally distributed were analyzed by Scheirer-Ray-Hare test followed by *post hoc* FDR test correction to account for multiple testing (FDR, $p < 0.05$).

TABLE 4 | Analysis of variance for fungal alpha diversity indices.

Statistical test		**ANOVA (F)**					**Scheirer-Ray-Hare (H)**
Alpha diversity indices		**Richness**	**Chao-1**	**ACE**	**Shannon**	**Equitability**	**Simpson reciprocal**
Breed (G)		0%	0.03%	0.01%	0.9%	1.69%	2.33%
Inputs (E)		2.61%	0.01%	0.13%	4.46% *	5.41%·	1.24%
G x E		7.4%	13.9% *	8.37%·	3.04%·	2.13%	1.71%
Variety		12.4%	11.15%	12.18%	1.05%	30.7%	21.22%
Block		4.8%	5.68%	3.66%	6.57% **	17.99% **	9.46%·
Variance explained		27.21%	30.77%	24.35%	57.78%	57.92%	35.97%
Direction of effects	Breed (G)	–	–	–	–	–	–
	Inputs (E)	–	–	–	w/o > inputs	w/o > inputs	–
	G x E	–	Anc: w/o < inputs; Mod: w/o < inputs	–	w/o: Anc > Mod	–	–

*Normally distributed indices were analyzed by ANOVA, while non-parametric indices were analyzed by Scheirer-Ray-Hare test. Percentages of explained variance are given, with asterisks indicating the significance of effects. "Block" is the factor identifying the three replicated blocks in the field. "Variety" is the sub-stratum of variance in the breeding factor, identifying five different wheat varieties inside each breeding type. The directions of significant effects are indicated (Anc = ancient; Mod = modern; w/o = without inputs), ·$p < 0.1$; *$p < 0.05$; **$p < 0.01$; ***$p < 0.001$.*

G × E interaction yielded unique OTUs in each category from families Ascobolaceae, Chaetomiaceae, Trebouxiaceae, and Mortierellaceae. More specifically, in the ancient varieties, 132 unique OTUs were found without inputs (featuring families Cladosporiaceae, Pleosporaceae, Pyronemataceae, and Trichocomaceae) and 115 with inputs (featuring families Herpotrichiellaceae, Hypocreales, Nectriaceae, Ophiostomataceae, Pyronemataceae, and Tremellaceae). In the modern varieties, 130 unique OTUs were found without inputs (featuring families Cladosporiaceae, Hypocreales, Nectriaceae, Ophiostomataceae, Plectosphaerellaceae, and Pyronemataceae) and 128 with inputs (featuring

families Herpotrichiellaceae, Hypocreales, Nectriaceae, Ophiocordycipitaceae, Ophiostomataceae, Plectosphaerellaceae, and Trichocomaceae). Noteworthy was the unique occurrence of Glomeromycota in ancient varieties without inputs and modern varieties with inputs. More specifically, the modern varieties with inputs have recruited six unique Glomeromycota OTUs from different phylogenetic origins: *Claroideoglomus*, *Diversispora*, *Gigaspora*, one unclassified Claroideoglomeraceae, and one unclassified Glomerales. In the ancient varieties without inputs, only one unique *Claroideoglomus* OTU (not the same as in modern with inputs) was recruited.

At the level of beta diversity (**Table 2**), the PERMANOVA showed a significant spatial heterogeneity (block, 5.4%, p = 0.011). Breeding type (2.5%, p = 0.052) and variety (34.7%, p = 0.02) had significant effects but not inputs (2.2%, p = 0.14). A separation between the modern and ancient varieties was observed on the constrained axis (CAP1: 2.8%, **Figure 2B**). Thirty-three fungal OTUs significantly responded to G, E, and G × E (**Supplementary Table 5**) and were mainly from Ascomycota, Basidiomycota, and Chytridiomycota. Twelve fungal OTUs were altered by breeding type, being enriched in the ancient varieties, and were mostly from families Helotiaceae, Erysiphaceae (*Blumeriagraminis*), Ascobolaceae, Nectriaceae (*Fusarium solani*), Leptosphaeriaceae, Sporormiaceae (*Preussiaflanaganii*), Russulaceae, and Lobulomycetaceae (*Clydaeavesicula*). Only one OTU (*Psathyrellapanaeoloides*) was enriched in the modern varieties. Six OTUs from various families were enriched by inputs (including *Blumeriagraminis*, *Fusarium solani,* and *Clydaeavesicula*), and three were decreased by inputs (including *Psathyrellapanaeoloides*). The G × E interaction altered 12 OTUs from various families, mostly between ancient varieties without inputs and modern varieties with inputs (e.g., *Blumeriagraminis and Psathyrellapanaeoloides*). The G × E interaction was also seen amongst ancient varieties depending on input application (*Didymellanegriana* and *Pseudeurotiumovale* favored no inputs, while *Cryptococcus uniguttulatus* favored inputs). Among noteworthy discriminant OTUs, an Ascobolaceae (OTU_3503, Pezizomycetes, Ascomycota) was found to be impacted by G (ancient > modern), E (without > with inputs), and G × E (ancient varieties without inputs > modern with inputs), a *Psathyrellapanaeoloides* (OTU_31, Basidiomycota) whose abundance was increased by 178 folds in the modern varieties with inputs compared to the ancient ones without inputs, and a Russulaceae (OTU-113, Basidiomycota) whose abundance was increased by 30 folds in the ancient varieties with inputs compared to those without. To summarize (**Supplementary Table 7**), breeding type (G) and phenotypic plasticity (G × E) were equally important in the fungi component of the microbiota (P). Breeding type (G) affected the community structure, with 13 OTUs enriched in the ancient varieties and only one in the modern varieties but did not alter the diversity indices. Phenotypic plasticity (G × E) had an overall important effect on alpha diversity, with diversity reduction in inputs only for the ancient varieties and an effect on the abundance of 12 OTUs between the modern varieties with inputs and the ancient ones without inputs.

Mycorrhizal Colonization

The breeding type had an impact on the intensity of mycorrhizal colonization in the root system (M, 4.3%, p = 0.005), on mycorrhizal root fragments (m, 4.5%, p = 0.009), on the arbuscular abundance in the root system (A, 4.7%, p = 0.018), and on mycorrhizal root fragments (a, 3.82%, p = 0.002), all being in favor of higher values in the modern varieties than in the ancient ones (**Figure 4**, **Table 5** and **Supplementary Table 6**). Inputs had an impact only on M (2.6%, p = 0.027) and m (2.6%, p = 0.046), being higher without inputs. The G × E interaction had no effect. Varieties in each breeding type had an effect on m (22.46%, p = 0.01), M (23.63%, p = 9.6E-4), and a (19.77%, p = 0.03). Spatial heterogeneity slightly affected M (block: 4.13%, p = 0.02). The frequency of mycorrhization "F" was not affected. The PERMANOVA on all the indices revealed a significant effect of breeding type in favor of higher values in the modern varieties (2.8%, p = 0.008, **Table 2** and **Supplementary Table 4**). The effect of varieties nested in each breeding type was also significant (18.8%, p = 0.007), as well as spatial heterogeneity (block: 2.8%, p = 0.046). To summarize (**Supplementary Table 7**), the mycorrhizal indices were primarily altered by breeding type (G), as mycorrhization was stronger in the modern varieties. The addition of inputs (E) decreased the intensity of mycorrhizal colonization in the root system and root fragments. The G × E interaction had no effects.

Network Analysis

Poisson Log-Normal (PLN) models reached stable solutions (refer to the two separated networks in **Supplementary Figure 5**), resulting in two networks with comparable sizes in terms of nodes (modern network: 141 nodes, sparsifying penalty = 0.22, R^2 = 0.993; ancient network: 158 nodes, sparsifying penalty = 0.21, R^2 = 0.993). To better visualize the specific and common parts between the two networks, we merged them and clustered nodes based on their membership (either unique or common, **Figure 5**). The intersection revealed 81 OTUs in common, while 77 and 60 were, respectively, specific to the network of either ancient or modern varieties. Similar phylogenetic compositions were found for both networks, with a dominance of Ascomycota, Proteobacteria, Actinobacteria, and Bacteroidetes OTUs. Eight keystone species gathering 40% of edges were identified (**Supplementary Figure 5**). The network of the ancient varieties had significantly higher complexity than that of the modern ones for all the tested indices. In the network of the ancient varieties, three keystone OTUs centralized most edges, including an Ascobolaceae (OTU_3503, Pezizomycetes, Ascomycota, degree = 34), an unclassified fungus (OTU_123, Ascomycota, degree = 26), and a *Cellvibrio* (OTU_886, Gammaproteobacteria, degree = 20). In the network of the modern varieties, one keystone OTU centralized most edges, *Lectera longa* (OTU_37, Sordariomycetes, degree = 54). Among common OTUs, four keystones centralized most edges: an unclassified Sordariomycetes (OTU_71, Ascomycota, degree = 38), a *Janthinobacteria* (OTU_1532, Oxalobacteraceae, Betaproteobacteria, degree = 18), a *Mortierella* (OTU_112, Mortierellomycota, degree = 13), a *Pedobacter*

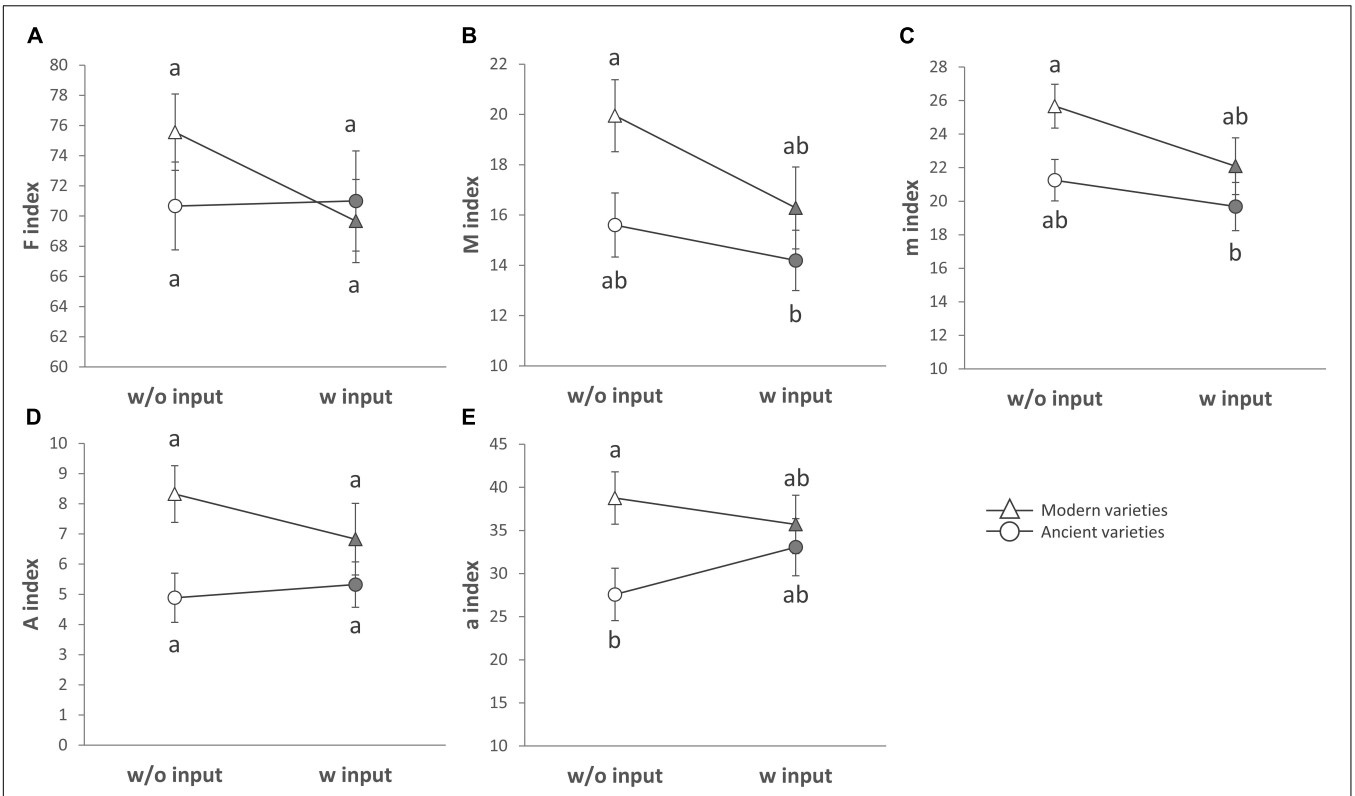

FIGURE 4 | Mycorrhizal colonization for breeding types and inputs that are presented as reaction norms. Panels are respectively showing **(A)** the frequency of root fragments with mycorrhizal structures on the root system scale, intensity of mycorrhizal colonization on the root **(B)** system scale, or **(C)** restricted to mycorrhizal root fragments **(D)** arbuscule abundance on the root system scale or **(E)** restricted to mycorrhizal root fragments for each type of breeding (modern varieties with triangles, ancient varieties with circles) in response to the presence of inputs. Significance was inferred by ANOVA under Tukey's HSD *post hoc* test for normally distributed data (honest significant differences, $p < 0.05$). Data that were not normally distributed were analyzed by Scheirer-Ray-Hare test followed by *post hoc* FDR test correction to account for multiple testing (FDR, $p < 0.05$).

TABLE 5 | Analysis of variance for mycorrhization indices.

Statistical test		**ANOVA (F)**			**Scheirer-Ray-Hare (H)**	
Alpha diversity indices		**M**	**m**	**a**	**F**	**A**
Breed (G)		4.26%**	4.53%**	3.82%*	0.1%	4.7%*
Inputs (E)		2.65%*	2.59%*	0.12%	0.73%	0.53%
G x E		0.52%	0.39%	1.45%	1.55%	2.19%
Variety		23.63%***	22.46%**	19.77%*	2.7%	8.99%
Block		4.13%*	3.86%·	1.29%	3.77%	2.33%
Batch		13.67%***	4.43%**	9.06%***	26.64%***	13.57%***
Variance explained		48.86%	38.26%	35.52%	35.49%	32.3%
Direction of effects	Breed (G)	Mod > Anc	Mod > Anc	Mod > Anc	–	Mod > Anc
	Inputs (E)	w/o > inputs	w/o > inputs	–	–	–
	G x E	–	–	–	–	–

*Normally distributed indices were analyses by ANOVA, while non-parametric indices were analyzed by Scheirer-Ray-Hare test. Percentages of explained variance are given, with asterisks indicating the significance of effects. "Block" is the factor identifying the three replicated blocks in the field. "Variety" is the sub-stratum of variance in the breeding factor, identifying five different wheat varieties inside each breeding type. "Series" refers to the two different batches of staining of mycorrhiza. The directions of significant effects are indicated (Anc = ancient; Mod = modern; w/o = without inputs), ·p < 0.1; *p < 0.05; **p < 0.01; ***p < 0.001.*

(Sphingobacteriaceae, Bacteroidetes, degree = 11). Six OTUs in this network were previously detected as being "discriminant taxa" (refer to "Network" in **Supplementary Table 5**). Among them, Ascobolaceae (OTU_3503, Pezizomycetes, Ascomycota, degree = 34) was an important discriminant OTU being affected by G, E, and G × E (**Supplementary Table 5**). To summarize, each network had its own set of OTUs. The ancient network was more complex, including more keystone species than in the

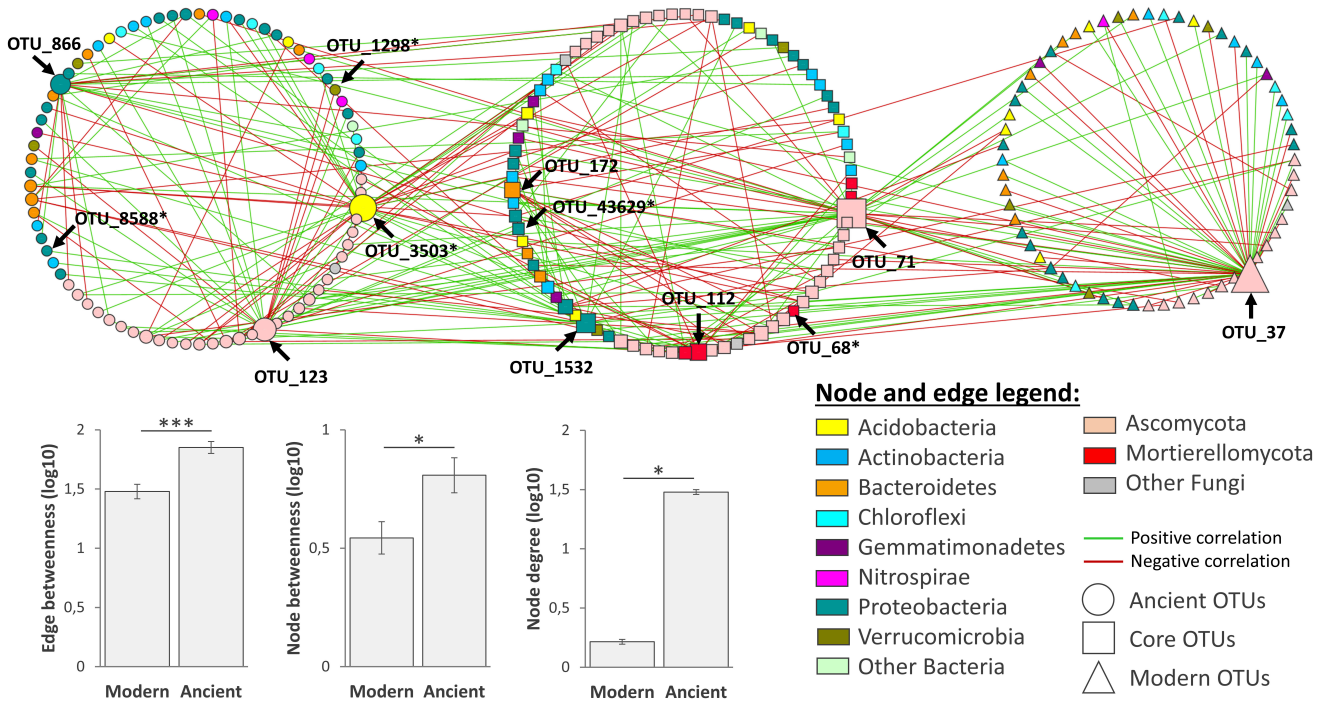

FIGURE 5 | Combined network analysis of rhizosphere microbiota associated to the modern (N = 26) and ancient (N = 24) wheat varieties. The modern and ancient networks were constructed using dominant OTUs based on partial correlations obtained with Poisson Log Normal models combining the bacterial and fungal datasets together (~1 + block + offset). For visualization, both networks were merged into one and clustered in three to feature: (i) unique OTUs of the ancient network on the left, (ii) common OTUs in the middle, and (iii) modern OTUs on the right. OTUs of interest (keystone or discriminant OTUs from **Supplementary Table 5**) are indicated with an arrow. Bar charts represent average network complexity indices estimated from edges or nodes (Kruskal–Wallis test, $^{*}p < 0.05$; $^{***}p < 0.001$).

modern network. Among keystone OTUs in the ancient network, the OTU_3503 Ascobolaceae was the most centralized one, being sensitive to G, E, and G × E.

A summary figure was established based on the main results obtained on the bacterial and fungal communities and mycorrizha colonization (**Figure 6**).

DISCUSSION

Modern wheat varieties were selected and are generally grown with inputs, whereas ancient varieties were selected before 1960, at a time where inputs were not used in a systematic way, and are generally grown today in organic farming without synthetic inputs. This link between genotype (G) and agricultural practices modifying the environment (E) prevents the assessment of the relative importance of individual factors (E and G) and their interaction (G × E) on plant-microbiota relationships. Our results are a first attempt to quantify the importance of these effects in the field. As such, spatial variability was important to consider by setting up three repeated blocks (**Supplementary Figure 2**) included in statistical models. This spatial variability was expected and had a relatively low effect on our recorded parameters (0.1~18%). In addition, it was important to assess the variability inside each breeding type by considering variety-specific variations across the modern and ancient genotypes (by multi-stratum variance analysis). Indeed, the variety effect nested inside each breeding type (see model, **Supplementary Figure 1**) was sometimes important (1.1–49.9%). However, both spatial and variety effects did not prevent the detection of significant effects associated with our factors of interest.

Effects of Breeding on Rhizosphere Microbiota

Breeding type (G) was the most structuring factor explaining the outcome of rhizosphere microbiota (**Supplementary Table 7**). The recent selection effort from ancient to modern varieties had a more pronounced effect on bacteria than on fungal alpha diversity, with modern varieties having more diversity than ancient ones. All the mycorrhiza indices (except F) were higher with the modern varieties than with the ancient ones. Therefore, our results invalidated the first hypothesis that modern varieties are associated with less diverse communities than ancient ones. This result is in line with the reduced selectivity of modern varieties regarding rhizosphere microbial recruitment as compared to ancient ones (Kiers et al., 2007). Besides, in terms of community structures (beta diversity), breeding had a small effect on both bacterial and fungal communities (2.5–2.6%). Different but not opposite results were reported in the literature about the recent selection effort on rhizosphere microbial community structure: (i) no clear difference in bacterial community structure between ancient (three varieties) and modern (one variety) breeding types (Cangioli et al., 2022); (ii) stronger effect on

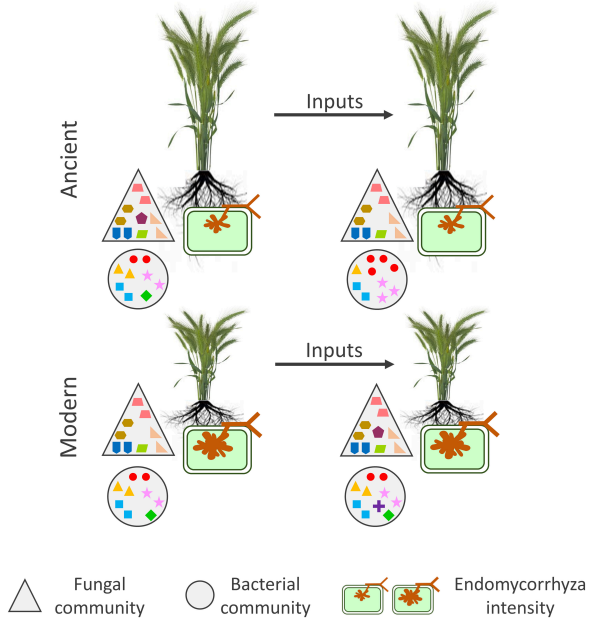

FIGURE 6 | Summary picture of the main effects detected by PERMANOVA on the alpha-diversity indices and mycorrhizal colonization parameters. The figure depicts ancient (tall plants) and modern (short plants) rhizosphere microbiota with and without inputs. The big triangles and circles depict the fungal and bacterial communities, respectively. The mycorrhiza is depicted as a green cell with an arbuscular structure inside. The symbols inside the big triangles and circles represent OTUs. PERMANOVA results are shown in **Table 2**. Only results from G, E, and G x E are shown. For the fungal community, input addition led to slight reduction in estimated richness for the ancient varieties and slight increase for the modern varieties. For the bacterial community, inputs reduced the richness and evenness for the ancient varieties but led to slight increase in richness for the modern varieties. For the mycorrhiza, the modern varieties had more pronounced colonization than the ancient varieties.

bacterial community structure between modern (five varieties) and ancient (three varieties) breeding types (Kavamura et al., 2020). However, small effects like ours were already observed with domestication (from wild relatives to cultivated varieties) (Özkurt et al., 2020; Spor et al., 2020) likely associated with a "relaxed" selective force (Hassani et al., 2020). In addition, a very strong effect of breeding was noticed on the structure of the rhizosphere microbiota network, featuring common but also specific OTUs of modern or ancient varieties. For the modern varieties, the organization was less complex than for the ancient ones. The fact that fewer keystone nodes were detected in the modern network, with clear centralization around *Lectera longa*, could be interpreted as a potential weakness in terms of stability if that one node was to be lost. Noteworthy, while the ancient network had several keystone OTUs, the modern network only had one keystone Lectera OTU. This genus contains crop pathogens (Cannon et al., 2012; Ares et al., 2021) and their abundance was shown to be an important predictor of wheat yield (Yergeau et al., 2020). As for the literature and our study, there is no consensus on the impact of plant breeding on rhizosphere microbiota diversity. A decrease in the diversity of symbiotic rhizobia associations was reported in domesticated legumes (Kim et al., 2014; Sangabriel-Conde et al., 2015). Mutch and Young (2004) reported limited interactions with symbionts in domesticated pea and broad bean compared with wild relatives in non-agricultural soil without inputs. Some studies found more nuanced results: Leff et al. (2017) reported domestication effects on the fungal rhizosphere community of sunflowers but not bacteria. Brisson et al. (2019) reported no effect on diversity but differences in co-occurrence networks among inbred maize lines, modern hybrids, and teosinte. Finally, Kinnunen-Grubb et al. (2020) reported faster bacterial colonization in the rhizosphere of modern wheat cultivars than in that of ancestors, potentially due to the relaxed ability of modern varieties to select beneficial microbial partners (Kiers and Denison, 2008) *via* the notable changes in root exudate complexity (Pérez-Jaramillo et al., 2017). Our results concur with this interpretation, as the ancient varieties were enriched with specific bacterial and fungal taxa together with a more complex network structure featuring more keystone nodes, unlike the modern ones that had higher diversity but lesser keystones, indicating that their selective force was potentially relaxed. Similarly, Kiers et al. (2007) showed that ancient soybean varieties were more performant in maintaining high seed production when infected with a mixture of effective and ineffective rhizobium strains, unlike modern ones. However, a meta-analysis on the effect of breeding on mycorrhizal association found that modern varieties (> 1950) were more responsive in terms of increased biomass than old varieties (1900–1950) and ancestors (< 1900) (Lehmann et al., 2012). Thus, the fact that modern varieties establish either adaptive or non-adaptive interactions with soil microbiota is still an open question (refer to Ghalambor et al., 2007).

Effects of the Environment on Rhizosphere Microbiota

The presence/absence of inputs (E) had a marginal impact compared to the other effects (**Supplementary Table 7**) likely due to the narrow range of environmental conditions covered in our study (fixed pedo-climatic conditions, with or without inputs). The abundance of several OTUs was altered by inputs (up to 55.7 fold increase with inputs compared to no inputs, and only up to 4.6 fold increase without inputs compared to inputs). This weak effect might be explained by several reasons, including the preceding crop, soil fertility, application frequencies, and doses. The preceding crop was a legume (*Vicia faba*), which may have left sufficient organic nitrogen in the soil to hide our mineral fertilization effect. Regarding soil fertility, a study reports shifts in bacterial community composition only in soils with low C and N concentrations (Ramirez et al., 2010, 2012). Since the C and N concentrations in our soil presented a medium value (26.7 $g.kg^{-1}$ organic carbon and 2.11 $g.kg^{-1}$ total nitrogen), nitrogen was likely not a limiting factor. Likewise, the effects of inputs on rhizosphere microbiota become noticeable when the treatments were repeated several times (Yang et al., 2012; Schlatter et al., 2017) or when the doses were increased (Kavamura et al., 2018; Chen et al., 2019). Since our purpose was to match local agricultural practices in terms of products and doses, this

might explain the observed weak effects. When noted, the effect of inputs was negative on microbial communities in terms of bacterial and fungal evenness, as well as mycorrhizal colonization intensity (likely without functional consequence since arbuscular development was maintained). The results are in line with the literature (Dunn et al., 2021) and support our second hypothesis that the presence of inputs decreases, although slightly, the microbial diversity in the rhizosphere. This decrease in diversity was expected for several reasons. First, the addition of fertilizers can change bacterial communities. Grunert et al. (2019) reported that the addition of an inorganic fertilizer reduced the diversity of tomato rhizosphere microbiota. Second, the effect of fungicide could have suppressed some fungal taxa. Although supposed to target specific fungal pathogens, fungicides may impact the entire rhizosphere fungal community (Esmaeili Taheri et al., 2015). Furthermore, some fungi could benefit from the decreased abundance of dominant species, thus increasing community evenness. Third, we speculated that herbicide application could have reduced microbial diversity by impacting microorganisms associated with weed plant species.

Effects of Phenotypic Plasticity on Rhizosphere Microbiota

We advocate that the lack of consensus in the literature regarding the effect of plant domestication and recent breeding efforts on plant-microbiota association might partly stem from the interaction between genotype and the environment. Indeed, differences in microbiota diversity between modern and ancient varieties can depend on input application. Phenotypic plasticity, a ubiquitous aspect of organisms, describes the ability of a genotype to produce different phenotypes in response to environmental variations (Gause, 1947; Bradshaw, 1965). Variations in the morphology, immunity, or exudation of a given genotype influence the rhizosphere, seen here as an "extended phenotype" (de la Fuente Cantó et al., 2020) or the "microbiota as a phenotype" (Oyserman et al., 2021). However, changes in the environment such as input applications could influence soil microbiota and lead to the recruitment of different rhizosphere microbiota. Indeed, we found that phenotypic plasticity, the G × E interaction, had an important impact on plant-microbiota relationships. It was, after breeding type, the second most structuring force (**Supplementary Table 7**) and could have potentially been higher provided that a wider range of environmental conditions was investigated. For bacterial alpha diversity, the effect of phenotypic plasticity (5.7%) was in the same range as the breeding type (7.4%), while for fungi, the breeding type had no effect, whereas phenotypic plasticity was significant and relatively important (10.5%). The ancient varieties had a decreased bacterial and fungal diversity due to inputs, whereas the modern varieties were not affected. Furthermore, the presence of core fractions uniquely detected in each G × E modalities reinforces the idea that a real interaction occurred. This was particularly true for Glomeromycota, as previously reported by Lehmann et al. (2012), whose occurrence in our core fractions of breeding types depended on inputs. Furthermore, the discriminant analysis revealed that phenotypic plasticity was altering the same number of OTUs than breeding type, especially between modern varieties with inputs compared to ancient varieties without inputs. This was obvious with OTU_3503, a keystone of the ancient network, whose abundance in the rhizosphere was further decreased by the interaction of breeding and inputs. Thus, the G × E interaction was important in understanding the variations of microbial diversity, validating our third hypothesis that the effects of the recent selection efforts on microbiota diversity depend on the presence of inputs. However, phenotypic plasticity had no impact on mycorrhizal colonization or on the beta diversity of bacterial and fungal communities. Cases of interaction between genotype and environment were reported for other plant species and traits (e.g., maize yield variations across North America: $G = 7\%$, $E = 43\%$, and $G \times E = 6\%$; Gage et al., 2017). Regarding plant-microbiota interactions, G × E was shown to affect the phyllosphere, and to a lesser extent, the rhizosphere microbiota of *Boechera stricta* (Brassicaceae), with stronger effects on evenness than the genotype itself (Wagner et al., 2016). Although not referring to phenotypic plasticity, a study on domestication reported that the fungal community of a wild rice relative was more affected by a fungicide than a cultivated one (Shi et al., 2019), which is consistent with our results. This lower sensitivity of microbiota to the effect of inputs with modern varieties could be explained either by an ecological or a genetic mechanism. In the light of our results and those from Shi et al. (2019), the fungicide treatment might explain that phenotypic plasticity is detrimental to fungi in the ancient varieties but not in the modern varieties perhaps because of the more easily degradable exudates released in the rhizosphere of the modern varieties (Pérez-Jaramillo et al., 2016, 2018). However, since the bacterial community was also affected by phenotypic plasticity, we cannot exclude that plasticity was due to genetic difference: our discriminant OTU analysis suggests that the modern varieties could have lost their ability to regulate rhizosphere microbiota according to soil fertility, which changed with the addition of fertilizer. The lack of regulation in modern varieties is coherent with the reported relaxed selective force they exert on their rhizosphere microbiota (Kiers et al., 2007; Hassani et al., 2020). In that regard, our sequencing results revealed that G × E was responsible for the differential recruitment of unique OTUs among the Glomeromycora phylum, which was more pronounced in the modern varieties with inputs. While likely without functional consequences based on our microscopic mycorrhizal observations, this might indicate that the relaxed selection of the modern varieties is accentuated with inputs. Since they were selected with inputs, the modern varieties might have experienced a lower range of variation in soil fertility than the ancient ones. This modified regulation in plant-microbiota interaction is consistent with results from Gage et al. (2017), showing that variation in phenotypic plasticity is disproportionately controlled by regulatory genes compared to other traits. To prevent the environmental impacts of agriculture, incentives to reduce chemical inputs are increasing. From that perspective, the choice of varieties that promote intrinsic microbial community properties such as richness and evenness is an important lever (Bakker et al., 2012). As reports on the importance of the interaction between genotype and environment on plant microbiota increase, it is high time to put emphasis on plant and microbe genes involved in phenotypic

plasticity, for instance through breeding programs. This could allow for the selection of varieties without *a priori* on agricultural practices they will be exposed to, especially regarding synthetic inputs. This perspective is realistic since genes responsible for yield (i.e., mean trait value) and phenotypic plasticity (i.e., variance) are distinct (Gage et al., 2017), theoretically enabling their concomitant selection by breeders to spawn plastic varieties with enhanced reaction capacity toward a changing environment while maintaining decent yields (Kusmec et al., 2017).

DATA AVAILABILITY STATEMENT

The raw sequence data used in this study has been deposited to the SRA (Sequence Read Archive), https://www.ncbi.nlm.nih.gov/sra, with the following accession numbers: Bacteria: PRJNA701534, Fungi: PRJNA702900. Any further queries should be directed to the corresponding author.

AUTHOR CONTRIBUTIONS

MB conceived the research. EP, CD, and MB carried out the experiment. DW, LC, and TR did the mycorrhiza observations. SJ dealt with the bioinformatics and statistical analyses and edited the figures and tables. MB wrote the article, with significant contribution of SJ. All authors contributed to the article and approved the submitted version.

FUNDING

SJ was funded by the University of Bourgogne Franche-Comté *via* an ISITE-BFC International Junior Fellowship award (AAP3:RA19028.AEC.IS). The salary of TR was funded by the Bourgogne Franche-Comté region via the FABER program (grant no. 2017-9201AAO049S01302).

ACKNOWLEDGMENTS

We thank Institut Agro Dijon for the experiment facilities. We are grateful to Jean-Philippe Guillemin, Wilfried Queyrel, and Etienne Gaujour for their advice on wheat culture and the management of the experimental site and Jacques Le Gouis and François Balfourier for providing information on the origins of the ancient varieties. We thank Tariq Shah for his contribution to the bibliographical search. We also thank Graines de Noé and, especially, Hélène Montaz for providing seeds of the ancient varieties, as well as RAGT Semences, Secobra, Saaten Union, and Limagrain for providing the modern varieties.

SUPPLEMENTARY MATERIAL

The Supplementary Material for this article can be found online at: https://www.frontiersin.org/articles/10.3389/fevo.2022.903008/full#supplementary-material

REFERENCES

Ai, C., Liang, G., Sun, J., Wang, X., He, P., Zhou, W., et al. (2015). Reduced dependence of rhizosphere microbiome on plant-derived carbon in 32-year long-term inorganic and organic fertilized soils. *Soil Biol. Biochem.* 80, 70–78. doi: 10.1016/j.soilbio.2014.09.028

An, G. H., Kobayashi, S., Enoki, H., Sonobe, K., Muraki, M., Karasawa, T., et al. (2010). How does arbuscular mycorrhizal colonization vary with host genotype? An example based on maize (*Zea* mays) germplasms. *Plant Soil* 327, 441–453. doi: 10.1007/s11104-009-0073-3

Ares, A., Costa, J., Joaquim, C., Pintado, D., Santos, D., Monika, M., et al. (2021). Effect of Low-Input Organic and Conventional Farming Systems on Maize Rhizosphere in Two Portuguese Open-Pollinated Varieties (OPV), "Pigarro" (Improved Landrace) and "SinPre" (a Composite Cross Population). *Front. Microbiol.* 12:636009. doi: 10.3389/fmicb.2021.636009

Baker, G. C., Smith, J. J., and Cowan, D. A. (2003). Review and re-analysis of domain-specific 16S primers. *J. Microbiol. Methods* 55, 541–555. doi: 10.1016/j.mimet.2003.08.009

Bakker, M. G., Manter, D. K., Sheflin, A. M., Weir, T. L., and Vivanco, J. M. (2012). Harnessing the rhizosphere microbiome through plant breeding and agricultural management. *Plant Soil* 360, 1–13. doi: 10.1007/s11104-012-1361-x

Berendsen, R. L., Pieterse, C. M. J., and Bakker, P. (2012). The rhizosphere microbiome and plant health. *Trends Plant Sci.* 17, 478–486. doi: 10.1016/j.tplants.2012.04.001

Berry, D., and Widder, S. (2014). Deciphering microbial interactions and detecting keystone species with co-occurrence networks. *Front. Microbiol.* 5:219. doi: 10.3389/fmicb.2014.00219

Bradshaw, A. D. (1965). Evolutionary significance of phenotypic plasticity in plants. *Adv. Genet.* 13, 115–155. doi: 10.1016/S0065-2660(08)60048-6

Brisson, V. L., Schmidt, J. E., Northen, T. R., Vogel, J. P., and Gaudin, A. C. (2019). Impacts of maize domestication and breeding on rhizosphere microbial community recruitment from a nutrient depleted agricultural soil. *Sci. Rep.* 9, 1–14. doi: 10.1038/s41598-019-52148-y

Bulgarelli, D., Garrido-Oter, R., Münch, P. C., Weiman, A., Dröge, J., Pan, Y., et al. (2015). Structure and function of the bacterial root microbiota in wild and domesticated barley. *Cell Host Microbe* 17, 392–403. doi: 10.1016/j.chom.2015.01.011

Cangioli, L., Mancini, M., Napoli, M., Fagorzi, C., Orlandini, S., Vaccaro, F., et al. (2022). Differential Response of Wheat Rhizosphere Bacterial Community to Plant Variety and Fertilization. *Int. J. Mol. Sci.* 23:3616. doi: 10.3390/ijms23073616

Cannon, P. F., Buddie, A. G., Bridge, P. D., Neergaard, E. D., Lübeck, M., and Askar, M. M. (2012). Lectera, a new genus of the Plectosphaerellaceae for the legume pathogen Volutella colletotrichoides. *MycoKeys* 3:28. doi: 10.3897/mycokeys.3.3065

Chaluvadi, S., and Bennetzen, J. L. (2018). Species-associated differences in the below-ground microbiomes of wild and domesticated Setaria. *Front. Plant Sci.* 9:1183. doi: 10.3389/fpls.2018.01183

Chen, S., Waghmode, T. R., Sun, R., Kuramae, E. E., Hu, C., and Liu, B. (2019). Root-associated microbiomes of wheat under the combined effect of plant development and nitrogen fertilization. *Microbiome* 7:136. doi: 10.1186/s40168-019-0750-2

Chiquet, J., Robin, S., and Mariadassou, M. (2019). "Variational inference for sparse network reconstruction from count data," in *International Conference on Machine Learning*, eds K. Chaudhuri, and R. Salakhutdinov (Long Beach, CA: PMLR), 1162–1171.

Chowdhury, S. P., Babin, D., Sandmann, M., Jacquiod, S., Sommermann, L., Sørensen, S. J., et al. (2019). Effect of long-term organic and mineral fertilization strategies on rhizosphere microbiota assemblage and performance of lettuce. *Environ. Microbiol.* 21, 1462–2920. doi: 10.1111/1462-2920.14631

Csardi, G., and Nepusz, T. (2006). The igraph software package for complex network research. *InterJ. Complex Syst.* 1695, 1–9.

Danchin, É, Charmantier, A., Champagne, F., Mesoudi, A., Pujol, B., and Blanchet, S. (2011). Beyond DNA: integrating inclusive inheritance into an extended theory of evolution. *Nat. Rev. Genet.* 12, 475–486. doi: 10.1038/nrg3028

de la Fuente Cantó, C., Simonin, M., King, E., Moulin, L., Bennett, M. J., Castrillo, G., et al. (2020). An extended root phenotype: the rhizosphere, its formation and impacts on plant fitness. *Plant J.* 103, 951–964. doi: 10.1111/tpj.14781

de Mendiburu, F., and Yaseen, M. (2020). *agricolae: Statistical Procedures for Agricultural Research". R package version 1.4.0*. Available Online at: https://myaseen208.com/agricolae/

Deng, S., Caddell, D. F., and Coleman-Derr, D. (2021). Genome wide association study reveals plant loci controlling heritability of the rhizosphere microbiome. *ISME J.* 15, 3181–3194. doi: 10.1038/s41396-021-00993-z

Dixon, P. (2003). VEGAN, a package of R functions for community ecology. *J. Veg. Sci.* 14, 927–930. doi: 10.1111/j.1654-1103.2003.tb02228.x

Dunn, L., Lang, C., Marilleau, N., Terrat, S., Biju-Duval, L., Lelièvre, M., et al. (2021). Soil microbial communities in the face of changing farming practices: a case study in an agricultural landscape in France. *PLoS One* 16:e0252216. doi: 10.1371/journal.pone.0252216

Egerton-Warburton, L. M., Johnson, N. C., and Allen, E. B. (2007). Mycorrhizal community dynamics following nitrogen fertilization: a cross-site test in five grasslands. *Ecol. Monogr.* 77, 527–544. doi: 10.1890/06-1772.1

Esmaeili Taheri, A., Hamel, C., and Gan, Y. (2015). Pyrosequencing reveals the impact of foliar fungicide application to chickpea on root fungal communities of durum wheat in subsequent year. *Fungal Ecol.* 15, 73–81. doi: 10.1016/j.funeco.2015.03.005

Estensmo, E. L. F., Sundy, M., Morgado, L., Martin-Sanchez, P. M., Skrede, I., and Kauserud, H. (2021). The influence of intraspecific sequence variation during DNA metabarcoding: a case study of eleven fungal species. *Mol. Ecol. Resour.* 21, 1141–1148. doi: 10.1111/1755-0998.13329

Falconer, D. S. (1989). *Introduction to Quantitative Genetics*. London, UK: Longman.

Gage, J. L., Jarquin, D., Romay, C., Lorenz, A., Buckler, E. S., Kaeppler, S., et al. (2017). The effect of artificial selection on phenotypic plasticity in maize. *Nat. Commun.* 8:1348. doi: 10.1038/s41467-017-01450-2

Gause, G. F. (1947). Problems of evolution. *Trans. Conn. Acad. Arts Sci.* 37, 17–68.

Geisseler, D., and Scow, K. M. (2014). Long-term effects of mineral fertilizers on soil microorganisms - A review. *Soil Biol. Biochem.* 75, 54–63. doi: 10.1016/j.soilbio.2014.03.023

Ghalambor, C. K., McKay, J. K., Carroll, S. P., and Reznick, D. N. (2007). Adaptive versus non-adaptive phenotypic plasticity and the potential for contemporary adaptation in new environments. *Funct. Ecol.* 21, 394–407. doi: 10.1111/j.1365-2435.2007.01283.x

Grunert, O., Robles-Aguilar, A. A., Hernandez-Sanabria, E., Schrey, S. D., Reheul, D., Van Labeke, M. C., et al. (2019). Tomato plants rather than fertilizers drive microbial community structure in horticultural growing media. *Sci. Rep.* 9, 1–15. doi: 10.1038/s41598-019-45290-0

Hassani, M. A., Özkurt, E., Franzenburg, S., and Stukenbrock, E. H. (2020). Ecological Assembly Processes of the Bacterial and Fungal Microbiota of Wild and Domesticated Wheat Species. *Phytobiomes J.* 4, 217–224. doi: 10.1094/PBIOMES-01-20-0001-SC

Herlemann, D. P., Labrenz, M., Jurgens, K., Bertilsson, S., Waniek, J. J., and Andersson, A. F. (2011). Transitions in bacterial communities along the 2000 km salinity gradient of the Baltic Sea. *ISME J.* 5, 1571–1579. doi: 10.1038/ismej.2011.41

Hetrick, B. A. D., Wilson, G. W. T., and Cox, T. S. (1992). Mycorrhizal dependence of modern wheat varieties, landraces, and ancestors. *Can. J. Bot.* 70, 2032–2040. doi: 10.1139/b92-253

Hu, L., Robert, C. A. M., Cadot, S., Zhang, X., Ye, M., Li, B., et al. (2018). Root exudate metabolites drive plant-soil feedbacks on growth and defense by shaping the rhizosphere microbiota. *Nat. Commun.* 9:2738. doi: 10.1038/s41467-018-05122-7

Ihrmark, K., Bödeker, I. T. M., Cruz-Martinez, K., Friberg, H., Kubartova, A., Schenck, J., et al. (2012). New primers to amplify the fungal ITS2 region – evaluation by 454-sequencing of artificial and natural communities. *FEMS Microbiol. Ecol.* 82, 666–677. doi: 10.1111/j.1574-6941.2012.01437.x

Jacquiod, S., Puga-Freitas, R., Spor, A., Mounier, A., Monard, C., Mougel, C., et al. (2020). A core microbiota of the plant-earthworm interaction conserved across soils. *Soil Biol. Biochem.* 144:107754. doi: 10.1016/j.soilbio.2020.107754

Jacquiod, S., Spor, A., Wei, S., Munkager, V., Bru, D., Sørensen, S. J., et al. (2022). Artificial selection of stable rhizosphere microbiota leads to heritable plant phenotype changes. *Ecol. Lett.* 25, 189–201. doi: 10.1111/ele.13916

Kapulnik, Y., and Kushnir, U. (1991). Growth dependency of wild, primitive and modern cultivated wheat lines on vesicular-arbuscular mycorrhiza fungi. *Euphytica* 56, 27–36. doi: 10.1007/BF00041740

Kavamura, V. N., Hayat, R., Clark, I. M., Rossmann, M., Mendes, R., Hirsch, P. R., et al. (2018). Inorganic Nitrogen Application Affects Both Taxonomical and Predicted Functional Structure of Wheat Rhizosphere Bacterial Communities. *Front. Microbiol.* 9:1074. doi: 10.3389/fmicb.2018.01074

Kavamura, V. N., Robinson, R. J., Hughes, D., Clark, I., Rossmann, M., Soares de Melo, I., et al. (2020). Wheat Dwarfing Influences Selection of the Rhizosphere Microbiome. *Sci. Rep.* 10:1452. doi: 10.1038/s41598-020-58402-y

Kiers, E. T., and Denison, R. F. (2008). Sanctions, cooperation, and the stability of plant-rhizosphere mutualisms. *Annu. Rev. Ecol. Evol. Syst.* 39, 215–236. doi: 10.1146/annurev.ecolsys.39.110707.173423

Kiers, E. T., Hutton, M. G., and Denison, R. F. (2007). Human selection and the relaxation of legume defences against ineffective rhizobia. *Proc. R. Soc. B Biol. Sci.* 274, 3119–3126. doi: 10.1098/rspb.2007.1187

Kim, B. H., Ramanan, R., Cho, D. H., Oh, H. M., and Kim, H. S. (2014). Role of Rhizobium, a plant growth promoting bacterium, in enhancing algal biomass through mutualistic interaction. *Biomass Bioenergy* 69, 95–105. doi: 10.1016/j.biombioe.2014.07.015

Kinnunen-Grubb, M., Sapkota, R., Vignola, M., Nunes, I. M., and Nicolaisen, M. (2020). Breeding selection imposed a differential selective pressure on the wheat root-associated microbiome. *FEMS Microbiol. Ecol.* 96:fiaa196. doi: 10.1093/femsec/fiaa196

Kusmec, A., Srinivasan, S., Nettleton, D., and Schnable, P. S. (2017). Distinct genetic architectures for phenotype means and plasticities in Zea mays. *Nat. Plants* 3, 715–723. doi: 10.1038/s41477-017-0007-7

Laitinen, R. A. E., and Nikoloski, Z. (2019). Genetic basis of plasticity in plants. *J. Exp. Bot.* 70, 739–745. doi: 10.1093/jxb/ery404

Lambers, H., Mougel, C., Jaillard, B., and Hinsinger, P. (2009). Plant-microbe-soil interactions in the rhizosphere: an evolutionary perspective. *Plant Soil* 321, 83–115. doi: 10.3389/fpls.2021.636709

Lebeis, S. L., Paredes, S. H., Lundberg, D. S., Breakfield, N., Gehring, J., McDonald, M., et al. (2015). Salicylic acid modulates colonization of the root microbiome by specific bacterial taxa. *Science* 349, 860–864. doi: 10.1126/science.aaa8764

Leff, J. W., Lynch, R. C., Kane, N. C., and Fierer, N. (2017). Plant domestication and the assembly of bacterial and fungal communities associated with strains of the common sunflower. *New Phytol.* 214, 412–423. doi: 10.1111/nph.14323

Lehmann, A., Barto, E. K., Powell, J. R., and Rillig, M. C. (2012). Mycorrhizal responsiveness trends in annual crop plants and their wild relatives-a meta-analysis on studies from 1981 to 2010. *Plant Soil* 355, 231–250. doi: 10.1007/s11104-011-1095-1

Leiser, W. L., Olatoye, M. O., Rattunde, H. F. W., Neumann, G., Weltzien, E., and Haussmann, B. I. (2016). No need to breed for enhanced colonization by arbuscular mycorrhizal fungi to improve low-P adaptation of West African sorghums. *Plant Soil* 401, 51–64. doi: 10.1007/s11104-015-2437-1

Lemanceau, P., Blouin, M., Muller, D., and Moënne-Loccoz, Y. (2017). Let the core microbiota be functional. *Trends Plant Sci.* 22, 583–595. doi: 10.1016/j.tplants.2017.04.008

Lundberg, D. S., Lebeis, S. L., Paredes, S. H., Yourstone, S., Gehring, J., Malfatti, S., et al. (2012). Defining the core Arabidopsis thaliana root microbiome. *Nature* 488, 86–90. doi: 10.1038/nature11237

Mendes, R., Kruijt, M., de Bruijn, I., Dekkers, E., van der Voort, M., Schneider, J. H. M., et al. (2011). Deciphering the rhizosphere microbiome for disease-suppressive bacteria. *Science* 332, 1097–1100. doi: 10.1126/science.1203980

Milla, R., Osborne, C. P., Turcotte, M. M., and Violle, C. (2015). Plant domestication through an ecological lens. *Trends Ecol. Evol.* 30, 463–469. doi: 10.1016/j.tree.2015.06.006

Mutch, L. A., and Young, J. P. W. (2004). Diversity and specificity of Rhizobium leguminosarumbiovar viciae on wild and cultivated legumes. *Mol. Ecol.* 13, 2435–2444. doi: 10.1111/j.1365-294X.2004.02259.x

Oyserman, B. O., Cordovez, V., Flores, S. S., Leite, M. F. A., Nijveen, H., Medema, M. H., et al. (2021). Extracting the GEMs:Genotype, Environment,and Microbiome Interactions ShapingHost Phenotypes. *Front. Microbiol.* 11:574053. doi: 10.3389/fmicb.2020.574053

Özkurt, E., Hassani, M. A., Sesiz, U., Künzel, S., Dagan, T., Özkan, H., et al. (2020). Seed-Derived Microbial Colonization of Wild Emmer and Domesticated Bread Wheat (*Triticum dicoccoides* and *T. aestivum*) Seedlings Shows Pronounced Differences in Overall Diversity and Composition. *mBio* 11:e02637–20. doi: 10.1128/mBio.02637-20

Peiffer, J. A., Spor, A., Koren, O., Jin, Z., Tringe, S. G., Dangl, J. L., et al. (2013). Diversity and heritability of the maize rhizosphere microbiome under field conditions. *Proc. Natl. Acad. Sci. U.S.A.* 110, 6548–6553. doi: 10.1073/pnas.1302837110

Pérez-Jaramillo, J. E., Carrión, V. J., Bosse, M., Ferrão, L. F., de Hollander, M., Garcia, A. A. F., et al. (2017). Linking rhizosphere microbiome composition of wild and domesticated Phaseolus vulgaris to genotypic and root phenotypic traits. *ISME J.* 11, 2244–2257. doi: 10.1038/ismej.2017.85

Pérez-Jaramillo, J. E., Carrión, V. J., de Hollander, M., and Raaijmakers, J. M. (2018). The wild side of plant microbiomes. *Microbiome* 6:143. doi: 10.1186/s40168-018-0519-z

Pérez-Jaramillo, J. E., Mendes, R., and Raaijmakers, J. M. (2016). Impact of plant domestication on rhizosphere microbiome assembly and functions. *Plant Mol. Biol.* 90, 635–644. doi: 10.1007/s11103-015-0337-7

Porter, S. S., and Sachs, J. L. (2020). Agriculture and the disruption of plant–microbial symbiosis. *Trends Ecol. Evol.* 35, 426–439. doi: 10.1016/j.tree.2020.01.006

R Core Team (2020). *R: A Language and Environment for Statistical Computing*. Vienna: R Foundation for Statistical Computing.

Ramirez, K. S., Craine, J. M., and Fierer, N. (2012). Consistent effects of nitrogen amendments on soil microbial communities and processes across biomes. *Glob. Chang. Biol.* 18, 1918–1927. doi: 10.1111/j.1365-2486.2012.02639.x

Ramirez, K. S., Lauber, C. L., Knight, R., Bradford, M. A., and Fierer, N. (2010). Consistent effects of nitrogen fertilization on soil bacterial communities in contrasting systems. *Ecology* 91, 3463–3470. doi: 10.1890/10-0426.1

Robinson, M. D., McCarthy, D. J., and Smyth, G. K. (2009). edgeR: a bioconductor package for differential expression analysis of digital gene expression data. *Bioinformatics* 26, 139–140. doi: 10.1093/bioinformatics/btp616

Sangabriel-Conde, W., Maldonado-Mendoza, I. E., Mancera-López, M. E., Cordero-Ramírez, J. D., Trejo-Aguilar, D., and Negrete-Yankelevich, S. (2015). Glomeromycota associated with Mexican native maize landraces in Los Tuxtlas, Mexico. *Appl. Soil Ecol.* 87, 63–71. doi: 10.1016/j.apsoil.2014.10.017

Schlatter, D. C., Yin, C., Hulbert, S., Burke, I., and Paulitz, T. (2017). Impacts of Repeated Glyphosate Use on Wheat-Associated Bacteria Are Small and Depend on Glyphosate Use History. *Appl. Environ. Microbiol.* 83:e01354–17. doi: 10.1128/AEM.01354-17

Schmalhausen, I. I. (1949). *Factors of Evolution: The Theory of Stabilizing Selection*. Philadelphia, PA: Blakiston.

Schöler, A., Jacquiod, S., Vestergaard, G., Schulz, S., and Schloter, M. (2017). Analysis of soil microbial communities based on amplicon sequencing of marker genes. *Biol. Fertil. Soils* 53, 485–489. doi: 10.1007/s00374-017-1205-1

Shannon, P., Markiel, A., Ozier, O., Baliga, N. S., Wang, J. T., Ramage, D., et al. (2003). Cytoscape: a software environment for integrated models of biomolecular interaction networks. *Genome Res.* 13, 2498–2504. doi: 10.1101/gr.1239303

Shi, S., Tian, L., Xu, S., Ji, L., Nasir, F., Li, X., et al. (2019). The rhizomicrobiomes of wild and cultivated crops react differently to fungicides. *Arch. Microbiol.* 201, 477–486. doi: 10.1007/s00203-018-1586-z

Smale, M. (1997). The Green Revolution and wheat genetic diversity: some unfounded assumptions. *World Dev.* 25, 1257–1269. doi: 10.1016/S0305-750X(97)00038-7

Sokal, R. R., and Rohlf, F. J. (1995). *Biometry: The Principles and Practice of Statistics in Biological Research*, 3rd Edn. New York, NY: W.H. Freeman.

Spor, A., Roucou, A., Mounier, A., Bru, D., Breuil, M. C., Fort, F., et al. (2020). Domestication-driven changes in plant traits associated with changes in the assembly of the rhizosphere microbiota in tetraploid wheat. *Scientific* 10:12234. doi: 10.1038/s41598-020-69175-9

Stearns, S. C. (1989). The evolutionary significance of phenotypic plasticity. *BioScience* 39, 436–445. doi: 10.2307/1311135

Szoboszlay, M., Lambers, J., Chappell, J., Kupper, J. V., Moe, L. A., and McNear, D. H. Jr. (2015). Comparison of root system architecture and rhizosphere microbial communities of Balsas teosinte and domesticated corn cultivars. *Soil Biol. Biochem.* 80, 34–44. doi: 10.1016/j.soilbio.2014.09.001

Trouvelot, A., Kough, J. L., and Gianinazzi-Pearson, V. (1986). "Mesure du taux de mycorhization VA d'un système radiculaire. Recherche de méthodes d'estimation ayant une signification fonctionnelle," in *Physiological and Genetical Aspects of Mycorrhizae. Proceedings of the 1st European Symposium on Mycorrhizae*, eds V. Gianinazzi-Pearson and S. Gianinazzi (Paris: Institut National de la Recherche Agronomique), 217–221.

Turcotte, M. M., Lochab, A. K., Turley, N. E., and Johnson, M. T. (2015). Plant domestication slows pest evolution. *Ecol. Lett.* 18, 907–915. doi: 10.1111/ele.12467

Vierheilig, H., Coughlan, A. P., Wyss, U., and Piché, Y. (1998). Ink and vinegar, a simple staining technique for arbuscular-mycorrhizal fungi. *Appl. Environ. Microbiol.* 64, 5004–5007. doi: 10.1128/AEM.64.12.5004-5007.1998

Voss-Fels, K. P., Stahl, A., Wittkop, B., Lichthardt, C., Nagler, S., Rose, T., et al. (2019). Breeding improves wheat productivity under contrasting agrochemical input level. *Nat. Plants* 5, 706–714. doi: 10.1038/s41477-019-0445-5

Wagner, M. R., Lundberg, D. S., Tijana, G., Tringe, S. G., Dangl, J. L., and Mitchell-Olds, T. (2016). Host genotype and age shape the leaf and root microbiomes of a wild perennial plant. *Nat. Commun.* 7, 1–15. doi: 10.1038/ncomms12151

Weese, D. J., Heath, K. D., Dentinger, B. T., and Lau, J. A. (2015). Long-term nitrogen addition causes the evolution of less-cooperative mutualists. *Evolution* 69, 631–642. doi: 10.1111/evo.12594

White, T., Bruns, T., and Lee, S. (1990). "Amplification and direct sequencing of fungal ribosomal RNA genes for phylogenetics," in *PCR Protocols: a Guide to Methods and Applications*, eds M. A. Innis, D. H. Gelfand, J. J. Sninsky, and T. White (London: Academic Press), 315–322. doi: 10.1016/B978-0-12-372180-8.50042-1

Yang, C., Hamel, C., Vujanovic, V., and Gan, Y. T. (2012). Non-target effects of foliar fungicide application on the rhizosphere: diversity of nifH gene and nodulation in chickpea field. *J. Appl. Microbiol.* 112, 966–974. doi: 10.1111/j.1365-2672.2012.05262.x

Yergeau, É, Quiza, L., and Tremblay, J. (2020). Microbial indicators are better predictors of wheat yield and quality than N fertilization. *FEMS Microbiol. Ecol.* 96:fiz205. doi: 10.1093/femsec/fiz205

Conflict of Interest: The authors declare that the research was conducted in the absence of any commercial or financial relationships that could be construed as a potential conflict of interest.

Publisher's Note: All claims expressed in this article are solely those of the authors and do not necessarily represent those of their affiliated organizations, or those of the publisher, the editors and the reviewers. Any product that may be evaluated in this article, or claim that may be made by its manufacturer, is not guaranteed or endorsed by the publisher.

frontiers | Frontiers in Ecology and Evolution

TYPE Perspective
PUBLISHED 25 August 2022
DOI 10.3389/fevo.2022.957708

OPEN ACCESS

EDITED BY
Joan Roughgarden,
Stanford University, United States

REVIEWED BY
Scott F. Gilbert,
University of Helsinki, Finland

*CORRESPONDENCE
Eugene Rosenberg
eros@tauex.tau.ac.il

SPECIALTY SECTION
This article was submitted to Coevolution, a section of the journal Frontiers in Ecology and Evolution

RECEIVED 31 May 2022
ACCEPTED 05 August 2022
PUBLISHED 25 August 2022

CITATION
Rosenberg E (2022) Rapid acquisition of microorganisms and microbial genes can help explain punctuated evolution. *Front. Ecol. Evol.* 10:957708. doi: 10.3389/fevo.2022.957708

Rapid acquisition of microorganisms and microbial genes can help explain punctuated evolution

Eugene Rosenberg[1,2]*

[1]Tel Aviv University, Tel Aviv, Israel, [2]Department of Biochemistry and Molecular Biology, The George S. Wise Faculty of Life Sciences, Tel Aviv University, Tel Aviv, Israel

The punctuated mode of evolution posits that evolution occurs in rare bursts of rapid evolutionary change followed by long periods of genetic stability (stasis). The accepted cause for the rapid changes in punctuated evolution is special ecological circumstances – selection forces brought about by changes in the environment. This article presents a complementary explanation for punctuated evolution by the rapid formation of genetic variants in animals and plants by the acquisition of microorganisms from the environment into microbiomes and microbial genes into host genomes by horizontal gene transfer. Several examples of major evolutionary events driven by microorganisms are discussed, including the formation of the first eukaryotic cell, the ability of some animals to digest cellulose and other plant cell-wall complex polysaccharides, dynamics of root system architecture, and the formation of placental mammals. These changes by cooperation were quantum leaps in the evolutionary development of complex bilolgical systems and can contribute to an understanding of the mechanisms underlying punctuated evolution.

KEYWORDS

holobiont, punctuated evolution, horizontal gene transfer, gene variation, placental mammals, hologenomes, microbiome

Introduction

The punctuated equilibrium mode of evolution, although first introduced by Simpson (1944), is generally attributed to the paleontologists Eldredge and Gould (Eldredge, 1971; Eldredge and Gould, 1972; Gould and Eldredge, 1977). Punctuated evolution posits genetic stability followed by rare bursts of rapid evolutionary change. Once a species appears in the fossil record, the population will become stable, showing little evolutionary change for most of its geological history. This state of little or no morphological change is called stasis. In contrast, phyletic gradualism is a more gradual, continuous model of evolution that occurs uniformly by the steady and slow transformation of whole lineages. Eldredge and Gould argued that the degree of gradualism, commonly attributed to Charles Darwin (Rhodes, 1983), is virtually nonexistent in the fossil record and that stasis dominates the history of most fossil

species. According to Gould and Eldredge (2016), "Phyletic gradualism was an *a priori* assertion from the start—it was never "seen" in the rocks; it expressed the cultural and political biases of 19th-century liberalism." More studies that are recent have provided support for the theory of punctuated evolution (Erwin and Anstey, 1995; Palmer et al., 2012; Cross et al., 2016; Gemmell et al., 2019; Schmidt and Wolf, 2021).

What is the accepted explanation for the bursts of rapid evolutionary change? The most common cause designated to the rapid changes in punctuated evolution is special ecological circumstances, which select specific genetic variants in the population (Rhodes, 1983). For example, when a species acquires a gene that allows it to exploit some feature of the changed or changing environment, such as a new environmental niche, the species may then show rapid changes in other traits as it adapts to this new niche (Milligan, 1986). Another example is extreme events, such as volcanism and asteroid impacts, which can be major drivers of evolutionary change by providing new niches (Grant et al., 2017).

This article presents complementary mechanisms for the understanding of punctuated evolution, derived from a consideration of the role of microorganisms in the evolution of animals and plants (Margulis, 1999; Margulis and Sagan, 2003; Rosenberg and Zilber-Rosenberg, 2018). Although never specifically referring to punctuated evolution, the symbiogenesis theory of Margulis posits that organisms come about primarily through the merger of separate organisms.

Punctuated evolution driven by acquisition of microorganisms

One of the most profound evolutionary events was the formation of the eukaryotic cell by the acquisition of one bacterium by another. Mitochondria and chloroplasts were probably formed by the acquisition of Alphaproteobacteria (Roger et al., 2017) and cyanobacteria (Ponce-Toledo et al., 2017), respectively. The nucleus of eukaryotic cells was possibly generated by the acquisition of an Archaea (Williams et al., 2020) or a virus (Takemura, 2020). Thus, it is generally accepted that eukaryotes were not formed by the slow process of mutation but, rather, by endosymbiosis, followed by the gradual conversion of the endosymbiont into an organelle. After the eukaryotic cell was formed, the acquisition of bacteria and viruses has continued to play a fundamental role in the evolution of eukaryotes to this day. Today, all eukaryotes (plants and animals) are not individuals but complex systems referred to as holobionts, composed of the host and myriad microorganisms living on or in them.

Prokaryotes were on this planet for 2.1 billion years before there were any animals or plants (Mikhailovsky and Gordon, 2021). During this time, they evolved enormous biochemical diversity and split into two domains: Bacteria and Archaea. Mutation and evolution in prokaryotes is much faster than in eukaryotes because they are haploid single cells, they multiply rapidly, and they readily exchange genetic information (Pepper, 2014). Animals and plants come into random contact with billions of microorganisms during their lifetime *via* air, water, and through interaction with organic and inorganic surfaces. Occasionally, some of these microbes find a niche and, under appropriate conditions, amplify on or in the host and affect the phenotype of the holobiont. Unlike mutation, which causes changes in existing genomes, the acquisition of a microbe introduces thousands of new genes into the holobiont. This way, rather than reinventing the wheel, animals and plants can acquire pre-evolved genetic information in the form of microbes. It is likely that, after the microbe is acquired, mutations and selection occur in both the microbe and host to optimize the interaction.

A major evolutionary event driven by the acquisition of microbes was the ability of some animals to digest cellulose and other plant cell-wall-complex polysaccharides. With few exceptions (Sharma et al., 2016), animal genomes do not code for the synthesis of cellulose-degrading enzymes. Instead, animals such as ruminants and termites rely totally on anaerobic cellulolytic microorganisms that are present in the internal space of their digestive tract. How did they gain access to these specialized microbes? It seems likely that at least some of the cellulose-degrading bacteria in ruminants originated from the consumption of grass, straw, and foliage that contained these bacteria on their surfaces (Sari et al., 2017). Gilbert (2020) discusses the ability of symbionts to promote development supporting the evolution of herbivory. It has been suggested that the first ruminant evolved in Southeast Asia about 50 million years ago from a small forest-dwelling omnivore, and, later, ruminants evolved from this original taxon (Hackmann and Spain, 2010).

Following the original acquisition of an anaerobic cellulose-degrading bacterium by a mammal, and, along the way, additional ones, there would be a strong selection for optimizing the interaction between the bacterium and the host, including changes in the host size, shape, internal organs, and teeth. These new adaptations helped ruminants leave more descendants and become one of the most widespread groups of large mammals they are today. A key point is that the evolution of ruminants was driven initially by the acquisition of cellulose-degrading bacteria. Large amounts of cellulose were already available in the environment as a selective force (Sarkar et al., 2009). The higher ruminants (Pecorans) are believed to have rapidly evolved in the Mid-Eocene, giving rise to five distinct extant families: Antilocapridae, Giraffidae, Moschidae, Cervidae, and Bovidae (Decker et al., 2009). The acquisition of cellulose-degrading bacteria made this rapid radiation possible.

Another example of how the acquisition of a microbial symbiont can lead to rapid evolution is the evolution and expansion of shallow-water scleractinian corals, following

the uptake of dinoflagellates roughly 240 million years ago (Frankowiak et al., 2016). The coral-dinoflagellate photosymbiosis allowed for growth in a nutrient-poor, low-productivity marine environment. Isotopic data support the role of photosymbiosis during the sudden Triassic expansion of coral reefs (Stanley, 2003). At present, we are living through a punctuated evolution event in the opposite direction. Global warming is causing disruption of coral symbioses, loss of coral reefs, and changed distributions of corals (Loya et al., 2001).

The acquisition of microorganisms not only played a crucial role in the emergence of chloroplasts, as discussed above but also in the continuing evolution of plants (Cordovez et al., 2019). One of the interesting contributions of microbiota to plants is the synthesis of the hormone auxin, indole-3-acetic acid. Auxin underpins plant development and growth (Frick and Strader, 2018). Bacteria and filamentous fungi, attached to roots in the rhizosphere, synthesize auxin (Wagi and Ahmed, 2019), which initiates several growth and developmental processes in plants, such as root hair and tip growth, formation of lateral roots, and the dynamics of root system architecture (Zamioudis et al., 2013). These auxin-producing microorganisms were, and probably still are, the driving force behind the evolution of plant synapses and other interactive behaviors of higher plants.

In conclusion, this section demonstrated that acquired beneficial microbes have the potential to be amplified and to spread rapidly to other holobionts in a manner similar to pathogen epidemics. This could accelerate the rate of adaptation and evolution of whole groups of holobionts. Such evolutionary changes by cooperation sometimes brought about quantum leaps in the development of biological complex systems. Gilbert (2019) has recently reviewed some of the literature on evolution by symbiosis but does not relate them to punctuated evolution.

Punctuated evolution driven by horizontal gene transfer

Horizontal gene transfer (HGT), also known as lateral gene transfer, refers to the movement of genetic material, and together with it genetic information across normal mating barriers, between more or less distantly related organisms. Thus, it differs from the standard vertical transmission of genes from parent to offspring. HGT enables the acquisition of novel traits *via* non-Mendelian inheritance of genetic material. HGT is generally associated with gene transfer between different types of bacteria and is a well-known and ubiquitous evolutionary mechanism in prokaryotes (Soucy et al., 2015; Kloub et al., 2021). An average of 81% of the genes in 181 sequenced prokaryotic genomes has been subject to HGT during the long history of prokaryotic evolution (Dagan et al., 2008). It was observed that HGT is more frequent than mutation in *E. coli* colonizing the mammalian gut (Frazão et al., 2019). Most prokaryotes possess different classes of mobile genetic elements that allow for the acquisition, loss, or rearrangement of sometimes large regions of their genome. Transposons, plasmids, genomic islands, and viruses, including bacteriophages, mediate HGT. One of the best-studied examples of HGT in bacteria is the evolution of antibiotic resistance (Maclean and San Millan, 2019). I would like to suggest that HGT could play a vital role in the genetic adaptation that is suggested to occur during punctuated evolution as a result of environmental changes. This can be achieved first by HGT between microorganisms within holobionts and, second, by HGT between these microorganisms and their host.

HGT between bacteria that are part of plant, animal, and human holobionts can bring about evolutionary change. For example, the ability of Far East Asian people to break down agar (an abundant ingredient in their diet since antiquity) originated from HGT between bacteria in their gut. Agar-decomposing genes, present in a marine bacterium, were transferred to a human gut bacterium, *Bacteroides plebeius*, by HGT as a result of eating food that contained raw seaweed (Hehemann et al., 2010). Although HGT usually occurs between bacteria in the same ecological niche, apparently the marine bacterium was present in the gut long enough to have some of its genes transferred to the resident gut bacterium. These genes code for the porphyranases that degrade the polysaccharide agarose of agar (Li et al., 2014). Westerners lack these enzymes and, therefore, cannot digest agar. The bacteria with the transferred genes spread throughout the Far East Asian population by vertical and horizontal transmission (Hehemann et al., 2012; Porter and Martens, 2017). This is an interesting example of a very fast, but minor, metabolic evolutionary change that could not be observed in fossil records.

The recent availability of a large number of high-quality sequences of fungus, plant, and animal genomes has led to the conclusion that HGT in these organisms has been more frequent events than observed previously (Li et al., 2018). It should be noted that the observable HGT events are probably only those occurring relatively late in evolutionary time scales since early ones are already masked by many genetic mutation events (Nielsen et al., 2014). Sixty sequenced fungal genomes contained 713 horizontally transferred genes from bacteria (Naranjo-Ortiz and Gabaldón, 2020). Invertebrate genomes contain numerous bacterial, fungal, and viral genes (reviewed by Drezen et al., 2017). For example, the genomes of 12 *Drosophila* species showed, on average, 40 foreign genes that had been horizontally transferred from bacteria and fungi (Crisp et al., 2015). When the *Drosophila* species were placed on a phylogenetic tree, there was a correspondence between the number of HGT events and the length of each branch, suggesting that HGT has occurred throughout *Drosophila* evolution and is likely to be ongoing (Serrato-Capuchina and Matute, 2018).

The evolutionary significance of HGT in plants has been reviewed by Wickell and Li (2020). Analysis of the 13.7-megabase genome of the extremophile red alga *Galdieria sulphuraria* indicated that 5% of its protein-coding genes were

acquired by HGT from bacteria and archaea (Schönknecht et al., 2013). Genomic data have uncovered that 57 gene families in the moss *Physcomitrella patens* genome were derived from prokaryotes, fungi, or viruses by HGT (Yue et al., 2012). Many of these genes are involved in essential or plant-specific activities, such as xylem formation, plant defense, nitrogen recycling, and the biosynthesis of starch, polyamines, hormones, and glutathione. Clearly, HGT has played an important role in the direction and the rate of evolution in plants (Ma et al., 2022).

Horizontally transferred genes can also be found in vertebrates (Dunning Hotopp, 2018). It was estimated that the human genome contains 1,467 HGT regions, involving 642 known genes (Huang et al., 2017). However, it is not clear when these HGT events took place. In one study, Crisp et al. (2015) reported that 145 human genes, which are not present in other primates, were probably attributed to HGT. The majority of the 145 genes identified in the study came from bacteria, but some originated from viruses and yeasts. Popov et al. (2019) have suggested that viruses and intracellular microbial pathogens were the modes of acquisition of bacterial genes into the human genome.

A major event in the evolution of mammals, the formation of placental mammals, which includes humans, was driven by the acquisition of the gene coding for the protein syncytin from a retrovirus by HGT (Dupressoir et al., 2012). It is assumed that the ancestor of placental mammals was solitary, seasonally breeding, insectivorous, and likely nocturnal (Wu et al., 2017). The original function of syncytin in such an ancestor was to allow retroviruses to fuse host cells so that they could move from one cell to another. Now, syncytin is necessary for the development of the placental syncytium, an essential part of the mother-fetus barrier. Endogenous retroviruses have been shown to be involved in placentation in various mammalian species Nakaya and Miyazawa, 2015; Hao et al., 2020, demonstrating that this event occurred a number of times during evolution. Moreover, recent molecular dating estimates for placental mammals echo fossil inferences for an explosive diversification about 76 million years ago (Halliday et al., 2015; Phillips and Fruciano, 2018). These data are consistent with the punctuated theory of evolution.

Discussion

Evolution depends both on a selective force and variants in the population that can benefit from this selected force. With regard to punctuated evolution, the rare bursts of rapid evolutionary change are generally attributed to extreme environmental events, such as large changes in temperature, and mass extinctions caused by volcanism or asteroid impact (Marshall, 2015; Grant et al., 2017). These extreme events set up strong selection pressures on organisms and are analogs of the dramatic changes documented in the fossil record. When an organism acquires a genetic variation that allows it to exploit some feature of the changed environment–a new environmental niche–the species may then show rapid changes in other traits as it adapts to this new niche (Milligan and Wood, 1986).

This article presents data demonstrating that the rate of formation of variants in the population can also help explain punctuated evolution. According to neo-Darwinian theory, formulated in the 1940s, genetic variation is ultimately generated by mutation (Hershberg, 2015; Ibraimov, 2020). However, evolving a novel function by mutation is a very slow process. For example, it was reported that laboratory adaptive evolution of *E. coli* to grow on a novel substrate, 1,2-propanediol, took ∼700 generations (Lee and Palsson, 2010), and the ability to grow on citrate required ∼31,000 generations (Lenski, 2017). One would expect that evolution by mutation in animals and plants would be much slower than in bacteria (Weller and Wu, 2015).

Acquisition of microorganisms from the environment and horizontal gene transfer bring forth underappreciated rapid modes of genetic variation (Zilber-Rosenberg and Rosenberg, 2021). Rather than "reinvent the wheel," holobionts have the ability to acquire genes and clusters of genes in a single step that initially evolved in microorganisms. If the acquisition provides a selective advantage to the holobiont, then it will multiply in the population by vertical and horizontal transfer and lead to the evolution of new species. Furthermore, changes in the composition of the microbiome have been shown to drive speciation in *Nasonia* wasps (Brucker and Bordenstein, 2013) and two house mice subspecies (Wang et al., 2015).

What is often not appreciated is that acquisition of microbiota can not only affect the metabolism of animals and plants but also their morphology. Examples include the hindgut of termites (Brune, 2014), rumen (Jami and Mizrahi, 2012), the squid eye organ (Nyholm and McFall-Ngai, 2004), and the nodule of legumes (Velázquez et al., 2017), In each of these examples, the morphology of the holobiont has undergone an evolutionary change while optimizing the interaction of the host with its microbiota for the benefit of the holobiont.

Cooperation is a fundamental property of all biological systems, from genes and cells to animals and societies. Evolutionary history can be viewed as a series of major transitions in which replicating units came together and formed new, more complex levels of biological organization (West et al., 2015). As examples, in this article, I discussed how eukaryotic cells were formed from the union of archaea and eubacteria, the formation of ruminants by the acquisition of cellulose-decomposing bacteria, the emergence of coral reefs by acquiring endosymbiotic algae, and the evolution of placental mammals by acquiring a viral gene. All of these examples would be expected to give rise to rapid evolution (punctuated evolution), even if they might not be observed directly in the fossil record.

In conclusion, the evidence described in this paper that the acquisition of microorganisms and microbial genes played an important role in the rapid evolution of animals and plants may contribute to a better understanding of the mechanisms underlying punctuated evolution. Finally, it should be noted that there are other mechanisms that have been suggested to play a role in punctuated evolution, including (i) regulatory gene evolution (Davidson, 2006; Tomoyasu et al., 2009), (ii) developmental plasticity wherein genes follow phenotypes (West-Eberhard, 2005; Standen et al., 2014), and (iii) stress-induced activation of cryptic genetic pathways (Love and Wagner, 2022). These mechanisms clearly contribute to specific examples of punctuated evolution. However, the major evolutionary events discussed in this article, the formation of eukaryotes, the ability of some animals to digest cellulose, and the formation of placental mammals are more readily understood by the acquisition of microbes and microbial genes.

Data availability statement

The original contributions presented in the study are included in the article/supplementary material, further inquiries can be directed to the corresponding author.

Author contributions

The author confirms being the sole contributor of this work and has approved it for publication.

Acknowledgments

The author thanks the Reviewer of this manuscript, Scott Gilbert, for his excellent criticisms and suggestions.

Conflict of interest

The author declares that the research was conducted in the absence of any commercial or financial relationships that could be construed as a potential conflict of interest.

Publisher's note

References

Brucker, R. M., and Bordenstein, S. R. (2013). Speciation by symbiosis. *Trends Ecol. Evol.* 27, 443–451. doi: 10.1016/j.tree.2012.03.011

Brune, A. (2014). Symbiotic digestion of lignocellulose in termite guts. *Nat. Rev. Microbiol* 12, 168–180. doi: 10.1038/nrmicro3182

Cordovez, V., Dini-Andreote, F., Carrión, V. J., et al. (2019). Ecology and evolution of plant microbiomes. *Annu. Rev. Microbiol* 73, 69–88. doi: 10.1146/annurev-micro-090817-062524

Crisp, A., Boschetti, C., Perry, M., Tunnacliffe, A., and Mickleme, G. (2015). Expression of multiple horizontally acquired genes is a hallmark of both vertebrate and invertebrate genomes. *Genome Biol.* 16, 50. doi: 10.1186/s13059-015-0607-3

Cross, W. C. H., Graham, T. A., and Wright, N. A. (2016). New paradigms in clonal evolution: punctuated equilibrium in cancer. *J. Pathol.* 240, 126–136. doi: 10.1002/path.4757

Dagan, T., Artzy-Randrup, Y., and Martin, W. (2008). Modular networks and cumulative impact of lateral transfer in prokaryote genome evolution. *Proc. Natl. Acad. Sci. USA* 105, 10039–10044. doi: 10.1073/pnas.0800679105

Davidson, E. H. (2006). *The Regulatory Genome: Gene Regulatory Networks in Development and Evolution*. San Diego: Academic Press.

Decker, J. E., Pires, J. C., Conant, G. C., and Taylor, J. F. (2009). Resolving the evolution of extant and extinct ruminants with high-throughput phylogenomics. *Proc. Natl. Acad. Sci. USA*. 1006, 18644–18649 doi: 10.1073/pnas.0904691106

Drezen, J. M., Gauthier, J., Josse, T., Bézier, A., Herniou, E., and Huguet, E. (2017). Foreign DNA acquisition by invertebrate genomes. *J. Invertebr. Pathol.* 147, 157–168. doi: 10.1016/j.jip.2016.09.004

Dunning Hotopp, J. C. D. (2018). Grafting or pruning in the animal tree: lateral gene transfer and gene loss?. *BMC Genom.* 19, 470. doi: 10.1186/s12864-018-4832-5

Dupressoir, A., Lavialle, C., and Heidmann, T. (2012). From ancestral infectious retroviruses to bona fide cellular genes: role of the captured syncytins in placentation. *Placenta.* 33, 663–671. doi: 10.1016/j.placenta.2012.05.005

Eldredge, N. (1971). The allopatric model and phylogeny in Paleozoic invertebrates. *Evolution* 25, 156–167. doi: 10.1111/j.1558-5646.1971.tb01868.x

Eldredge, N., and Gould, S. J. (1972). "Punctuatedequilibria: an alternative to phyletic gradualism," in *Models in Paleobiology*, eds Schopf, T. J. M. and Cooper, F., (Freeman Cooper: San Francisco, Calif). 82–115.

Erwin, D. H., and Anstey, R. L. (1995). "Speciation in the fossil record," in New Approaches to Speciation in the Fossil Record, eds Erwin, D. H. and Anstey, R. L. (New York: Columbia University Press), 11–39.

Frankowiak, K., Wang, X. T., Sigman, D. M., Gothmann, A. M., Kitahara, M. V., Mazur, M., et al. (2016). Photosymbiosis and the expansion of shallow-water corals. *Sci. Adv.* 2, e1601122. doi: 10.1126/sciadv.1601122

Frazão, N., Sousa, A., and Lässig, M. (2019). Horizontal gene transfer overrides mutation in *Escherichia coli* colonizing the mammalian gut. *Proc. Natl. Acad. Sci. USA* 116, 17906–17915. doi: 10.1073/pnas.1906958116

Frick, E. M., and Strader, L. C. (2018). Roles for IBA-derived auxin in plant development. *J. Exp. Bot.*69, 169–177. doi: 10.1093/jxb/erx298

Gemmell, M. R., Trewick, S. A., Hills, S. F. K., and Morgan-Richards, M. (2019). Phylogenetic topology and timing of New Zealand olive shells are consistent with punctuated equilibrium. *J. Zoo. Syst. Evol. Res.* 58, 209–220. doi: 10.1111/jzs.12342

Gilbert, S. F. (2019). Evolutionary transitions revisited: Holobiont evo-devo. *J. Exp. Zoo. Mol. Dev. Biol.* 332, 307–314. doi: 10.1002/jez.b.22903

Gilbert, S. F. (2020). Developmental symbiosis facilitates the multiple origins of herbivory. *Evol. Dev.* 22, 154–164. doi: 10.1111/ede.12291

Gould, S. J., and Eldredge, N. (1977). Punctuated equilibria: the tempo and mode of evolution reconsidered. *Paleobiology* 3, 115–151. doi: 10.1017/S0094837300005224

Gould, S. J., and Eldredge, N. (2016).*Punctuated Equilibria: The Tempo and Mode of Evolution Reconsidered*. Cambridge, UK: Cambridge University Press.

Grant, P. R., Grant, B. R., Huey, R. B., Johnson, M. T. J., Knoll, A. H., and Schmitt, J. (2017). Evolution caused by extreme events. *Phil.Trans. R. Soc. B* 372, 0146. doi: 10.1098/rstb.2016.0146

Hackmann, T. J., and Spain, J. N. (2010). Invited review: Ruminant ecology and evolution: Perspectives useful to ruminant livestock research and production. *J. Dairy Sci.* 93, 1320–1334. doi: 10.3168/jds.2009-2071

Halliday, T. J. D., Upchurch, P., and Goswami, A. (2015). Resolving the relationships of Paleocene placental mammals. *Biol. Rev.* 92, 521–550. doi: 10.1111/brv.12242

Hao, Y., Lee, H. J., Baraboo, M., Burch, K., Maurer, T., Somarelli, J. A., et al. (2020). Baby genomics: Tracing the evolutionary changes that gave rise to placentation. *Genome Biol. Evol.* 12, 35–47. doi: 10.1093/gbe/evaa026

Hehemann, J. H., Correc, G., Barbeyron, T., Helbert, W., Mirjam Czjzek, M., and Michel, G. (2010). Transfer of carbohydrate-active enzymes from marine bacteria to Japanese gut microbiota. *Nature* 464, 908–914. doi: 10.1038/nature08937

Hehemann, J. H., Kelly, A. G., Pudlo, N., and Borastonet, A. B. (2012). Bacteria of the human gut microbiome catabolize red seaweed glycans with carbohydrate-active enzyme updates from extrinsic microbes. *Proc. Natl. Acad. Sci. USA* 109, 19786–19791. doi: 10.1073/pnas.1211002109

Hershberg, R. (2015). Mutation–the engine of evolution: Studying mutation and its role in the evolution of bacteria. *Cold Spring Harb. Perspect. Biol.* 7, a018077. doi: 10.1101/cshperspect.a018077

Huang, J., Liang, X., Xuan, Y., Geng, C., Li, Y., Lu, H., et al. (2017). A reference human genome dataset of the BGISEQ-500 sequencer. *Gigascience.* 6, 1–9. doi: 10.1093/gigascience/gix024

Ibraimov,. A. I. (2020). Why the mechanisms of biological evolution are still not revealed? *Curr. Res. Biochem. Mol. Biol.* 1, 1–8. doi: 10.33702/crbmb.2020.1.1.1

Jami, E., and Mizrahi, I. (2012). Composition and similarity of bovine rumen microbiota across individual animals. *PLoS ONE* 7, e33306. doi: 10.1371/journal.pone.0033306

Kloub, L., Gosselin, S., Fullmer, M.,Graf, J., Gogarten, J. P., and Bansal, M. S. (2021). Systematic detection of large-scale multi-gene horizontal transfer in prokaryotes. *Mol. Biol. Evol.* 38, 2639–2659. doi: 10.1093/molbev/msab043

Lee, D.-H., and Palsson, B. O. (2010). Adaptive evolution of *Escherichia coli* K-12 MG1655 during growth on a nonnative carbon source, L-1,2-propanediol. *Appl. Environ. Microbiol.* 76, 4158–4168. doi: 10.1128/AEM.00373-10

Lenski, R. (2017). Experimental evolution and the dynamics of adaptation and genome evolution in microbial populations. *ISME J.* 11, 2181–2194. doi: 10.1038/ismej.2017.69

Li, M., Li, G., Zhu, L., Yin, Y., Zhao, X., Xiang, C., et al. (2014). Isolation and characterization of an agaro-oligosaccharide (AO)-hydrolyzing bacterium from the gut microflora of Chinese individuals. *PLoS ONE* 9, e91106. doi: 10.1371/journal.pone.0091106

Li, M., Zhao, J., and Tang, N., et al. (2018). Horizontal gene transfer from bacteria and plants to the arbuscular mycorrhizal fungus Rhizophagus irregularis. *Front. Plant Sci.* 9, 701. doi: 10.3389/fpls.2018.00701

Love, A. C., and Wagner, G. P. (2022). Co-option of stress mechanisms in the origin of evolutionary novelties. *Evolution* . 76, 394–413. doi: 10.1111/evo.14421

Loya, Y., Sakai, K., Yamazato, K., Nakano, Y., Sambali, H., and van Woesik, R. (2001). Coral bleaching: the winners and the losers. *Ecol. Lett.* 4, 122–131. doi: 10.1046/j.1461-0248.2001.00203.x

Ma, J., Wang, S., Zhu, X., Sun, G., Chang, G., Li, L., et al. (2022). Major episodes of horizontal gene transfer drove the evolution of land plants. Mol. Plant. 15, 857–871. doi: 10.1016/j.molp.2022.02.001

Maclean, R. C., and San Millan, A. (2019). The evolution of antibiotic resistance. *Science* 13, 1082–1083. doi: 10.1126/science.aax3879

Margulis, L. (1999). *Symbiotic Planet: A New Look at Evolution*. New York: Basic Books.

Margulis, L., and Sagan, D. (2003). *Acquiring Genomes: A Theory of the Origin of Species*. New York: Basic Books.

Marshall, C. R. (2015). How stable are food webs during a mass extinction? *Science* 350, 38–39. doi: 10.1126/science.aad2729

Mikhailovsky, G. E., and Gordon, R. (2021). LUCA to LECA, the Lucacene: A model for the gigayear delay from the first prokaryote to eukaryogenesis. *Biosystems* 205, 104415. doi: 10.1016/j.biosystems.2021.104415

Milligan, B. G. (1986). Punctuated evolution induced by ecological change. *Am. Nat.* 127, 522–532. doi: 10.1086/284500

Milligan, C. L., and Wood, C. M. (1986). Intracellular and extracellular acid-base status and H+ exchange with the environment after exhaustive exercise in the Rainbow trout. *J. Exp. Biol.* 123, 93–121. doi: 10.1242/jeb.123.1.93

Nakaya, Y., and Miyazawa, T. (2015). The roles of syncytin-like proteins in ruminant placentation. *Viruses*. 7, 2928–2942. doi: 10.3390/v7062753

Naranjo-Ortiz, M. A., and Gabaldón, T. (2020). Fungal evolution: cellular, genomic and metabolic complexity. *Biol. Rev.* 95, 1198–1232. doi: 10.1111/brv.12605

Nielsen, K. M., Bøhn, T., and Jeffrey, P., Townsend, J. P. (2014). Detecting rare gene transfer events in bacterial populations. *Front. Microbiol.* 4, 415. doi: 10.3389/fmicb.2013.00415

Nyholm, S. V., and McFall-Ngai, M. (2004). The winnowing: establishing the squid vibrio symbiosis. *Nat. Rev. Microbiol.* 2, 632–642. doi: 10.1038/nrmicro957

Palmer, S. A., Clapham, A. J., Rose, P., Freitas, F. O., Owen, B. D., Beresford-Jones, D., et al. (2012). Archaeogenomic evidence of punctuated genome evolution in *Gossypium*. *Mol. Biol.* Evol. 29, 2031–2038. doi: 10.1093/molbev/mss070

Pepper, J. W. (2014). The evolution of bacterial social life: from the ivory tower to the front lines of public health. *Evol. Med. Public Health* 2014, 65–68. doi: 10.1093/emph/eou010

Phillips, M. J., and Fruciano, C. (2018). The soft explosive model of placental mammal evolution. *BMC Evol. Biol.* 18, 104. doi: 10.1186/s12862-018-1218-x

Ponce-Toledo, R. I., Deschamps, P., López-García, P., Zivanovic, Y., Benzerara, K., and Moreira, D. (2017). An early-branching freshwater cyanobacterium at the origin of plastids. *Curr. Biol.* 27, 386–391. doi: 10.1016/j.cub.2016.11.056

Popov, N. N., Sklyar, N. I., Kolotova, Y. T., Davidenko, M. B., and Voronkina, I. A. (2019). New coding sequences formation by viruses with the help of horizontal transfer and gene duplication. *Ann. Mechnikov Instit.* 1, 7–12. Available online at: https://europub.co.uk/articles/-A-613590

Porter, N. T., and Martens, E. C. (2017). The critical roles of polysaccharides in gut microbial ecology and physiology. *Annu. Rev. Microbiol.* 71, 349–369. doi: 10.1146/annurev-micro-102215-095316

Rhodes, F. H. T. (1983). Gradualism, punctuated equilibrium and the origin of species. *Nature* 305, 269–272. doi: 10.1038/305269a0

Roger, A. J., Muñoz-Gómez, S. A., and Kamikawa, R. (2017). The origin and diversification of mitochondria. *Curr. Biol.* 27, 1177–1192. doi: 10.1016/j.cub.2017.09.015

Rosenberg, E., and Zilber-Rosenberg, I. (2018). The hologenome concept of evolution after 10 years. *Microbiome* 6, 78. doi: 10.1186/s40168-018-0457-9

Sari, W. N., Darmawi, S., and Fahrimal, Y. (2017). Isolation and identification of a cellulolytic Enterobacter from rumen of Aceh cattle. *Vet. World* 10, 1515–1520. doi: 10.14202/vetworld.2017.1515-1520

Sarkar, P., Bosneaga, E., and Auer, M. (2009). Plant cell walls throughout evolution: towards a molecular understanding of their design principles. *J. Exp. Bot.* 60, 3615–3635. doi: 10.1093/jxb/erp245

Schmidt, K. E., and Wolf, F. (2021). Punctuated evolution of visual cortical circuits? Evidence from the large rodent Dasyprocta leporina, and the tiny primate Microcebus murinus. *Curr. Opin. Neurobiol.* 71, 110–118. doi: 10.1016/j.conb.2021.10.007

Schönknecht,. G., Chen, W. H., Ternes, C. M., Barbier, G. G., Shrestha, R. P., Stanke, M., et al. (2013). Gene transfer from bacteria and archaea facilitated evolution of an extremophilic eukaryote. *Science* 339, 1207–1210. doi: 10.1126/science.1231707

Serrato-Capuchina, A., and Matute, D. R. (2018). The role of transposable elements in speciation. *Genes*. 9:254.

Sharma, A., Tewari, R., Rana, S. S., Soni, T., and Soni, S. K. (2016). Cellulases: Classification, methods of determination and industrial applications. *Appl. Biochem. Biotechnol.* 179, 1346–1380. doi: 10.1007/s12010-016-2070-3

Simpson, G. G. (1944). *Tempo and Mode in Evolution*. New York: Columbia Univ. Press.

Soucy, S. M., Huang, J., and Gogarten, J. P. (2015). Horizontal gene transfer: building the web of life. *Nat. Rev. Genet*. 16, 472–482. doi: 10.1038/nrg3962

Standen, E. M., Du, T. Y., and Larsson, H. C. E. (2014). Developmental plasticity and the origin of tetrapods. *Nature* 513, 54–58. doi: 10.1038/nature13708

Stanley, G. D. (2003). The evolution of modern corals and their early history. *Earth-Sci. Rev*. 60, 195–225. doi: 10.1016/S0012-8252(02)00104-6

Takemura, M. (2020). Medusavirus ancestor in a proto-eukaryotic cell: updating the hypothesis for the viral origin of the nucleus. *Front. Microbiol.* 2020, 11. doi: 10.3389/fmicb.2020.571831

Tomoyasu, Y., Arakane, Y., Kramer, J., and Denell, R. E. (2009). Repeated co-options of exoskeleton formation during wing-to-elytron evolution in beetles. *Curr. Biol.* 19, 2057–2065. doi: 10.1016/j.cub.2009.11.014

Velázquez, E., Carro, L., Flores-Félix, J. D., et al. (2017). The *legume nodule microbiome: A source of plant growth-promoting bacteria*," in *Probiotics and Plant Health*, eds Kumar, V., Kumar, M., Sharma, S. and Prasad, R. (Singapore: Springer).

Wagi, S., and Ahmed, A. (2019). *Bacillus* spp.: potent microfactories of bacterial IAA. *PeerJ* 7, e7258. doi: 10.7717/peerj.7258

Wang, J., Kalyan, S., Steck, N., et al. (2015). Analysis of intestinal microbiota in hybrid house mice reveals evolutionary divergence in a vertebrate hologenome. *Nat. Commun* 6, 6440. doi: 10.1038/ncomms7440

Weller, C., and Wu, M. (2015). A generation-time effect on the rate of molecular evolution in bacteria. *Evolution* 69, 643–652. doi: 10.1111/evo.12597

West, S. A., Fisher, R. M., Gardner, A., and Kiers, E. T. (2015). Major evolutionarytransitions in individuality. *Proc. Natl. Acad. Sci. USA* 112, 10112–10119. doi: 10.1073/pnas.1421402112

West-Eberhard, M. J. (2005). Developmental plasticity and the origins of species differences. *PNAS* 102, 6543–6549. doi: 10.1073/pnas.0501844102

Wickell, D. A., and Li, F.-W. (2020). On the evolutionary significance of horizontal gene transfers in plants. *New Phytol.* 225, 113–117. doi: 10.1111/nph.16022

Williams, T. A., Cox, C. J., Foster, P. G., Szöllosi, G. J., and Embley, T. M. (2020). Phylogenomics provides robust support for a two-domains tree of life. *Nat. Ecol. Evol.* 4, 138–147. doi: 10.1038/s41559-019-1040-x

Wu, J., Yonezawa, T., and Kishino, H. (2017). Rates of molecular evolution suggest natural history of life history traits and a post-k-pg nocturnal bottleneck of placentals. *Curr. Biol.* 27, 3025–3033.e5. doi: 10.1016/j.cub.2017.08.043

Yue, J., Hu, X., Sun, H., Yang, Y., Yang, Y., and Huang, J. (2012). Widespread impact of horizontal gene transfer on plant colonization of land. *Nat. Commun.* 3, 1152. doi: 10.1038/ncomms2148

Zamioudis, C., Mastranesti, P., Dhonukshe, P., et al. (2013). Unraveling root developmental programs initiated by beneficial *Pseudomonas* spp. bacteria. *Plant Physiol.*162, 304–318. doi: 10.1104/pp.112.212597

Zilber-Rosenberg, I., and Rosenberg, E. (2021). Microbial-driven genetic variation in holobionts. *FEMS Microbiol. Rev.* 45, fuab022. doi: 10.1093/femsre/fuab022

frontiers | Frontiers in Ecology and Evolution

TYPE Original Research
PUBLISHED 27 March 2023
DOI 10.3389/fevo.2023.1112742

OPEN ACCESS

EDITED BY
Ty N. F. Roach,
University of Hawaii at Manoa,
United States

REVIEWED BY
Sheila A. Kitchen,
California Institute of Technology,
United States
Shelley Templeman,
James Cook University,
Australia

*CORRESPONDENCE
Michael Kühl
✉ mkuhl@bio.ku.dk

†These authors share first authorship

SPECIALTY SECTION
This article was submitted to Coevolution, a section of the journal Frontiers in Ecology and Evolution

RECEIVED 30 November 2022
ACCEPTED 06 March 2023
PUBLISHED 27 March 2023

CITATION
Lyndby NH, Murray MC, Trampe E, Meibom A and Kühl M (2023) The mesoglea buffers the physico-chemical microenvironment of photosymbionts in the upside-down jellyfish *Cassiopea* sp. *Front. Ecol. Evol.* 11:1112742. doi: 10.3389/fevo.2023.1112742

The mesoglea buffers the physico-chemical microenvironment of photosymbionts in the upside-down jellyfish *Cassiopea* sp.

Niclas Heidelberg Lyndby[1†], Margaret Caitlyn Murray[2†], Erik Trampe[2], Anders Meibom[1,3] and Michael Kühl[2*]

[1]Laboratory for Biological Geochemistry, School of Architecture, Civil and Environmental Engineering, Ecole Polytechnique Fédérale de Lausanne, Lausanne, Switzerland, [2]Marine Biological Section, Department of Biology, University of Copenhagen, Helsingør, Denmark, [3]Center for Advanced Surface Analysis, Institute of Earth Sciences, University of Lausanne, Lausanne, Switzerland

Introduction: The jellyfish *Cassiopea* has a conspicuous lifestyle, positioning itself upside-down on sediments in shallow waters thereby exposing its photosynthetic endosymbionts (Symbiodiniaceae) to light. Several studies have shown how the photosymbionts benefit the jellyfish host in terms of nutrition and O_2 availability, but little is known about the internal physico-chemical microenvironment of *Cassiopea* during light–dark periods.

Methods: Here, we used fiber-optic sensors to investigate how light is modulated at the water-tissue interface of *Cassiopea* sp. and how light is scattered inside host tissue. We additionally used electrochemical and fiber-optic microsensors to investigate the dynamics of O_2 and pH in response to changes in the light availability in intact living specimens of *Cassiopea* sp.

Results and discussion: Mapping of photon scalar irradiance revealed a distinct spatial heterogeneity over different anatomical structures of the host, where oral arms and the manubrium had overall higher light availability, while shaded parts underneath the oral arms and the bell had less light available. White host pigmentation, especially in the bell tissue, showed higher light availability relative to similar bell tissue without white pigmentation. Microprofiles of scalar irradiance into white pigmented bell tissue showed intense light scattering and enhanced light penetration, while light was rapidly attenuated over the upper 0.5 mm in tissue with symbionts only. Depth profiles of O_2 concentration into bell tissue of live jellyfish showed increasing concentration with depth into the mesoglea, with no apparent saturation point during light periods. O_2 was slowly depleted in the mesoglea in darkness, and O_2 concentration remained higher than ambient water in large (> 6 cm diameter) individuals, even after 50 min in darkness. Light–dark shifts in large medusae showed that the mesoglea slowly turns from a net sink during photoperiods into a net source of O_2 during darkness. In contrast, small medusae showed a more dramatic change in O_2 concentration, with rapid O_2 buildup/consumption in response to light–dark shifts; in a manner similar to corals. These effects on O_2 production/consumption were also reflected in moderate pH fluctuations within the mesoglea. The mesoglea thus buffers O_2 and pH dynamics during dark-periods.

KEYWORDS

symbiosis, jellyfish, microenvironment, photosynthesis, respiration, light

Introduction

Symbiont-bearing jellyfish in the genus *Cassiopea* exhibit a conspicuous lifestyle by settling upside-down on sediment, exposing the subumbrella and oral arms to light. The oral side (i.e., the subumbrella side) of the medusa is particularly dense in intracellular microalgal symbionts, which are dinoflagellates of the family Symbiodiniaceae (Lampert, 2016). In contrast to corals where symbionts are found in endoderm cells, symbiont algae in *Cassiopea* are kept in clusters in host-specialized amoebocyte cells, directly below the epidermis in the mesoglea of the bell and oral arms (Colley and Trench, 1985; Estes et al., 2003). Similar to many photosymbiotic corals and anemones, *Cassiopea* rely on a metabolic exchange of carbon and nitrogen between the host animal and its algal symbionts (Welsh et al., 2009; Freeman et al., 2016; Lyndby et al., 2020). Translocation of autotrophically acquired carbon from the algal symbionts to the host covers a significant part of its daily carbon requirement, estimated to be at a similar or greater level than what is known from reef-building corals (Muscatine et al., 1981; Verde and McCloskey, 1998).

While most photosymbiotic cnidarians require a rather stable environment to maintain a healthy symbiosis, *Cassiopea* appears extraordinarily resilient to fluctuating environmental conditions (Goldfarb, 1914; Morandini et al., 2017; Aljbour et al., 2019; Klein et al., 2019; Banha et al., 2020) and are increasingly regarded as an invasive species (Mills, 2001; Morandini et al., 2017). *Cassiopea* are typically found in shallow waters (e.g., lagoons, around seagrass beds, and mangroves) in tropical and subtropical regions (Drew, 1972; Hofmann et al., 1996) that are prone to strong diel fluctuations in both temperature, and salinity, as well as high solar irradiance (Anthony and Hoegh-Guldberg, 2003; Veal et al., 2010). Human activities in such coastal ecosystems can further add to strong fluctuations in both nutrient input, O_2 availability, and pH (Stoner et al., 2011; Klein et al., 2017; Rowen et al., 2017; Arossa et al., 2021).

The photobiology and optical properties of marine symbiont-bearing cnidarians have been studied in detail in reef-building corals, showing adaptations in host growth patterns, microscale holobiont light modulation, and colony-wide symbiont organization to enable and optimize symbiont photosynthesis for the benefit of the host (e.g., Falkowski et al., 1984; Kühl et al., 1995; Wangpraseurt et al., 2014b; Lyndby et al., 2019; Kramer et al., 2021; Bollati et al., 2022). Studies have shown that *in vivo* light exposure of symbionts is modulated on a holobiont level to enhance photosynthesis, including alleviating photodamage and bleaching (Lesser and Farrell, 2004; Enriquez et al., 2005; Marcelino et al., 2013; Wangpraseurt et al., 2017), altering inter-and intracellular pH (e.g., Kühl et al., 1995; Gibbin et al., 2014), and directly affecting holobiont temperature (Jimenez et al., 2008, 2012; Lyndby et al., 2019). Recently, these experimental insights were integrated in a first multiphysics model of radiative, heat and mass transfer in corals, simulating how coral tissue structure and composition can modulate the internal light, O_2 and temperature microenvironment of corals (Taylor Parkins et al., 2021; Murthy et al. 2023). Given a similar global distribution and a benthic lifestyle relying on host-symbiont metabolic interactions, it is feasible to assume that *Cassiopea* exhibit similar traits, but few studies have investigated to what extent *Cassiopea* modulate their physicochemical microenvironment (Klein et al., 2017; Arossa et al., 2021).

In this study, we use a combination of optical and electro-chemical microsensors to investigate the internal microenvironment of *Cassiopea* sp. medusae. We explore how light is modulated by host morphology and distinct anatomical features. Furthermore, we show how the size of animals and the thickness of their bell mesoglea affects the intracellular physicochemical microenvironment of intact, living *Cassiopea* sp. medusae.

Methods

Cassiopea maintenance

Medusae of *Cassiopea* sp. were acquired *via* DeJong Marinelife (Netherlands) in 2018, and since cultivated at the aquarium facility at the Marine Biology Section in Helsingør, University of Copenhagen (Denmark). According to the commercial provider, the obtained specimens originated from Cuba indicating the species *Cassiopea xamachana* or *C. frondosa*, but no species identification was performed. The medusae were kept in artificial seawater (ASW; 25°C, 35 ppt, pH of 8.1) in a 60 l glass aquarium, under a 12 h-12 h day-night cycle using LED lamps (Tetra, Pacific Sun) providing an incident photon irradiance (400–700 nm) of ~300 µmol photons m^{-2} s^{-1}, as measured with a cosine corrected mini quantum sensor (MQS-B, Walz, Germany), connected to a calibrated irradiance meter (ULM-500, Walz, Germany). Animals were fed with living *Artemia* sp. nauplii twice a week, and 25% of the aquarium water was replaced with fresh filtered ASW (FASW) 1 h after feeding. Additionally, water was continuously filtered using an internal filter pump, a filter sock (200 µm), and a UV filter. Additionally, an air pump was used to ensure water remained oxygenated at all times.

Light measurements

Photon scalar irradiance

Mapping of photon scalar irradiance in µmol photons m^{-2} s^{-1} (PAR; 400–700 nm) on the jellyfish tissue surface was performed with a submersible spherical micro quantum sensor (3.7 mm diameter; US-SQS/L, Walz, Germany) connected to a calibrated irradiance meter (ULM-500, Walz, Germany). Measurements were conducted inside an aquarium tank filled with ASW and the inside covered with a black cloth to avoid internal reflections from the container. The medusa was placed in the aquarium and illuminated vertically from above by a fiber-optic tungsten-halogen lamp (KL-2500 LCD, Schott GmbH, Germany), equipped with a collimating lens. Photon scalar irradiance was measured holding the sensor at a ~ 45° angle, while measuring light on the surface of the animal within 7 areas of interest (AOI) of one animal (Figure 1B). Measurements were normalized against the incident downwelling photon irradiance, as measured over the black cloth covering the inside of the container relative to each AOI on the animal.

Spectral scalar irradiance and reflectance

Both spectral scalar irradiance and reflectance measurements required the medusa to be fixed in place on a large rubber stopper using hypodermic needles, and placed in a container filled with seawater. Incident light was provided vertically from above with a fiber-optic

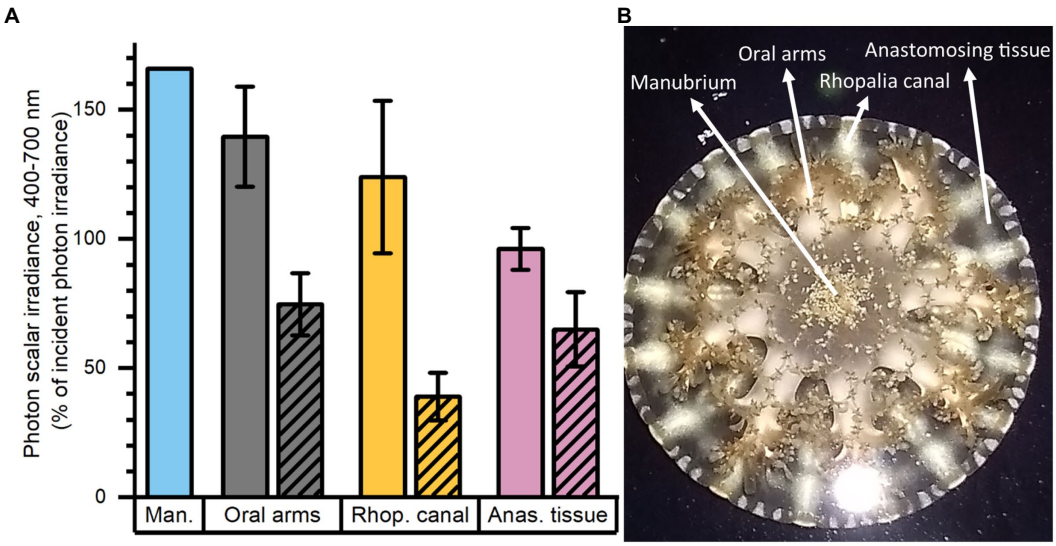

FIGURE 1
Normalized photon scalar irradiance (PAR, 400–700nm) measured at **(A)** the manubrium center (Man.), oral arms, rhopalia canals (Rhop. canal) and anastomosing tissue (Anas. tissue) on a single adult medusa of *Cassiopea*. Bright colors indicate values measured above, and shaded colors the values below the medusa. **(B)** Overview of the specimen with exemplary positions for measurements (white arrows). Light intensities were mapped at the tissue-water interface (above and below the medusa) at respective anatomical structures (n=7–17) using a submersible spherical quantum sensor (see Methods), and normalized against the incident photon irradiance intensity measured at the same sensor positions without the medusae above a black surface. Note, only one measurement was performed above the manubrium center.

halogen lamp (KL-2500 LCD, Schott GmbH, Germany) fitted with a collimating lens. Spectral scalar irradiance was measured using a fiber-optic scalar irradiance microprobe (spherical tip diameter ~ 100 µm; Rickelt et al., 2016). Spectral reflectance was measured using a fiber-optic field radiance probe (400 µm diameter; Kühl, 2005). Both sensors were connected to a fiber-optic spectrometer (USB2000+; Ocean Optics, USA), and spectral information was acquired using SpectraSuite software (Ocean Optics, USA). Sensors were mounted on a manual micromanipulator (MM33, Märzhäuser Wetzlar GmbH, Germany) attached to a heavy-duty stand to facilitate precise positioning of sensors on the medusa. Sensors were positioned visually using a dissection microscope, while ensuring oral arms and other anatomical features did not shade the tissue studied. The spectral reflectance probe was positioned by first moving the sensor to the surface of the medusa, then moving the sensor 1 mm away. Similarly, the scalar irradiance probe was first positioned to touch the surface tissue of the medusa (depth = 0 µm) and was then moved into the medusa in vertical steps of 200 µm. Both sensors were held by the micromanipulator in an angle of 45° relative to the incident light. The recorded spectral scalar irradiance was normalized against the incident, downwelling spectral irradiance measured over the black cloth covering the inside of the container relative to each measuring position on the medusae. The recorded spectral reflection spectra were normalized against a reference spectrum measured with an identical setup over a 99% white reflectance standard (Spectralon, Labsphere) in air.

Microscale measurements of O_2 and pH

General setup

For all O_2 and pH measurements, individual medusae were placed in a cylindrical plexiglass chamber with aerated, filtered ASW. Medusae were illuminated with a fiber-optic halogen lamp (KL-2500 LED, Schott GmbH, Germany) equipped with a collimating lens, and providing defined levels of incident photon irradiance (0, 42, 105, 160, 300, and 580 µmol photons m^{-2} s^{-1}; 400–700 nm), as measured for specific lamp settings with a calibrated photon irradiance meter equipped with a spherical micro quantum sensor (ULM-500 and US-SQS/L, Heinz Walz GmbH, Germany).

Concentration profiles and dynamics were measured above and inside anastomosing bell tissue of 3 small (25–48 mm, bell thickness < 4 mm) and 2 large (63–67 mm, thickness of bell >8 mm) medusae. Anastomosing tissue, i.e., connective tissue, comprise the large and mainly brown or transparent parts of the bell disk, making up the space between the rhopalia canals (Figure 1B). The microsensor tip was carefully positioned at the tissue surface-water interface while watching the tissue surface under a dissection microscope. For profiling, the sensor was inserted in vertical steps of 100 µm until reaching the approximate center of the mesoglea, relative to the subumbrella and exumbrella bell epidermis.

Oxygen measurements

The O_2 concentration measurements were done using a robust fiber-optic O_2 optode (OXR230 O_2 sensor, 230 µm diameter tip, < 2 s response time; PyroScience GmbH, Germany) connected to a fiber-optic O_2 meter (FireSting, PyroScience GmbH, Germany). The sensor was linearly calibrated in O_2-free and 100% air saturated seawater at experimental temperature and salinity. The sensor was mounted slightly angled relative to the incident light (to avoid shadowing) on a motorized micromanipulator (MU1, PyroScience GmbH, Germany) attached to a heavy-duty stand, facilitating visual sensor positioning with a dissection microscope. Data acquisition was done using the manufacturer's software (Profix, PyroScience GmbH, Germany). Measurements were performed at room temperature (22°C) in a dark

room under defined light conditions, and the temperature was continuously recorded in the experimental chamber with a submersible temperature sensor (TSUB21, PyroScience GmbH, Germany) connected to the O_2 meter.

For light–dark measurements, the O_2 sensor tip was inserted approximately midway between sub-and exumbrella epidermis (depth ranging from ~800 to 3,000 µm from the surface depending on the specimen size). Once the depth of interest was reached, the local O_2 concentration dynamics were measured at 10 s intervals during experimental manipulation of the light. Local rates of net photosynthesis and post-illumination respiration were estimated from the measured linear slope of O_2 concentration versus time measurements (using linear fits in the software OriginPro 2020b; OriginLab Corp., USA) under light and dark conditions, respectively. The local gross photosynthesis was then estimated as the sum of the absolute values of net photosynthesis and respiration.

The O_2 concentration depth profiles were recorded at vertical depth intervals of 100–200 µm during constant light or darkness. The measurements were recorded once the O_2 concentration reached a steady-state at each depth, starting from deepest inside the tissue and moving the sensor up until the sensor tip was retracted up into the overlaying turbulent water column (100% air saturation).

pH measurements

pH was measured using a pH glass microelectrode (PH-100, 100 µm tip diameter, response time < 10 s, Unisense, Denmark) combined with an external reference electrode and connected to a high impedance mV-meter (Unisense, Denmark). A motorized micromanipulator (MU1, PyroScience GmbH, Germany) was used for positioning of the sensor, and data were recorded using SensorTrace Logger software (Unisense, Denmark). Prior to measurements the sensor was calibrated at room temperature using IUPAC standard buffer solutions at pH 4, 7, and 9 (Radiometer Analytical, France). Dynamic changes in mesoglea pH levels were measured during experimental dark–light transitions and vice versa. pH depth profiles were measured under constant light or darkness, and were recorded from the middle of the bell and up into the water column in steps of 200 µm, until the sensor tip was retracted into the overlying turbulent water column (pH level of 8.1–8.4).

Results

Light microenvironment

Photon scalar irradiance

Macroscopic mapping of integral photon scalar irradiance of photosynthetically active radiation (PAR, 400–700 nm) in 4 distinct regions of an intact, living *Cassiopea* sp. revealed a heterogeneous light field across the medusa tissue facing the incident light as well as across the tissue. The manubrium center experienced the highest scalar irradiance reaching 166% of incident photon irradiance (Figure 1). Oral arms experienced a photon scalar irradiance reaching 140 ± 19% of incident photon irradiance, while light availability just below the oral arms was significantly lower (75 ± 12% of incident photon irradiance). The light levels of rhopalia canals reached 124 ± 30% of incident photon irradiance and light levels of anastomosing tissue reached 96 ± 8% of incident photon irradiance on the subumbrella side. On the exumbrella side, more light penetrated the anastomosing tissue (65 ± 14% of incident photon irradiance), while the least amount of light penetrated through the rhopalia canals (39 ± 9% of incident photon irradiance).

Reflectance

The oral arms and rhopalia canals of *Cassiopea* reflected more light than the manubrium and anastomosing tissue, with oral arms reflecting 9.5%, rhopalia canals 7%, the manubrium 4.8%, and anastomosing tissue 3% of incident irradiance (Figure 2).

Spectral scalar irradiance

Depth profiles of spectral scalar irradiance in live *Cassiopea* tissue showed spectral absorption signatures of chlorophyll (Chl) *a* (430–440, 675 nm), Chl *c* (460, 580–590, and 635 nm), and peridinin (480–490 nm), throughout the anastomosing tissue and near rhopalia canals (Figure 3). Spectral scalar irradiance at the tissue–water interface (0 µm) revealed a local enhancement near the rhopalia canals, while light was more readily absorbed on anastomosing tissue. Depth profiles show a steady attenuation of light within the first 400 µm of the bell near rhopalia canals (Figure 3A). In contrast, scalar irradiance was slightly enhanced at 200 and 400 µm in the anastomosing tissue, until a strong attenuation was observed at 600 µm depth (Figure 3B).

Chemical microenvironment

Oxygen depth profiles

The O_2 concentration depth profiles were measured in a *Cassiopea* sp. medusa (45 mm Ø) under a saturating photon irradiance of 300 µmol photons m^{-2} s^{-1} (Figure 4). The O_2 concentration increased strongly in deeper parts of the bell tissue below 1 mm depth, rising from 315 (± 21) to 445 (± 40) µmol O_2 l^{-1} at a depth of 3.7 mm. A maximal O_2 concentration was measured at 4 mm, reaching ~500 µmol O_2 l^{-1} (not shown in figure).

Similarly, O_2 depth profiles were measured in darkness in 3 different medusae (38–67 mm Ø), with either 0, 15, or 50 min of darkness prior to the profile (Figure 5). Profiles reveal high O_2 depletion in the top 1 mm layer of the bell with increasing length of dark incubation, while measurements deeper into the bell showed a less dramatic decrease of O_2 concentration in the mesoglea of the medusae.

Light-dependent oxygen dynamics

The O_2 dynamics measured approximately in the middle of the mesoglea between the sub-and exumbrella epidermis showed a delayed response to changes in light in large individuals, while the response in smaller medusae appeared immediately after a light–dark switch or vice versa (Figure 6). The O_2 concentration measured in 2 large and 3 small medusae showed that the O_2 content continued to increase in the mesoglea of large medusae several minutes after light was turned off, indicative of diffusive supply from the surrounding tissue with a higher symbiont density and/or photosynthetic activity prior to onset of darkness (Figure 7).

Locally measured photosynthesis versus photon irradiance curves showed that photosynthesis increased linearly with irradiance until saturation was approached at ~300 µmol photons m^{-2} s^{-1} (Figure 8).

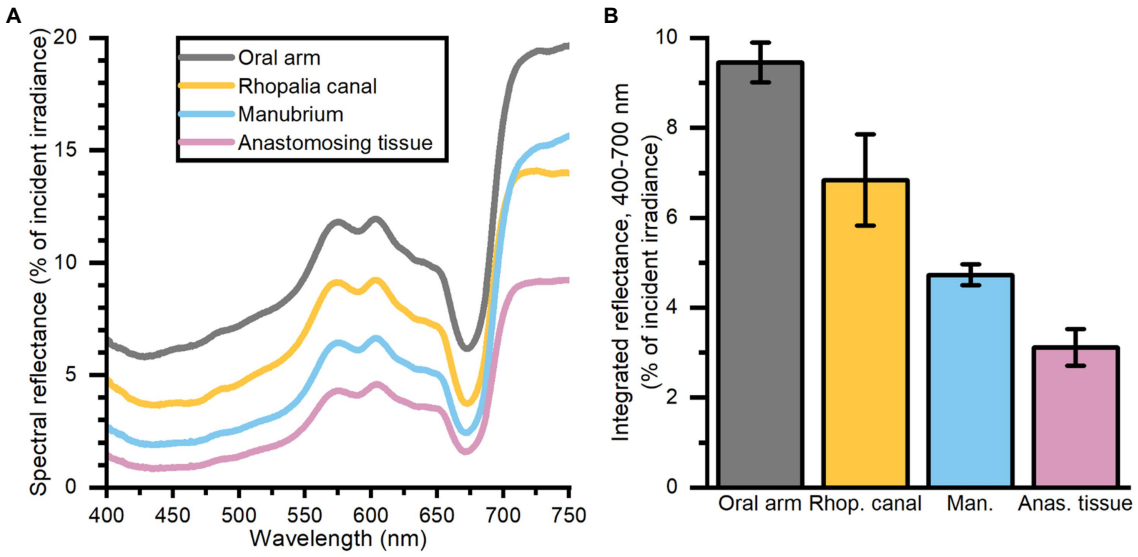

FIGURE 2
Spectral reflectance (in % of incident irradiance) **(A)** measurements, and integrated reflectance (400–700nm) **(B)** averaged for 4 areas of interest depicting differing morphological tissue regions of one large *Cassiopea* medusa. Data represent mean±SEM (n=3 for each tissue type). For increased clarity standard errors are not shown in panel **(A)**, but are reflected in the ±SEM shown for integrated values in panel **(B)**.

At saturating irradiance, net photosynthesis rates in bell tissue ranged from 0.08 µmol O_2 l^{-1} s^{-1} in large individuals, to 0.18 µmol O_2 l^{-1} s^{-1} in small medusae. Similarly, the estimated gross photosynthesis was roughly 2-fold higher in small medusae, at 0.26 µmol O_2 l^{-1} s^{-1} vs. 0.14 µmol O_2 l^{-1} s^{-1} in large medusae. Post-illumination respiration rates were 0.04–0.07 µmol O_2 l^{-1} s^{-1} in large medusae regardless of illumination, while post-illumination respiration in small medusae increased to a maximum of 0.18 µmol O_2 l^{-1} s^{-1} at maximum photon irradiance (580 µmol photons m^{-2} s^{-1}). The respiration at saturating photon irradiance (300 µmol photons m^{-2} s^{-1}) was 0.08 µmol O_2 l^{-1} s^{-1} in tissue of small medusae.

Spatio-temporal dynamics of pH

pH depth profiles measured after a combined 15 min light, 15 min darkness incubation showed that pH dropped rapidly to below ambient water pH at the bell tissue-water interface (0 µm) in both the large and small medusae (Figure 9). pH then increased rapidly again within the first 1,000 µm of the bell tissue (to above ambient water pH), and kept increasing to a maximum depth of 4,000 µm to a final pH of ~8.8 for both specimens. The pH dynamics over experimental light–dark shifts showed a similar pattern to what was observed with O_2 dynamics: pH changed relatively quickly in the small medusa, while a much longer delay (usually >10 min after the light change) was observed with the large medusa (Figure 10).

Discussion

Cassiopea harbors optical microniches

Light availability in the host is a key factor for an efficient photosymbiosis. It has been shown that host morphology and tissue plasticity, host pigmentation, and symbiont density can modulate the scattering and absorption of photons in tissue of reef-building corals, creating optical microniches in a colony (D'Angelo et al., 2008; Wangpraseurt et al., 2014b, 2019; Bollati et al., 2022); and we note that the coral skeleton is also important for the coral light microenvironment (e.g., Enriquez et al., 2005; Enríquez et al., 2017). In *Cassiopea*, we found distinct spatial heterogeneity over the surface tissue in various regions of an adult medusa (Figure 1). Local photon scalar irradiance was highest near apical parts of the animal, while it dropped by 30–80% underneath the same anatomical structures (Figure 1A). The largest decrease was observed between measurements on the subumbrella and exumbrella epidermis along the rhopalia canal, which dropped by 80% on the exumbrella side. Additionally, spatial heterogeneity was observed over the subumbrella bell tissue, with rhopalia canals experiencing on average ~30% higher photon flux compared to the anastomosing tissue right next to it.

Depth profiles of spectral scalar irradiance measured in tissue close to rhopalia canals and in anastomosing tissue showed that light scattered differently within the upper 600 µm of the two regions (Figure 3). Profiles in anastomosing tissue showed small variations in spectral scalar irradiance measured in the top 400 µm of this region (Figure 3B). Such small variations indicate the presence of a dense symbiont population spread out in the top 400 µm of the mesoglea, between the subumbrella epidermis and the gastric network (Estes et al., 2003). Similar studies on corals have shown that light can be scattered by host tissue and symbionts in the surface layers, enhancing the chance of photon absorption (Wangpraseurt et al., 2012, 2014a; Jacques et al., 2019). In contrast, we observed a strong light attenuation over the first 400 µm of the tissue near rhopalia canals, with an initial enhancement of local scalar irradiance that quickly attenuated to levels below what was observed at the same depth in anastomosing tissue (Figure 3B). *Cassiopea* contain distinct white striated patterns in dense layers along the rhopalia canals in the bell and under oral arms (see white patches in Figure 1B; Bigelow, 1900). While little is known about host pigments in *Cassiopea* and other rhizostome jellyfish (Hamaguchi et al., 2021; Lawley et al., 2021),

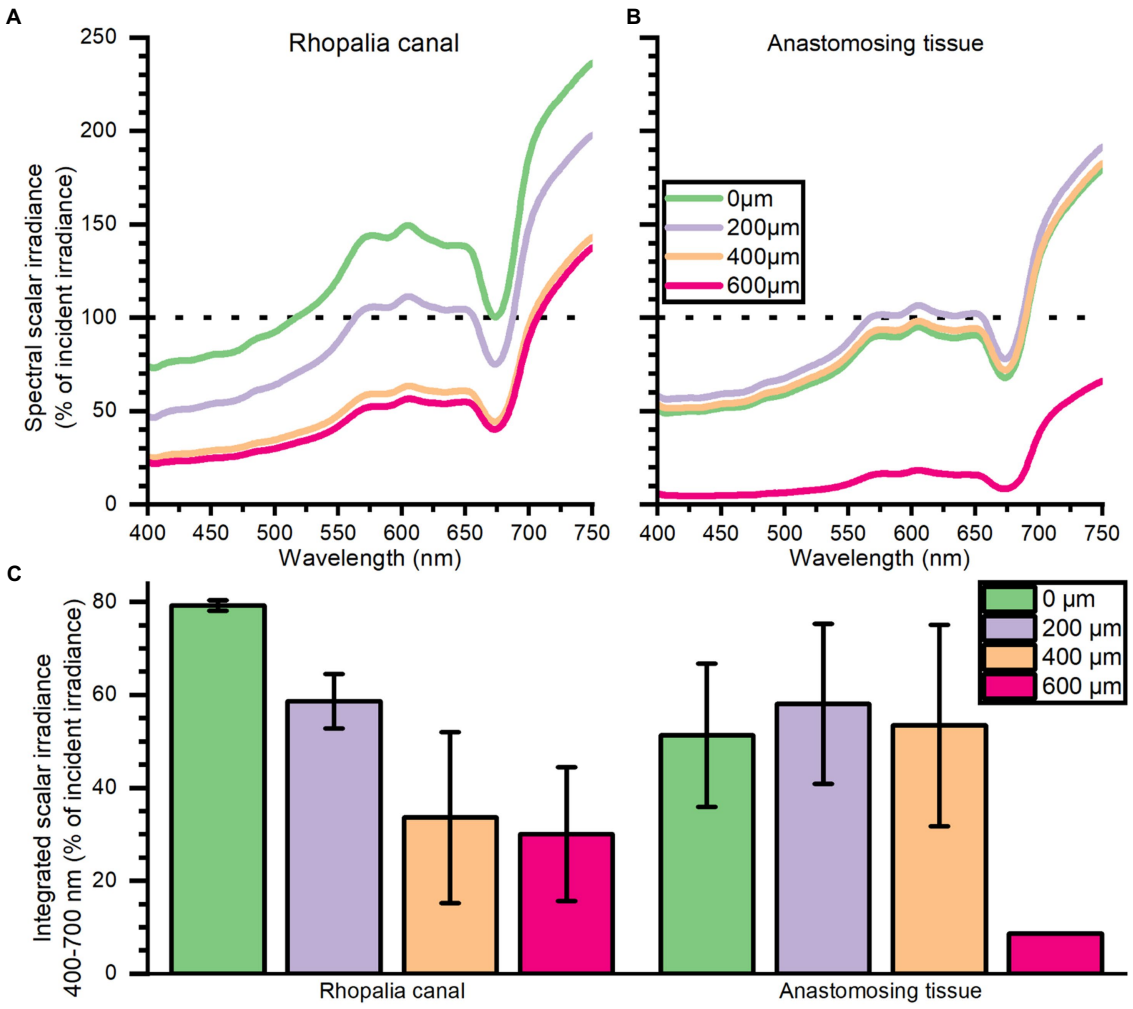

FIGURE 3
Spectral scalar irradiance (in % of incident irradiance) measured near the subumbrella rhopalia canal **(A)** and anastomosing tissue **(B)**, and integrated scalar irradiance (400–700nm) **(C)**. Data represent mean±SEM of 2 rhopalia canals and 3 anastomosing tissue areas (except for the 600µm). For increased clarity standard errors are not shown in panel **(A,B)**, but are reflected in the ±SEM shown for integrated values in panel **(C)**.

our reflection data (compare for example rhopalia canal with anastomosing tissue in Figure 2) suggests that the white pigmented tissue can play a role in scattering and reflection of light in *Cassiopea* medusae, similar to host pigments and the skeleton in reef-building corals (Wangpraseurt et al., 2014a; Jacques et al., 2019). More detailed analyses are required to understand the full potential of light-modulating host pigments in *Cassiopea*, and how the holobiont might respond and grow under various light regimes.

Cassiopea harbors its photosymbionts in a buffered chemical microenvironment

We investigated the light-driven dynamics of O_2 and pH on the surface and inside the bell tissue of *Cassiopea* medusae. Depth profiles of O_2 concentration measured at saturating irradiance showed the presence of a diffusive boundary layer (DBL) over the bell tissue (Figure 5). In light, the O_2 concentration increased towards the bell tissue-water interface and continued to increase as the sensor penetrated deeper into the tissue and mesoglea (Figure 4). We measured to a maximum depth of 4 mm into the mesoglea reaching an O_2 concentration of roughly 2-fold that of the surrounding seawater concentration. A similar study, measuring O_2 in cut-off oral arms of *Cassiopea* sp., found that O_2 concentration was highest near symbiont populations (i.e., near the epidermis), while it decreased to a more constant level deeper into the oral arm mesoglea (Arossa et al., 2021). However, our measured depth profiles in bell tissue did not show any indication that O_2 buildup would stagnate or decrease at this point, suggesting even higher concentrations might be possible in the bell mesoglea relative to oral arms. Passive accumulation of O_2 has been reported in non-symbiotic jellyfish like *Aurelia labiata* (Thuesen et al., 2005), which was found to build up O_2 in the mesoglea when in O_2-rich water, indicating that the mesoglea can act as a natural reservoir for O_2 in jellyfish. However, similar to measurements in oral arms of *Cassiopea* sp. (Arossa et al., 2021), measured depth profiles of O_2 concentrations in non-symbiotic jellyfish like *Aurelia* appear to have the highest O_2 concentration near the tissue-water interface, with a steady decline towards the center of the bell (Thuesen et al., 2005). In contrast our measurements indicate that the presence of photosynthetic endosymbionts harbored within amoebocytes in the

mesoglea (Colley and Trench, 1985; Medina et al., 2021) leads to internal O_2 production and accumulation in deeper tissue layers during photo periods (Kühl et al., 1995; Arossa et al., 2021).

The diffusion of O_2 through cnidarian tissue and mesoglea has received little attention. However, Brafield and Chapman (1983) determined an O_2 diffusion coefficient of 7.69×10^{-6} cm^2 s^{-1} in the mesoglea of the sea anemone *Calliactis* sp. Such a low diffusion coefficient in the mesoglea (as compared to seawater) will impede mass transfer, especially in cnidarians with a particularly thick mesoglea like jellyfish and sea anemones, and is probably a key factor in the observed buffering of O_2 dynamics in the *Cassiopea* sp. bell. We further investigated the dynamics of O_2 in darkness and found that the top 1 mm layer of *Cassiopea* bell tissue turned from a net O_2 source into a sink (Figure 5). Measurements in the DBL showed a switch from a net export from the tissue into the surrounding seawater to a diffusive import of O_2 from the seawater within the first 15 min (compare DBLs in Figure 5). A more pronounced depletion of O_2 was observed in the top 1 mm of the bell after 50 min darkness. The higher O_2 consumption near the subumbrella epidermis probably reflects the presence of abundant musculature required for bell pulsation and motility of jellyfish (Blanquet and Riordan, 1981; Thuesen et al., 2005; Aljbour et al., 2017), as well as the presence of a dense population of endosymbionts (Estes et al., 2003; Lampert, 2016). Both have previously been ascribed to heavy diel fluctuations of O_2 measured in *Cassiopea* oral arms (Arossa et al., 2021). However, the O_2 concentration remained high at depths deeper than 1 mm into the bell even after 50 min of darkness, reflecting a lower cell density and diffusive transport of O_2.

In the present study, experimental light–dark shifts performed on intact small (< 5 cm) and large (> 6 cm) *Cassiopea* sp. showed that the O_2 concentration in small medusae with a (relatively) thin bell of 2 mm thickness changed almost immediately in response to light–dark shifts similar to observed O_2 dynamics in corals and dissected oral arms of *Cassiopea* (Figure 6A; Kühl et al., 1995; Arossa et al., 2021). Unlike the fast response observed in small medusae, larger medusae with a thicker bell tissue showed a much slower response of O_2 levels to changes in light (Figure 6B). In fact, detailed O_2 dynamics measured in several large and small medusae revealed a consistent pattern where O_2 would continue to build up in the thick mesoglea of larger medusae for a few minutes after onset of darkness (Figure 7). These observations indicate that O_2 generated in other regions with higher photosynthetic activity due to higher light levels and/or higher symbiont density can

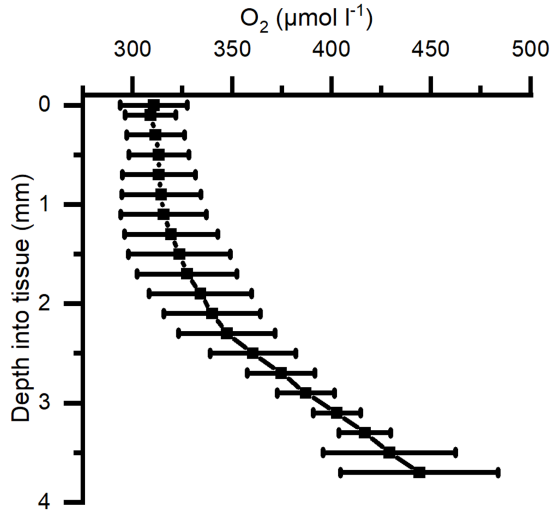

FIGURE 4
Average of depth profiles of O_2 concentration in *Cassiopea* tissue measured under a photon irradiance (400–700nm) of 300µmol photons m^{-2} s^{-1} in the bell of a medusae. n=3 biological replicates with 1 profile each.

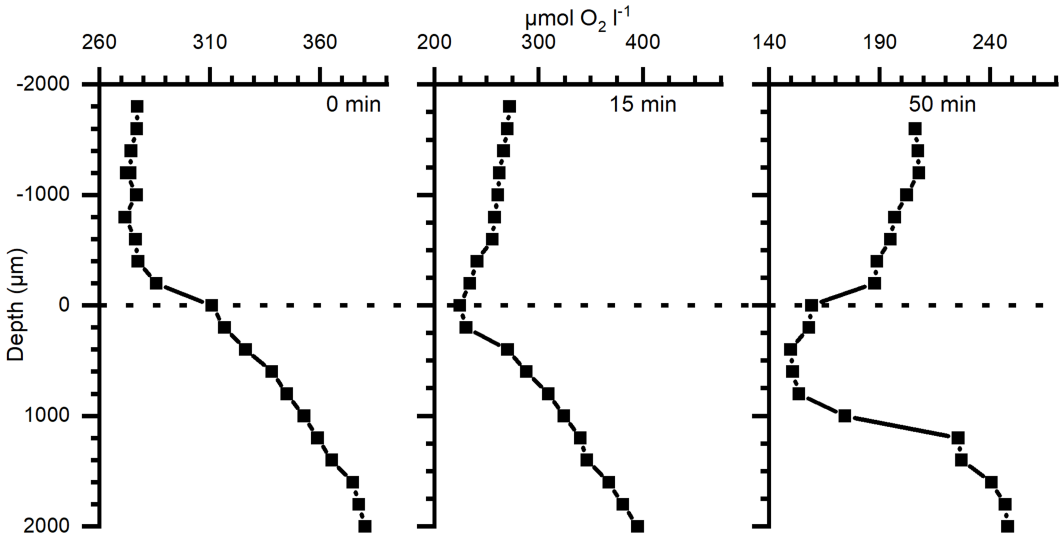

FIGURE 5
Depth profiles of O_2 concentration in bell tissue of three different *Cassiopea* specimens (38–67mm Ø) incubated in darkness for 0, 15, and 50min, respectively (38, 67, and 63mm Ø individual, respectively), prior to measurements. Zero depth indicates the tissue-water interface, and 2,000µm the deepest into the tissue. Note differences in the *x*-axis scales.

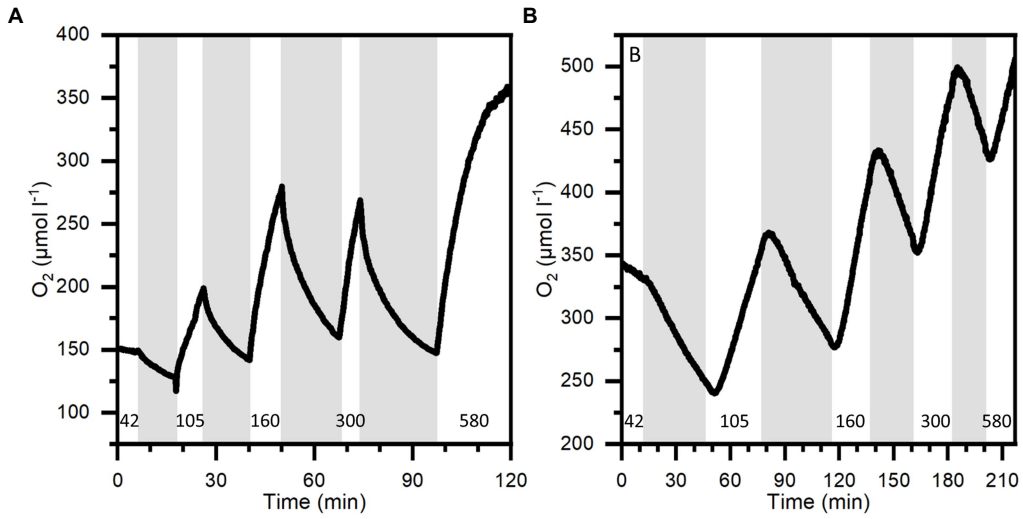

FIGURE 6
O_2 dynamics at 1mm depth into the bell of a small medusa **(A)** and 3mm into the bell of a large medusa **(B)** during light–dark shifts. Gray areas indicate dark shifts and white areas indicate photo periods of increasing incident photon irradiance (400–700nm) noted with numbers in units of µmol photons m^{-2} s^{-1}. Note differences in *x*- and *y*-axes.

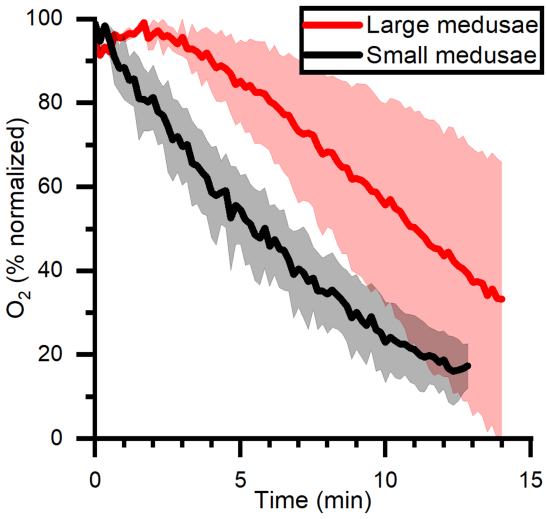

FIGURE 7
O_2 dynamics measured in mid-bell mesoglea (roughly halfway deep in the bells) of large and small medusae from onset of darkness at 0min, after a previous illumination with an incident photon irradiance (400–700nm) of 580µmol photons m^{-2} s^{-1}. Data is normalized against maximum oxygen concentration measured in each medusa, and then averaged for large (*n*=2) and small (*n*=3) individuals ±SEM.

diffuse into and accumulate in the mesoglea, from where it is not efficiently exchanged with the surrounding water due to the relatively low O_2 diffusivity in mesoglea (Brafield and Chapman, 1983).

Furthermore, an inverse relationship between medusa size and photosynthetic rate have previously been reported (Verde and McCloskey, 1998). We observed a similar inverse relationship, with smaller medusae on average reaching roughly 2-fold higher photosynthetic rates (net and gross) at photon irradiances above 200 µmol photons m^{-2} s^{-1} (Figure 8). Post-illumination respiration also increased in small individuals, while larger medusae did not show changes to respiration after illumination. The combined effect of the diffusive properties of mesoglea, the relative thickness of the mesoglea, and the overall size of the animal together explain why the O_2 dynamics is more pronounced in medusae (and other cnidarians) with a thin mesoglea like in juvenile *Cassiopea* bell or oral arms, while the O_2 dynamics in medusae with a thick mesoglea is much more buffered.

Consistent with the measured O_2 dynamics, we found that pH changes in the mesoglea were affected by changes in light, because pH increases due to photosynthetic carbon fixation in the light and decreases during darkness due to respiration (Figure 10). This relationship between photosynthesis, respiration, and pH seems prevalent in symbiotic cnidaria (e.g., Kühl et al., 1995; de Beer et al., 2000; Chan et al., 2016; Klein et al., 2017; Arossa et al., 2021), largely driven by the shifting equilibrium between carbonate species (i.e.; CO_2, H_2CO_3, HCO_3^-, CO_3^{2-}) and the balance between photosynthesis and respiration. de Beer et al. (2000) found that pH in coral tissue followed the trend of O_2 during experimental light–dark shifts but with a delayed response (seconds to minutes), and attributed the delay to hypothetic processes, such as proton pumps and other similar cross-tissue transport, that would buffer pH in coral polyps (Palmer and Van Eldik, 1983). External buffering has also been reported in polyps of *Cassiopea*, where Klein et al. (2017) found that polyps retained their internal pH at ambient water pH during the night, and only symbiotic polyps would increase their internal pH during photoperiods due to a shifting carbonate equilibrium. We observed a similar, but much longer (>10 min) delay before a pH change was observed in the mesoglea of large medusa after light–dark shifts (Figure 10B). While external buffering is likely to occur in medusae of *Cassiopea* as well, the pH dynamics inside the mesoglea is probably more affected by diffusive transport phenomena. Depth profiles done in both small and large medusae thus show that within 15 min of darkness the top 1 mm of the bell tissue became more acidic relative

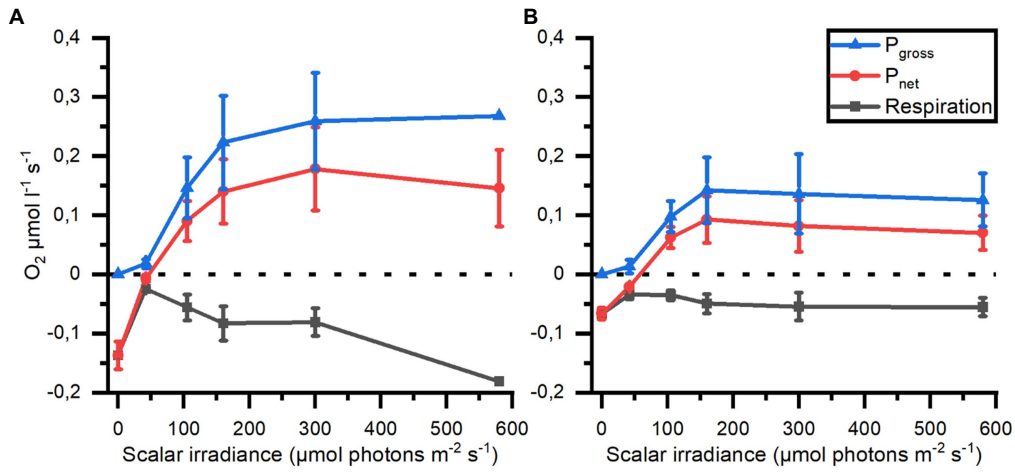

FIGURE 8
Respiration, net (P_{net}) and gross photosynthesis (P_{gross}) measured in mesoglea of small (**A**; *n*=3) and large (**B**; *n*=2) medusae as a function of photon scalar irradiance (400–700nm).

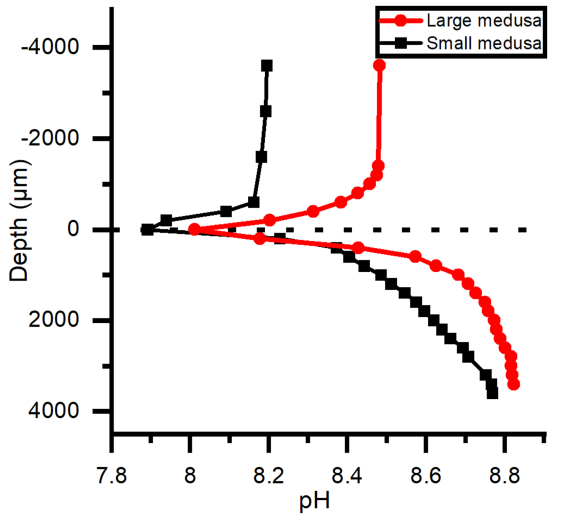

FIGURE 9
pH depth profiles measured in the bells of a small and large medusae, where 0µm is tissue surface and 4,000µm is the deepest inside the tissue. Both individuals were kept under an incident photon irradiance (400–700nm) of 580µmol photons m^{-2} s^{-1} light for >15min and then in darkness for ~15min before profiles were done.

to ambient water pH (0.3–0.5 pH lower; Figure 9), while pH in deeper tissue layers (> 1,000 µm into the bell) remained alkaline and above ambient water pH. This strongly suggest that the mesoglea has a buffering effect on pH in the bell tissue of *Cassiopea*.

The buffering capacity of the mesoglea could be of benefit for both host and symbionts. A reservoir of O_2 can for example act as a steady supply of O_2 to both host musculature, needed for bell pulsation, and to symbionts during dark periods or exposure to hypoxia (Thuesen et al., 2005). Similarly, buffering pH could lower the possibility of the holobiont experiencing cellular acidosis (Smith and Raven, 1979; Gibbin et al., 2014) that would otherwise disrupt cell-function (Madshus, 1988). Thus, symbionts harbored in amoebocytes in the *Cassiopea* mesoglea may exist in a more stable ecological niche as compared to algae in corals that are more prone to rapid chemical dynamics. We speculate that the buffering of the chemical microenvironment in the mesoglea of *Cassiopea*, might also be reflected in the fact that *Cassiopea* medusae generally seem to only engage with a specific type of Symbiodiniaceae. Indeed, specific strains of Symbiodiniaceae have been speculated to be favored by different hosts in symbiotic cnidarians (Schoenberg and Trench, 1980; Biquand et al., 2017), including *Cassiopea* (Colley and Trench, 1983; Fitt, 1985). While specificity is generally attributed to a combination of symbiont cell size and a hospitable host microenvironment (Biquand et al., 2017), Fitt (1985) found a correlation between symbiont cell size and respective photosynthesis and respiration rates, and proposed that only specific symbiont strains are able to establish symbiosis due to metabolic rates matching the hosts specific microenvironment. As such, the *Cassiopea*-Symbiodiniaceae symbiosis may be successful even in extreme environments as *Cassiopea* is capable of maintaining less stress-tolerant species due to the buffering nature of the *Cassiopea* chemical microenvironment.

Summary

Cassiopea tissue exhibits optical properties similar to those previously identified in reef-building coral tissue. Both macroscale host anatomy and microscale structures play a role in modulating the internal light field experienced by the symbionts *via* light scattering. Precisely how these structures affect symbiont photosynthesis remains to be explored further. Furthermore, our microsensor measurements indicated a buffering of chemical dynamics in the thick mesoglea matrix of *Cassiopea* sp. medusae, suggesting that the internal physico-chemical microenvironment of the holobiont remains more constant when experiencing abrupt changes in light conditions. This is in strong contrast to the rapid

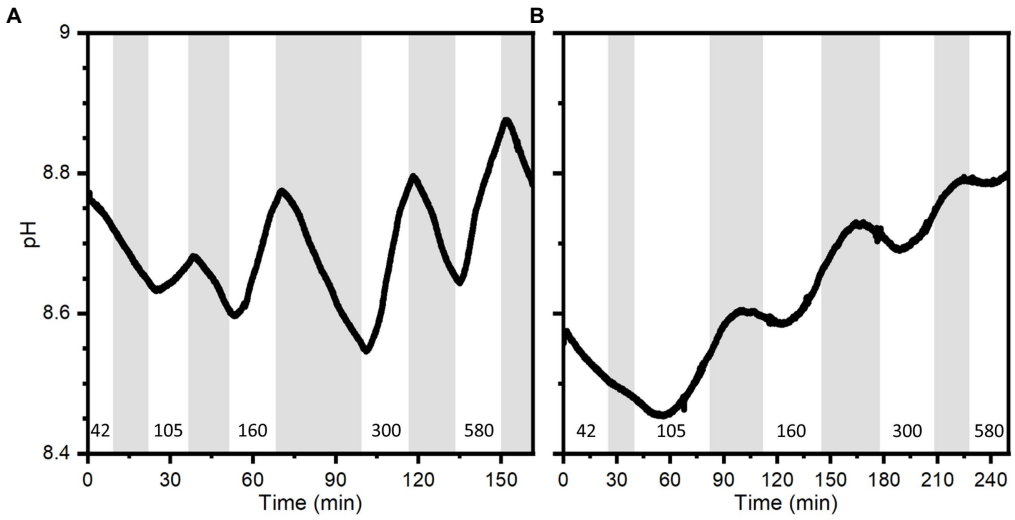

FIGURE 10
pH dynamics measured with a pH microsensor positioned at a depth of 1.6mm into the bell of a small medusa **(A)** and 2mm into the bell of a large medusa **(B)** during experimental light–dark shifts. Gray areas indicate dark shifts and white areas indicate photo periods of increasing incident photon irradiance (400–700nm) noted with numbers in units of µmol photons m^{-2} s^{-1}. Note difference in *x*-axes.

dynamics seen in coral tissue, which has a much thinner mesoglea and where the endosymbionts are found within endoderm cells. We hypothesize that the stabilization of the internal host microenvironment can be beneficial to the holobiont during unfavorable external environmental conditions such as hypoxia, where stored O_2 in the mesoglea might act as an important reserve for keeping internal homeostasis. This may also be key to the apparent success of *Cassiopea* to invade and persist in coastal tropical habitats with strong environmental fluctuations, that often preclude coral colonization. However, further studies are required to determine the effect of the buffering capacity of large individuals in combination with true environmental stressors over short and long periods.

Data availability statement

The original contributions presented in the study are included in the article/supplementary material, further inquiries can be directed to the corresponding author.

Author contributions

MM, NL, ET, and MK designed the experiment. MM, ET, and MK acquired data. MM, NL, ET, and MK analysed data. NL wrote the article with editorial help from all authors, who also approved the submitted version.

Funding

This study was supported by an Investigator award from the Gordon and Betty Moore Foundation (MK; Grant no. GBMF9206, https://doi.org/10.37807/GBMF9206) and the Swiss National Science Foundation (AM; Grant no. 200021_179092).

Acknowledgments

We thank Sofie Lindegaard Jakobsen for excellent technical assistance with keeping *Cassiopea* specimens used in this study.

Conflict of interest

The authors declare that the research was conducted in the absence of any commercial or financial relationships that could be construed as a potential conflict of interest.

Publisher's note

References

Aljbour, S. M., Zimmer, M., Al-Horani, F. A., and Kunzmann, A. (2019). Metabolic and oxidative stress responses of the jellyfish *Cassiopea* sp. to changes in seawater temperature. *J. Sea Res.* 145, 1–7. doi: 10.1016/j.seares.2018.12.002

Aljbour, S. M., Zimmer, M., and Kunzmann, A. (2017). Cellular respiration, oxygen consumption, and trade-offs of the jellyfish *Cassiopea* sp. in response to temperature change. *J. Sea Res.* 128, 6–97. doi: 10.1016/j.seares.2017.08.006

Anthony, K. R. N., and Hoegh-Guldberg, O. (2003). Variation in coral photosynthesis, respiration and growth characteristics in contrasting light microhabitats: an analogue to plants in forest gaps and understoreys? *Funct. Ecol.* 17, 246–259. doi: 10.1046/j.1365-2435.2003.00731.x

Arossa, S., Barozzi, A., Callegari, M., Klein, S. G., Parry, A. J., Hung, S.-H., et al. (2021). The internal microenvironment of the symbiotic jellyfish *Cassiopea* sp. from the Red Sea. *Front. Mar. Sci.* 8:705915. doi: 10.3389/fmars.2021.705915

Banha, T. N. S., Mies, M., Güth, A. Z., Pomory, C. M., and Sumida, P. Y. G. (2020). Juvenile *Cassiopea andromeda* medusae are resistant to multiple thermal stress events. *Mar. Biol.* 167:173. doi: 10.1007/s00227-020-03792-w

Bigelow, R. P. (1900). *The Anatomy and Development of Cassiopea xamachana*. Boston, MA: Boston Society of Natural History.

Biquand, E., Okubo, N., Aihara, Y., Rolland, V., Hayward, D. C., Hatta, M., et al. (2017). Acceptable symbiont cell size differs among cnidarian species and may limit symbiont diversity. *ISME J.* 11, 1702–1712. doi: 10.1038/ismej.2017.17

Blanquet, R. S., and Riordan, G. P. (1981). An ultrastructural study of the Subumbrellar musculature and Desmosomal complexes of *Cassiopea xamachana* (Cnidaria: Scyphozoa). *Trans. Am. Microsc. Soc.* 100, 109–119. doi: 10.2307/3225794

Bollati, E., Lyndby, N. H., D'Angelo, C., Kühl, M., Wiedenmann, J., and Wangpraseurt, D. (2022). Green fluorescent protein-like pigments optimise the internal light environment in symbiotic reef-building corals. *elife* 11:e73521. doi: 10.7554/eLife.73521

Brafield, A. E., and Chapman, G. (1983). Diffusion of oxygen through the Mesogloea of the sea anemone *Calliactis parasitica*. *J. Exp. Biol.* 107, 181–187. doi: 10.1242/jeb.107.1.181

Chan, N. C. S., Wangpraseurt, D., Kühl, M., and Connolly, S. R. (2016). Flow and coral morphology control coral surface pH: implications for the effects of ocean acidification. *Front. Mar. Sci.* 3:10. doi: 10.3389/fmars.2016.00010

Colley, N. J., and Trench, R. K. (1983). Selectivity in phagocytosis and persistence of symbiotic algae by the scyphistoma stage of the jellyfish *Cassiopeia xamachana*. *Proc. R. Soc. London. Ser. B. Biol. Sci.* 219, 61–82.

Colley, N. J., and Trench, R. K. (1985). Cellular events in the reestablishment of a symbiosis between a marine dinoflagellate and a coelenterate. *Cell Tissue Res.* 239, 93–103. doi: 10.1007/BF00214908

D'Angelo, C., Denzel, A., Vogt, A., Matz, M. V., Oswald, F., Salih, A., et al. (2008). Blue light regulation of host pigment in reef-building corals. *Mar. Ecol. Prog. Ser.* 364, 97–106. doi: 10.3354/meps07588

de Beer, D., Kühl, M., Stambler, N., and Vaki, L. (2000). A microsensor study of light enhanced Ca^{2+} uptake and photosynthesis in the reef-building hermatypic coral *Favia* sp. *Mar. Ecol. Prog. Ser.* 194, 75–85. doi: 10.3354/meps194075

Drew, E. A. (1972). The biology and physiology of alga-invertebrate symbioses. I. Carbon fixation in *Cassiopea* sp. at aldabra atoll. *J. Exp. Mar. Biol. Ecol.* 9, 65–69. doi: 10.1016/0022-0981(72)90007-X

Enríquez, S., Méndez, E. R., Hoegh-Guldberg, O., and Iglesias-Prieto, R. (2017). Key functional role of the optical properties of coral skeletons in coral ecology and evolution. *Proc. Biol. Sci.* 284:20161667. doi: 10.1098/rspb.2016.1667

Enriquez, S., Méndez, E. R., and Iglesias-Prieto, R. (2005). Multiple scattering on coral skeletons enhances light absorption by symbiotic algae. *Limnol. Oceanogr.* 50, 1025–1032. doi: 10.4319/lo.2005.50.4.1025

Estes, A. M., Kempf, S. C., and Henry, R. P. (2003). Localization and quantification of carbonic anhydrase activity in the symbiotic scyphozoan *Cassiopea xamachana*. *Biol. Bull.* 204, 278–289. doi: 10.2307/1543599

Falkowski, P. G., Dubinsky, Z., Muscatine, L., and Porter, J. W. (1984). Light and the bioenergetics of a symbiotic coral. *Bioscience* 34, 705–709. doi: 10.2307/1309663

Fitt, W. K. (1985). "Effect of different strains of the zooxanthella *Symbiodinium microadriaticum* on growth and survival of their coelenterate and molluscan hosts," in *Proceedings of The Fifth International Coral Reef Congress*. eds. C. Gabrie and M. Harmelin (Tahit), 131–136.

Freeman, C. J., Stoner, E. W., Easson, C. G., Matterson, K. O., and Baker, D. M. (2016). Symbiont carbon and nitrogen assimilation in the *Cassiopea-Symbiodinium* mutualism. *Mar. Ecol. Prog. Ser.* 544, 281–286. doi: 10.3354/meps11605

Gibbin, E. M., Putnam, H. M., Davy, S. K., and Gates, R. D. (2014). Intracellular pH and its response to CO_2-driven seawater acidification in symbiotic versus non-symbiotic coral cells. *J. Exp. Biol.* 217, 1963–1969. doi: 10.1242/jeb.099549

Goldfarb, A. J. (1914). "Changes in salinity and their effects upon the regeneration of *Cassiopea xamachana*," in Papers from the Tortugas Laboratory of the Carnegie Institution of Washington (Washington, DC: Carnegie Institution of Washington, pp. 83–94.

Hamaguchi, Y., Iida, A., Nishikawa, J., and Hirose, E. (2021). Umbrella of *Mastigias papua* (Scyphozoa: Rhizostomeae: Mastigiidae): hardness and cytomorphology with remarks on colors. *Plankton Benthos Res.* 16, 221–227. doi: 10.3800/pbr.16.221

Hofmann, D. K., Fitt, W. K., and Fleck, J. (1996). Checkpoints in the life-cycle of *Cassiopea* spp.: control of metagenesis and metamorphosis in a tropical jellyfish. *Int. J. Dev. Biol.* 40, 331–338.

Jacques, S. L., Wangpraseurt, D., and Kühl, M. (2019). Optical properties of living corals determined with diffuse reflectance spectroscopy. *Front. Mar. Sci.* 6:472. doi: 10.3389/fmars.2019.00472

Jimenez, I. M., Kühl, M., Larkum, A. W. D., and Ralph, P. J. (2008). Heat budget and thermal microenvironment of shallow-water corals: do massive corals get warmer than branching corals? *Limnol. Oceanogr.* 53, 1548–1561. doi: 10.4319/lo.2008.53.4.1548

Jimenez, I. M., Larkum, A. W. D., Ralph, P. J., and Kühl, M. (2012). Thermal effects of tissue optics in symbiont-bearing reef-building corals. *Limnol. Oceanogr.* 57, 1816–1825. doi: 10.4319/lo.2012.57.6.1816

Klein, S. G., Pitt, K. A., Lucas, C. H., Hung, S.-H., Schmidt-Roach, S., Aranda, M., et al. (2019). Night-time temperature reprieves enhance the thermal tolerance of a symbiotic cnidarian. *Front. Mar. Sci.* 6:453. doi: 10.3389/fmars.2019.00453

Klein, S. G., Pitt, K. A., Nitschke, M. R., Goyen, S., Welsh, D. T., Suggett, D. J., et al. (2017). *Symbiodinium* mitigate the combined effects of hypoxia and acidification on a noncalcifying cnidarian. *Glob. Chang. Biol.* 23, 3690–3703. doi: 10.1111/gcb.13718

Kramer, N., Tamir, R., Ben-Zvi, O., Jacques, S. L., Loya, Y., and Wangpraseurt, D. (2021). Efficient light-harvesting of mesophotic corals is facilitated by coral optical traits. *Funct. Ecol.* 36, 406–418. doi: 10.1111/1365-2435.13948

Kühl, M. (2005). Optical microsensors for analysis of microbial communities. *Meth Enzymol.* 397, 166–199. doi: 10.1016/S0076-6879(05)97010-9

Kühl, M., Cohen, Y., Dalsgaard, T., Jørgensen, B. B., and Revsbech, N. P. (1995). Microenvironment and photosynthesis of zooxanthellae in scleractinian corals studied with microsensors for O_2, pH and light. *Mar. Ecol. Prog. Ser.* 117, 159–172. doi: 10.3354/meps117159

Lampert, K. P. (2016). "Cassiopea and its zooxanthellae," in *The Cnidaria, Past, Present and Future*. eds. S. Goffredo and Z. Dubinsky (Cham: Springer), 415–423.

Lawley, J. W., Carroll, A. R., and McDougall, C. (2021). Rhizostomins: a novel pigment family from Rhizostome jellyfish (Cnidaria, Scyphozoa). *Front. Mar. Sci.* 8:752949. doi: 10.3389/fmars.2021.752949

Lesser, M. P., and Farrell, J. H. (2004). Exposure to solar radiation increases damage to both host tissues and algal symbionts of corals during thermal stress. *Coral Reefs* 23, 367–377. doi: 10.1007/s00338-004-0392-z

Lyndby, N. H., Holm, J. B., Wangpraseurt, D., Ferrier-Pagès, C., and Kühl, M. (2019). Bio-optical properties and radiative energy budgets in fed and unfed scleractinian corals (*Pocillopora* sp.) during thermal bleaching. *Mar. Ecol. Prog. Ser.* 629, 1–17. doi: 10.3354/meps13146

Lyndby, N. H., Radecker, N., Bessette, S., Jensen, L. H. S., Escrig, S., Trampe, E., et al. (2020). Amoebocytes facilitate efficient carbon and nitrogen assimilation in the *Cassiopea*-Symbiodiniaceae symbiosis. *Proc. R. Soc. B* 287:20202393. doi: 10.1098/rspb.2020.2393

Madshus, I. H. (1988). Regulation of intracellular pH in eukaryotic cells. *Biochem. J.* 250, 1–8. doi: 10.1042/bj2500001

Marcelino, L. A., Westneat, M. W., Stoyneva, V., Henss, J., Rogers, J. D., Radosevich, A., et al. (2013). Modulation of light-enhancement to symbiotic algae by light-scattering in corals and evolutionary trends in bleaching. *PLoS One* 8:e61492. doi: 10.1371/journal.pone.0061492

Medina, M., Sharp, V., Ohdera, A., Bellantuono, A., Dalrymple, J., Gamero-Mora, E., et al. (2021). "The upside-down jellyfish *Cassiopea xamachana* as an emerging model system to study cnidarian–algal symbiosis" in *Handbook of Marine Model Organisms in Experimental Biology* (Boca Raton, FL: CRC Press), 149–171.

Mills, C. E. (2001). Jellyfish blooms: are populations increasing globally in response to changing ocean conditions? *Hydrobiologia* 451, 55–68. doi: 10.1023/A:1011888006302

Morandini, A. C., Stampar, S. N., Maronna, M. M., and Da Silveira, F. L. (2017). All non-indigenous species were introduced recently? The case study of *Cassiopea* (Cnidaria: Scyphozoa) in Brazilian waters. *J. Mar. Biol. Assoc. U. K.* 97, 321–328. doi: 10.1017/S0025315416000400

Murthy, S., Picioreanu, C., and Kühl, M. (2023). Modeling the radiative, thermal and chemical microenvironment of 3D scanned corals. *bioRXiv [Preprint]*. doi: 10.1101/2023.01.31.526450

Muscatine, L., Mccloskey, L. R., and Marian, R. E. (1981). Estimating the daily contribution of carbon from zooxanthellae to coral animal respiration. *Limnol. Oceanogr.* 26, 601–611. doi: 10.4319/lo.1981.26.4.0601

Palmer, D. A., and Van Eldik, R. (1983). The chemistry of metal carbonato and carbon dioxide complexes. *Chem. Rev.* 83, 651–731. doi: 10.1021/cr00058a004

Rickelt, L. F., Lichtenberg, M., Trampe, E. C. L., and Kühl, M. (2016). Fiber-optic probes for small-scale measurements of scalar irradiance. *Photochem. Photobiol.* 92, 331–342. doi: 10.1111/php.12560

Rowen, D. J., Templeman, M. A., and Kingsford, M. J. (2017). Herbicide effects on the growth and photosynthetic efficiency of *Cassiopea maremetens*. *Chemosphere* 182, 143–148. doi: 10.1016/j.chemosphere.2017.05.001

Schoenberg, D. A., and Trench, R. K. (1980). Genetic variation in *Symbiodinium* (=*Gymnodinium*) microadriaticum Freudenthal, and specificity in its Symbiosis with marine invertebrates. II. Morphological variation in Symbiodinium microadriaticum. *Proc. Roy. Soc. B* 207, 429–444.

Smith, F. A., and Raven, J. A. (1979). Intracellular pH and its regulation. *Annu. Rev. Plant Physiol.* 30, 289–311. doi: 10.1146/annurev.pp.30.060179.001445

Stoner, E. W., Layman, C. A., Yeager, L. A., and Hassett, H. M. (2011). Effects of anthropogenic disturbance on the abundance and size of epibenthic jellyfish *Cassiopea* spp. *Mar. Pollut. Bull.* 62, 1109–1114. doi: 10.1016/j.marpolbul.2011.03.023

Taylor Parkins, S. K., Murthy, S., Picioreanu, C., and Kühl, M. (2021). Multiphysics modelling of photon, mass and heat transfer in coral microenvironments. *J. R. Soc. Interface* 18:20210532. doi: 10.1098/rsif.2021.0532

Thuesen, E. V., Rutherford, L. D., Brommer, P. L., Garrison, K., Gutowska, M. A., and Towanda, T. (2005). Intragel oxygen promotes hypoxia tolerance of scyphomedusae. *J. Exp. Biol.* 208, 2475–2482. doi: 10.1242/jeb.01655

Veal, C. J., Carmi, M., Dishon, G., Sharon, Y., Michael, K., Tchernov, D., et al. (2010). Shallow-water wave lensing in coral reefs: a physical and biological case study. *J. Exp. Biol.* 213, 4304–4312. doi: 10.1242/jeb.044941

Verde, E. A., and McCloskey, L. R. (1998). Production, respiration, and photophysiology of the mangrove jellyfish *Cassiopea xamachana* symbiotic with zooxanthellae: effect of jellyfish size and season. *Mar. Ecol. Prog. Ser.* 168, 147–162. doi: 10.3354/meps168147

Wangpraseurt, D., Holm, J. B., Larkum, A. W. D., Pernice, M., Ralph, P. J., Suggett, D. J., et al. (2017). *In vivo* microscale measurements of light and photosynthesis during coral bleaching: evidence for the optical feedback loop? *Front. Microbiol.* 8:59. doi: 10.3389/fmicb.2017.00059

Wangpraseurt, D., Jacques, S., Lyndby, N., Holm, J. B., Pages, C. F., and Kühl, M. (2019). Microscale light management and inherent optical properties of intact corals studied with optical coherence tomography. *J. R. Soc. Interface* 16:20180567. doi: 10.1098/rsif.2018.0567

Wangpraseurt, D., Larkum, A. W. D., Franklin, J., Szabó, M., Ralph, P. J., and Kühl, M. (2014a). Lateral light transfer ensures efficient resource distribution in symbiont-bearing corals. *J. Exp. Biol.* 217, 489–498. doi: 10.1242/jeb.091116

Wangpraseurt, D., Larkum, A. W. D., Ralph, P. J., and Kühl, M. (2012). Light gradients and optical microniches in coral tissues. *Front. Microbiol.* 3:316. doi: 10.3389/fmicb.2012.00316

Wangpraseurt, D., Polerecky, L., Larkum, A. W. D., Ralph, P. J., Nielsen, D. A., Pernice, M., et al. (2014b). The *in situ* light microenvironment of corals. *Limnol. Oceanogr.* 59, 917–926. doi: 10.4319/lo.2014.59.3.0917

Welsh, D. T., Dunn, R. J. K., and Meziane, T. (2009). Oxygen and nutrient dynamics of the upside down jellyfish (*Cassiopea* sp.) and its influence on benthic nutrient exchanges and primary production. *Hydrobiologia* 635, 351–362. doi: 10.1007/s10750-009-9928-0

frontiers | Frontiers in Ecology and Evolution

TYPE Original Research
PUBLISHED 20 April 2023
DOI 10.3389/fevo.2023.1152183

OPEN ACCESS

EDITED BY
Jennifer L. Matthews,
University of Technology Sydney, Australia

REVIEWED BY
Daniel Powell,
University of the Sunshine Coast, Australia
Jarosław Bryk,
University of Huddersfield, United Kingdom

*CORRESPONDENCE
Rita Rebollo
✉ rita.rebollo@inrae.fr
Anna Zaidman-Rémy
✉ anna.zaidman@insa-lyon.fr

†These authors have contributed equally to this work

SPECIALTY SECTION
This article was submitted to Coevolution, a section of the journal Frontiers in Ecology and Evolution

RECEIVED 27 January 2023
ACCEPTED 20 March 2023
PUBLISHED 20 April 2023

CITATION
Vallier A, Dell'Aglio E, Ferrarini MG, Hurtado O, Vincent-Monégat C, Heddi A, Rebollo R and Zaidman-Rémy A (2023) Transcriptomic-based selection of reference genes for quantitative real-time PCR in an insect endosymbiotic model. *Front. Ecol. Evol.* 11:1152183. doi: 10.3389/fevo.2023.1152183

Transcriptomic-based selection of reference genes for quantitative real-time PCR in an insect endosymbiotic model

Agnès Vallier†, Elisa Dell'Aglio†, Mariana Galvão Ferrarini, Ophélie Hurtado, Carole Vincent-Monégat, Abdelaziz Heddi, Rita Rebollo* and Anna Zaidman-Rémy*

Université de Lyon, INRAE, INSA Lyon, BF2I, UMR 203, Villeurbanne, France

Reference genes are a fundamental tool for analyses of gene expression by real-time quantitative PCR (qRT-PCR), in that they ensure the correct comparison between conditions, stages, or treatments. Because of this, selection of appropriate genes to use as references is crucial for proper application of the technique. Nevertheless, efforts to find appropriate, stably expressed transcripts are still lacking, in particular in the field of insect science. Here, we took advantage of a massive transcriptomic high-throughput analysis of various developmental stages of the gut and associated-bacteriomes of the cereal weevil *Sitophilus oryzae* and identified a subset of stably expressed genes with the potential to be used as housekeeping genes from the larva to the adult stage. We employed several normalization techniques to select the most suitable genes among our subset. Our final selection includes two genes–*TAO*, and *YTH3*–which can also be used to compare transcript abundance at various developmental stages in symbiotic insects, and in insects devoid of endosymbionts (aposymbiotic). Since they are well conserved, these genes have the potential to be useful for many other insect species. This work confirms the interest in using large-scale, unbiased methods for reference gene selection.

KEYWORDS

real-time PCR, insect, symbiosis, transcriptomic, normalization

1. Introduction

Although high-throughput transcriptomic analyses are becoming more affordable and accessible, analysis of a subset of transcripts with quantitative real-time PCR (qRT-PCR) (Higuchi et al., 1992) is still routinely required in laboratory practice, exploratory experiments, experimental validations as well as diagnostics protocols (Kubista et al., 2006). The instrumentation for qRT-PCR is common in molecular biology facilities, along with established guidelines [MIQE guidelines (Bustin et al., 2009)], making it a highly affordable and reliable technique. However, the qRT-PCR accuracy relies on the use of a control method for data normalization that is often achieved by comparing the expression level of target genes against stably expressed transcripts from so-called reference genes, housekeeping genes or constitutively expressed genes. These transcripts must be stably expressed in the

biological samples and experimental conditions that are tested, in order to be used as a comparison to evaluate changes in the expression of the transcripts of interest.

Hence, an appropriate set of qRT-PCR reference genes must be established for each experimental condition, species and tissue examined (Bustin et al., 2009). However, historically, only a small group of highly stably expressed genes has been used and tested in various conditions and species. A review summarizing recent work on reference genes in 78 insect species from 2008 to 2017 has shown that the majority of reports focused on the same gene candidates, including *Actin, Tubulin, Glyceraldehyde 3-phosphate dehydrogenase* (*GAPDH*) and the ribosomal gene *18S* (Lü et al., 2018). All these genes displayed great stability and high expression levels in various experimental conditions, tissues and species, but none appeared to be a universal "passe-partout," as highlighted now that transcriptomic analyses are routinely employed in different tissues and at different developmental stages. For example, *GAPDH* (Dveksler et al., 1992) often shows stable expression between insect tissues and treatments but is not often adapted for comparisons between developmental stages (Fu et al., 2013; Pan et al., 2015).

Since the production of transcriptomic data is becoming more and more affordable, it is now possible to choose the best set of reference genes for each species, condition, and treatment, by comparing whole transcriptomes instead of limiting the choice to a set of potential candidates. Examples of this non-aprioristic process are already available for various organisms, including plants (Yim et al., 2015; Liang et al., 2020; Lopes et al., 2021), mammals (Zhang et al., 2020), and human tissues (Caracausi et al., 2017), but not yet for insects, notably, Coleoptera. Around 400 thousand Coleoptera species have been described to date, including terrestrial and aquatic species (Zhang, 2013; Zhang et al., 2018). True weevils, or Curculionidae, are one of the largest animal families and include major agronomic pests, such as the cereal weevil (*Sitophilus* spp.), which is responsible for important damage to fields and stored grains (Longstaff, 1981).

As most insects thriving on a nutritionally unbalanced diet, *S. oryzae* shares a symbiotic relationship with an intracellular Gram-negative bacterium called *Sodalis pierantonius* (Mansour, 1930; Heddi et al., 1999; Oakeson et al., 2014). *S. pierantonius* is housed within specific host cells, the bacteriocytes, forming a unique bacteriome organ attached to the gut during all larval stages (Pierantoni, 1927; Mansour, 1930). Throughout *S. oryzae*'s metamorphosis, the bacteriocytes migrate along the midgut and endosymbionts subsequently infect cells in the apexes of gut caeca (Maire et al., 2020). These coordinated changes result in the formation of multiple bacteriomes along the midgut by the completion of metamorphosis. In these bacteriomes, endosymbionts exponentially increase in number in the emerging adult, before being recycled by an apoptotic-autophagic mechanism following the first week of adult life (Vigneron et al., 2014). Analyzing transcriptomic regulations across weevil's development is required to fully understand *S. oryzae* and *S. pierantonius* relationship, and to uncover key pathways profitable for integrative pest management strategies. We have recently conducted a thorough analysis of the gut (and associated bacteriomes) transcriptome of *S. oryzae* across its development from larval stages up to bacterial clearance in adults (**Figure 1**; Ferrarini et al., 2023). In this work, we took advantage of the recent transcriptomic profile of *S. oryzae* during development (Ferrarini et al., 2023) to select a set of reliable reference genes for qRT-PCR analyses, with high stability and conservation among insects. The identified transcripts will be of use for the comparison of transcript abundance across multiple developmental stages in *S. oryzae*, gene silencing conditions, and comparisons with artificially obtained aposymbiotic weevils. These genes also have a great potential for being suitable reference transcripts in other insects, as well as in many other eukaryotes.

2. Materials and methods

2.1. Insect rearing and sampling

The symbiotic *S. oryzae* population was sampled in Azergues valley, France in 1984, and has been reared in laboratory conditions ever since. The aposymbiotic strain was obtained by heat treatment in 2010, following a protocol described previously (Nardon, 1973). *S. oryzae* symbiotic and artificially obtained aposymbiotic weevils were reared in a climate chamber (27.5°C, 70% relative humidity, no light source) on wheat grains as a food source and substrate for egg laying. In these conditions, the timespan between egg laying and the emergence of adults from the grain is 1 month for symbiotic weevils, and 5 weeks for aposymbiotic ones. Adults emerging from the grain are fully formed, although their cuticle is reinforced during the 5 days following emergence from the grain, together with sexual maturation (Maire et al., 2019). The time between the end of metamorphosis and emergence has been calculated to be around 3 days (Vigneron et al., 2014). Since our studies are mainly focused on *S. oryzae* transcript levels in the gut, from larval stages to the symbiotic clearance (around day 9 of adulthood), we tested candidate reference genes on gut samples (which contains the bacteriomes) harvested from the last larval stage (L4) to day 9 of adulthood (D9), including pupae (P), and intermediate adult stages (D1, D3, D5, and D7).

For sampling, weevils were immersed in buffer TA (35 mM Tris/HC_l, 25 mM KC_l, 10 mM $MgCl_2$, 250 mM sucrose, pH 7.5) and dissected under a stereomicroscope. Three biological samples per time point were collected, each composed of five guts and their bacteriomes. All samples were collected on ice in 1.5 mL RNAse-free tubes and stored at −80°C until use.

2.2. Transcriptomic analysis

RNAseq datasets were processed in our previous publication (Ferrarini et al., 2023), and raw reads are available at BioProject PRJNA918957. Briefly, quality check was performed with FastQC v0.11.8 (Andrews, 2010), and raw reads were quality trimmed using trim_galore from Cutadapt v0.6.7 (Martin, 2011), then mapped to the *S. oryzae*'s genome (GCA_002938485.2 Soryzae_2.0) using STAR v2.7.3a (Dobin et al., 2013). Then, uniquely mapping reads were counted with featureCounts v2.0.1 (Liao et al., 2014), and mapping quality was assessed by multiqc v1.13 (Ewels et al., 2016). Differential expression analysis was conducted with SarTOOLS, taking advantage of a global linear model from Deseq2 (Love et al., 2014, 2), and log2 fold changes and adjusted *p*-values were obtained for sequential pairwise comparisons, i.e., L4 vs. D1, D1 vs. D3 etc.,

TABLE 1 candidate reference genes.

Accession name	Gene ID	Gene annotation	Gene function	References
LOC115875935	*TAO*	Serine/threonine-protein kinase Tao	G-protein signaling cascade, regulates DNA damage response, apoptosis and cytoskeleton	Hutchison et al., 1998; Timm et al., 2006
LOC115876598	*RAP1*	Ras-related protein Rap1	Small GTPase, regulates cell adhesion, cell junction formation, and integrin-mediated signaling	Caron, 2003
LOC115877543	*YTH3*	YTH domain-containing family protein 3	Transcriptional regulator involved in the degradation of N6-methyladenosine (m6A)-containing mRNA and non-coding RNAs	Zaccara and Jaffrey, 2020
LOC115882250	*PAN3*	PAN (Poly-A Nuclease)2-PAN3 deadenylation complex subunit Pan3	Transcriptional regulator, part of a poly-A degradation complex	Brown et al., 1996; Garneau et al., 2007
LOC115883196	*KIAA*	Transmembrane protein KIAA1109 homolog	Synaptic development and function, regulation of regulating synaptic plasticity	Kursula, 2014
LOC115889772	*CYCT1*	Cyclin-T1	Subunit of the positive transcription elongation factor b (P-TEFb), promotes RNA polymerase II transcription elongation	Shim et al., 2002
LOC115890036	*PP12A*	Protein phosphatase 1 regulatory subunit 12A	Subunit of the myosin phosphatase complex responsible for the interaction between actin and myosin	Takahashi et al., 1997; Hughes et al., 2020
LOC115890441	*PP43*	Serine/threonine-protein phosphatase 4 regulatory subunit 3	Ser/Thr phosphatase conserved in yeasts, mammals, insects, plants	Gingras et al., 2005; Kataya et al., 2017; Karman et al., 2020
LOC115891122	*TFIIF*	General transcription factor IIF subunit 1	Transcription initiation factor, part of the pre-initiation complex	Aso et al., 1992; Luse, 2012
LOC115881082	*GAPDH*	Glyceraldehyde 3-phosphate dehydrogenase	Glycolysis, gene regulation and DNA repair	Sirover, 1999
LOC115890765	*SYN1A*	Syntaxin-1	Intracellular vesicle traffic, synaptic vesicle fusion	Zhou et al., 2000

and can be found in the Supplementary material of our previous report (Ferrarini et al., 2023). Most graphic outputs are either performed in R, using ggplot2 (Wickham, 2009) or with GraphPad Prism software.

2.3. Primer design for candidate reference genes

Primers for each candidate reference gene and *GAPDH* were designed with Primer3 software (Kõressaar et al., 2018, 3), with "best annealing" at 55°C, amplicon length between 70 and 120 nucleotides (**Table 2**). Forward and reverse primers were always located in two different exons in order to span at least one intron. In the case of multiple predicted isoforms for each transcript, the primers were designed so that they could amplify all of them. Primer sequences were checked by BLAST (Camacho et al., 2009) to ensure their specificity in the target genome.

2.4. RNA extraction and transcript amplification

Total RNA was purified from samples using the RNAqueous Micro kit (Ambion) and its DNAse treatment, following the manufacturer's instructions. Final RNA concentration was measured with a Nanodrop® spectrophotometer (Thermo Scientific), and RNA quality was checked using agarose gel electrophoresis. Reverse transcription to cDNA was carried out using the iScript cDNA Synthesis Kit (Bio-Rad), which relies on a blend of oligo(dT) and random primers. Reverse transcription was performed starting from 1 µg of total RNA. Transcript amplification by qRT-PCR was performed with a CFX Connect Real-Time detection system (Bio-Rad) using the LightCycler Fast Start DNA Master SYBR Green I kit (Roche Diagnostics) as previously described (Maire et al., 2019). Each reaction contained 5 µl of Master Sybr Green mix, 0.5 µl of each primer (10 µM), 1.5 µl RNAse Free water, and 2.5 µl of 1:5 diluted cDNA. Primers for amplification are listed in **Table 2**. After 5 min at 95°C, the cycling conditions were: 45 cycles at 95°C for 10 s, 56°C for 20 s, and 72°C for 30 s. A melting curve was obtained at the end of each PCR by heating for 30 s at 66°C, then increasing the temperature up to 95°C (increment rates of 0.11°C/s). For every candidate gene, three biological and two technical replicates were tested for each developmental stage, together with a standard curve made with PCR products as templates, at concentrations spanning from 0.2 fg/µl to 2 pg/µl of amplicon, to calculate the reaction efficiency and ensure linearity of the amplification. The data from each transcript were collected within the same plate.

10.3389/fevo.2023.1152183

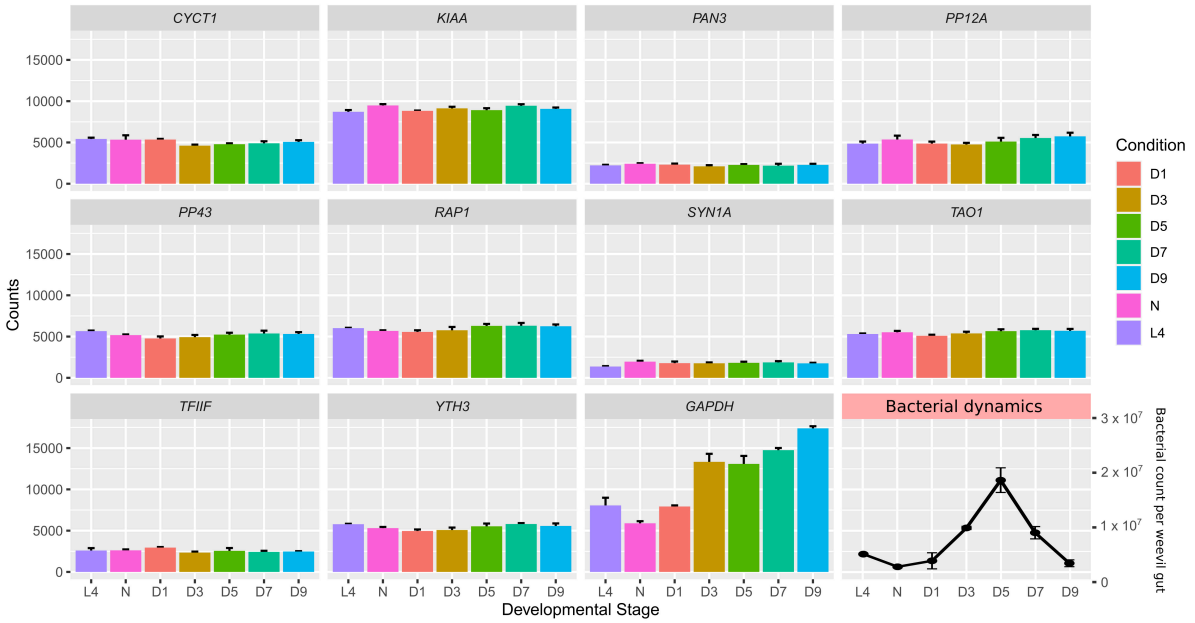

FIGURE 1

Expression profile of all candidate housekeeping genes in *Sitophilus oryzae* gut-bacteriome samples analyzed by transcriptomics at various developmental stages. L4: larval stage 4; P: pupae; D1: 1-day-old adults; D3: 3-day-old adults; D5: 5-day-old adults; D7: 7-day-old adults; D9: 9-day-old adults. Data represent normalized counts at each developmental stage (Ferrarini et al., 2023). Error bars represent standard deviation. Bacterial dynamics is represented in the bottom right corner, adapted from Dell'Aglio et al. (2023).

TABLE 2 Primers and amplification parameters used for each candidate reference gene selected for qRT-PCR normalization.

Gene name	Locus	Primer sequences (FW and REV)	Tm FW/REV (°C)	Amplicon length (bp)	Average Ct	Efficiency (%)	R^2
CYCT1	LOC115889772	CAGGACATGGGGCAAAGACTA	59.72	102	25.66	96.5	1
		TGGGAAGTCAGTGAAGGAGTG	59.31				
KIAA	LOC115883196	CCGCATCATTGCGGGTAAAA	59.55	100	38.01	61.6	0.999
		GAACTAGCGCTGGGTAACGA	59.83				
PAN3	LOC115882250	AGTTGACAGTTACCACGAGCTT	59.90	91	26.03	91.3	1
		GTACATGGAGGCCTGATAGCC	60.00				
PP12A	LOC115890036	TGCTCAAGGACGAGATTCGG	59.83	97	24.00	96.2	0.999
		GCCAACCATTCTTTGGCGTC	60.39				
PP43	LOC115890441	GCGCCGGATATTGGTTCTGA	60.53	89	24.23	95.5	1
		CCTTGAGGGCGACCAGTTT	59.93				
RAP1	LOC115876598	CGGCATCGCCCGATACAA	60.28	107	32.57	78.4	1
		CCCCCTGACCCAAGTACTACA	60.95				
SYNT1	LOC115890765	ACAGGGAGAGGTGTAAAGCG	59.39	109	27.60	94.4	1
		AAGACGGTAGAAGTTCCTTGTTCT	59.66				
TAO	LOC115875935	CGGTTCATTCTGTTGGGGTGT	60.82	94	24.09	94.4	1
		TTCGTTGTTCCATCCTCGCC	60.67				
TFIIF	LOC115891122	GACCCGATGATCAGCCTTGG	60.53	92	24.67	97.1	1
		TGTGTTTTCTGAGACACCCCC	60.13				
YTH3	LOC115877543	GAATTCAGCAGCTCATCCAGC	59.67	101	24.82	91.2	1
		ATGTTCCTCCACTGCCATAATAAC	58.87				
GAPDH	LOC115881082	TGACCGTCAGGTTAGGCAAA	59.24	94	20.03	96.9	1
		TAGCCCAGGATGCCCTTCA	60.31				

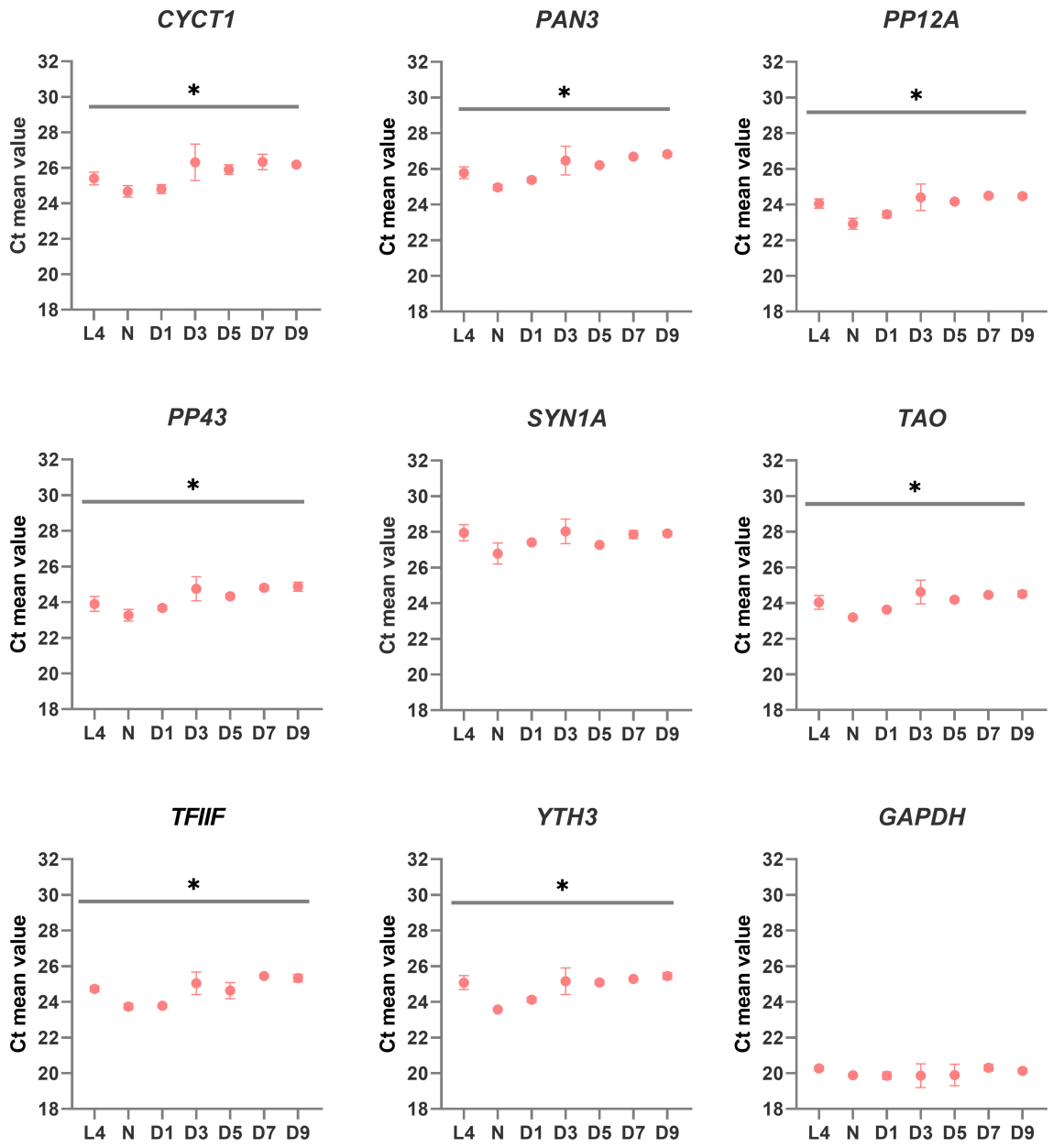

FIGURE 2
Quantitative real-time PCR (qRT-PCR) expression profile of candidate reference genes in *Sitophilus oryzae* gut-bacteriome samples. Graphs represent the mean Ct value for each developmental stage. One-way ANOVA was performed to assess differences between the means of all developmental stages. Asterisks denote statistical significance (ANOVA with Kruskal-Wallis test, $^*p \leq 0.05$). Error bars represent standard deviation.

2.5. Candidate reference gene comparisons

To evaluate the reliability of each candidate reference gene, we compared the average cycle threshold (Ct) of each developmental stage and the percentage covariance (CV%) value for each gene (Boda et al., 2009; Sundaram et al., 2019). We then compared the rankings of various web-based algorithms: GeNorm (Vandesompele et al., 2002), the ΔCt method (Silver et al., 2006), BestKeeper (Pfaffl et al., 2004), and Reffinder (Xie et al., 2012). Each candidate reference gene was compared, ranked and evaluated through the tools described.

3. Results and discussion

3.1. Choice of candidate reference genes based on transcriptome data

To find *S. oryzae* reference genes to be used across gut and bacteriomes development (from larval stage 4 to 9-day-old adults), we scanned a comprehensive transcriptomic dataset spanning *S. oryzae* life cycle (Ferrarini et al., 2023). Candidate reference genes should be stable between conditions, highly expressed, and present transcript isoforms suitable for primer design. There are 17 957 genes in *S. oryzae* (Parisot et al., 2021) and our previous analysis

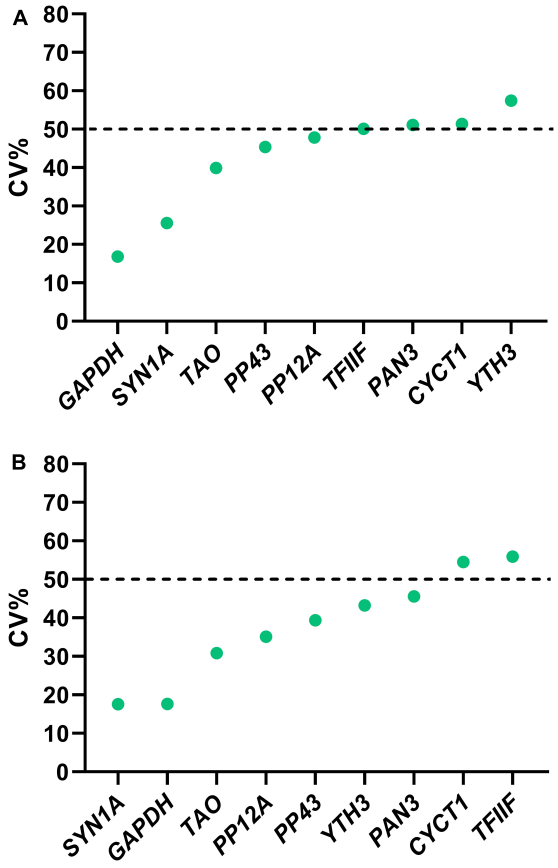

FIGURE 3
CV% values for the selected candidate reference genes, calculated on the linearized 2-Ct converted Ct values at all *Sitophilus oryzae* developmental stages considered in **Figure 2**. **(A)** CV% measured considering all developmental stages. **(B)** CV% calculated considering only adult stages. Only genes with a CV% lower than 50 were selected for further analysis.

showed that 11 908 were differentially expressed between sequential conditions (Ferrarini et al., 2023). In order to find stable genes across development, we removed genes presenting an adjusted p-value < 0.05 between time points (∼1 500 remaining genes), along with a significant log2 fold change lower than −1 or higher than 1 between two consecutive stages, yielding 100 candidate genes. A selection was made by prioritizing highly expressed genes (mean expression level higher than 1000), in order to improve qRT-PCR detection, decreasing the candidate list to only 19 genes. Among the resulting pre-selected 19 genes, we visually selected those with the most steady expression along the development. We eliminated genes encoding regulators, which are more likely to change in expression according to the experimental conditions. Among the remaining genes, we avoided uncharacterized genes, abundant in the *S. oryzae* genome. These filtering steps resulted in selecting nine potential reference genes for experimental validation (**Table 1** and **Figure 1**). The selected genes spanned various predicted biological functions, to reduce the risk of co-regulation among them and to facilitate the future use of the same genes in other organisms.

Finally, we also included *GAPDH*, a very common reference gene in our model and similar model organisms, and the homolog of syntaxin-1 (*SYN1A*), a protein involved in intracellular vesicle traffic, especially in neurons (Zhou et al., 2000), previously selected as a suitable reference gene by Lord et al. (2010) for *Tribolium castaneum*, the most widely studied member of Coleoptera. These genes were included in the study as a point of comparison for the newly selected genes. Both genes showed little variation between time points (**Figure 1**). Altogether, a set of 11 candidate genes were then submitted for further analysis.

3.2. Expression profiles of candidate reference genes

While the transcriptomic analysis suggests the candidate genes are stable across *S. oryzae*'s gut development, it is important to verify that it is indeed possible to amplify such transcripts in an accurate manner by qRT-PCR. A preliminary PCR test allowed amplification of all predicted transcripts from gut cDNA pools, obtaining fragments compatible with the predicted amplicon sizes. Subsequent qRT-PCR quantification from gut samples (larval stage L4, pupal stage P, and adult stages D1, D3, D5, D7, and D9) was successful for nine out of eleven genes, leading to acceptable efficiency and linearity (**Table 2**). Two exceptions were the primers for *KIAA* and *RAP1*, which did not lead to acceptable fragment amplification under standard conditions (efficiency values of 61.6 and 78.4, respectively; average Ct values of 38.01 and 32.58, respectively); and were therefore excluded from the list of potential candidates (**Table 2**). Moreover, although successful, *YTH3* expression levels appear lower than expected based on the transcriptomic analysis. Discrepancies between amplification in qRT-PCR and normalized read counts could be due to low primer efficiency, a tendency to primer dimerization, or suboptimal amplification of transcripts in our standardized qRT-PCR protocol, as well as differences in normalization strategies between the two techniques. One should also note that for qRT-PCR, larval samples consisted of bacteriomes and whole guts, while in the previous transcriptomic dataset on which the candidate reference gene selection was based, only larval bacteriomes were dissected (Ferrarini et al., 2023).

The mean Ct values of amplicons for each candidate reference gene at each developmental stage are reported in **Figure 2**. The gene with the lowest average Ct was *GAPDH* (mean for all stages: 20.0), followed by *PP12A* (mean for all stages: 23.99) and *PP43* (mean for all stages: 24.66). All average Ct values are considered low (*GAPDH*) or medium (all other genes) and are therefore suitable for estimating gene expression of various target genes with different expression profiles. Statistical analysis of Ct values revealed that the mean expression level for the majority of the genes is subjected to mild variations between developmental stages (see asterisks in **Figure 2**), except for *GAPDH* and *SYN1A*.

3.3. Evaluation of expression stability and ranking of candidate reference genes

To identify the most suitable reference gene to compare transcript expression across *S. oryzae* development, we relied on the comparison of statistical methods recently conducted by

TABLE 3 Ranking of candidate reference genes for various *Sitophilus oryzae* developmental stages, according to the ΔCt method, BestKeeper, NormFinder, GeNorm, and Reffinder.

	ΔCt		BestKeeper		NormFinder		GeNorm		Reffinder	
Rank	Gene name	Mean st. dev.	Gene name	R	Gene name	SV	Gene name	M	Gene name	GM
1	TAO	0.378	SYN1A	0.245	TAO	0.189	TAO	0.378	TAO	1,189
2	SYN1A	0.460	TAO	0.408	SYN1A	0.309	SYN1A	0.378	SYN1A	1,414
3	PP12A	0.505	PP43	0.490	PP12A	0.398	PP43	0.415	PP43	3,464
4	PP43	0.505	GAPDH	0.490	PP43	0.398	PP12A	0.448	PP12A	3,663
5	GAPDH	0.505	PP12A	0.612	GAPDH	0.398	GAPDH	0.471	GAPDH	4,729

The rankings were obtained for all developmental stages. SV, stability value; GM, geomean of ranking values.

TABLE 4 Ranking of candidate reference genes for various *Sitophilus oryzae* developmental stages, according to the ΔCt method, BestKeeper, NormFinder, GeNorm, and Reffinder.

	ΔCt		BestKeeper		NormFinder		GeNorm		Reffinder	
Rank	Gene name	Mean st. dev.	Gene name	Stability	Gene name	SV	Gene name	M	Gene name	GM
1	TAO	0.396	SYN1A	0.245	TAO	0.178	YTH3	0.00	TAO	1,682
2	YTH3	0.4	TAO	0.408	YTH3	0.282	PP12A	0.00	YTH3	2,115
3	PP12A	0.4	PP43	0.490	PP12A	0.282	PAN3	0.252	PP12A	2,711
4	PAN3	0.474	GAPDH	0.490	SYN1A	0.343	TAO	0.333	SYN1A	3,162
5	SYN1A	0.477	YTH3	0.612	PAN3	0.356	SYN1A	0.389	PAN3	4,527
6	PP43	0.496	PP12A	0.612	PP43	0.382	PP43	0.419	PP43	5,045
7	GAPDH	0.548	PAN3	0.653	GAPDH	0.461	GAPDH	0.456	GAPDH	6,086

The rankings were obtained for adult stages only. SV, stability value; GM, geomean of ranking values.

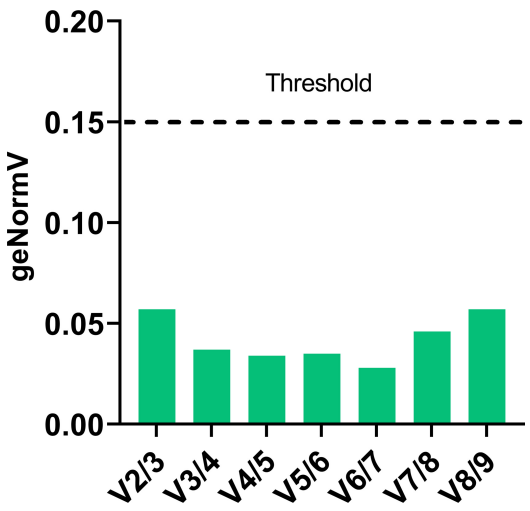

FIGURE 4
Optimal number of reference genes for normalization in *S. oryzae* at various developmental stages. The pairwise variation values obtained from GeNorm analyses were used to determine the minimum number of reference genes for normalization. The value of Vn/Vn + 1 < 0.15 indicates that the minimum number of reference genes to be used for qPCR data normalization is n.

Sundaram et al. (2019). After describing the merits and limitations of various comparison algorithms, the authors suggested the following as the best pipeline for the identification of reliable reference genes: (i) visual estimation of expression variation across stages, (ii) analysis of CV% values [(Boda et al., 2009); a cut-off of 50 is recommended]; and (iii) ranking of the remaining candidate reference genes by the NormFinder algorithm (Andersen et al., 2004).

Since the visual estimation of expression variation across stages was already performed and showed mild variation for most genes (**Figure 2**), we calculated the CV% value for each candidate reference gene. The CV% values of four out of nine genes (*YTH3*, *CYCT1*, *PAN3*, and *TFIIF*) across all developmental stages are indeed higher than 50 (**Figure 3A**), reflecting variations observed in particular at the pupal stage (**Figure 2**). When only adult stages were considered (**Figure 3B**), only two genes still displayed CV% values higher than 50 (*CYCT1* and *TFIIF*). After excluding genes with CV% higher than 50, we ran the NormFinder algorithm together with other common reference gene ranking algorithms: GeNorm (Vandesompele et al., 2002), the ΔCt method (Silver et al., 2006), BestKeeper (Pfaffl et al., 2004), and Reffinder (Xie et al., 2012). To note, all ranking systems used here are relative to the set of genes that have been chosen and input in the system. Hence, the important information here is the rank that the genes obtain (i.e., their classification), relative to the others. Including the *GAPDH* and *SYN1A* genes that are routinely used as "standard" reference genes ensure a point of comparison with the candidate genes we found in our process. Rankings according to all prediction tools are reported in **Table 3** for all stages, and in **Table 4** for adult stages only. Overall, each of these methods provided good stability values for all the preselected

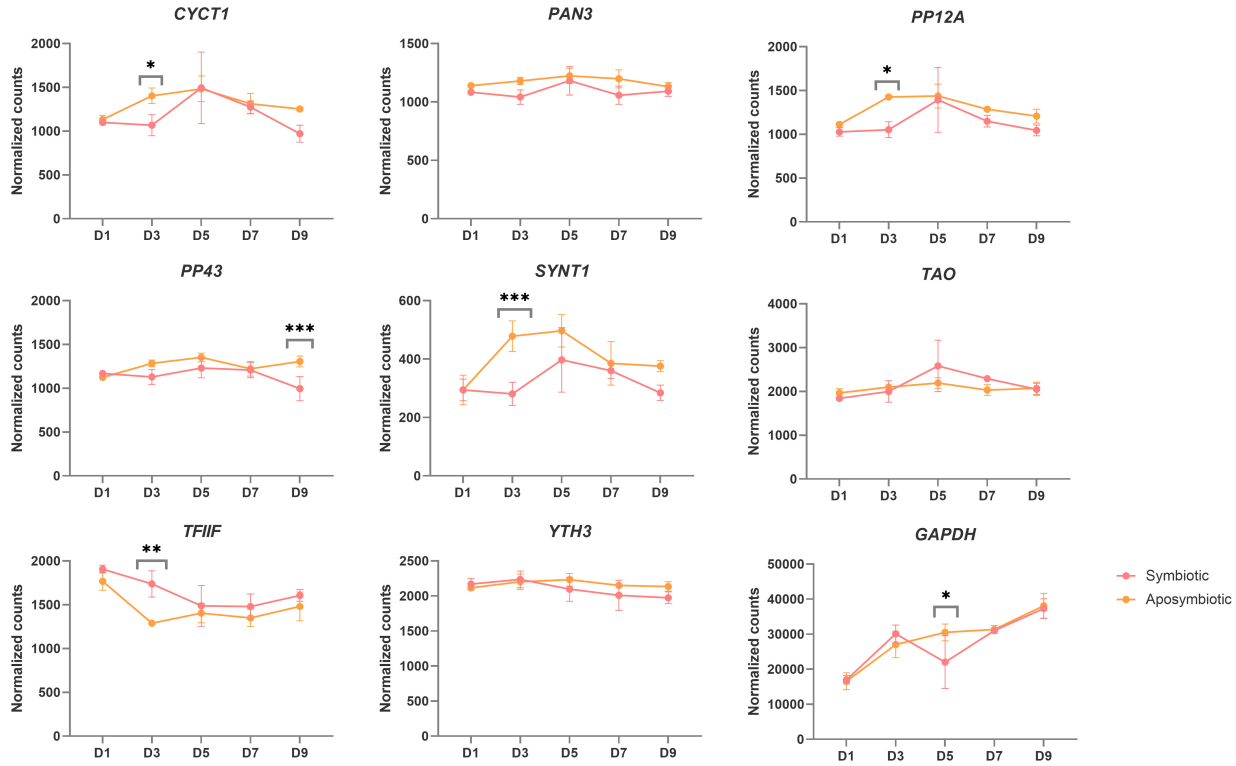

FIGURE 5
Normalized counts of selected candidate reference genes from previous RNAseq data obtained from symbiotic and aposymbiotic weevils (Ferrarini et al., 2023). Stars denote the adjusted *p*-value between symbiotic and aposymbiotic weevils at a given time point, upon DESEQ2 analysis (see section "2. Materials and methods"). *Adjpvalue < 0.05, ** < 0.005, *** < 0.0005. Three genes show no differences between symbiotic and aposymbiotic weevils at any given time point and constitute good candidates for symbiotic/aposymbiotic qRT-PCR comparisons: *pan3*, *tao*, and *yth3*.

candidate genes, with a consensus for *TAO* and *SYN1A* at all stages and for *TAO*, *PP12A*, and *YTH3* in adult stages only. *GAPDH* was often ranked last among these set of candidate reference genes.

3.4. Determination of the minimum number of reference genes for qPCR normalization

The pairwise variation value (V) between the ranked genes was calculated with the geNorm algorithm and used to estimate the stability of the normalization factor with the addition of one normalization gene at a time. The cut-off value for pairwise variation used was 0.15 (Vandesompele et al., 2002), meaning that as soon as the value of V drops below 0.15 the number of reference genes was considered suitable for correct standardization of gene expression. The V value for the set of candidate reference genes was always lower than 0.15 (**Figure 4**). This indicates that two reference genes, which is the minimal number of reference genes accepted by the MIQE guidelines (Bustin et al., 2009), are sufficient for standardization of gene expression across *S. oryzae* development in the gut, from the L4 larval stages to D9 adults. It also shows that any combination of the proposed nine reference genes is suitable for normalization.

3.5. Assessment of candidate reference genes for transcript comparisons between symbiotic and aposymbiotic insects

Weevils artificially deprived of symbionts by heat treatment (aposymbiotic) do survive under laboratory standard conditions, although their fitness is partially compromised, e.g., the larval development takes longer, fertility is lower (Nardon, 1973), and aposymbiotic adults are unable to fly (Nardon et al., 1998). In aposymbiotic weevils, the insect cuticle, which is derived from aromatic amino acids mainly supplied by the bacteria, does not fully develop but remains thinner and more delicate (Vigneron et al., 2014). In order to pinpoint symbiosis-specific transcriptional changes, the transcriptomic profiles obtained for symbiotic weevils (Ferrarini et al., 2023) should be compared with the expression profiles obtained at the same stage in aposymbiotic weevils. We took advantage of existing transcriptomic datasets produced from adult symbiotic and aposymbiotic weevils at different adult stages, to compare the expression of all candidate genes between symbiotic stages (**Figure 5**; Ferrarini et al., 2023). Differential expression analysis of all nine candidate genes between symbiotic and aposymbiotic weevils shows only three genes are equally expressed between symbiotic conditions: *PAN3*, *TAO*, and *YTH3*. Two of these genes were chosen as suitable candidates for symbiotic

analysis, *TAO* and *YTH3* and should constitute a good set for symbiotic/aposymbiotic comparisons.

4. Conclusion

In this work, we relied on transcriptomic data to select a set of nine new candidate reference genes for *S. oryzae*, which we compared with *GAPDH*, a very common reference gene (Bustin, 2000), and *SYN1A*, which has been previously used as a reference gene for *T. castaneum* (Lord et al., 2010). By combining differential expression data filtering, visual inspection, CV% analysis and a variety of gene stability ranking algorithms, we were able to select stable gut transcripts in *S. oryzae* adult stages, but also for stages spanning from larvae to adult, including metamorphosis. In particular, all the preselected candidate genes scored well in all ranking systems, with a general preference for *TAO* and *SYN1A* when all developmental stages (from larval stage 4 to 9-day-old adults) were considered, and for *TAO*, *PP12A*, and *YTH3* in adult stages only. Interestingly, for all the various algorithms used to rank the reliability of reference genes, the newly selected genes were always more suitable than the highly popular *GAPDH*, although the latter ranked better in terms of CV% values.

Our selection approach was guided by the stability of expression levels of various transcripts and their abundance in transcriptomic data (Ferrarini et al., 2023), and on the presumed housekeeping function of each gene on the basis of the available literature and sequence alignments with homologs from other species. Indeed, all the candidates that were successfully quantified by qPCR, and in particular *TAO* and *YTH3*, which were chosen for comparing symbiotic and aposymbiotic weevils, have been previously associated with important cell functions, such as DNA repair and RNA transcription, suggesting they are likely good candidates as reference genes for many other tissues and organisms (**Table 1**).

In conclusion, we identified stable reference genes across *S. oryzae* development with potential application in various other animal species. This work also demonstrates the potential of transcriptomic data as a guide for reference gene selection to obtain comparable or better performances in comparison to traditional ones–a strategy still neglected in insect studies.

Data availability statement

The original contributions presented in this study are included in the article, further inquiries can be directed to the corresponding authors.

Author contributions

AZ-R and RR conceived the study with the help from AH. MF performed the gene selection from high throughput transcriptomic data, with inputs from CV-M, AV, ED, AH, and AZ-R. AV, ED, and OH produced and treated the gene expression data. AV, ED, and RR performed the statistical analysis. AZ-R, RR, AV, AH, and ED wrote the manuscript. All authors read and approved the manuscript.

Funding

This work was funded by the ANR UNLEASH (ANR UNLEASH-CE20-0015-01–RR) and ANR GREEN (ANR-17-CE20-0031-01–AH).

Conflict of interest

The authors declare that the research was conducted in the absence of any commercial or financial relationships that could be construed as a potential conflict of interest.

Publisher's note

All claims expressed in this article are solely those of the authors and do not necessarily represent those of their affiliated organizations, or those of the publisher, the editors and the reviewers. Any product that may be evaluated in this article, or claim that may be made by its manufacturer, is not guaranteed or endorsed by the publisher.

References

Andersen, C. L., Jensen, J. L., and Ørntoft, T. F. (2004). Normalization of real-time quantitative reverse transcription-PCR data: a model-based variance estimation approach to identify genes suited for normalization, applied to bladder and colon cancer data sets. *Cancer Res.* 64, 5245–5250. doi: 10.1158/0008-5472.CAN-04-0496

Andrews, S. (2010). *FastQC A Quality Control tool for High Throughput Sequence Data*. Available online at: https://www.bioinformatics.babraham.ac.uk/projects/fastqc/ (accessed December 23, 2022).

Aso, T., Vasavada, H. A., Kawaguchi, T., Germino, F. J., Ganguly, S., Kitajima, S., et al. (1992). Characterization of cDNA for the large subunit of the transcription initiation factor TFIIF. *Nature* 355, 461–464. doi: 10.1038/355461a0

Boda, E., Pini, A., Hoxha, E., Parolisi, R., and Tempia, F. (2009). Selection of reference genes for quantitative real-time RT-PCR studies in mouse brain. *J. Mol. Neurosci. MN* 37, 238–253. doi: 10.1007/s12031-008-9128-9

Brown, C. E., Tarun, S. Z., Boeck, R., and Sachs, A. B. (1996). PAN3 encodes a subunit of the Pab1p-dependent poly(A) nuclease in Saccharomyces cerevisiae. *Mol. Cell. Biol.* 16, 5744–5753. doi: 10.1128/MCB.16.10.5744

Bustin, S. A. (2000). Absolute quantification of mRNA using real-time reverse transcription polymerase chain reaction assays. *J. Mol. Endocrinol.* 25, 169–193. doi: 10.1677/jme.0.0250169

Bustin, S. A., Benes, V., Garson, J. A., Hellemans, J., Huggett, J., Kubista, M., et al. (2009). The MIQE guidelines: minimum information for publication of quantitative real-time PCR experiments. *Clin. Chem.* 55, 611–622. doi: 10.1373/clinchem.2008.112797

Camacho, C., Coulouris, G., Avagyan, V., Ma, N., Papadopoulos, J., Bealer, K., et al. (2009). BLAST+: architecture and applications. *BMC Bioinformatics* 10:421. doi: 10.1186/1471-2105-10-421

Caracausi, M., Piovesan, A., Antonaros, F., Strippoli, P., Vitale, L., and Pelleri, M. C. (2017). Systematic identification of human housekeeping genes possibly useful

as references in gene expression studies. *Mol. Med. Rep.* 16, 2397–2410. doi: 10.3892/mmr.2017.6944

Caron, E. (2003). Cellular functions of the Rap1 GTP-binding protein: a pattern emerges. *J Cell Sci.* 116(Pt 21), 435–440. doi: 10.1242/jcs.00707

Dell'Aglio, E., Lacotte, V., Peignier, S., Rahioui, I., Benzaoui, F., Vallier, A., et al. (2023). Weevil carbohydrate intake triggers endosymbiont proliferation: a trade-off between host benefit and endosymbiont burden. *mBio* 1–14. doi: 10.1128/mbio.03333-22

Dobin, A., Davis, C. A., Schlesinger, F., Drenkow, J., Zaleski, C., Jha, S., et al. (2013). STAR: ultrafast universal RNA-seq aligner. *Bioinformatics* 29, 15–21. doi: 10.1093/bioinformatics/bts635

Dveksler, G. S., Basile, A. A., and Dieffenbach, C. W. (1992). Analysis of gene expression: use of oligonucleotide primers for glyceraldehyde-3-phosphate dehydrogenase. *PCR Methods Appl.* 1, 283–285. doi: 10.1101/gr.1.4.283

Ewels, P., Magnusson, M., Lundin, S., and Käller, M. (2016). MultiQC: summarize analysis results for multiple tools and samples in a single report. *Bioinformatics* 32, 3047–3048. doi: 10.1093/bioinformatics/btw354

Ferrarini, M. G., Vallier, A., Vincent-Monégat, C., Dell'Aglio, E., Gillet, B., Hughes, S., et al. (2023). Coordinated host and endosymbiont gene expression governs endosymbiont growth and elimination in the cereal weevil *Sitophilus* spp. *bioRxiv* [Preprint]. doi: 10.1101/2023.04.03.535335

Fu, W., Xie, W., Zhang, Z., Wang, S., Wu, Q., Liu, Y., et al. (2013). Exploring valid reference genes for quantitative real-time PCR analysis in *Plutella xylostella* (*Lepidoptera*: *Plutellidae*). *Int. J. Biol. Sci.* 9, 792–802. doi: 10.7150/ijbs.5862

Garneau, N. L., Wilusz, J., and Wilusz, C. J. (2007). The highways and byways of mRNA decay. *Nat. Rev. Mol. Cell Biol.* 8, 113–126. doi: 10.1038/nrm2104

Gingras, A.-C., Caballero, M., Zarske, M., Sanchez, A., Hazbun, T. R., Fields, S., et al. (2005). A novel, evolutionarily conserved protein phosphatase complex involved in cisplatin sensitivity. *Mol. Cell. Proteomics MCP* 4, 1725–1740. doi: 10.1074/mcp.M500231-MCP200

Heddi, A., Grenier, A.-M., Khatchadourian, C., Charles, H., and Nardon, P. (1999). Four intracellular genomes direct weevil biology: nuclear, mitochondrial, principal endosymbiont, and Wolbachia. *Proc. Natl. Acad. Sci. U.S.A.* 96, 6814–6819. doi: 10.1073/pnas.96.12.6814

Higuchi, R., Dollinger, G., Walsh, P. S., and Griffith, R. (1992). Simultaneous amplification and detection of specific DNA sequences. *Biotechnol. Nat. Publ. Co.* 10, 413–417. doi: 10.1038/nbt0492-413

Hughes, J. J., Alkhunaizi, E., Kruszka, P., Pyle, L. C., Grange, D. K., Berger, S. I., et al. (2020). Loss-of-function variants in PPP1R12A: from isolated sex reversal to Holoprosencephaly spectrum and urogenital malformations. *Am. J. Hum. Genet.* 106, 121–128. doi: 10.1016/j.ajhg.2019.12.004

Hutchison, M., Berman, K. S., and Cobb, M. H. (1998). Isolation of TAO1, a protein kinase that activates MEKs in stress-activated protein kinase cascades. *J. Biol. Chem.* 273, 28625–28632. doi: 10.1074/jbc.273.44.28625

Karman, Z., Rethi-Nagy, Z., Abraham, E., Fabri-Ordogh, L., Csonka, A., Vilmos, P., et al. (2020). Novel perspectives of target-binding by the evolutionarily conserved PP4 phosphatase. *Open Biol.* 10, 200343. doi: 10.1098/rsob.200343

Kataya, A. R. A., Creighton, M. T., Napitupulu, T. P., Saetre, C., Heidari, B., Ruoff, P., et al. (2017). PLATINUM SENSITIVE 2 LIKE impacts growth, root morphology, seed set, and stress responses. *PLoS One* 12:e0180478. doi: 10.1371/journal.pone.0180478

Kõressaar, T., Lepamets, M., Kaplinski, L., Raime, K., Andreson, R., and Remm, M. (2018). Primer3_masker: integrating masking of template sequence with primer design software. *Bioinforma. Oxf. Engl.* 34, 1937–1938. doi: 10.1093/bioinformatics/bty036

Kubista, M., Andrade, J. M., Bengtsson, M., Forootan, A., Jonák, J., Lind, K., et al. (2006). The real-time polymerase chain reaction. *Mol. Aspects Med.* 27, 95–125. doi: 10.1016/j.mam.2005.12.007

Kursula, P. (2014). Structural basis of synaptic adhesion and signaling by Calsyntenin-1. *Proc. Natl. Acad. Sci. U.S.A.* 111, 3956–3957. doi: 10.1073/pnas.1401919111

Liang, L., He, Z., Yu, H., Wang, E., Zhang, X., Zhang, B., et al. (2020). Selection and validation of reference genes for gene expression studies in *Codonopsis pilosula* based on Transcriptome sequence data. *Sci. Rep.* 10:1362. doi: 10.1038/s41598-020-58328-5

Liao, Y., Smyth, G. K., and Shi, W. (2014). featureCounts: an efficient general purpose program for assigning sequence reads to genomic features. *Bioinforma. Oxf. Engl.* 30, 923–930. doi: 10.1093/bioinformatics/btt656

Longstaff, B. C. (1981). Biology of the grain pest species of the genus *Sitophilus* (*Coleoptera*: Curculionidae): a critical review. *Prot. Ecol.* 3, 83–130.

Lopes, J. M. L., de Matos, E. M., de Queiroz Nascimento, L. S., and Viccini, L. F. (2021). Validation of reference genes for quantitative gene expression in the *Lippia alba* polyploid complex (*Verbenaceae*). *Mol. Biol. Rep.* 48, 1037–1044. doi: 10.1007/s11033-021-06183-6

Lord, J. C., Hartzer, K., Toutges, M., and Oppert, B. (2010). Evaluation of quantitative PCR reference genes for gene expression studies in *Tribolium castaneum* after fungal challenge. *J. Microbiol. Methods* 80, 219–221. doi: 10.1016/j.mimet.2009.12.007

Love, M. I., Huber, W., and Anders, S. (2014). Moderated estimation of fold change and dispersion for RNA-seq data with DESeq2. *Genome Biol.* 15:550. doi: 10.1186/s13059-014-0550-8

Lü, J., Yang, C., Zhang, Y., and Pan, H. (2018). Selection of reference genes for the normalization of RT-qPCR data in gene expression studies in insects: a systematic review. *Front. Physiol.* 9:1560. doi: 10.3389/fphys.2018.01560

Luse, D. S. (2012). Rethinking the role of TFIIF in transcript initiation by RNA polymerase II. *Transcription* 3, 156–159. doi: 10.4161/trns.20725

Maire, J., Parisot, N., Galvao Ferrarini, M., Vallier, A., Gillet, B., Hughes, S., et al. (2020). Spatial and morphological reorganization of endosymbiosis during metamorphosis accommodates adult metabolic requirements in a weevil. *Proc. Natl. Acad. Sci. U.S.A.* 117, 19347–19358. doi: 10.1073/pnas.2007151117

Maire, J., Vincent-Monégat, C., Balmand, S., Vallier, A., Hervé, M., Masson, F., et al. (2019). Weevil pgrp-lb prevents endosymbiont TCT dissemination and chronic host systemic immune activation. *Proc. Natl. Acad. Sci. U.S.A.* 116, 5623–5632. doi: 10.1073/pnas.1821806116

Mansour, K. (1930). Memoirs: preliminary Studies on the Bacterial Cell-mass (Accessory Cell-mass) of Calandra Oryzae (Linn.): the Rice Weevil. *J. Cell Sci.* s2- 73, 421–435. doi: 10.1242/jcs.s2-73.291.421

Martin, M. (2011). Cutadapt removes adapter sequences from high-throughput sequencing reads. *EMBnet.journal* 17, 10–12. doi: 10.14806/ej.17.1.200

Nardon, P. (1973). Obtention d'une souche asymbiotique chez le charançon *Sitophilus sasakii* Tak: différentes méthodes d'obtention et comparaison avec la souche symbiotique d'origine. *CR Acad Sci Paris D* 277, 981–984.

Nardon, P., Grenier, A., and Heddi, A. (1998). Endocytobiote control by the host in the weevil *Sitophilus oryzae*, *Coleoptera*, Curculionidae. *Symbiosis* 25:237.

Oakeson, K. F., Gil, R., Clayton, A. L., Dunn, D. M., von Niederhausern, A. C., Hamil, C., et al. (2014). Genome degeneration and adaptation in a nascent stage of symbiosis. *Genome Biol. Evol.* 6, 76–93. doi: 10.1093/gbe/evt210

Pan, H., Yang, X., Siegfried, B. D., and Zhou, X. (2015). A comprehensive selection of reference genes for RT-qPCR analysis in a predatory lady beetle, Hippodamia convergens (*Coleoptera*: Coccinellidae). *PLoS One* 10:e0125868. doi: 10.1371/journal.pone.0125868

Parisot, N., Vargas-Chávez, C., Goubert, C., Baa-Puyoulet, P., Balmand, S., Beranger, L., et al. (2021). The transposable element-rich genome of the cereal pest *Sitophilus oryzae*. *BMC Biol.* 19:241. doi: 10.1186/s12915-021-01158-2

Pfaffl, M. W., Tichopad, A., Prgomet, C., and Neuvians, T. P. (2004). Determination of stable housekeeping genes, differentially regulated target genes and sample integrity: BestKeeper–Excel-based tool using pair-wise correlations. *Biotechnol. Lett.* 26, 509–515. doi: 10.1023/b:bile.0000019559.84305.47

Pierantoni, U. (1927). L'organo simbiotico nello svillupo di *Calandra oryzae*. *Rend R. Acad Sci Fis Mat Napoli* 27, 21–33. doi: 10.1080/11250006009438308

Shim, E. Y., Walker, A. K., Shi, Y., and Blackwell, T. K. (2002). CDK-9/cyclin T (P-TEFb) is required in two postinitiation pathways for transcription in the *C. elegans* embryo. *Genes Dev.* 16, 2135–2146. doi: 10.1101/gad.999002

Silver, N., Best, S., Jiang, J., and Thein, S. L. (2006). Selection of housekeeping genes for gene expression studies in human reticulocytes using real-time PCR. *BMC Mol. Biol.* 7:33. doi: 10.1186/1471-2199-7-33

Sirover, M. (1999). New insights into an old protein: the functional diversity of mammalian glyceraldehyde-3-phosphate dehydrogenase. *Biochim Biophys Acta*. 1432, 159–184. doi: 10.1016/s0167-4838(99)00063-0

Sundaram, V. K., Sampathkumar, N. K., Massaad, C., and Grenier, J. (2019). Optimal use of statistical methods to validate reference gene stability in longitudinal studies. *PLoS One* 14:e0219440. doi: 10.1371/journal.pone.0219440

Takahashi, N., Ito, M., Tanaka, J., Nakano, T., Kaibuchi, K., Odai, H., et al. (1997). Localization of the gene coding for myosin phosphatase, target subunit 1 (MYPT1) to human chromosome 12q15-q21. *Genomics* 44, 150–152. doi:10.1006/geno.1997.4859

Timm, T., Matenia, D., Li, X.-Y., Griesshaber, B., and Mandelkow, E.-M. (2006). Signaling from MARK to tau: regulation, cytoskeletal crosstalk, and pathological phosphorylation. *Neurodegener. Dis.* 3, 207–217. doi:10.1159/000095258

Vandesompele, J., De Preter, K., Pattyn, F., Poppe, B., Van Roy, N., De Paepe, A., et al. (2002). Accurate normalization of real-time quantitative RT-PCR data by geometric averaging of multiple internal control genes. *Genome Biol.* 3:RESEARCH0034. doi: 10.1186/gb-2002-3-7-research0034

Vigneron, A., Masson, F., Vallier, A., Balmand, S., Rey, M., Vincent-Monégat, C., et al. (2014). insects recycle endosymbionts when the benefit is over. *Curr. Biol.* 24, 2267–2273. doi: 10.1016/j.cub.2014.07.065

Wickham, H. (2009). *ggplot2*. New York, NY: Springer New York, doi: 10.1007/978-0-387-98141-3

Xie, F., Xiao, P., Chen, D., Xu, L., and Zhang, B. (2012). miRDeepFinder: a miRNA analysis tool for deep sequencing of plant small RNAs. *Plant Mol. Biol* doi: 10.1007/s11103-012-9885-2 [Epub ahead of print].

Yim, A. K.-Y., Wong, J. W.-H., Ku, Y.-S., Qin, H., Chan, T.-F., and Lam, H.-M. (2015). Using RNA-Seq data to evaluate reference genes suitable for gene expression studies in soybean. *PLoS One* 10:e0136343. doi:10.1371/journal.pone.0136343

Zaccara, S., and Jaffrey, S. R. (2020). A unified model for the function of YTHDF proteins in regulating m6A-modified mRNA. *Cell* 181, 1582.e18–1595.e18. doi: 10.1016/j.cell.2020.05.012

Zhang, J., Deng, C., Li, J., and Zhao, Y. (2020). Transcriptome-based selection and validation of optimal house-keeping genes for skin research in goats (*Capra hircus*). *BMC Genomics* 21:493. doi: 10.1186/s12864-020-06912-4

Zhang, S.-Q., Che, L.-H., Li, Y., Liang, D., Pang, H., Ślipiński, A., et al. (2018). Evolutionary history of *Coleoptera* revealed by extensive sampling of genes and species. *Nat. Commun.* 9:205. doi: 10.1038/s41467-017-02644-4

Zhang, Z.-Q. (2013). Animal biodiversity: an outline of higher-level classification and survey of taxonomic richness (Addenda 2013). *Zootaxa* 3703, 1–82. doi: 10.11646/zootaxa.3703.1.1

Zhou, Q., Xiao, J., and Liu, Y. (2000). Participation of syntaxin 1A in membrane trafficking involving neurite elongation and membrane expansion. *J. Neurosci. Res.* 61, 321–328.

frontiers | Frontiers in Ecology and Evolution

TYPE Original Research
PUBLISHED 22 May 2023
DOI 10.3389/fevo.2023.1083315

OPEN ACCESS

EDITED BY
Jennifer L. Matthews,
University of Technology Sydney, Australia

REVIEWED BY
Mathias Wegner,
Alfred Wegener Institute Helmholtz Centre for Polar and Marine Research (AWI), Germany
Luke P. Miller,
San Diego State University, United States

*CORRESPONDENCE
Bayden D. Russell
✉ brussell@hku.hk

RECEIVED 28 October 2022
ACCEPTED 28 April 2023
PUBLISHED 22 May 2023

CITATION
Hemraj DA, Falkenberg LJ, Cheung K, Man L, Carini A and Russell BD (2023) Acidification and hypoxia drive physiological trade-offs in oysters and partial loss of nutrient cycling capacity in oyster holobiont.
Front. Ecol. Evol. 11:1083315.
doi: 10.3389/fevo.2023.1083315

Acidification and hypoxia drive physiological trade-offs in oysters and partial loss of nutrient cycling capacity in oyster holobiont

Deevesh Ashley Hemraj[1,2,3], Laura J. Falkenberg[4], Khan Cheung[1,2], Lauren Man[1,5], Alessia Carini[1,2] and Bayden D. Russell[1,2,6,7]*

[1]The Swire Institute of Marine Science and Area of Ecology and Biodiversity, School of Biological Sciences, The University of Hong Kong, Pokfulam, Hong Kong SAR, China, [2]The Joint Laboratory for Marine Ecology and Environmental Sciences (JLMEES), The Swire Institute of Marine Science, The University of Hong Kong, Pokfulam, Hong Kong SAR, China, [3]Department of Ecoscience, Aarhus University, Roskilde, Denmark, [4]Simon F.S. Li Marine Science Laboratory, School of Life Sciences, The Chinese University of Hong Kong, Shatin, Hong Kong SAR, China, [5]Department of Geography, University of Victoria, Victoria, BC, Canada, [6]Institute for Climate and Carbon Neutrality, The University of Hong Kong, Pokfulam, Hong Kong SAR, China, [7]LabEx ICONA International CO_2 Natural Analogues Network, Shimoda, Japan

Introduction: Reef building oysters provide vast ecological benefits and ecosystem services. A large part of their role in driving ecological processes is mediated by the microbial communities that are associated with the oysters; together forming the oyster holobiont. While changing environmental conditions are known to alter the physiological performance of oysters, it is unclear how multiple stressors may alter the ability of the oyster holobiont to maintain its functional role.

Methods: Here, we exposed oysters to acidification and hypoxia to examine their physiological responses (molecular defense and immune response), changes in community structure of their associated microbial community, and changes in water nutrient concentrations to evaluate how acidification and hypoxia will alter the oyster holobiont's ecological role.

Results: We found clear physiological stress in oysters exposed to acidification, hypoxia, and their combination but low mortality. However, there were different physiological trade-offs in oysters exposed to acidification or hypoxia, and the combination of stressors incited greater physiological costs (i.e., >600% increase in protein damage and drastic decrease in haemocyte counts). The microbial communities differed depending on the environment, with microbial community structure partly readjusted based on the environmental conditions. Microbes also seemed to have lost some capacity in nutrient cycling under hypoxia and multi-stressor conditions (~50% less nitrification) but not acidification.

Discussion: We show that the microbiota associated to the oyster can be enriched differently under climate change depending on the type of environmental change that the oyster holobiont is exposed to. In addition, it may be the primary impacts to oyster physiology which then drives changes to the associated microbial community. Therefore, we suggest the oyster holobiont may lose some of its nutrient cycling properties under hypoxia and multi-stressor conditions although the oysters can regulate their physiological processes to maintain homeostasis on the short-term.

KEYWORDS

oyster holobiont, oyster physiology, acidification, hypoxia, oyster reef

Introduction

Reef building oysters provide numerous ecological functions in coastal marine systems. Along with building structural complexity on the benthos which provides habitat for many marine species, oysters also drive crucial ecological processes such as biogeochemical cycling and benthic-pelagic coupling (Ray and Fulweiler, 2021). Key to these processes are the microbial communities associated with oysters; together forming the oyster holobiont. The activity of the microbial communities associated with oysters are key for the oysters themselves and for the ecological processes performed by the oyster holobiont as a whole (Green et al., 2012; Dubé et al., 2019; Stevick et al., 2021). For example, the oyster holobiont contributes to reduction of eutrophication through simultaneous bio-deposition from the oyster and denitrification stimulated by microbial conversion of biologically reactive nitrogen to nitrogen gas (Ray and Fulweiler, 2021). However, it remains unclear how changing environments, especially driven by climate change, can impact the ecological performance of the oyster holobiont.

Rapid changes in coastal marine environments, directly or indirectly driven by anthropogenic activity, can cause strong physiological responses in fauna. These responses influence how organisms perform their ecological roles within their ecosystem (Vaquer-Sunyer and Duarte, 2008; Hughes et al., 2020). The decline in the capability of organisms to perform their ecological roles can subsequently manifest into broader consequences, such as the loss of some ecological processes within the ecosystem (Diaz and Rosenberg, 1995; Lemasson et al., 2017; Vizzini et al., 2017; Ullah et al., 2018). In the case of sessile habitat forming species, such as oysters, stressful environmental change like acidification or hypoxia can cause physiological impairment that includes oxidative stress, reduced metabolic activity, or haemocyte apoptosis (Boyd and Burnett, 1999; David et al., 2005; Timmins-Schiffman et al., 2014; Wang et al., 2016). These physiological impairments can lead to broader consequences including changes in energy homeostasis, reduced growth, increased susceptibility to diseases, or mortality (Wang et al., 2016; Lutier et al., 2022), and therefore impact the ecological functions of oysters (Lemasson et al., 2017). On the other hand, the extent of alteration to oyster associated microbes in relation to changing environments remains debatable with some studies indicating limited changes (Zhou et al., 2016; Ge et al., 2021; Garner et al., 2022), while others showing significant changes, especially with longer exposure to environmental change (King et al., 2019; Scanes et al., 2021a,b; Unzueta-Martínez et al., 2021).

Among the multiple environmental stressors that can affect oysters and their associated microbial communities, acidification and hypoxia are likely to have profound impact on the oyster holobiont because the already large pH variability within coastal systems (especially around estuaries) could become more extreme with climate change (Rivest et al., 2017). In addition, hypoxic events have become more frequent because of increased coastal eutrophication (Vaquer-Sunyer and Duarte, 2008). Finally, given the simultaneous increase in eutrophication and warming of coastal systems, the co-occurrence of acidification and hypoxia will become more prevalent as overall increases in system metabolic demands will consume more oxygen and release more carbon dioxide (Cai, 2011; Gobler and Baumann, 2016). Therefore, examining how acidification and hypoxia will impact the oyster holobiont and its function can provide important information for oyster reef restoration or oyster aquaculture activities, both of which attract large efforts and financial investments globally (Bayraktarov et al., 2016).

One of the key ecological roles filled by the oyster holobiont is as an intermediary that links biogeochemical cycles in the sediment and water column through filtration and bio-deposition (Smyth et al., 2013; Ray and Fulweiler, 2021). Organic matter (generally from phytoplankton) from the water column is filtered and digested, and substantial denitrification (conversion of NO_3^- to N_2 gas) can by the microbiome within the oysters' digestive system (the microbial community that naturally occurs within the oyster) (Ray et al., 2019). Unassimilated matter released as bio-deposits (faeces and pseudo-faeces) that contain a large amount of ammonium (NH_4^+) is then cycled, through nitrification, to NO_2^- and NO_3^- by microbes on the oysters' shell or in the sediment/water column (Ray et al., 2019). These biologically reactive nitrogen species (NO_2^- and NO_3^-) are further denitrified by microbes in the sediment or water column, or utilised by epiphytes (Ray et al., 2019). Importantly, changes in water conditions can alter the nutrient cycling capacity of oysters (Hoellein et al., 2015) by influencing the oysters' physiology, and hence the amount of nitrogen that is processed (Jeppesen et al., 2018), and by changing the microbial community associated with oysters (King et al., 2019; Unzueta-Martínez et al., 2021; Scanes et al., 2021a,b).

Here, we tested the impact of acidification, hypoxia, and their combination on the oyster holobiont; the physiological traits of the oyster, associated microbial community, and the resulting changes in nutrient cycling. While is it well documented that acidification or hypoxia can drive deteriorative physiological responses in oysters (Timmins-Schiffman et al., 2014), the impact of stressful environmental conditions on the whole oyster holobiont remains unclear. We hypothesised that acidification and hypoxia would drive physiological trade-offs in oysters, which would shift the microbial communities associated with them and thus alter the biogeochemical cycling capacity of the oyster holobiont. To test this hypothesis, we exposed oyster holobionts to hypoxia, acidification, or their combination. We then quantified the level of protein damage, oxidative stress, and immune response of oysters exposed to each condition. Finally, we identified the microbial community associated with the oysters and measured the concentration of different nutrients within experimental treatments to estimate the relationship between oysters, microbes and nutrient cycle. Together, these results provide a broader understanding of how climate driven changes in coastal environmental conditions may impact the oyster holobiont as a whole and affect their nutrient cycling capacity.

Methods

Oyster collection

Oysters were sampled from a natural community at Shui Hau Wan, Hong Kong, during low tide at salinity 33 psu and temperature 23°C. This community is comprised of *Magallana angulata* and *Magallana sikamea*. Visual separation of species before the experiment was attempted, however, the exact separation of species remained uncertain because of the morphological similarity of these two species and their co-occurrence at the site (Lau et al., 2020). DNA barcoding using mantle tissues of about 50% of the total oysters used in the

experiment showed that the community was composed of 60% *M. sikamea* and 40% *M. angulata* (only oysters that were used for tissue sampling as described below were used for DNA barcoding). Oysters were brought to the laboratory and kept in 100 L holding tanks for 10 days for acclimation and fed daily with Shellfish Diet 1800 (Reed Mariculture Inc., United States). During this period, oysters were cleaned to remove all fouling from their shells and half the seawater in the holding tanks was changed daily to maintain water quality. Salinity in the holding tanks was 35 psu and temperature was maintained at 23°C using 300-watt submersible aquarium water heaters.

Experimental setup

After acclimation, oysters were transferred into 5 L experimental containers. Five replicate containers per treatment condition ($n = 5$) were used, each containing 12 individual oysters of mixed sizes. We used 12 oysters per replicate to allow for enough individuals for sampling tissue to measure molecular defence and for sampling haemolymph for quantifying immune response (different individuals were used) in case this sampling created stress or mortality in the oysters. Treatment conditions for the experiments were ambient control (C), hypoxia (H), acidification (A), and hypoxia × acidification (HA) (n = 5 containers per treatment). Treatments were achieved by bubbling pre-mixed gases through the seawater in each experimental container. Hypoxia conditions were created by adding N_2 to air to achieve 5% O_2 (equivalent to 2 mgO_2/L) and acidification conditions were created by mixing CO_2 to air to achieve 0.1% CO_2 (equivalent to 1,000 ppm). To create HA conditions CO_2 was added directly to the hypoxia mixture, while control conditions involved bubbling air into the seawater. All gases were mixed using electronic multi-gas flow controllers (Cole Parmer Masterflex Gas Mass Flowmeter) and manual air flow controllers (Cole Parmer Masterflex Variable-Area Flowmeter). To maintain stable treatment conditions, each gas was constantly bubbled in the appropriate experimental containers and a thin sheet of styrofoam was placed on the surface of the water to limit air/water gas exchange. At the beginning of the experiment, containers were filled with seawater pre-adjusted to the treatment conditions, then placed in a water bath at 23°C, controlled by an external water chiller (Hailea, Model HC.2200BH). Oysters were fed *ad libitum* with Shellfish Diet 1800 and a two-thirds water change was performed daily with seawater pre-adjusted to the treatment conditions. The experiment was maintained for 16 days, and oyster mortality recorded daily during water change.

Water chemistry

Water quality (pH and DO) was monitored three times each day (in the morning, after the water change, and in the afternoon). Water pH and temperature were monitored with a Mettler Tolledo Seven2Go pH meter. Oxygen concentrations were monitored with a Fibox 4 (PreSens) to which an oxygen dip probe was connected, and salinity wat monitored using a refractometer. To determine the exact pCO_2 levels, water samples (70 mL) for total alkalinity were taken once daily. Total alkalinity was measured using a Metrohm Titrator. Finally, pCO_2 levels were calculated using CO2Sys_v2.1 (Supplementary Table S1).

Oyster molecular defence

To estimate the effects of hypoxia, acidification, or HA on oyster physiology (i.e., protein damage and oxidative stress), the concentration of Hsp-70, total antioxidant capacity (TAC), and malondialdehyde (MDA) were measured from the gill tissue of oysters. At the end of the experiment, one oyster from each container was dissected to remove the gills, which were immediately frozen in liquid nitrogen and stored at −80°C until further use. Prior to measuring Hsp-70, TAC and MDA, gill tissue samples were thawed and immediately cut and weighed separately for each assay. For all assays, gill tissue samples were homogenised using a TissueLyser 2 at 30 hertz for 1 min. Total protein was measured using a BCA total protein kit (Pierce) following manufacturer's protocols. Hsp 70 was measured using a Mouse Heat Shock Protein 70 m Hsp-70 Elisa Kit (CUSABIO) following manufacturer's protocols. TAC and MDA were measured using an OxiSelect Total Antioxidant Capacity (TAC) Assay Kit (Cell Biolabs) and an OxiSelect TBARS (MDA Quantification) Assay Kit (Cell Biolabs), respectively, following manufacturer's protocols.

Oyster immune response

To quantify the haemocyte populations and measure the level of phagocytosis in oysters from different treatments, haemolymph samples were collected from the pericardial cavity of two new individuals from each experimental container (total of 10 individuals per treatment) at the end of the experiment using a one millilitre syringe and fine needle. Haemolymph samples were immediately placed on ice to prevent coagulation. For cell counts and identification, haemolymph samples were prepared following Wang et al. (2016). In brief, 0.5 mL haemolymph from each individual was fixed with 4% paraformaldehyde, then cells counted and identified using microscopy. Preserved cells were counted and separated as granulocytes and agranulocytes using a haemocytometer mounted on a light microscope. Phagocytic activity was measured immediately after haemolymph sampling using undiluted haemolymph samples following Goedken and De Guise (2004). In brief, 0.5 mL fresh haemolymph was mixed with one micrometre fluorescent latex beads at a ratio of approximately 100 beads/haemocyte. Samples were incubated for 1 hour at 20°C, then analysed on a FACS Aria 2 flow cytometer (Becton Dickinson). 10,000 events were set as a limit and the number of haemocytes that had engulfed zero, one, two or three beads were quantified based on their fluorescence peaks. Filtered seawater, fresh haemolymph samples without added beads, and filtered seawater with beads only were used as controls to clearly separate different populations. The percentage composition of haemocytes that had engulfed zero, one, two, and three beads were calculated as a function of the total haemocyte population.

Microbial community

To identify the effects of treatment conditions on the microbial communities associated with oysters, we sampled the microbes after 12 days of experimental exposure. Microbial samples were taken after day 12 rather than 16 (end of whole experiment) in order to have time

to process all samples and ensure no additional sampling was required. We collected 1 litre of water from each oyster container, before water change and feeding. To differentiate between microbes that were already present in the water from microbes that were associated with the oysters, we also collected 1 litre of water from the control containers that did not contain any oysters ($n = 3$ per treatment). These containers had the same water change regime as the containers with oysters and therefore water in both the controls (no oyster) and treatment containers (with oyster) had been incubated for the same time period between water change and sampling (approximately 20 h). Water samples were filtered on autoclaved 0.2 µm mixed cellulose esters membrane filter papers (Millipore) using a vacuum pump and filtration system (Rocker Scientific). Filter papers were immediately frozen in liquid nitrogen and stored at −80°C until analysis. DNA was extracted from the membrane filter papers using a Qiagen PowerSoil kit following manufacturer's protocol. DNA concentrations were checked with a nanodrop (Thermo Scientific) and quality checked on an agarose gel. Two extraction blanks were included to quantify the level of contamination that originated from the extraction kit or the extraction process.

Prior to sequencing library preparation, DNA concentrations were measured with a Qubit dsDNA BR Assay Kit on a Qubit 2.0 fluorometer (Thermo Scientific); the concentrations of DNA samples were subsequently normalized to 20 ng/µL by diluting with nuclease free water (Thermo Scientific). Amplicon sequencing libraries targeting the 16S rRNA V4-V5 region were prepared following the TaggiMatrix protocol (Glenn et al., 2019). The targeted locus was amplified with the primer pairs 515F-Y/926R (Parada et al., 2016); all primers included a variable length internal index (5–8 bp). The genes were amplified in 25 µL reactions with NEBNext® Ultra™ II Q5® Master Mix (New England Biolabs), which combined 12.5 µL of the PCR master mix, 1.25 µL of each primer, 5 µL of DNA template, and 5 µL of nuclease free water. The cycling conditions were as follows: 30 s at 98°C; 20 cycles of 10 s at 98°C, 15 s at 62°C, 20 s at 72°C; 2 min at 72°C. PCR products were purified with AMPure XP magnetic beads (Beckman Coulter) in 1:1 ratio and inspected on 1.5% agarose gel. Two PCR blanks were included for each amplicon to monitor contamination originated from the PCR process.

Purified amplicons were pooled together in equal concentrations for a second round of PCR with iTru indexed primers (Glenn et al., 2019). The second PCR was performed in triplicate, in 50 µL reaction volume with NEBNext® Ultra™ II Q5® Master Mix (New England Biolabs) following manufacturer's instructions. The reaction conditions were as follows: initial denaturation of 30 s at 98°C; 8 cycles of 10 s at 98°C and 75 s at 65°C; and a final extension step at 65°C for 5 min. PCR products were purified with AMPure XP magnetic beads (Beckman Coulter) in 1:1 ratio and inspected on 1.5% agarose gel. The amplicon libraries were then pooled with other amplicon sequencing libraries and sequenced on Illumina MiSeq with MiSeq Reagent Kit version 3 (2 × 300 bp) in the Centre for PanorOmic Sciences, LKS Faculty of Medicine, HKU.

Raw sequencing reads were adapter trimmed and demultiplexed with cutadapt v3.1 (Martin, 2011), and subsequently imported into Qiime2 2020.11 (Bolyen et al., 2019). Read pairs were denoised and merged using DADA2 (Callahan et al., 2016), with the forward and reverse reads truncated to 290 bp and 210 bp, respectively. In order to perform taxonomic classification of the sequencing reads, we used the Silva 138 database as recommended in Qiime2. A feature classifier was trained on the Silva 138 99% OTUs full length sequences dataset; to improve the accuracy of the Naïve Bayes classifier, the dataset was subset so that only the region of the target sequences was used for training the classifier (Bokulich et al., 2018). This yielded a spreadsheet of taxonomic classifications and the number of hits based on our sequences.

Nutrient cycling

After sampling for microbial communities, water samples for measuring nutrient concentrations were taken by filtering 50 mL of water from all experimental treatments (control, hypoxia, acidification, and HA), with and without oysters, into a sterile centrifuge tube using a syringe-mounted 0.22 µm filter (Millipore). Water for nutrient samples were collected immediately after sampling for microbial communities, and from the same experimental container, to capture the microbial community and nutrient concentrations in the water as closely as possible. Filtered water samples were stored at −20°C until analysis. Ammonium concentration was analysed by spectrophotometry on a 96 well-plate following Grasshoff et al. (2009). A gradient of standards was prepared using ammonium sulphate dissolved in MilliQ water (100, 40, 20, 10, 5, 1, and 0.5 µmol/L). 250 µL of standard and sample were then pipetted in a 96 well-plate followed by addition of 10 µL phenol, 5 µL citrate buffer, and 10 µL hypochlorite. The solutions were mixed using the "shake" function on the spectrophotometer and incubated at 37°C for 30 min followed by cool down for 30 min and measurement at 630 nm on the spectrophotometer. Concentrations of nitrate and nitrite were measured following García-Robledo et al. (2014). Standards were prepared using sodium nitrate and sodium nitrite dissolved in MilliQ water (100, 40, 20, 10, 5, 1, and 0.5 µmol/L). 200 µL of standard and sample were then pipetted in a 96 well-plate followed by addition of 20 µL of Greiss reagent. The solutions were mixed using the 'shake' function on the spectrophotometer and incubated at 60°C for 20 min followed by cool down for 30 min and measurement at 540 nm on the spectrophotometer. Standards were used to plot a calibration curve based on known nutrient concentrations and spectrophotometer readings, which was then used to determine nutrient concentrations in samples.

Data analyses

Prior to formal analysis, all data were tested for normality and homoscedasticity using a Shapiro–Wilk test and a Bartlett test, respectively. To identify differences in Hsp-70, MDA, TAC, haemocyte community, phagocytic activity, and nutrient concentrations among treatments (control, hypoxia, acidification, and HA), we undertook two-factor permutational-ANOVAs (factors: Hypoxia, Acidification, two levels in each) on Euclidean distance matrices ($3 < n < 15$ per treatment depending on the variable measured, see Supplementary Tables S2, S3) followed by pairwise tests for significant terms in PERMANOVA. Microbial community data were grouped by phylum and were log (X + 1) transformed prior to analysis because of the large number of zero values within the data set. To identify differences in community structures among treatments, we performed a two-factor permutational-MANOVA (factor: Hypoxia,

Acidification) on Bray–Curtis similarity matrix (n = 4). When significant effects were detected, post-hoc pairwise tests were used to determine which treatments differed. We then used an Analysis of Similarity (ANOSIM) to identify the amount of overlap (similarity/dissimilarity) in the community between treatments. Specific microbial phyla that contributed to the differences between treatments were identified using a Similarity Percentage test (SIMPER). The microbial community data were then plotted on a heatmap and a dendrogram was used for hierarchical clustering of microbial phyla. All permutational-MANOVA, ANOSIM, and SIMPER tests were performed on PRIMER+PERMANOVA (version 7). All normality tests, homoscedasticity tests, and hierarchical clustering of microbial phyla for heatmap were performed on R (version 4.12) using the packages "stats" and "gplots."

Results

Oyster molecular defence

Throughout the experiment, less than 10% of oysters died across all experimental treatments (total 14 individuals died out of 240: 3 in control, 2 in acidification, 4 in hypoxia, and 5 in HA). However, experimental treatments drove differences in the physiological responses of oysters (Figure 1; Supplementary Table S2). Hsp-70 production was independently influenced by hypoxia and acidification (Supplementary Table S2). Oysters exposed to HA produced the highest concentrations of Hsp-70 (Figure 1A); approximately 600% more than oysters in the control ($t_7 = 3.1738$, $p = 0.023$; Supplementary Table S2), and 500% more than those exposed to acidification ($t_8 = 3.0245$, $p = 0.012$). Oysters from HA conditions also seemed to produce higher concentrations of Hsp-70 than those from hypoxic conditions, however these were not significant, likely because of large variability (Figure 1A; $t_7 = 2.0412$, $p = 0.078$). Oysters from hypoxic conditions produced approximately 120% more Hsp-70 than those from control conditions (Figure 1A; $t_6 = 2.3148$, $p = 0.029$), but were within the same range as those from acidified conditions ($t_7 = 1.2772$, $p = 0.247$). Finally, oysters from acidification conditions did not produce significantly higher Hsp-70 concentrations than those from control conditions (Figure 1A; $t_7 = 1.2131$, $p = 0.317$).

Overall, oysters from the different conditions produced similar concentrations of MDA (Figure 1B; Supplementary Table S2), except for acidification, meaning that oxidative stress was high in oysters exposed to acidification. Oysters exposed to acidification produced a higher concentration of MDA compared to those exposed to control and HA conditions (Figure 1B; $t_5 = 3.6523$, $p = 0.029$, $t_6 = 3.4242$, $p = 0.043$, respectively), but not compared to hypoxia ($t_5 = 2.5796$ $p = 0.101$: Supplementary Table S1). Finally, no difference in TAC was observed across treatments (Figure 1C; Supplementary Table S2).

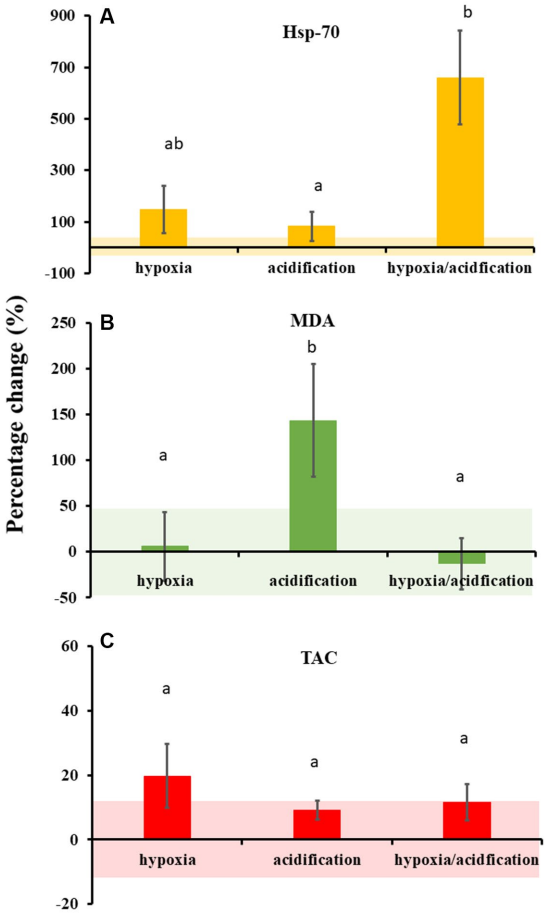

FIGURE 1
Percentage change relative to control (mean±SE) in heat shock protein 70 (Hsp-70; **(A)**), malondialdehyde (MDA; **(B)**), and total oxidative capacity (TAC; **(C)**) measured from oysters exposed to hypoxia, acidification, or both. Coloured bands around the x-axis denote the variation (mean±SE) in oysters exposed to control conditions. Concentrations of Hsp-70, MDA and TAC in control conditions were 0.0014 (±0.0007) ng/mg, 0.071 (±0.03) µM/mg, and 0.0014 (±0.0002) mM/mg, respectively. Note the difference in scale for each graph. Letters denote significant differences.

Oyster immune response

The number of granulocytes in oysters were influenced by both acidification and hypoxia (Supplementary Table S3) demonstrating that the immune system was impaired. Oysters exposed to HA and acidification produced fewer granulocytes compared to control or hypoxia oysters (Figure 2A; Supplementary Table S3). The number of agranulocytes in oysters, were also influenced by acidification and hypoxia, and their interaction (Supplementary Table S3). Agranulocyte numbers in oysters from HA conditions were lower than those exposed to hypoxia or acidification (Figure 2A; $t_{33} = 3.6789$, $p = 0.002$, and $t_{32} = 2.3893$, $p = 0.026$, respectively), with counts in the latter two being similar ($t_{31} = 1.0456$, $p = 0.314$), and lower than those in the control ($t_{27} = 5.2238$, $p = 0.001$, and $t_{28} = 5.8149$, $p = 0.001$, respectively).

The overall communities of haemocyte (both granulocytes and agranulocytes) were significantly influenced by hypoxia, acidification, or their combination (HA), with the proportion of granulocyte to agranulocyte also differing (1:1.5 granulocyte to agranulocyte in controls; Figure 2A; Supplementary Table S3). The haemocyte community in oysters exposed to hypoxia were different from those exposed to other experimental treatments in terms of counts and proportion of granulocyte to agranulocyte (more granulocyte than agranulocyte; ratio = 1:0.8; Supplementary Table S3). Oysters exposed

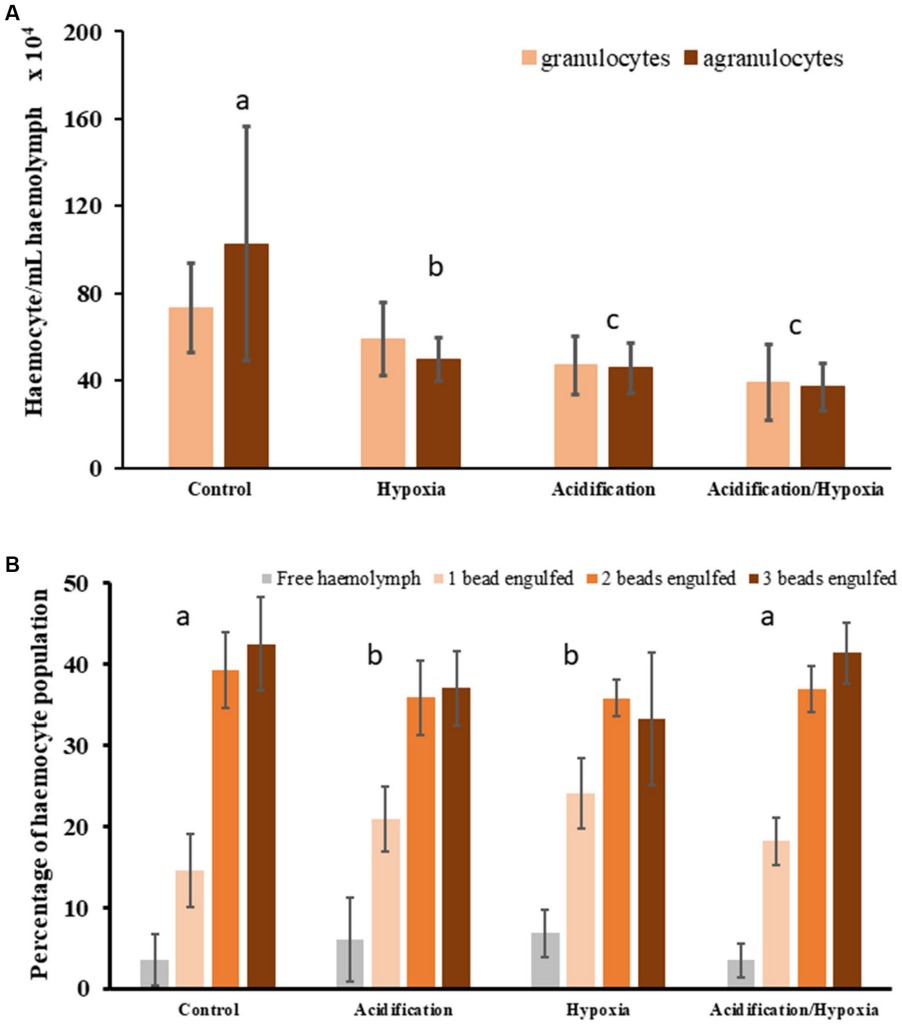

FIGURE 2
Oyster haemocyte counts (mean±SE) differentiated as granulocytes and agranulocytes **(A)** and oyster phagocytic activity measured as the number of fluorescent beads engulfed by haemocytes (mean±SE) **(B)**. Letters and circles denote significantly different treatment groups.

to HA and acidification had similar haemocyte community, that is, similar counts and proportion of granulocyte to agranulocyte (1:1) to each other (Figure 2A; $t_{33} = 1.7916$ $p = 0.059$), but also the lowest counts among all treatments (Figure 2A).

The phagocytic activity, that is the percentage of haemocytes that engulfed one, two, three, or no beads, was influenced by hypoxia and acidification which each independently reduced overall phagocytic activity relative to control (fewer haemocytes engulfed 2 or 3 beads: Figure 3; Supplementary Table S3). However, HA produced similar phagocytic activity as control conditions as suggested by the proportion of haemocytes engulfing 2 or 3 beads (Figure 2B; Supplementary Table S3). Although oysters exposed to HA had lower counts of haemocytes, their activity in terms of engulfment of beads, was similar to oysters from control conditions (Figure 2B; $t_{16} = 1.227$, $p = 0.212$). Overall, a larger proportion of haemocytes from both control and HA engulfed two or three beads, with very few engulfing none. The phagocytic activity in oysters exposed to hypoxia and acidification were similar to each other (Figure 2B; $t_{17} = 1.4234$, $p = 0.148$). While the majority of haemocytes from these treatments still engulfed two or three beads, a large proportion also engulfed only one or no beads (Figure 2B).

Microbial community

There was a clear difference in the microbial community structure when oysters were present oysters, irrespective of the treatment, compared when oysters were absent (Figure 3; *Pseudo*-$F_{3,30} = 101.01$, $p = 0.001$). The microbial community associated with oysters was characterised by microbes that are commonly observed in the environment (benthos, water column) or as part of the microbiome of organisms (e.g., the phyla Latescibacterota and Acidobacteriota), but also multiple other phyla associated with organic matter degradation (e.g., Hydrogenedentes, Sumerlaeota) or inorganic nutrient cycling (e.g., Desulfobacterota, Nitrospinota, 'uncultured' NB1-j, Planctomycetota). The community structure of microbes associated with oysters also differed among the four treatments (Supplementary Table S4), albeit with some overlap in the number of phyla (ANOSIM: $0.2 < R$ statistic < 0.5). Therefore, differences among the communities were driven by turnover in a few taxa rather than wholesale community change. The community in acidified conditions was distinguished by the presence of bacteria resistant to extreme environments (e.g., phylum Deinococcota), organic carbon fermenting bacteria (e.g., phylum Fermentibacterota), and

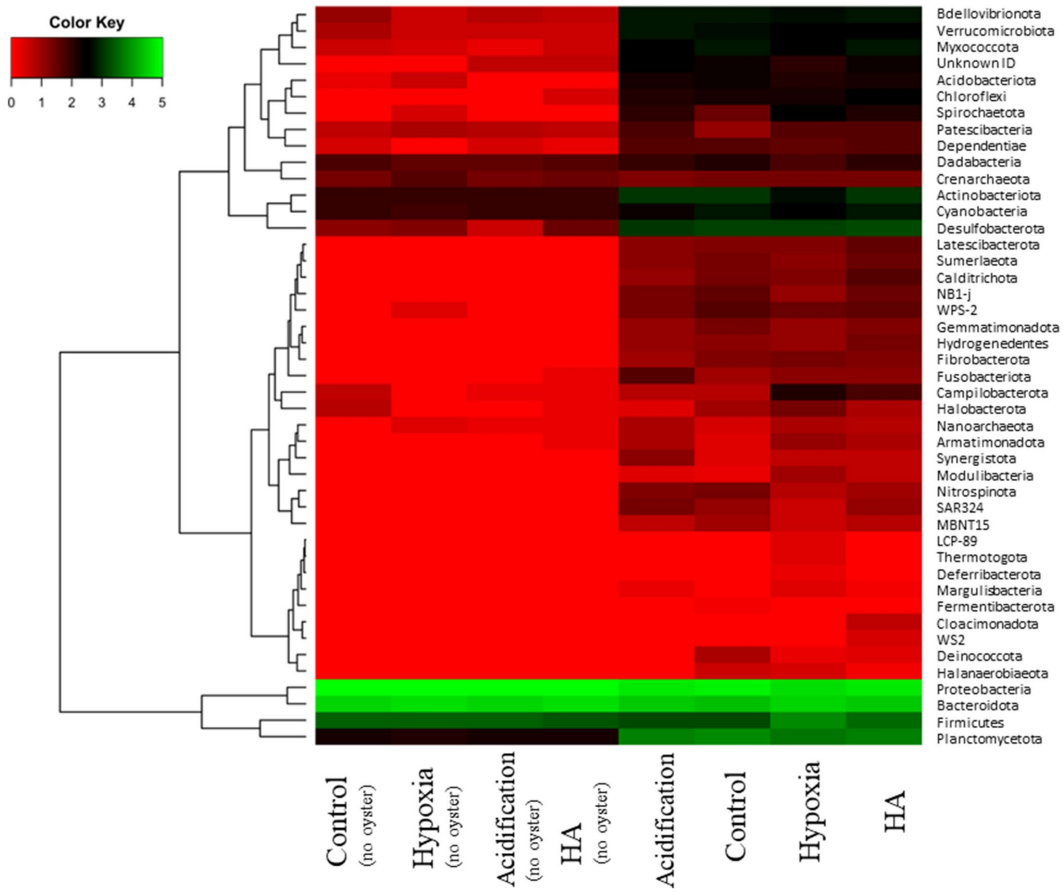

FIGURE 3
Heatmap comparing abundance of microbial phyla (log x+1) in the presence or absence of oysters under control, acidification, hypoxia, and hypoxia/acidification (HA) conditions.

nitrite-oxidizing bacteria (e.g., phylum Nitrospinota) (Figure 3). On the other hand, the community in hypoxic conditions was primarily distinguished by the presence of bacteria from multiple phyla that thrive in anaerobic conditions (e,g., Deferribacterota, Halanaerobiaeota, Modulibacteria, and Thermotogota). In addition, pathogenic bacteria, such as from the phyla Firmicutes and Spirochaetoses, contributed more to the hypoxic community compared to all other treatments. Finally, in the HA treatment, the microbial community was characterised by anaerobic bacteria and organic carbon degraders (e.g., phyla Calditrichota, Cloacimonadota, and Hydrogenedentes).

Nutrient cycling

The concentration of ammonium and nitrite were very low (close to zero) in the absence of oysters under all treatments (Figure 4). In contrast, the concentrations of both were high (> 15 µmol/L for ammonium and > 35 µmol/L for nitrite) in all experimental conditions when oysters were present. The concentrations of ammonium was higher in control and acidification treatments when oysters were present compared to when they were absent (up to 25 µmol/L g; Figure 4; $t_6 = 5.0176$, $p = 0.016$ and $t_6 = 3.4189$, $p = 0.047$, respectively), but these concentrations were low compared to the concentration of nitrite in both control and acidification conditions in the presence of oysters (both over 40 µmol/L; $t_6 = 7.8128$, $p = 0.019$ and $t_6 = 13.198$, $p = 0.018$, respectively). Finally, nitrate concentrations remained unchanged in the presence or absence of oysters or between different treatments (Figure 4). The concentrations of ammonium were two times higher under hypoxia and HA conditions compared to acidification (Figure 4; $t_7 = 3.3436$, $p = 0.009$ and $t_8 = 2.5076$, $p = 0.036$). The concentrations of ammonium were higher under hypoxia compared to control conditions (Figure 4; $t_7 = 2.9393$, $p = 0.024$), and while the concentrations under HA seemed higher, they were not statistically significant ($t_8 = 2.1081$, $p = 0.057$). No differences were found in nitrite concentrations between treatments, except for acidification where nitrite was lower compared to control conditions (Figure 4; $t_8 = 2.2273$, $p = 0.027$). Finally, the concentration of nitrate under hypoxia and HA were both less than that in acidification (Figure 4; $t_7 = 3.2422$, $p = 0.014$ and $t_8 = 32.5526$, $p = 0.007$, respectively).

Discussion

Climate change is projected to drive more extreme fluctuations in environmental conditions, potentially exposing organisms to periods of physiologically stressful conditions, especially with compound changes in two or more environmental conditions. For habitat forming

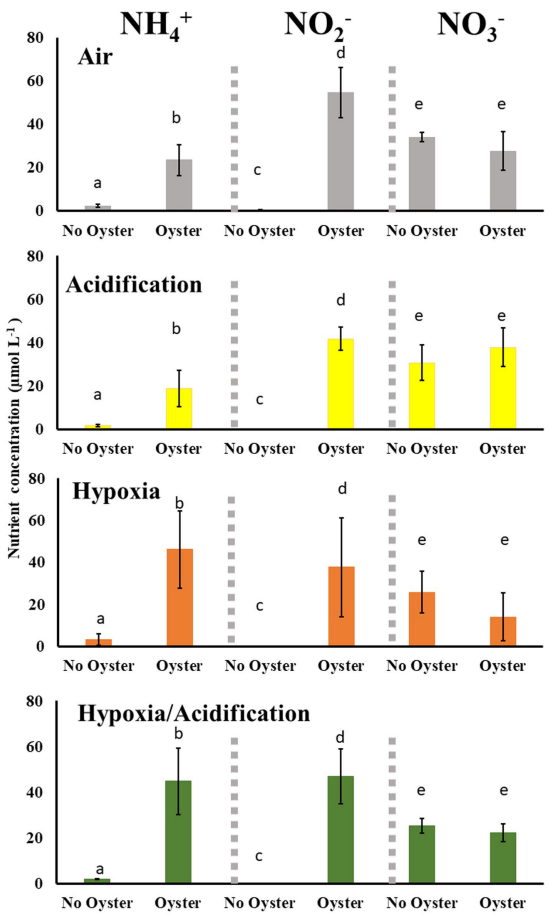

FIGURE 4
Ammonium (NH_4^+), Nitrite (NO_2^-) and Nitrate (NO_3^-) concentrations (mean±SE) measured from seawater in the presence and absence of oysters under control, acidification, hypoxia, and Hypoxia/acidification conditions. Letters denote significantly different concentrations for each nutrient in the presence and absence of oysters within each treatment.

organisms (e.g., oysters, mussels, seagrasses, or corals), physiological stress can quickly cascade into ecosystem-wide consequences (Wernberg et al., 2013) through changes in performance of the organism that result in changes in their function (e.g., loss of habitat forming capacity or changes in ecological processes in which they are involved). Here, we show that acidification, and its combination with hypoxia (HA), were particularly stressful to oysters and caused a large molecular response. Simultaneously, acidification, hypoxia, and HA impaired the immune response of oysters. More importantly, however, changes to the oyster-associated microbial community under altered conditions drove a loss in efficiency of nutrient cycling in hypoxic and HA conditions.

The physiological response of oysters differed based on the type of environmental stressor they were exposed to, but, overall, both molecular processes and immune response were impacted. Oysters exposed to acidification produced a higher concentration of MDA, suggesting an increased lipid peroxidation and oxidative stress (Tsikas, 2017), a response commonly observed in oysters exposed to acidification (Tomanek et al., 2011; Mackenzie et al., 2014; Wang et al., 2016, 2020). Simultaneously, oysters exposed to acidification produced fewer haemocytes and the phagocytic capacity of these haemocytes was also reduced. The reduction of haemocytes and phagocytosis is generally representative of stressful conditions (Mackenzie et al., 2014) and here it could be indicative of two responses. First, energy may have been redistributed towards production of MDA for reduction of oxidative stress within the organism, at the expense of the immune system (trade-off mechanism; Rauw, 2012). Second, oxidative stress within the haemolymph may have reduced phagocytic capacity of haemocytes by impacting cell membrane strength (e.g., Xie et al., 2017; Cao et al., 2018). The low haemocyte production and phagocytic activity means that extended exposure to acidification can severely impact oyster immune capacity, both through impaired molecular response and immune response, and, therefore, increase their susceptibility to pathogens.

Oysters exposed to hypoxia did not respond through changes to molecular defence, but their immune capacity was significantly lowered. Specifically, we found that both the number of granulocytes and agranulocytes in oysters were reduced indicating a reduction in innate immune capacity (Jiang et al., 2016). Depressed immune capacity (haemocyte counts and phagocytic activity) under hypoxic conditions has been observed in a range of organisms (Wang et al., 2012; Chen et al., 2017; Wang et al., 2017; Shen et al., 2019; Zhan et al., 2022), and is often considered a major contributor to mortality because of the associated susceptibility to pathogenic load (Ellis et al., 2011). In our experiment, exposure to hypoxic conditions for 16 days did not have major lethal consequences likely because of the controlled conditions that organisms were reared in (that is natural pathogens were not as prevalent as they could be in the natural environment). However, considering that hypoxic conditions on the benthos can last for days up to months (Levin et al., 2009; Qian et al., 2018), and oysters inhabit dynamic coastal environments where pathogens are more prevalent (either occurring in the natural environment or resulting from anthropogenic discharge), it is likely that prolonged hypoxia will drive higher mortality rates of oysters in natural ecosystems.

The coupled impact of acidification and hypoxia tends to be synergistically negative on organismal physiology (Gobler et al., 2014; Gobler and Baumann, 2016) and can cause rapid mortality (Chan et al., 2019). In our experiment, oysters produced substantially more Hsp-70 under combined hypoxic and acidified conditions and their haemocyte counts decreased considerably. Yet, the phagocytic activity (proportion of cells that engulf beads) remained similar to that of oysters from the control conditions (i.e., most cells engulfed three and few engulfed less than two beads) and, most importantly, mortality remained low. This combination of responses suggests that oysters under HA conditions likely experienced acute physiological stress. As the production and chaperoning action of HSPs are ATP-dependent processes that require high levels of aerobic metabolism and come at a high energetic cost (Feder and Hofmann, 1999; Sokolova et al., 2012), our results suggest that a large amount of energy may have been directed towards the production of Hsp-70 chaperones that serve to maintain protein integrity (Mayer and Bukau, 2005). The increased Hsp-70 production suggests that the organisms experienced protein damage, a condition commonly driven by excessive oxidative stress that rapidly affects the structure and activity of proteins (Reichmann et al., 2018). Therefore, rather than

allocating energy towards reduction of oxidative stress (e.g., MDA), oysters may have allocated energy towards maintaining the structure of the rapidly deteriorating proteins (by producing Hsp-70 chaperones). Finally, the low counts of haemocytes but strong phagocytic capacity indicates that energy may have also been invested towards efficient immune response, such as through repair of haemocyte cell membrane (Xie et al., 2017), rather than production of more haemocytes. The investment in repairing haemocyte cell membranes could be driven by an increasing pathogenic load or deteriorating tissue that required haemocytes to respond (Bachère et al., 2015), but the large amount of energy already allocated to Hsp-70 production meant that production of new haemocyte may be too costly, and maintenance of already existing haemocytes provided a better trade-off. Overall, these results suggest that the combined effects of hypoxia and acidification are physiologically costly to oysters and can rapidly increase their susceptibility to pathogens.

The microbial community associated with the oysters was affected by exposure to different environmental stressors. Considering that the microbial community structure was modified (enriched differently) in different environmental conditions, it is conceivable that short-term rapid environmental change will drive some extent of oyster holobiont restructuring in natural systems (e.g., some microbes that were more suited to exploit or survive in the acidification, hypoxia, or both conditions, and, therefore, became more prevalent in these conditions). While oyster holobiont research remains limited, similar changes in some microbial taxonomic groups within the holobiont have been observed when exposed to similar environmental stressors for the Sydney rock oysters (*Saccostrea glomerata*; Scanes et al., 2021a,b), some sponges (Ribes et al., 2016; Posadas et al., 2022) and some corals (Bourne et al., 2016; Meunier et al., 2021). However, complete/broader turnover of associated microbial communities is not often observed (Meron et al., 2012; Bourne et al., 2016; Zhou et al., 2016; Ge et al., 2021). Broader host associated microbial community turnover is more likely to occur after long-term exposure to changed environments, such as in oysters exposed to 2,800 ppm pCO_2 for 80 days (Unzueta-Martínez et al., 2021) or clams exposed to several years of increased temperature (Neu et al., 2021). Our results, along with findings from other studies, therefore, suggest that host associated microbial communities can be subject to important shifts in enrichment that cause compositional changes driven by alterations to their environment.

The two times lower concentration of ammonium than nitrite (ratio of approximately 1:2) suggest perhaps low ammonium release through bio-deposits by oysters but, importantly, efficient nitrification rates by microbes in both control and acidification. In contrast, the doubled ammonium concentration in hypoxic and HA conditions compared acidification, and to some extent, control conditions suggest more ammonium release by oysters in hypoxic and HA conditions. A probable explanation of for the increased ammonium concentrations is that increased stress induced higher filtration rates (energy acquisition), which lead to more ammonium excretion. While we did not directly measure filtration rates, the linkage between physiological stress, filtration rates and ammonium releases has previously been established (e.g., Guzmán-Agüero et al., 2013). The 1:1 ratio of ammonium to nitrite in hypoxic and HA conditions also suggest approximately 50% less efficient nitrification compared to control or acidification conditions. Therefore, the changes in ammonium and nitrite concentrations measured in our study suggest high nitrification capacity by microbes in the acidification treatment, that is a possible increase in nitrification by microbes in acidified conditions compared to control or other treatments. Under hypoxia and the combination of stressors, however, the high concentration of both ammonium and nitrite measured in the experiment suggest ammonium release by oysters (e.g., through excretion) may be higher and that although nitrification was maintained, there was loss of nitrification efficiency/capacity under hypoxia and HA conditions.

Overall, our study shows that the oyster holobiont can maintain some reduced nutrient cycling capacity under acidification or hypoxic conditions, or their combination, as long as the host itself can regulate its physiological processes. The enrichment of microbial communities seemed to change mostly in an exploitive manner based on the environmental conditions. However, it is also clear that processes such as nitrification become less efficient in hypoxic and combined hypoxic and acidified conditions. On the other hand, oyster molecular defence and immune capacity was impacted under both acidification and hypoxia, and even more so under the combined stressors. While mortality was low under all altered conditions, the decreased immune capacity coupled with other physiological impairments would likely render oysters vulnerable to pathogens and other future environmental stressors. If there was a resultant increase in mortality and decline in oyster populations this would drive a drastic loss of the functions associated with the oyster holobiont. The negative impact of climate change on oyster physiology and holobiont functions, therefore, has implications for the future of oyster reefs whereby the increase hypoxic and acidified conditions in coastal environments could render conservation and restoration efforts less able to achieve their full potential.

Data availability statement

The original contributions presented in the study are publicly available. This data can be found here: University of Hong Kong (HKU) Data Repository, accession 10.25442/hku.22717084.v1; NCBI BioProject, accession PRJNA903533.

Author contributions

DH: conceptualization, methodology, formal analysis, investigation, and writing – original draft. LF: conceptualization, methodology, writing – review & editing, and funding acquisition. KC: conceptualization, methodology, formal analysis, investigation, and writing – review & editing. LM: investigation and writing – review & editing. AC: conceptualization, methodology, investigation, and writing – review & editing. BR: conceptualization, methodology, writing – original draft, review & editing, and funding acquisition. All authors contributed to the article and approved the submitted version.

Funding

This project was funded by a Faculty of Science (HKU) Rising Star Fund grant to BR, a University of Hong Kong Post-Doctoral Fellowship to DH, and CUHK funding to LF. The computations were performed using research computing facilities offered by Information Technology Services, the University of Hong Kong.

Conflict of interest

The authors declare that the research was conducted in the absence of any commercial or financial relationships that could be construed as a potential conflict of interest.

Publisher's note

Supplementary material

The Supplementary material for this article can be found online at: https://www.frontiersin.org/articles/10.3389/fevo.2023.1083315/full#supplementary-material

References

Bachère, E., Rosa, R. D., Schmitt, P., Poirier, A. C., Merou, N., Charrière, G. M., et al. (2015). The new insights into the oyster antimicrobial defense: cellular, molecular and genetic view. *Fish Shellfish Immunol.* 46, 50–64. doi: 10.1016/j.fsi.2015.02.040

Bayraktarov, E., Saunders, M. I., Abdullah, S., Mills, M., Beher, J., Possingham, H. P., et al. (2016). The cost and feasibility of marine coastal restoration. *Ecol. Appl.* 26, 1055–1074. doi: 10.1890/15-1077

Bokulich, N. A., Kaehler, B. D., Rideout, J. R., Dillon, M., Bolyen, E., Knight, R., et al. (2018). Optimizing taxonomic classification of marker-gene amplicon sequences with QIIME 2's q2-feature-classifier plugin. *Microbiome* 6, 1–17. doi: 10.1186/s40168-018-0470-z

Bolyen, E., Rideout, J. R., Dillon, M. R., Bokulich, N. A., Abnet, C. C., Al-Ghalith, G. A., et al. (2019). Reproducible, interactive, scalable and extensible microbiome data science using QIIME 2. *Nat. Biotechnol.* 37, 852–857. doi: 10.1038/s41587-019-0209-9

Bourne, D. G., Morrow, K. M., and Webster, N. S. (2016). Insights into the coral microbiome: underpinning the health and resilience of reef ecosystems. *Annu. Rev. Microbiol.* 70, 317–340. doi: 10.1146/annurev-micro-102215-095440

Boyd, J. N., and Burnett, L. E. (1999). Reactive oxygen intermediate production by oyster hemocytes exposed to hypoxia. *J. Exp. Biol.* 202, 3135–3143. doi: 10.1242/jeb.202.22.3135

Cai, W. J. (2011). Estuarine and coastal ocean carbon paradox: CO2 sinks or sites of terrestrial carbon incineration? *Annu. Rev. Mar. Sci.* 3, 123–145. doi: 10.1146/annurev-marine-120709-142723

Callahan, B. J., McMurdie, P. J., Rosen, M. J., Han, A. W., Johnson, A. J. A., and Holmes, S. P. (2016). DADA2: high-resolution sample inference from Illumina amplicon data. *Nat. Methods* 13, 581–583. doi: 10.1038/nmeth.3869

Cao, R., Wang, Q., Yang, D., Liu, Y., Ran, W., Qu, Y., et al. (2018). CO2-induced ocean acidification impairs the immune function of the Pacific oyster against *Vibrio splendidus* challenge: an integrated study from a cellular and proteomic perspective. *Sci. Total Environ.* 625, 1574–1583. doi: 10.1016/j.scitotenv.2018.01.056

Chan, F., Barth, J. A., Kroeker, K. J., Lubchenco, J., and Menge, B. A. (2019). The dynamics and impact of ocean acidification and hypoxia. *Oceanography* 32, 62–71. doi: 10.5670/oceanog.2019.312

Chen, N., Wu, M., Tang, G. P., Wang, H. J., Huang, C. X., Wu, X. J., et al. (2017). Effects of acute hypoxia and reoxygenation on physiological and immune responses and redox balance of Wuchang bream (*Megalobrama amblycephala* Yih, 1955). *Front. Physiol.* 8:375. doi: 10.3389/fphys.2017.00375

David, E., Tanguy, A., Pichavant, K., and Moraga, D. (2005). Response of the Pacific oyster *Crassostrea gigas* to hypoxia exposure under experimental conditions. *FEBS J.* 272, 5635–5652. doi: 10.1111/j.1742-4658.2005.04960.x

Diaz, R. J., and Rosenberg, R. (1995). Marine benthic hypoxia: a review of its ecological effects and the behavioural responses of benthic macrofauna. *Oceanogr. Mar. Biol.* 33, 245–203.

Dubé, C. E., Ky, C. L., and Planes, S. (2019). Microbiome of the black-lipped pearl oyster *Pinctada margaritifera*, a multi-tissue description with functional profiling. *Front. Microbiol.* 10:1548. doi: 10.3389/fmicb.2019.01548

Ellis, R. P., Parry, H., Spicer, J. I., Hutchinson, T. H., Pipe, R. K., and Widdicombe, S. (2011). Immunological function in marine invertebrates: responses to environmental perturbation. *Fish Shellfish Immunol.* 30, 1209–1222. doi: 10.1016/j.fsi.2011.03.017

Feder, M. E., and Hofmann, G. E. (1999). Heat-shock proteins, molecular chaperones, and the stress response: evolutionary and ecological physiology. *Annu. Rev. Physiol.* 61, 243–282. doi: 10.1146/annurev.physiol.61.1.243

García-Robledo, E., Corzo, A., and Papaspyrou, S. (2014). A fast and direct spectrophotometric method for the sequential determination of nitrate and nitrite at low concentrations in small volumes. *Mar. Chem.* 162, 30–36. doi: 10.1016/j.marchem.2014.03.002

Garner, N., Ross, P. M., Falkenberg, L. J., Seymour, J. R., Siboni, N., and Scanes, E. (2022). Can seagrass modify the effects of ocean acidification on oysters? *Mar. Pollut. Bull.* 177:113438. doi: 10.1016/j.marpolbul.2022.113438

Ge, R., Liang, J., Yu, K., Chen, B., Yu, X., Deng, C., et al. (2021). Regulation of the coral-associated Bacteria and Symbiodiniaceae in *Acropora valida* under ocean acidification. *Front. Microbiol.* 12:767174. doi: 10.3389/fmicb.2021.767174

Glenn, T. C., Nilsen, R. A., Kieran, T. J., Sanders, J. G., Bayona-Vásquez, N. J., Finger, J. W., et al. (2019). Adapterama I: universal stubs and primers for 384 unique dual-indexed or 147,456 combinatorially-indexed Illumina libraries (iTru & iNext). *Peer J* 7:e7755. doi: 10.7717/peerj.7755

Gobler, C. J., and Baumann, H. (2016). Hypoxia and acidification in ocean ecosystems: coupled dynamics and effects on marine life. *Biol. Lett.* 12:20150976. doi: 10.1098/rsbl.2015.0976

Gobler, C. J., DePasquale, E. L., Griffith, A. W., and Baumann, H. (2014). Hypoxia and acidification have additive and synergistic negative effects on the growth, survival, and metamorphosis of early life stage bivalves. *Plo S one* 9:e83648. doi: 10.1371/journal.pone.0083648

Goedken, M., and De Guise, S. (2004). Flow cytometry as a tool to quantify oyster defence mechanisms. *Fish Shellfish Immunol.* 16, 539–552. doi: 10.1016/j.fsi.2003.09.009

Grasshoff, K., Kremling, K., and Ehrhardt, M. eds., (2009). *Methods of Seawater Analysis*. John Wiley & Sons, Hoboken, NJ.

Green, D. S., Boots, B., and Crowe, T. P. (2012). Effects of non-indigenous oysters on microbial diversity and ecosystem functioning. *PLoS One* 7:e48410. doi: 10.1371/journal.pone.0048410

Guzmán-Agüero, J. E., Nieves-Soto, M., Hurtado, M. Á., Pina-Valdez, P., and Garza-Aguirre, M. D. C. (2013). Feeding physiology and scope for growth of the oyster *Crassostrea corteziensis* (Hertlein, 1951) acclimated to different conditions of temperature and salinity. *Aquac. Int.* 21, 283–297. doi: 10.1007/s10499-012-9550-4

Hoellein, T. J., Zarnoch, C. B., and Grizzle, R. E. (2015). Eastern oyster (*Crassostrea virginica*) filtration, biodeposition, and sediment nitrogen cycling at two oyster reefs with contrasting water quality in Great Bay estuary (New Hampshire, USA). *Biogeochemistry* 122, 113–129. doi: 10.1007/s10533-014-0034-7

Hughes, D. J., Alderdice, R., Cooney, C., Kühl, M., Pernice, M., Voolstra, C. R., et al. (2020). Coral reef survival under accelerating ocean deoxygenation. *Nat. Clim. Chang.* 10, 296–307. doi: 10.1038/s41558-020-0737-9

Jeppesen, R., Rodriguez, M., Rinde, J., Haskins, J., Hughes, B., Mehner, L., et al. (2018). Effects of hypoxia on fish survival and oyster growth in a highly eutrophic estuary. *Estuar. Coasts* 41, 89–98. doi: 10.1007/s12237-016-0169-y

Jiang, S., Jia, Z., Zhang, T., Wang, L., Qiu, L., Sun, J., et al. (2016). Functional characterisation of phagocytes in the Pacific oyster *Crassostrea gigas*. *Peer J* 4:e2590. doi: 10.7717/peerj.2590

King, W. L., Jenkins, C., Seymour, J. R., and Labbate, M. (2019). Oyster disease in a changing environment: decrypting the link between pathogen, microbiome and environment. *Mar. Environ. Res.* 143, 124–140. doi: 10.1016/j.marenvres.2018.11.007

Lau, S. C. Y., Thomas, M., Hancock, B., and Russell, B. D. (2020). Restoration potential of Asian oysters on heavily developed coastlines. *Restor. Ecol.* 28, 1643–1653. doi: 10.1111/rec.13267

Lemasson, A. J., Fletcher, S., Hall-Spencer, J. M., and Knights, A. M. (2017). Linking the biological impacts of ocean acidification on oysters to changes in ecosystem services: a review. *J. Exp. Mar. Biol. Ecol.* 492, 49–62. doi: 10.1016/j.jembe.2017.01.019

Levin, L. A., Ekau, W., Gooday, A. J., Jorissen, F., Middelburg, J. J., Naqvi, S. W. A., et al. (2009). Effects of natural and human-induced hypoxia on coastal benthos. *Biogeosciences* 6, 2063–2098. doi: 10.5194/bg-6-2063-2009

Lutier, M., Di Poi, C., Gazeau, F., Appolis, A., Le Luyer, J., and Pernet, F. (2022). Revisiting tolerance to ocean acidification: insights from a new framework combining physiological and molecular tipping points of Pacific oyster. *Glob. Chang. Biol.* 28, 3333–3348. doi: 10.1111/gcb.16101

Mackenzie, C. L., Lynch, S. A., Culloty, S. C., and Malham, S. K. (2014). Future oceanic warming and acidification alter immune response and disease status in a commercial shellfish species, *Mytilus edulis* L. *PLoS One* 9:e99712. doi: 10.1371/journal.pone.0099712

Mayer, M. P., and Bukau, B. (2005). Hsp70 chaperones: cellular functions and molecular mechanism. *Cell. Mol. Life Sci.* 62, 670–684. doi: 10.1007/s00018-004-4464-6

Meron, D., Rodolfo-Metalpa, R., Cunning, R., Baker, A. C., Fine, M., and Banin, E. (2012). Changes in coral microbial communities in response to a natural pH gradient. *ISME J.* 6, 1775–1785. doi: 10.1038/ismej.2012.19

Meunier, V., Geissler, L., Bonnet, S., Rädecker, N., Perna, G., Grosso, O., et al. (2021). Microbes support enhanced nitrogen requirements of coral holobionts in a high CO2 environment. *Mol. Ecol.* 30, 5888–5899. doi: 10.1111/mec.16163

Neu, A. T., Hughes, I. V., Allen, E. E., and Roy, K. (2021). Decade-scale stability and change in a marine bivalve microbiome. *Mol. Ecol.* 30, 1237–1250. doi: 10.1111/mec.15796

Parada, A. E., Needham, D. M., and Fuhrman, J. A. (2016). Every base matters: assessing small subunit rRNA primers for marine microbiomes with mock communities, time series and global field samples. *Environ. Microbiol.* 18, 1403–1414. doi: 10.1111/1462-2920.13023

Posadas, N., Baquiran, J. I. P., Nada, M. A. L., Kelly, M., and Conaco, C. (2022). Microbiome diversity and host immune functions influence survivorship of sponge holobionts under future ocean conditions. *ISME J.* 16, 58–67. doi: 10.1038/s41396-021-01050-5

Qian, W., Gan, J., Liu, J., He, B., Lu, Z., Guo, X., et al. (2018). Current status of emerging hypoxia in a eutrophic estuary: the lower reach of the Pearl River estuary, China. *Estuar. Coast. Shelf Sci.* 205, 58–67. doi: 10.1016/j.ecss.2018.03.004

Rauw, W. M. (2012). Immune response from a resource allocation perspective. *Front. Genet.* 3:267. doi: 10.3389/fgene.2012.00267

Ray, N. E., and Fulweiler, R. W. (2021). Meta-analysis of oyster impacts on coastal biogeochemistry. *Nat. Sustain.* 4, 261–269. doi: 10.1038/s41893-020-00644-9

Ray, N. E., Henning, M. C., and Fulweiler, R. W. (2019). Nitrogen and phosphorus cycling in the digestive system and shell biofilm of the eastern oyster *Crassostrea virginica*. *Mar. Ecol. Prog. Ser.* 621, 95–105. doi: 10.3354/meps13007

Reichmann, D., Voth, W., and Jakob, U. (2018). Maintaining a healthy proteome during oxidative stress. *Mol. Cell* 69, 203–213. doi: 10.1016/j.molcel.2017.12.021

Ribes, M., Calvo, E., Movilla, J., Logares, R., Coma, R., and Pelejero, C. (2016). Restructuring of the sponge microbiome favors tolerance to ocean acidification. *Environ. Microbiol. Rep.* 8, 536–544. doi: 10.1111/1758-2229.12430

Rivest, E. B., Comeau, S., and Cornwall, C. E. (2017). The role of natural variability in shaping the response of coral reef organisms to climate change. *Curr. Clim. Change Rep.* 3, 271–281. doi: 10.1007/s40641-017-0082-x

Scanes, E., Parker, L. M., Seymour, J. R., Siboni, N., King, W. L., Danckert, N. P., et al. (2021a). Climate change alters the haemolymph microbiome of oysters. *Mar. Pollut. Bull.* 164:111991. doi: 10.1016/j.marpolbul.2021.111991

Scanes, E., Parker, L. M., Seymour, J. R., Siboni, N., King, W. L., Wegner, K. M., et al. (2021b). Microbiome response differs among selected lines of Sydney rock oysters to ocean warming and acidification. *FEMS Microbiol. Ecol.* 97:fiab 09. doi: 10.1093/femsec/fiab099

Shen, Y., Huang, Z., Liu, G., Ke, C., and You, W. (2019). Hemolymph and transcriptome analysis to understand innate immune responses to hypoxia in Pacific abalone. *Comp. Biochem. Physiol. Part D Genomics Proteomics* 30, 102–112. doi: 10.1016/j.cbd.2019.02.001

Smyth, A. R., Geraldi, N. R., and Piehler, M. F. (2013). Oyster-mediated benthic-pelagic coupling modifies nitrogen pools and processes. *Mar. Ecol. Prog. Ser.* 493, 23–30. doi: 10.3354/meps10516

Sokolova, I. M., Frederich, M., Bagwe, R., Lannig, G., and Sukhotin, A. A. (2012). Energy homeostasis as an integrative tool for assessing limits of environmental stress tolerance in aquatic invertebrates. *Mar. Environ. Res.* 15, 1–18. doi: 10.1016/j.marenvres.2012.04.003

Stevick, R. J., Post, A. F., and Gómez-Chiarri, M. (2021). Functional plasticity in oyster gut microbiomes along a eutrophication gradient in an urbanized estuary. *Anim. Microbiome* 3, 1–17. doi: 10.1186/s42523-020-00066-0

Timmins-Schiffman, E., Coffey, W. D., Hua, W., Nunn, B. L., Dickinson, G. H., and Roberts, S. B. (2014). Shotgun proteomics reveals physiological response to ocean acidification in *Crassostrea gigas*. *BMC Genomics* 15, 1–18. doi: 10.1186/1471-2164-15-951

Tomanek, L., Zuzow, M. J., Ivanina, A. V., Beniash, E., and Sokolova, I. M. (2011). Proteomic response to elevated P CO2 level in eastern oysters, *Crassostrea virginica*: evidence for oxidative stress. *J. Exp. Biol.* 214, 1836–1844. doi: 10.1242/jeb.055475

Tsikas, D. (2017). Assessment of lipid peroxidation by measuring malondialdehyde (MDA) and relatives in biological samples: analytical and biological challenges. *Anal. Biochem.* 524, 13–30. doi: 10.1016/j.ab.2016.10.021

Ullah, H., Nagelkerken, I., Goldenberg, S. U., and Fordham, D. A. (2018). Climate change could drive marine food web collapse through altered trophic flows and cyanobacterial proliferation. *PLoS Biol.* 16:e2003446. doi: 10.1371/journal.pbio.2003446

Unzueta-Martínez, A., Downey-Wall, A. M., Cameron, L. P., Ries, J. B., Lotterhos, K. E., and Bowen, J. L. (2021). Ocean acidification alters the diversity and structure of oyster associated microbial communities. *Limnol. Oceanogr.* 6, 348–359. doi: 10.1002/lol2.10214

Vaquer-Sunyer, R., and Duarte, C. M. (2008). Thresholds of hypoxia for marine biodiversity. *Proc. Natl. Acad. Sci.* 105, 15452–15457. doi: 10.1073/pnas.0803833105

Vizzini, S., Martínez-Crego, B., Andolina, C., Massa-Gallucci, A., Connell, S. D., and Gambi, M. C. (2017). Ocean acidification as a driver of community simplification via the collapse of higher-order and rise of lower-order consumers. *Sci. Rep.* 7, 1–10. doi: 10.1038/s41598-017-03802-w

Wang, Q., Cao, R., Ning, X., You, L., Mu, C., Wang, C., et al. (2016). Effects of ocean acidification on immune responses of the Pacific oyster *Crassostrea gigas*. *Fish Shellfish Immunol.* 49, 24–33. doi: 10.1016/j.fsi.2015.12.025

Wang, Y., Hu, M., Cheung, S. G., Shin, P. K. S., Lu, W., and Li, J. (2012). Immune parameter changes of hemocytes in green-lipped mussel Perna viridis exposure to hypoxia and hyposalinity. *Aquaculture* 356-357, 22–29. doi: 10.1016/j.aquaculture.2012.06.001

Wang, X., Huang, W., Wei, S., Shang, Y., Gu, H., Wu, F., et al. (2020). Microplastics impair digestive performance but show little effects on antioxidant activity in mussels under low pH conditions. *Environ. Pollut.* 258:113691. doi: 10.1016/j.envpol.2019.113691

Wang, Q. F., Shen, W. L., Hou, C. C., Liu, C., Wu, X. F., and Zhu, J. Q. (2017). Physiological responses and changes in gene expression in the large yellow croaker *Larimichthys crocea* following exposure to hypoxia. *Chemosphere* 169, 418–427. doi: 10.1016/j.chemosphere.2016.11.099

Wernberg, T., Smale, D. A., Tuya, F., Thomsen, M. S., Langlois, T. J., De Bettignies, T., et al. (2013). An extreme climatic event alters marine ecosystem structure in a global biodiversity hotspot. *Nat. Clim. Chang.* 3, 78–82. doi: 10.1038/nclimate1627

Xie, J., Zhao, C., Han, Q., Zhou, H., Li, Q., and Diao, X. (2017). Effects of pyrene exposure on immune response and oxidative stress in the pearl oyster, Pinctada martensii. *Fish Shellfish Immunol.* 63, 237–244. doi: 10.1016/j.fsi.2017.02.032

Zhan, Y., Zha, S., Peng, Z., Lin, Z., and Bao, Y. (2022). Hypoxia-mediated immunotoxicity in the blood clam Tegillarca granosa. *Mar. Environ. Res.* 177:105632. doi: 10.1016/j.marenvres.2022.105632

Zhou, G., Yuan, T., Cai, L., Zhang, W., Tian, R., Tong, H., et al. (2016). Changes in microbial communities, photosynthesis and calcification of the coral *Acropora gemmifera* in response to ocean acidification. *Sci. Rep.* 6, 1–9. doi: 10.1038/srep35971

frontiers | Frontiers in Ecology and Evolution

TYPE Review
PUBLISHED 22 June 2023
DOI 10.3389/fevo.2023.1083341

OPEN ACCESS

EDITED BY
Mark A. Elgar,
The University of Melbourne, Australia

REVIEWED BY
Saúl Huitzil,
Northwestern University, United States
Michael P. Doane,
Flinders University, Australia

*CORRESPONDENCE
Cody S. Clements
✉ cclments9@gatech.edu

RECEIVED 28 October 2022
ACCEPTED 19 May 2023
PUBLISHED 22 June 2023

CITATION
Clements CS and Hay ME (2023) Disentangling the impacts of macroalgae on corals via effects on their microbiomes.
Front. Ecol. Evol. 11:1083341.
doi: 10.3389/fevo.2023.1083341

Disentangling the impacts of macroalgae on corals via effects on their microbiomes

Cody S. Clements* and Mark E. Hay

School of Biological Sciences and Center for Microbial Dynamics and Infection, Georgia Institute of Technology, Atlanta, GA, United States

Tropical reefs are commonly transitioning from coral to macroalgal dominance, but the role of macroalgae in coral decline remains inadequately understood. A growing body of research suggests that algae may harm corals via disruptions to the homeostasis of the coral holobiont, including resident microbial communities, but the processes that mediate these potential microbial effects and the spatial scales at which they operate are uncertain. Resolving the relative importance and context dependencies of microbially-mediated algal-coral competition is critical for understanding and predicting coral dynamics as reefs further degrade. In this review, we examine the current state of knowledge surrounding algal impacts on corals via disruption of their microbiomes, with a particular focus on the mechanisms hypothesized to mediate microbial effects, the scales at which they are thought to operate, and the evidence from laboratory- and field-based studies for their existence and ecological relevance in the wild. Lastly, we highlight challenges for further advancing the field.

KEYWORDS

coral reef, coral, microbiome, macroalgae, coral-algal competition, microbial interactions, dysbiosis

1. Introduction

Microbiomes can alter the development, health, function, and behavior of humans and other hosts (Markle et al., 2013; McFall-Ngai et al., 2013; Gensollen et al., 2016). This realization generated an understandable interest in investigating the potential impacts of host microbiomes and their dynamics on the ecological health and function of a wide range of species playing critical roles in the structure and function of natural ecosystems (Ritchie, 2006; Barott and Rohwer, 2012; Krediet et al., 2013; McDevitt-Irwin et al., 2017). This is especially true for scleractinian corals, which are the foundation species of tropical reefs but have declined precipitously in recent decades as a variety of anthropogenic stressors increased in frequency and severity (e.g., overfishing, ocean warming, pollution, etc.; Bellwood et al., 2004; Hughes et al., 2010, 2018; Jackson et al., 2014). Mutualistic interactions among the coral animal, the symbiotic dinoflagellates that reside in and transfer photosynthates to the coral host, and a number of external symbionts, including crabs, shrimps, and fishes that protect corals from predators or competitors in return for a safer living space were already known and appreciated (Glynn, 1983; Stachowicz and Hay, 1999; Dixson and Hay, 2012). However, the possibility that this already "tangled bank" of symbiotic interactions might also depend on a wealth of undescribed mutualisms involving unappreciated microbes offered a new vision of deep biological complexities that proved irresistible for microbiologists and coral reef investigators (e.g., Ritchie, 2006; Vega Thurber et al., 2009; Barott and Rohwer, 2012; Haas et al., 2016;

Clements et al., 2020b). If appropriate microbiomes are critical to the wellbeing of this crucial group of foundation species, then understanding, and possibly remedying, microbial imbalances on corals might offer novel means for conserving or restoring reefs (Santoro et al., 2021; Voolstra et al., 2021).

These new insights initiated a wealth of studies involving coral microbiomes. Because corals were often replaced by macroalgae as reefs degraded, many investigations focused on the potential impacts of macroalgae on coral microbiomes and the role that algal-microbiome interactions might play in coral demise. We overview hypotheses and information on these interactions below. We do not attempt to be comprehensive of all studies to date, but rather try to elaborate major findings, issues, and remaining challenges.

Coral decline is often accompanied by increases in benthic algae, which compete with corals for space and now dominate the benthic landscape on numerous tropical reefs (Hughes, 1994; Mumby and Steneck, 2008; Roff and Mumby, 2012; Rasher et al., 2013). In general, competition with algae is expected to further exacerbate coral decline as macroalgae proliferate and interactions with remaining corals increase in frequency and intensity (Mumby et al., 2007; Bonaldo and Hay, 2014). Numerous studies have demonstrated that algal competitors suppress coral growth (River and Edmunds, 2001; Clements et al., 2018, 2020b), fecundity (Foster et al., 2008; Monteil et al., 2020), recruitment (Birrell et al., 2008), and survival (Box and Mumby, 2007); however, the extent to which algal competition is a driver of coral stress and demise versus a response to coral stress and demise due to other causes is uncertain (Bruno et al., 2009; Dudgeon et al., 2010; Mumby et al., 2012; Schmitt et al., 2019). These drivers may also be context dependent (e.g., Bruno et al., 2007; Mumby et al., 2007; Mumby and Steneck, 2008; Rasher et al., 2011; Vega Thurber et al., 2012; Clements et al., 2020b), making the general role of algae in suppressing corals via impacts on coral microbiomes uncertain.

Despite uncertainties, it has become common to assume that changes in coral microbiomes may be a driver of coral demise rather than a response to coral stresses from other sources (Barott and Rohwer, 2012; Haas et al., 2016; Nelson et al., 2022). The difficulties of separating microbial causes of coral demise from microbial responses to coral demise are complicated by a general inability to identify microbial pathogens causing coral diseases despite considerable efforts to do so (Barott and Rohwer, 2012; Vega Thurber et al., 2020). In many cases, coral diseases are correlated with a polyculture of different microbes; some may be pathogens, some detritivores responding to the dead tissues, a mix of both, or normally benign coral associates that become opportunistic detritivores or pathogens when corals are compromised by other stresses (Vega Thurber et al., 2020). Despite our enthusiasm for understanding the role that microbes may play in coral dynamics and responses to stress, it is necessary to remember that predictable co-occurrence need not indicate a *cause* rather than a *consequence* of demise. A consistent change in coral microbiomes as corals sicken need not indicate that the microbial changes are a *cause* rather than a *consequence* of the coral's demise. Additionally, it is common for studies of microbial shifts on reefs, or of the pathways the microbes are up-regulating (pathogenicity, etc.), to assume these shifts or changes in metabolism will lead to coral demise without investigating co-occurring changes in corals. Of the 45 studies we found addressing how shifts in microbes on coral reefs might impact corals, fewer than half (44%) assessed for effects on co-occurring corals (Supplementary Table S1).

Extensive investigations into the dynamics of coral-algal competition have been undertaken in recent decades—ranging from experimental field manipulations pairing corals and algae or excluding herbivores to assess the effects of algal proliferation, to broader scale correlations of coral recruitment and survivorship on algal-dominated versus coral-dominated reefs (Birrell et al., 2008; Beatty et al., 2018). Within some of these efforts, there was an interest in linking observed algal effects to the complex association between the coral animal and its associated microorganisms (protists, bacteria, archaea, fungi, and viruses)—collectively referred to as the coral microbiome. These associates can be integral to a variety of host functions that facilitate or hinder coral growth, health, and survival. Among the most well-known facilitators of coral health are endosymbiotic *Symbiodinium* algae that provide photosynthates to the coral host, but increasing evidence suggests that other associates such as bacteria also play integral roles in metabolism, nutrient dynamics, resistance to pathogens, and immune response (Thompson et al., 2014; Bourne et al., 2016), and may help corals tolerate or adapt to stressful conditions (Rosado et al., 2019; Santoro et al., 2021). Conversely, stresses associated with algal competition may disrupt these relationships, potentially compromising coral health (Zaneveld et al., 2017). These competing notions (microbiome changes as adaptive for versus detrimental to the holobiont) make it impossible to interpret the fitness-related consequences of microbiome change without a better "natural history" of the functional role of individual microbes, or consortia of microbes, to the well-being of the holobiont. An adequate natural history understanding is not presently available.

Harmful algal effects to corals observed at the macroscale, such as reduced coral growth, survival, and recruitment (Vermeij et al., 2009; Bulleri et al., 2018), commonly, but not always (Clements et al., 2020a,b), co-occur with alterations to the coral holobiont—often via changes in composition, abundances, or dispersion of resident microbes that are thought to be indicative of microbial dysbiosis (i.e., increases in harmful or loss of beneficial microbes; Vega Thurber et al., 2012; Zaneveld et al., 2017). Algal-induced microbiome changes are hypothesized to occur via several mechanisms that vary in their mode of action, and as a consequence, the potential extent and severity of their impacts. These are thought to include contact-mediated mechanisms that likely act at localized scales of centimeters or less near the coral-algal interface (Brown and Carpenter, 2015; Jorissen et al., 2016; Clements et al., 2020a,b), as well as via algal release into the water of compounds that may be advected to corals centimeters to meters downstream of algal competitors (Barott and Rohwer, 2012). Each has substantially different implications for potential trajectories of coral reef decline and recovery.

Algae have been implicated in disrupting the coral holobiont (e.g., reduced *Symbiodinium* densities; Quan-Young and Espinoza-Avalos, 2006), with most research to-date focused on disruptions to coral microbiomes (Rosenberg et al., 2007; McDevitt-Irwin et al., 2017). Indeed, microbially-mediated competition is now commonly stated to be among the primary processes involved in coral-algal interactions and a potential driver of coral decline (Barott and Rohwer, 2012; McDevitt-Irwin et al., 2017). However, the degree to which altered coral microbiomes are: i) a cause of coral decline, ii) a response to coral decline caused by other stresses, or iii) an adaptive response of the coral to alter its microbiome to better fit the new ecological conditions and enhance holobiont fitness is often unclear. The mechanisms by which algae affect coral holobionts appear

multifactorial, context-dependent, and not mutually exclusive. Resolving their ecological relevance and the spatial scales at which competing algae impact microbiome dynamics remains a challenge that has important implications for efforts to predict, manage, and restore coral populations on increasingly degraded reefs.

Below, we discuss the current state of knowledge surrounding algal effects on coral holobionts, with a special focus on whether, how, and under what conditions macroalgal effects on corals are mediated via impacts on coral microbiomes. Our goal is to examine the ecological scales at which these processes operate, the evidence to-date for their effects on corals, and how these may differ under the lab settings that facilitate careful monitoring versus the field conditions under which corals and macroalgae actually live and interact. We are particularly interested in exploring the relative importance of contact- versus water-mediated interactions in driving changes to coral microbial communities, as well the potential adaptive capacity and resilience of the coral host to such disruptions. These distinctions may prove critical for understanding the likelihood of various conservation measures proving effective under field conditions.

2. Algal effects via contact versus effects at a distance

The spatial scale at which algal-coral interactions occur and how this may vary with species combinations or environmental context can be critical for understanding these interactions. If contact is required, then corals may be able to counter or limit algal impacts via offensive sweeper tentacles (Wellington, 1980) or commensal crustaceans or fishes that remove nearby macroalgae (Stachowicz and Hay, 1999; Dixson and Hay, 2012). In contrast, if algae can damage corals at a distance by releasing water-soluble compounds that destabilize critical microbiomes on corals downstream (Barott and Rohwer, 2012), then ecological countermeasures by corals or their symbionts may be ineffective, leaving the longer-term option of evolving resistance to these effects as the primary avenue of response. In summary, it is important to understand whether algae function more as: i) "toxic paint brushes" damaging corals only on contact, ii) "sewage outfalls," spilling organic pollutants that damage downstream corals at a distance, or iii) some of both, depending on environmental circumstances and species combinations.

Numerous field- and laboratory-based studies have demonstrated adverse effects for corals that are directly contacted by macroalgae (McCook et al., 2001; Rasher and Hay, 2010; Bonaldo and Hay, 2014; Vieira et al., 2016b; Clements et al., 2018), with an increasing number also documenting concurrent shifts in coral microbiomes (Vega Thurber et al., 2012; Morrow et al., 2013; Zaneveld et al., 2016; Pratte et al., 2018; see Supplementary Table S1). Experiments focused on the mechanistic basis of these microbial dynamics or their ecological impacts are less common, but increasing evidence suggests that direct mechanisms such as algal abrasion or shading (Clements et al., 2020b), as well contact-mediated transfer of hydrophobic allelochemicals (Rasher and Hay, 2010; Rasher et al., 2011; Morrow et al., 2012, 2017), organic matter, or microbial pathogens (Nugues et al., 2004; Barott et al., 2012; Sweet et al., 2013; Vieira et al., 2016a), are capable of inducing microbiome changes that may, or may not, constitute dysbiosis (i.e., change can be damaging or an adaptive response).

Though it has been suggested that physical mechanisms play only a minor role in coral-algal competition (Barott and Rohwer, 2012; but see Box and Mumby, 2007), recent field-based manipulations demonstrated that biologically inert algal mimics reduced coral growth and photosynthetic efficiency, and altered resident microbial communities in a comparable manner to live algae common to degraded reefs (Morrow et al., 2012; Clements et al., 2020b), including species known to damage corals via allelopathy (*Galaxaura* spp.; Rasher and Hay, 2010; Rasher et al., 2011). Tank-based studies have also reported comparable effects on coral microbiomes between mimics and live algae, but this varied based on the coral-algal species pairs tested and was not consistently reflected in the physiological metrics being assessed (i.e., percent tissue bleaching, photosynthetic efficiency; Fong et al., 2020). Under ecologically realistic scenarios, contact-mediated stressors likely work in concert to alter the coral holobiont, potentially facilitating dysbiotic after-effects (e.g., pathogen invasion), but this will depend on the species involved and interaction context. It is also useful to recognize that microbiome changes need not be detrimental to a coral. Changes could be neutral or even beneficial allowing the coral to adapt to new stresses via its microbial associates. One way of addressing this is to measure correlates of coral fitness (e.g., growth or photosynthesis) as changes in microbiome dynamics are assessed under realistic field conditions. This is relatively rare—with only seven of the 45 studies in Supplementary Table S1 (~16%) conducting such experiments.

The potential for algae to harm corals at a distance through changes to coral microbiomes has gained considerable attention in the past two decades and is hypothesized to be an important contributor to coral decline (Barott and Rohwer, 2012; Haas et al., 2016; Nelson et al., 2022). Early lab studies demonstrated that algae held in small containers and separated from immediately adjacent coral by filters that should prevent passage of microbes caused coral damage without direct contact; this effect was suppressed or nullified by the addition of antibiotics (Smith et al., 2006). The coral damage in these experiments was associated with a decline in oxygen where corals were immediately adjacent to macroalgae, suggesting that dissolved organics (e.g., dissolved organic carbon = DOC) leaking from algae were fueling microbial growth, lowering O_2, and stressing or killing adjacent coral tissue via hypoxia. This, and related experiments (Haas et al., 2011, 2013, 2016; Nelson et al., 2011, 2013; Walsh et al., 2017), lead to positing the DOC, disease, and algae model (DDAM), suggesting that algae release bioavailable DOC into surrounding waters, that the released compounds stimulate growth and respiration of reef microbes, that the released DOC may produce effects centimeters to meters downstream (Barott and Rohwer, 2012), and that this harms corals via hypoxia (Haas et al., 2011). In this scenario, microbial community changes do not simply correlate with macroscale changes in reef benthic communities, but actively promote feedback loops that suppress corals and accelerate transitions towards degraded reefs dominated by macroalgae.

The above models are supported by laboratory investigations demonstrating microbial changes in seawater of various algal-associated dissolved organic compounds (Kline et al., 2006; Haas et al., 2011, 2013; Nelson et al., 2013) and adverse effects on corals at distances of centimeters or less (Jorissen et al., 2016; Fong et al., 2020). Limited field collections ($n = 2–4$) of water within, or near, the benthic boundary layer above an area dominated by a coral, macroalga, turf alga, or a zoanthid found differences in water microbiomes across these

collections and that all differed from water samples collected three meters above these substrates (Walsh et al., 2017), indicating localized but not reef-wide impacts. Walsh et al. (2017) also probed for functions and noted halos of microbiomes above turf algae were expressing functions suggesting pathogenic activity. However, many pathogens have a narrow host range and pathogenicity to corals, or damage to corals of any sort, was not assessed. Even when one probes for function, detects activation of pathogenicity, and knows the host that can be infected, there is no assurance that this will result in successful host attack. Microbial physiology alone is insufficient as a proof of coral damage; one needs to actually assess damage to nearby corals. Numerous studies do not do this (Supplementary Table S1). Several field studies do not find corals being damaged by seaweeds unless there is direct contact (Rasher and Hay, 2010; Rasher et al., 2011; Clements et al., 2018, 2020b), thus the potential effects of seaweeds on corals or their microbiomes across distance needs confirmation under field conditions. Of the 45 studies in Supplementary Table S1, only five tested for effects on coral microbiomes via dissolution over a distance (see Supplementary Table S1). Two were conducted in the field under natural conditions of flow and found no effects at cm scales (Barott et al., 2012; Clements et al., 2020b); two lab studies in closed containers demonstrated water-soluble effects (Smith et al., 2006; Fong et al., 2020) and one correlative field study found patterns suggestive of such effects (Briggs et al., 2021).

Several issues may constrain laboratory studies conducted in still enclosures or in containers with limited flow from translating to the field where flow, advection, turbulence, and various biotic processes may diminish or completely counter effects noted under laboratory conditions. As examples: i) DOC concentrations will accumulate in lab containers in a manner that might rarely occur given flow conditions in the field, ii) fragmenting macroalgae to place them in lab containers may cause more leakage of DOC or other algal metabolites than occurs under intact conditions in the field, and iii) if microbes are stimulated by DOC from algae, it is likely that they will colonize algal surfaces and draw DOC down as it emerges rather than leaving it to drift downstream to be used by other microbial competitors. This latter possibility is supported by a 4-year study of DOC and bacterioplankton concentrations in oceanic water as it passed from the ocean over the reef crest, lagoon, and fringing reefs in Mo'orea, French Polynesia, with the latter areas all supporting large areas of macroalgae. In this investigation, Nelson et al. (2011) found that both DOC and bacterioplankton declined significantly, rather than increasing, as low DOC oceanic water moved across these algal-rich reefs. A possible explanation is that microbial populations inhabiting the considerable surface areas of macroalgae were able to not only consume all DOC released by the macroalgae, but to also draw down further the low DOC concentrations from the oceanic waters. If this is the case, then DOC from macroalgae is unlikely to be affecting coral microbiomes at a distance.

A careful field study on reefs in Mo'orea, French Polynesia, found that algal-coral interactions and the effects of these on microbial concentrations in the water were highly context dependent and varied as a function of flow conditions, the types of algae involved, whether the up-stream or down-stream side of the coral was considered, etc. (Brown and Carpenter, 2015). These authors concluded that algal release of DOC and its negative effects on corals via microbially-mediated hypoxia, could likely occur, but only under constrained conditions of low flow, very small spatial scales, and certain algal-coral combinations (e.g., turf algae that could hold DOC in the diffusive boundary layer on the down current side of a massive coral). Field sampling by Walsh et al. (2017) also found effects on water sample microbiomes taken within centimeters of macroorganisms, but not at meter scales. More critically, when numerous macroalgae and corals were paired in the field on reefs in Fiji or Caribbean Panama, almost all algal damage to corals was detectable only on coral portions experiencing direct algal contact (i.e., in most pairings, no detectable damage occurred only millimeters away) and the damage seen in algal-coral pairings could be replicated via extracts of non-polar metabolites that would not be dispersed via dissolution into water (Rasher and Hay, 2010; Rasher et al., 2011).

Bolstering this effect of direct contact versus compounds dispersed via DOC dissolution, when corals (*Acropora millepora* and *Porites cylindrica*) were transplanted into dense algal beds, their growth was significantly suppressed, but when macroalgae were cleared for only centimeters around them—preventing direct contact—there was no effect on coral growth (Clements et al., 2018). Unfortunately, these investigations did not evaluate algal effects on coral microbiomes, but the types of tissue bleaching and death seen in earlier lab-based experiments (Smith et al., 2006) were not apparent in these field assays unless macroalgae were physically contacting corals.

A more recent lab-based experiment involving three coral species (*Merulina ampliata*, *Montipora stellata*, and *Pocillopora acuta*) found that microbiome composition of one species (*M. stellata*) was altered when in close proximity (~5 cm) to macroalgae (*Lobophora* sp. and *Hypnea pannosa*) in 3-liter tanks, but adverse effects on coral physiology (e.g., percent tissue bleaching, photosynthetic efficiency) required direct algal contact (Fong et al., 2020). Similarly, photosynthesis and growth of corals (*A. millepora*) in the field were suppressed when corals were in direct contact with live algae (*Sargassum polycystum* or *Galaxaura filamentosa*) or inert algal mimics, but were unaffected when algae or algal mimics were 1.5 cm distance away from corals and contact was prevented (Clements et al., 2020b). Coral microbiomes were also largely unaffected in composition, variability, or diversity by any of the treatments; however, a few uncommon taxa did differ among treatments. These experiments suggest that under most ecologically realistic field conditions, the negative impacts of macroalgae on corals are limited to contact and rarely affected by DOC liberated by the macroalgae.

3. Coral microbiome stability on algal- versus coral-dominated reefs

Determining the relevant ecological scales at which negative algal impacts operate not only depends on characteristics inherent to algae (e.g., ability to stimulate copiotrophic microbial activity via algal-induced DOC) and the abiotic environment (e.g., flow dynamics), but also the ability of the coral to maintain holobiont homeostasis despite external, potentially stressful, conditions (Sunagawa et al., 2010; Webster et al., 2016; Zhou et al., 2016; Marcelino et al., 2017; O'Brien et al., 2018; Reigel et al., 2021; Díaz-Almeyda et al., 2022). Studies assessing differences in microbiomes of corals from algal- versus coral-dominated reefs have yielded mixed results but suggest that some corals are regulating their microbiomes despite macroalgal dominance and that coarse-resolution microbial metrics alone may be ill-suited for assessing potential algal effects. For example, Beatty

et al. (2018) found that neither adults nor larvae of the coral *Pocillopora damicornis* differed significantly in microbiome composition between adjacent coral- and algal- dominated reefs in Fiji, but adult *P. damicornis* microbiomes were more variable (i.e., greater beta-dispersion) and enriched in low abundance (<2%) of potentially pathogenic taxa from the family Vibrionaceae (e.g., *Vibrio shilonii*).

As reported in other studies, Beatty et al. (2019) found that microbiome composition of benthic seawater differed between adjacent coral- and algal-dominated reefs, but in contrast to what might be expected in these differing environments, the community composition of microbiomes from three coral species (*A. millepora*, *P. damicornis*, and *P. cylindrica*) collected from these differing locations did not differ within species. However, one species (*A. millepora*) did exhibit greater microbiome dispersion, reduced abundance of a putative beneficial Endozoicimonaceae indicator taxon, and reduced ability to suppress a common coral pathogen (*Vibrio coralliilyticus*) when corals were sampled from macroalgal-dominated reefs versus coral-dominated reefs. When fragments of the same three coral species were reciprocally transplanted between paired coral- and algal-dominated reefs, two species (*A. millepora* and *P. damicornis*) exhibited differences in microbiome composition based on the type of site from which they were collected (both species) or transplanted to (*P. damicornis* only; Beatty et al., 2022). These differences were again largely driven by reduced relative abundances of Endozoicimonaceae and enrichment of Vibrionaceae sequences.

Together, the findings outlined above suggest that some corals maintain broad-scale microbiome community composition despite marked, and sometimes dramatic (Beatty et al., 2019, 2022), differences in macroalgal abundance and in the surrounding benthic and water column microbial community. They also suggest that relevant algal effects may involve more nuanced differences in coral microbiomes than coarse-scale metrics such as community composition (i.e., small or modest changes in rare microbes may produce important effects). Similar findings have been reported for other marine organisms, such as sponges and macroalgae, which can exhibit overall microbiome stability and minor shifts in less abundant taxa despite occurring on reefs differing in algal abundance and in water column microbiomes (Chen and Parfrey, 2018; Campana et al., 2021). It also is consistent with other studies that found stressor-induced changes to coral microbiomes (e.g., via corallivory, temperature, fish feces) were spatially and temporally constrained (Clements et al., 2020a; Ezzat et al., 2021), and dovetails with macroscale assessments of coral well-being (e.g., growth) that suggest algal effects require direct contact (Clements et al., 2018, 2020b) and that negative effects cease relatively quickly following algal removal (Clements et al., 2018; van Duyl et al., 2023).

Furthermore, none of the aforementioned comparisons precluded contact between coral and algae within algal-dominated sites and thus did not assess potential contact- versus water-mediated effects. We are aware of only one correlative field-based study that has attempted to assess microbial community changes as a function of benthic algal cover and algal contact. The authors' reported a mix of coral microbiome responses, including antagonistic effects of algal contact and macroalgal cover for broad-scale metrics such as microbiome composition and dispersion, as well as changes in relative abundances of specific microbes that were more pronounced based on algal contact than cover (Briggs et al., 2021). Higher-resolution investigations, including assessments of the "core microbiome" (Ainsworth et al., 2010, 2015; Bourne et al., 2016), more specific indicator taxa, or other microbial metrics (e.g., potency of pathogen-suppressing extracts; Beatty et al., 2019, 2022), may be necessary to reconcile disparate findings and adequately evaluate coral responses to changes in reef state and how these vary with direct contact versus close proximity.

4. Outstanding questions and challenges

Despite the considerable progress in studies of algal impacts on coral holobionts, questions remain concerning the mechanistic basis of algal-coral-microbiome interactions, their impacts on coral fitness, and how this may be impacting conservation, management, and restoration of degraded reefs. The majority of correlative studies assessing the relationship between algal cover and reef "microbialization" have focused on sampling and assessing differences in the microbiomes of water slightly above the substrate on coral- versus algal-dominated reefs (Haas et al., 2011, 2013, 2016; Nelson et al., 2013; Walsh et al., 2017; Meirelles et al., 2018; Silva et al., 2021)—but not to corals themselves (see Supplementary Table S1)—making it difficult to discern whether and how proposed models of indirect algal effects (e.g., DDAM) translate to microbial changes within the coral holobiont, or whether such changes have negative effects on coral fitness. These knowledge gaps represent a formidable challenge for future efforts to understand the impacts of algae on coral holobionts, but also an opportunity to foster greater integration and collaboration between field- and lab-based experimentalists whose complementary approaches can strengthen both fields via collaboration.

4.1. Understanding context-dependence

The ecologically relevant scales at which algae alter coral microbiomes, and the consequences of microbiome change for the host holobiont may have dramatically different implications for trajectories of coral decline or resilience. Laboratory-based experiments suggest that algae can influence coral microbiomes at limited distances ($\leq$ 5 cm; Jorissen et al., 2016; Fong et al., 2020) via water-mediated mechanisms, but manipulative field experiments to-date have yet to detect similar effects at this spatial scale (Brown and Carpenter, 2015; Clements et al., 2020b); thus, the ecological relevance of water-mediated processes thought to operate in the wild (e.g., DDAM; Haas et al., 2016) remain uncertain. Indirect algal effects on microbiomes *in situ* appear likely, but will depend on interaction context and may occur under only a limited set of conditions (Brown and Carpenter, 2015). Rigorous field studies under variable conditions of flow, turbulence, and advection need to be conducted to bound the conditions under which algal effects at a distance may occur.

4.2. A natural history of microbes is needed

We know too little of the real effects of particular microbes in nature. This is readily evident in coral reef ecosystems, which are being dramatically impacted by disease, but in many cases the specific causative

microbial agent(s) of disease remain unknown (Mera and Bourne, 2018; Vega Thurber et al., 2020). Our considerably greater understanding of human microbial pathogens has taken centuries and large amounts of human and financial capital to achieve since Pasture's initial studies. The history of successes and failures in human studies can help inform marine approaches (Pollock et al., 2011). Erecting and understanding the natural history and epidemiology of coral diseases will not be easy and may require reevaluating traditional etiological paradigms. For example, recent calls to move beyond the "one pathogen—one disease" model of coral disease (Vega Thurber et al., 2020) have followed from insights first gleaned from studies of human health, such as the polymicrobial nature of many diseases (Nelson et al., 2012; Lamont and Hajishengallis, 2015), the pathobiont concept (Chow et al., 2011), and the role of dysbiosis as an indicator of disease (Zaneveld et al., 2017) versus adaptation via microbiome alterations. Studies have begun and should continue to utilize these alternative frameworks for assessing algal effects.

4.3. Not "who is there?," but "what are they doing?"

To more rigorously understand the critical roles that microbial associates may play in coral health and function, we need to move beyond studies of descriptive co-occurrence to rigorous demonstrations of cause-effect relationships and the mechanisms involved in microbiome impacts on coral hosts. We need to go beyond broad-scale sequencing and evaluate active and core members of the microbiome, as well as the functions microbes are up- or down-regulating in different contexts. However, just as not all predator attacks are successful, not all microbes that induce pathogenicity or similar traits will successfully invade and infect a coral host. We will not understand the importance and dynamics of coral-microbiome interactions unless both host and microbes are studied synchronously and under realistic ecological conditions. Supplementary Table S1 suggests that we can improve on this. High prevalence in healthy corals does not negate a microbe's pathogenic potential (Shaver et al., 2017; Klinges et al., 2019), and even common commensals or mutualists may turn into pathogens under certain conditions (Seyedsayamdost et al., 2011). Multidisciplinary approaches are already underway to tackle these questions (Bourne et al., 2016; Barreto et al., 2021), including in studies of coral-algal interactions (Roach et al., 2020).

4.4. Cause versus effect

Disentangling cause versus effect is a problem that consistently confounds efforts to investigate links between various stressors and microbiome dynamics across a range of disciplines (Fischbach, 2018). This is further complicated by the multifactorial nature of stressors facing corals on most modern reefs (Bellwood et al., 2004). At present, we cannot consistently differentiate microbiome changes that destabilize the host and cause coral death, from microbiome changes that are a response to coral demise due to other drivers or from changes that may involve the coral adapting to a changing environment by "trading-out" microbial associates. In numerous cases, it is not even clear if coral disease/demise is due to changes in bacterial, fungal, ciliates, flatworms, or other coral associates (Mera and Bourne, 2018; Barton et al., 2020; Vega Thurber et al., 2020). In these instances, field experiments with compounds targeting these different groups may be useful. Making advances on the three challenges listed above may allow us to begin to separate and understand microbiome dynamics that are driving coral demise from those that are a response to coral stress or demise. Achieving that goal will represent a significant advance in the field.

Author contributions

All authors listed have made a substantial, direct, and intellectual contribution to the work and approved it for publication.

Funding

This work was supported by the U.S. National Science Foundation (grant no. OCE 1947522), the Teasley Endowment to the Georgia Institute of Technology, and the Anna and Harry Teasley Gift Fund.

Conflict of interest

The authors declare that the research was conducted in the absence of any commercial or financial relationships that could be construed as a potential conflict of interest.

Publisher's note

Supplementary material

The Supplementary material for this article can be found online at: https://www.frontiersin.org/articles/10.3389/fevo.2023.1083341/full#supplementary-material

References

Ainsworth, T. D., Krause, L., Bridge, T., Torda, G., Raina, J.-B., Zakrzewski, M., et al. (2015). The coral core microbiome identifies rare bacterial taxa as ubiquitous endosymbionts. *ISME J.* 9, 2261–2274. doi: 10.1038/ismej.2015.39

Ainsworth, T. D., Thurber, R. V., and Gates, R. D. (2010). The future of coral reefs: a microbial perspective. *Trends Ecol. Evol.* 25, 233–240. doi: 10.1016/j.tree.2009.11.001

Barott, K. L., Rodriguez-Mueller, B., Youle, M., Marhaver, K. L., Vermeij, M. J. A., Smith, J. E., et al. (2012). Microbial to reef scale interactions between the reef-building coral *Montastraea annularis* and benthic algae. *Proc. Biol. Sci.* 279, 1655–1664. doi: 10.1098/rspb.2011.2155

Barott, K. L., and Rohwer, F. L. (2012). Unseen players shape benthic competition on coral reefs. *Trends Microbiol.* 20, 621–628. doi: 10.1016/j.tim.2012.08.004

Barreto, M. M., Ziegler, M., Venn, A., Tambutté, E., Zoccola, D., Tambutté, S., et al. (2021). Effects of ocean acidification on resident and active microbial communities of *Stylophora pistillata*. *Front. Microbiol.* 12:707674. doi: 10.3389/fmicb.2021.707674

Barton, J. A., Bourne, D. G., Humphrey, C., and Hutson, K. S. (2020). Parasites and coral-associated invertebrates that impact coral health. *Rev. Aquac.* 12, 2284–2303. doi: 10.1111/raq.12434

Beatty, D. S., Clements, C. S., Stewart, F. J., and Hay, M. E. (2018). Intergenerational effects of macroalgae on a reef coral: major declines in larval survival but subtle changes in microbiomes. *Mar. Ecol. Prog. Ser.* 589, 97–114. doi: 10.3354/meps12465

Beatty, D. S., Clements, C. S., Valayil, J. M., Jarvis, S. Y., Ritchie, K. B., Stewart, F. J., et al. (2022). Variance of coral anti-pathogen defense in response to transplantation between coral- and macroalgal-dominated reefs. *Coral Reefs* 41, 1417–1431. doi: 10.1038/s41598-018-27891-3

Beatty, D. S., Valayil, J. M., Clements, C. S., Ritchie, K. B., Stewart, F. J., and Hay, M. E. (2019). Variable effects of local management on coral defenses against a thermally regulated bleaching pathogen. *Sci. Adv.* 5:eaay1048. doi: 10.1126/sciadv.aay1048

Bellwood, D. R., Hughes, T. P., Folke, C., and Nystrom, M. (2004). Confronting the coral reef crisis. *Nature* 429, 827–833. doi: 10.1038/nature02691

Birrell, C. L., McCook, L. J., Willis, B. L., and Diaz-Pulido, G. A. (2008). Effects of benthic algae on the replenishment of corals and the implications for the resilience of coral reefs. *Oceanogr. Mar. Biol. Annu. Rev.* 20081322, 25–63. doi: 10.1201/9781420065756.ch2

Bonaldo, R. M., and Hay, M. E. (2014). Seaweed-coral interactions: variance in seaweed allelopathy, coral susceptibility, and potential effects on coral resilience. *PLoS One* 9:e85786. doi: 10.1371/journal.pone.0085786

Bourne, D. G., Morrow, K. M., and Webster, N. S. (2016). Insights into the coral microbiome: underpinning the health and resilience of reef ecosystems. *Annu. Rev. Microbiol.* 70, 317–340. doi: 10.1146/annurev-micro-102215-095440

Box, S. J., and Mumby, P. J. (2007). Effect of macroalgal competition on growth and survival of juvenile Caribbean corals. *Mar. Ecol. Prog. Ser.* 342, 139–149. doi: 10.3354/meps342139

Briggs, A. A., Brown, A. L., and Osenberg, C. W. (2021). Local versus site-level effects of algae on coral microbial communities. *R. Soc. Open Sci.* 8:210035. doi: 10.1098/rsos.210035

Brown, A. L., and Carpenter, R. C. (2015). Water flow influences the mechanisms and outcomes of interactions between massive *Porites* and coral reef algae. *Mar. Biol.* 162, 459–468. doi: 10.1007/s00227-014-2593-5

Bruno, J. F., Selig, E. R., Casey, K. S., Page, C. A., Willis, B. L., Harvell, C. D., et al. (2007). Thermal stress and coral cover as drivers of coral disease outbreaks. *PLoS Biol.* 5:e124. doi: 10.1371/journal.pbio.0050124

Bruno, J. F., Sweatman, H., Precht, W. F., Selig, E. R., and Schutte, V. G. W. (2009). Assessing evidence of phase shifts from coral to macroalgal dominance on coral reefs. *Ecology* 90, 1478–1484. doi: 10.1890/08-1781.1

Bulleri, F., Thiault, L., Mills, S. C., Nugues, M. M., Eckert, E. M., Corno, G., et al. (2018). Erect macroalgae influence epilithic bacterial assemblages and reduce coral recruitment. *Mar. Ecol. Prog. Ser.* 597, 65–77. doi: 10.3354/meps12583

Campana, S., Demey, C., Busch, K., Hentschel, U., Muyzer, G., and de Goeij, J. M. (2021). Marine sponges maintain stable bacterial communities between reef sites with different coral to algae cover ratios. *FEMS Microbiol. Ecol.* 97:fiab115. doi: 10.1093/femsec/fiab115

Chen, M. Y., and Parfrey, L. W. (2018). Incubation with macroalgae induces large shifts in water column microbiota, but minor changes to the epibiota of co-occurring macroalgae. *Mol. Ecol.* 27, 1966–1979. doi: 10.1111/mec.14548

Chow, J., Tang, H., and Mazmanian, S. K. (2011). Pathobionts of the gastrointestinal microbiota and inflammatory disease. *Curr. Opin. Immunol.* 23, 473–480. doi: 10.1016/j.coi.2011.07.010

Clements, C. S., Burns, A. S., Stewart, F. J., and Hay, M. E. (2020a). Parasite-host ecology: the limited impacts of an intimate enemy on host microbiomes. *Anim. Microbiome* 2:42. doi: 10.1186/s42523-020-00061-5

Clements, C. S., Burns, A. S., Stewart, F. J., and Hay, M. E. (2020b). Seaweed-coral competition in the field: effects on coral growth, photosynthesis and microbiomes require direct contact. *Proc. Biol. Sci.* 287:20200366. doi: 10.1098/rspb.2020.0366

Clements, C. S., Rasher, D. B., Hoey, A. S., Bonito, V. E., and Hay, M. E. (2018). Spatial and temporal limits of coral-macroalgal competition: the negative impacts of macroalgal density, proximity, and history of contact. *Mar. Ecol. Prog. Ser.* 586, 11–20. doi: 10.3354/meps12410

Díaz-Almeyda, E. M., Ryba, T., Ohdera, A. H., Collins, S. M., Shafer, N., Link, C., et al. (2022). Thermal stress has minimal effects on bacterial communities of thermotolerant *Symbiodinium* cultures. *Front. Ecol. Evol.* 10:764086. doi: 10.3389/fevo.2022.764086

Dixson, D. L., and Hay, M. E. (2012). Corals chemically cue mutualistic fishes to remove competing seaweeds. *Science* 338, 804–807. doi: 10.1126/science.1225748

Dudgeon, S. R., Aronson, R. B., Bruno, J. F., and Precht, W. F. (2010). Phase shifts and stable states on coral reefs. *Mar. Ecol. Prog. Ser.* 413, 201–216. doi: 10.3354/meps08751

Ezzat, L., Merolla, S., Clements, C. S., Munsterman, K. S., Landfield, K., Stensrud, C., et al. (2021). Thermal stress interacts with surgeonfish feces to increase coral susceptibility to dysbiosis and reduce tissue regeneration. *Front. Microbiol.* 12:608. doi: 10.3389/fmicb.2021.620458

Fischbach, M. A. (2018). Microbiome: focus on causation and mechanism. *Cells* 174, 785–790. doi: 10.1016/j.cell.2018.07.038

Fong, J., Deignan, L. K., Bauman, A. G., Steinberg, P. D., McDougald, D., and Todd, P. A. (2020). Contact- and water-mediated effects of macroalgae on the physiology and microbiome of three indo-Pacific coral species. *Front. Mar. Sci.* 6:831. doi: 10.3389/fmars.2019.00831

Foster, N. L., Box, S. J., and Mumby, P. J. (2008). Competitive effects of macroalgae on the fecundity of the reef-building coral *Montastraea annularis*. *Mar. Ecol. Prog. Ser.* 367, 143–152. doi: 10.3354/meps07594

Gensollen, T., Iyer, S. S., Kasper, D. L., and Blumberg, R. S. (2016). How colonization by microbiota in early life shapes the immune system. *Science* 352, 539–544. doi: 10.1126/science.aad9378

Glynn, P. W. (1983). Increased survivorship on corals harboring crustacean symbionts. *Marine Biology Letter* 4, 105–111.

Haas, A. F., Fairoz, M. F. M., Kelly, L. W., Nelson, C. E., Dinsdale, E. A., Edwards, R. A., et al. (2016). Global microbialization of coral reefs. *Nat. Microbiol.* 1:16042. doi: 10.1038/nmicrobiol.2016.42

Haas, A. F., Nelson, C. E., Rohwer, F., Wegley-Kelly, L., Quistad, S. D., Carlson, C. A., et al. (2013). Influence of coral and algal exudates on microbially mediated reef metabolism. *PeerJ* 1:e108. doi: 10.7717/peerj.108

Haas, A. F., Nelson, C. E., Wegley Kelly, L., Carlson, C. A., Rohwer, F., Leichter, J. J., et al. (2011). Effects of coral reef benthic primary producers on dissolved organic carbon and microbial activity. *PLoS One* 6:e27973. doi: 10.1371/journal.pone.0027973

Hughes, T. P. (1994). Catastrophes, phase shifts, and large-scale degradation of a Caribbean coral reef. *Science* 265, 1547–1551. doi: 10.1126/science.265.5178.1547

Hughes, T. P., Anderson, K. D., Connolly, S. R., Heron, S. F., Kerry, J. T., Lough, J. M., et al. (2018). Spatial and temporal patterns of mass bleaching of corals in the Anthropocene. *Science* 359, 80–83. doi: 10.1126/science.aan8048

Hughes, T. P., Graham, N. A. J., Jackson, J. B. C., Mumby, P. J., and Steneck, R. S. (2010). Rising to the challenge of sustaining coral reef resilience. *Trends Ecol. Evol.* 25, 633–642. doi: 10.1016/j.tree.2010.07.011

Jackson, J., Donovan, M., Cramer, K., and Lam, V. (2014). *Status and Trends of Caribbean Coral Reefs: 1970–2012*. Washington, D.C. Global Coral Reef Monitoring.

Jorissen, H., Skinner, C., Osinga, R., de Beer, D., and Nugues, M. M. (2016). Evidence for water-mediated mechanisms in coral-algal interactions. *Proc. Biol. Sci.* 283:20161137. doi: 10.1098/rspb.2016.1137

Kline, D. I., Kuntz, N. M., Breitbart, M., Knowlton, N., and Rohwer, F. (2006). Role of elevated organic carbon levels and microbial activity in coral mortality. *Mar. Ecol. Prog. Ser.* 314, 119–125. doi: 10.3354/meps314119

Klinges, J. G., Rosales, S. M., McMinds, R., Shaver, E. C., Shantz, A. A., Peters, E. C., et al. (2019). Phylogenetic, genomic, and biogeographic characterization of a novel and ubiquitous marine invertebrate-associated Rickettsiales parasite, *Candidatus Aquarickettsia rohweri*, gen. Nov., sp. nov. *ISME J.* 13, 2938–2953. doi: 10.1038/s41396-019-0482-0

Krediet, C. J., Ritchie, K. B., Paul, V. J., and Teplitski, M. (2013). Coral-associated micro-organisms and their roles in promoting coral health and thwarting diseases. *Proc. Biol. Sci.* 280:20122328. doi: 10.1098/rspb.2012.2328

Lamont, R. J., and Hajishengallis, G. (2015). Polymicrobial synergy and dysbiosis in inflammatory disease. *Trends Mol. Med.* 21, 172–183. doi: 10.1016/j.molmed.2014.11.004

Marcelino, V. R., Morrow, K. M., van Oppen, M. J. H., Bourne, D. G., and Verbruggen, H. (2017). Diversity and stability of coral endolithic microbial communities at a naturally high pCO_2 reef. *Mol. Ecol.* 26, 5344–5357. doi: 10.1111/mec.14268

Markle, J. G. M., Frank, D. N., Mortin-Toth, S., Robertson, C. E., Feazel, L. M., Rolle-Kampczyk, U., et al. (2013). Sex differences in the gut microbiome drive hormone-dependent regulation of autoimmunity. *Science* 339, 1084–1088. doi: 10.1126/science.1233521

McCook, L. J., Jompa, J., and Diaz-Pulido, G. (2001). Competition between corals and algae on coral reefs: a review of evidence and mechanisms. *Coral Reefs* 19, 400–417. doi: 10.1007/s003380000129

McDevitt-Irwin, J. M., Baum, J. K., Garren, M., and Vega Thurber, R. L. (2017). Responses of coral-associated bacterial communities to local and global stressors. *Front. Mar. Sci.* 4:262. doi: 10.3389/fmars.2017.00262

McFall-Ngai, M., Hadfield, M. G., Bosch, T. C. G., Carey, H. V., Domazet-Lošo, T., Douglas, A. E., et al. (2013). Animals in a bacterial world, a new imperative for the life sciences. *Proc. Natl. Acad. Sci. U. S. A.* 110, 3229–3236. doi: 10.1073/pnas.1218525110

Meirelles, P. M., Soares, A. C., Oliveira, L., Leomil, L., Appolinario, L. R., Francini-Filho, R. B., et al. (2018). Metagenomics of coral reefs under phase shift and high hydrodynamics. *Front. Microbiol.* 9:2203. doi: 10.3389/fmicb.2018.02203

Mera, H., and Bourne, D. G. (2018). Disentangling causation: complex roles of coral-associated microorganisms in disease. *Environ. Microbiol.* 20, 431–449. doi: 10.1111/1462-2920.13958

Monteil, Y., Teo, A., Fong, J., Bauman, A. G., and Todd, P. A. (2020). Effects of macroalgae on coral fecundity in a degraded coral reef system. *Mar. Pollut. Bull.* 151:110890. doi: 10.1016/j.marpolbul.2020.110890

Morrow, K. M., Bromhall, K., Motti, C. A., Munn, C. B., and Bourne, D. G. (2017). Allelochemicals produced by brown macroalgae of the *Lobophora* genus are active against coral larvae and associated bacteria, supporting pathogenic shifts to *vibrio* dominance. *Appl. Environ. Microbiol.* 83:e02391-16. doi: 10.1128/AEM.02391-16

Morrow, K. M., Liles, M. R., Paul, V. J., Moss, A., and Chadwick, N. E. (2013). Bacterial shifts associated with coral–macroalgal competition in the Caribbean Sea. *Mar. Ecol. Prog. Ser.* 488, 103–117. doi: 10.3354/meps10394

Morrow, K. M., Ritson-Williams, R., Ross, C., Liles, M. R., and Paul, V. J. (2012). Macroalgal extracts induce bacterial assemblage shifts and sublethal tissue stress in Caribbean corals. *PLoS One* 7:e44859. doi: 10.1371/journal.pone.0044859

Mumby, P. J., Hastings, A., and Edwards, H. J. (2007). Thresholds and the resilience of Caribbean coral reefs. *Nature* 450, 98–101. doi: 10.1038/nature06252

Mumby, P. J., and Steneck, R. S. (2008). Coral reef management and conservation in light of rapidly evolving ecological paradigms. *Trends Ecol. Evol.* 23, 555–563. doi: 10.1016/j.tree.2008.06.011

Mumby, P. J., Steneck, R. S., and Hastings, A. (2012). Evidence for and against the existence of alternate attractors on coral reefs. *Oikos* 122, 481–491. doi: 10.1111/j.1600-0706.2012.00262.x

Nelson, C. E., Alldredge, A. L., McCliment, E. A., Amaral-Zettler, L. A., and Carlson, C. A. (2011). Depleted dissolved organic carbon and distinct bacterial communities in the water column of a rapid-flushing coral reef ecosystem. *ISME J.* 5, 1374–1387. doi: 10.1038/ismej.2011.12

Nelson, A., De Soyza, A., Perry, J. D., Sutcliffe, I. C., and Cummings, S. P. (2012). Polymicrobial challenges to Koch's postulates: ecological lessons from the bacterial vaginosis and cystic fibrosis microbiomes. *Innate Immun.* 18, 774–783. doi: 10.1177/1753425912439910

Nelson, C. E., Goldberg, S. J., Kelly, L. W., Haas, A. F., Smith, J. E., Rohwer, F., et al. (2013). Coral and macroalgal exudates vary in neutral sugar composition and differentially enrich reef bacterioplankton lineages. *ISME J.* 7, 962–979. doi: 10.1038/ismej.2012.161

Nelson, C. E., Wegley Kelly, L., and Haas, A. F. (2022). Microbial interactions with dissolved organic matter are central to coral reef ecosystem function and resilience. *Annu. Rev. Mar. Sci.* 15:431. doi: 10.1146/annurev-marine-042121-080917

Nugues, M. M., Smith, G. W., Hooidonk, R. J., Seabra, M. I., and Bak, R. P. M. (2004). Algal contact as a trigger for coral disease. *Ecol. Lett.* 7, 919–923. doi: 10.1111/j.1461-0248.2004.00651.x

O'Brien, P. A., Smith, H. A., Fallon, S., Fabricius, K., Willis, B. L., Morrow, K. M., et al. (2018). Elevated CO_2 has little influence on the bacterial communities associated with the pH-tolerant coral, massive *Porites* spp. *Front. Microbiol.* 9:2621. doi: 10.3389/fmicb.2018.02621

Pollock, F. J., Morris, P. J., Willis, B. L., and Bourne, D. G. (2011). The urgent need for robust coral disease diagnostics. *PLoS Pathog.* 7:e1002183. doi: 10.1371/journal.ppat.1002183

Pratte, Z. A., Longo, G. O., Burns, A. S., Hay, M. E., and Stewart, F. J. (2018). Contact with turf algae alters the coral microbiome: contact versus systemic impacts. *Coral Reefs* 37, 1–13. doi: 10.1007/s00338-017-1615-4

Quan-Young, L. I., and Espinoza-Avalos, J. (2006). Reduction of zooxanthellae density, chlorophyll a concentration, and tissue thickness of the coral *Montastraea faveolata* (Scleractinia) when competing with mixed turf algae. *Limnol. Oceanogr.* 51, 1159–1166. doi: 10.4319/lo.2006.51.2.1159

Rasher, D. B., and Hay, M. E. (2010). Chemically rich seaweeds poison corals when not controlled by herbivores. *Proc. Natl. Acad. Sci. U. S. A.* 107, 9683–9688. doi: 10.1073/pnas.0912095107

Rasher, D. B., Hoey, A. S., and Hay, M. E. (2013). Consumer diversity interacts with prey defenses to drive ecosystem function. *Ecology* 94, 1347–1358. doi: 10.1890/12-0389.1

Rasher, D. B., Stout, E. P., Engel, S., Kubanek, J., and Hay, M. E. (2011). Macroalgal terpenes function as allelopathic agents against reef corals. *Proc. Natl. Acad. Sci. U. S. A.* 108, 17726–17731. doi: 10.1073/pnas.1108628108

Reigel, A. M., Paz-García, D. A., and Hellberg, M. E. (2021). Microbiome of a reef-building coral displays signs of acclimation to a stressful shallow hydrothermal vent habitat. *Front. Mar. Sci.* 8:652633. doi: 10.3389/fmars.2021.652633

Ritchie, K. B. (2006). Regulation of microbial populations by coral surface mucus and mucus-associated bacteria. *Mar. Ecol. Prog. Ser.* 322, 1–14. doi: 10.3354/meps322001

River, G. F., and Edmunds, P. J. (2001). Mechanisms of interaction between macroalgae and scleractinians on a coral reef in Jamaica. *J. Exp. Mar. Bio. Ecol.* 261, 159–172. doi: 10.1016/s0022-0981(01)00266-0

Roach, T. N. F., Little, M., Arts, M. G. I., Huckeba, J., Haas, A. F., George, E. E., et al. (2020). A multiomic analysis of in situ coral-turf algal interactions. *Proc. Natl. Acad. Sci. U. S. A.* 117, 13588–13595. doi: 10.1073/pnas.1915455117

Roff, G., and Mumby, P. J. (2012). Global disparity in the resilience of coral reefs. *Trends Ecol. Evol.* 27, 404–413. doi: 10.1016/j.tree.2012.04.007

Rosado, P. M., Leite, D. C. A., Duarte, G. A. S., Chaloub, R. M., Jospin, G., Nunes da Rocha, U., et al. (2019). Marine probiotics: increasing coral resistance to bleaching through microbiome manipulation. *ISME J.* 13, 921–936. doi: 10.1038/s41396-018-0323-6

Rosenberg, E., Koren, O., Reshef, L., Efrony, R., and Zilber-Rosenberg, I. (2007). The role of microorganisms in coral health, disease and evolution. *Nat. Rev. Microbiol.* 5, 355–362. doi: 10.1038/nrmicro1635

Santoro, E. P., Borges, R. M., Espinoza, J. L., Freire, M., Messias, C. S. M. A., Villela, H. D. M., et al. (2021). Coral microbiome manipulation elicits metabolic and genetic restructuring to mitigate heat stress and evade mortality. *Sci. Adv.* 7. doi: 10.1126/sciadv.abg3088

Schmitt, R. J., Holbrook, S. J., Davis, S. L., Brooks, A. J., and Adam, T. C. (2019). Experimental support for alternative attractors on coral reefs. *Proc. Natl. Acad. Sci. U. S. A.* 116, 4372–4381. doi: 10.1073/pnas.1812412116

Seyedsayamdost, M. R., Case, R. J., Kolter, R., and Clardy, J. (2011). The Jekyll-and-Hyde chemistry of *Phaeobacter gallaeciensis*. *Nat. Chem.* 3, 331–335. doi: 10.1038/nchem.1002

Shaver, E. C., Shantz, A. A., McMinds, R., Burkepile, D. E., Vega Thurber, R. L., and Silliman, B. R. (2017). Effects of predation and nutrient enrichment on the success and microbiome of a foundational coral. *Ecology* 98, 830–839. doi: 10.1002/ecy.1709

Silva, L., Calleja, M. L., Ivetic, S., Huete-Stauffer, T., Roth, F., Carvalho, S., et al. (2021). Heterotrophic bacterioplankton responses in coral- and algae-dominated Red Sea reefs show they might benefit from future regime shift. *Sci. Total Environ.* 751:141628. doi: 10.1002/ecy.1709

Smith, J. E., Shaw, M., Edwards, R. A., Obura, D., Pantos, O., Sala, E., et al. (2006). Indirect effects of algae on coral: algae-mediated, microbe-induced coral mortality. *Ecol. Lett.* 9, 835–845. doi: 10.1111/j.1461-0248.2006.00937.x

Stachowicz, J. J., and Hay, M. E. (1999). Mutualism and coral persistence: the role of herbivore resistance to algal chemical defense. *Ecology* 80, 2085–2101. doi: 10.1890/0012-9658(1999)080[2085:MACPTR]2.0.CO;2

Sunagawa, S., Woodley, C. M., and Medina, M. (2010). Threatened corals provide underexplored microbial habitats. *PLoS One* 5:e9554. doi: 10.1371/journal.pone.0009554

Sweet, M. J., Bythell, J. C., and Nugues, M. M. (2013). Algae as reservoirs for coral pathogens. *PLoS One* 8:e69717. doi: 10.1371/journal.pone.0069717

Thompson, J. R., Rivera, H. E., Closek, C. J., and Medina, M. (2014). Microbes in the coral holobiont: partners through evolution, development, and ecological interactions. *Front. Cell. Infect. Microbiol.* 4:176. doi: 10.3389/fcimb.2014.00176

van Duyl, F. C., van Bleijswijk, J. D. L., Wuchter, C., Witte, H. J., Coolen, M. J. L., Bak, R. P. M., et al. (2023). Recovery patterns of the coral microbiome after relief of algal contact. *J. Sea Res.* 191:102309. doi: 10.1016/j.seares.2022.102309

Vega Thurber, R., Burkepile, D. E., Correa, A. M. S., Thurber, A. R., Shantz, A. A., Welsh, R., et al. (2012). Macroalgae decrease growth and alter microbial community structure of the reef-building coral. *Porites astreoides*. *PLoS One* 7:e44246. doi: 10.1371/journal.pone.0044246

Vega Thurber, R., Mydlarz, L. D., Brandt, M., Harvell, D., Weil, E., Raymundo, L., et al. (2020). Deciphering coral disease dynamics: integrating host, microbiome, and the changing environment. *Front. Ecol. Evolut.* 8:575927. doi: 10.3389/fevo.2020.575927

Vega Thurber, R., Willner-Hall, D., Rodriguez-Mueller, B., Desnues, C., Edwards, R. A., Angly, F., et al. (2009). Metagenomic analysis of stressed coral holobionts. *Environ. Microbiol.* 11, 2148–2163. doi: 10.1111/j.1462-2920.2009.01935.x

Vermeij, M. J. A., Smith, J. E., Smith, C. M., Vega Thurber, R., and Sandin, S. A. (2009). Survival and settlement success of coral planulae: independent and synergistic effects of macroalgae and microbes. *Oecologia* 159, 325–336. doi: 10.1007/s00442-008-1223-7

Vieira, C., Engelen, A. H., Guentas, L., Aires, T., Houlbreque, F., Gaubert, J., et al. (2016a). Species specificity of bacteria associated to the brown seaweeds Lobophora (Dictyotales, Phaeophyceae) and their potential for induction of rapid coral bleaching in *Acropora muricata*. *Front. Microbiol.* 7:316. doi: 10.3389/fmicb.2016.00316

Vieira, C., Thomas, O. P., Culioli, G., Genta-Jouve, G., Houlbreque, F., Gaubert, J., et al. (2016b). Allelopathic interactions between the brown algal genus Lobophora (Dictyotales, Phaeophyceae) and scleractinian corals. *Sci. Rep.* 6:18637. doi: 10.1038/srep18637

Voolstra, C. R., Suggett, D. J., Peixoto, R. S., Parkinson, J. E., Quigley, K. M., Silveira, C. B., et al. (2021). Extending the natural adaptive capacity of coral holobionts. *Nat. Rev. Earth Environ.* 2, 747–762. doi: 10.1038/s43017-021-00214-3

Walsh, K., Haggerty, J. M., Doane, M. P., Hansen, J. J., Morris, M. M., Moreira, A. P. B., et al. (2017). Aura-biomes are present in the water layer above coral reef benthic macro-organisms. *PeerJ* 5:e3666. doi: 10.7717/peerj.3666

Webster, N. S., Negri, A. P., Botté, E. S., Laffy, P. W., Flores, F., Noonan, S., et al. (2016). Host-associated coral reef microbes respond to the cumulative pressures of ocean warming and ocean acidification. *Sci. Rep.* 6:19324. doi: 10.1038/srep19324

Wellington, G. M. (1980). Reversal of digestive interactions between Pacific reef corals: mediation by sweeper tentacles. *Oecologia* 47, 340–343. doi: 10.1007/BF00398527

Zaneveld, J. R., Burkepile, D. E., Shantz, A. A., Pritchard, C. E., McMinds, R., Payet, J. P., et al. (2016). Overfishing and nutrient pollution interact with temperature to disrupt coral reefs down to microbial scales. *Nat. Commun.* 7:11833. doi: 10.1038/ncomms11833

Zaneveld, J. R., McMinds, R., and Vega Thurber, R. (2017). Stress and stability: applying the Anna Karenina principle to animal microbiomes. *Nat. Microbiol.* 2:17121. doi: 10.1038/nmicrobiol.2017.121

Zhou, G., Yuan, T., Cai, L., Zhang, W., Tian, R., Tong, H., et al. (2016). Changes in microbial communities, photosynthesis and calcification of the coral *Acropora gemmifera* in response to ocean acidification. *Sci. Rep.* 6:35971. doi: 10.1038/srep35971

frontiers | Frontiers in Ecology and Evolution

TYPE Original Research
PUBLISHED 10 August 2023
DOI 10.3389/fevo.2023.1079271

OPEN ACCESS

EDITED BY
Kevin R. Theis,
Wayne State University, United States

REVIEWED BY
Lauren Frances Messer,
University of Stirling, United Kingdom
Eva Majerová,
University of Hawaii at Manoa,
United States

*CORRESPONDENCE
Karla Heric
karla.heric@unimelb.edu.au

RECEIVED 25 October 2022
ACCEPTED 21 July 2023
PUBLISHED 10 August 2023

CITATION
Heric K, Maire J, Deore P, Perez-Gonzalez A and van Oppen MJH (2023) Inoculation with *Roseovarius* increases thermal tolerance of the coral photosymbiont, *Breviolum minutum*. *Front. Ecol. Evol.* 11:1079271. doi: 10.3389/fevo.2023.1079271

Inoculation with *Roseovarius* increases thermal tolerance of the coral photosymbiont, *Breviolum minutum*

Karla Heric[1]*, Justin Maire[1], Pranali Deore[1], Alexis Perez-Gonzalez[2] and Madeleine J. H. van Oppen[1,3]

[1]School of Biosciences, The University of Melbourne, Parkville, VIC, Australia, [2]Melbourne Cytometry Platform, Department of Microbiology and Immunology, The University of Melbourne, The Peter Doherty Institute of Infection and Immunity, Parkville, VIC, Australia, [3]Australian Institute of Marine Science, Townsville, QLD, Australia

Coral reefs are diverse marine ecosystems that have tremendous ecological and cultural value and support more than 25% of eukaryote marine biodiversity. Increased ocean temperatures and light intensity trigger coral bleaching, the breakdown of the relationship between corals and their photosymbionts, dinoflagellates of the family Symbiodiniaceae. This leaves corals without their primary energy source, thereby leading to starvation and, often, death. Coral bleaching is hypothesized to occur due to an overproduction of reactive oxygen species (ROS) by Symbiodiniaceae, which subsequently accumulate in coral tissues. Bacterial probiotics have been proposed as an approach to mitigate coral bleaching, by reducing ROS levels in the coral holobiont through bacterial antioxidant production. Both corals and Symbiodiniaceae are known to associate with bacteria. However, the Symbiodiniaceae-bacteria relationship, and its impact on Symbiodiniaceae thermal tolerance, remains a poorly studied area. In this study, cultured Symbiodiniaceae of the species *Breviolum minutum* were treated with antibiotics to reduce their bacterial load. The cultures were subsequently inoculated with bacterial isolates from the genus *Roseovarius* that were isolated from the same *B. minutum* culture and showed either high or low ROS-scavenging abilities. The *B. minutum* cultures were then exposed to experimental heat stress for 16 days, and their health was monitored through measurements of cell density and photochemical efficiency of photosystem II. It was found that *B. minutum* inoculated with *Roseovarius* with higher ROS-scavenging abilities showed greater cell growth at elevated temperatures, compared to cultures inoculated with a *Roseovarius* strain with lower ROS-scavenging abilities. This suggests that *Roseovarius* may play a role in Symbiodiniaceae fitness at elevated temperatures. Analysis of Symbiodiniaceae-associated bacterial communities through 16S rRNA gene metabarcoding revealed that *Roseovarius* relative abundance increased in *B. minutum* cultures following inoculation and with elevated temperature exposure, highlighting the contribution they may have in shielding *B. minutum*

from thermal stress, although other bacterial community changes may have also contributed to these observations. This study begins to unpick the relationship between Symbiodiniaceae and their bacteria and opens the door for the use of Symbiodiniaceae-associated bacteria in coral reef conservation approaches.

KEYWORDS

bacteria, probiotics, reactive oxygen species, Symbiodiniaceae, coral

Introduction

Coral reefs are diverse marine ecosystems with highly beneficial ecological functions, such as providing protection of coastlines from degradation, and housing fish which humans harvest for nutrition and economic growth (Cesar et al., 2003). Reef-building corals associate with photosymbionts, dinoflagellate algae in the family Symbiodiniaceae (LaJeunesse et al., 2018). Nutrient exchange occurs between the two organisms; corals provide Symbiodiniaceae with the compounds they require for photosynthesis such as CO_2 (Yellowlees et al., 2008) and in turn, Symbiodiniaceae translocate photosynthate to corals for use in host cellular processes (Fournier, 2013). However, corals are experiencing stress due to climate change-induced summer heatwaves and exposure to high light levels that typically occur during summer heatwaves (Hughes et al., 2017). Such stressors break down the symbiotic relationship between Symbiodiniaceae and corals, causing coral bleaching and starvation (Weis, 2008; Suggett & Smith, 2019). Coral bleaching amounts to widespread habitat destruction for reef-dwelling organisms (Munday, 2004).

One of the mechanisms believed to be responsible for coral bleaching is the excess production of reactive oxygen species (ROS) by the Symbiodiniaceae following thermal and high light-induced damage to the symbionts' photosystems (Szabó et al., 2020). ROS are products of reactions of photosystems I and II (PSI and PSII) within chloroplasts of Symbiodiniaceae (Mehler, 1951; Richter et al., 1990). Some ROS, such as singlet oxygen from hydrogen peroxide (H_2O_2), are hypothesized to diffuse from the photosynthetic algae to the coral host, disrupt the mitochondrial membrane (Fournier, 2013), damage DNA (Barzilai and Yamamoto, 2004) and trigger a cellular cascade resulting in the loss of the Symbiodiniaceae (Weis, 2008). Providing exogenous antioxidants to corals has been shown to prevent bleaching under thermal stress, thus confirming a role of ROS underpinning the bleaching response (Lesser et al., 1990; Lesser, 1997).

Several coral bleaching mitigation methods have been proposed that aim to increase thermal tolerance in both corals and Symbiodiniaceae (van Oppen et al., 2015). One approach currently gaining traction is the use of bacteria (i.e., bacterial probiotics and microbiome transplantation) to enhance coral thermal bleaching tolerance (Rosado et al., 2019; Doering et al., 2021; Maire & van Oppen, 2021; Peixoto et al., 2021; Santoro et al., 2021; Dungan et al., 2022; Doering et al., 2023). Both corals and Symbiodiniaceae associate with a diverse community of bacteria (Lawson et al., 2018; van Oppen and Blackall, 2019; Camp et al., 2020; Maire et al., 2021a). Bacteria are also found intracellularly in cultured and *in hospite* Symbiodiniaceae and on the extracellular surface of cultured Symbiodiniaceae (Maire et al., 2021c). Their contribution to nutrient acquisition or thermal stress tolerance is not well documented (Ritchie, 2012), but studies on other marine microalgae have demonstrated functional roles. For example, *Marinobacter* in the marine diatom *Pseudo-nitzschia multiseries* (Amin et al., 2015) aides siderophore production and assists with resolving issues of iron bioavailability and iron acquisition (Amin et al., 2012). Recently, Motone et al. (2020) showed that a bacterium belonging to the genus *Muricauda* (Flavobacteriia) enhanced heat and light tolerance in Symbiodiniaceae cultures (*Durusdinium* sp.). Through antibiotic treatment, bacteria from the class Flavobacteriia were entirely depleted prior to experimental stress exposure. When Symbiodiniaceae cultures were exposed to thermal and light stress, photochemical efficiency of photosystem II (PSII) decreased with a concurrent increase in ROS, an effect that was significantly higher in cultures treated with antibiotics. However, this effect was smaller in cultures that were re-inoculated with *Muricauda*. This restored tolerance was attributed to *Muricauda*'s production of the carotenoid zeaxanthin, an antioxidant that ultimately promotes Symbiodiniaceae thermal and light resistance by minimizing damage by ROS. Bacteria sourced from Symbiodiniaceae themselves could thus be good candidates for probiotic use, but the functional relationship between Symbiodiniaceae as well as their potential contribution to thermal tolerance is relatively unexplored (Matthews et al., 2020).

Here, we conducted microbiome manipulation using a bacterium belonging to the genus *Roseovarius*. *Roseovarius* spp. have previously shown to have traits such as the ability to neutralize ROS molecules (Yoch, 2002; Miller and Belas, 2004; Randle et al., 2020). *Breviolum minutum* cultures isolated from *Exaiptasia diaphana* collected at the Great Barrier Reef were treated with antibiotics, inoculated with *Roseovarius*, and exposed to thermal stress. It was hypothesized that *B. minutum* inoculated with *Roseovarius* that had antioxidant abilities would be more thermally tolerant compared to *B. minutum* inoculated with *Roseovarius* lacking antioxidant ability, or a no-inoculum control. This study provides the foundation for future research into Symbiodiniaceae-bacteria relationships, and more generally the study of bacterial roles in Symbiodiniaceae heat tolerance.

Materials and methods

Symbiodiniaceae cultures

Breviolum minutum MMSF01 were obtained from *Exaiptasia diaphana* (Aiptasia) from the central Great Barrier Reef (Tortorelli et al., 2020). Cultures were maintained in 15 mL Daigo's IMK medium (1X concentration), prepared with filtered red sea salt water (fRSSW, 34 ppt) in sterile 50 mL polypropylene culture flasks where media was changed fortnightly. These flasks were kept in a 12 h light:12 h dark incubator (50–60 µmol photons $m^{-2}s^{-1}$ of photosynthetically active radiation) at 26°C.

Antibiotic treatment

The method detailed by Costa et al. (2019) was adapted to minimize bacterial community diversity and bacterial load in *B. minutum* cultures. First, 10 mL of Symbiodiniaceae culture were mixed with 18.7 µL of 0.1% Triton X-100 solution, and gently shaken for 30 sec to remove any loosely associated bacteria. This solution was then centrifuged for 5 min at 5000 × *g* and subsequently suspended in 10 mL of an antibiotic cocktail solution containing rifampicin, nalidixic acid, carbenicillin, nystatin and erythromycin (Table S1) for two days, then centrifuged and resuspended in IMK 1X for five days and this process was repeated three times in August 2020. During this time, flasks were maintained for three weeks in the same light and temperature conditions as described above. Following this antibiotic treatment, 50 uL Symbiodiniaceae culture were transferred to 1% agar plates that contained IMK (1X concentration), ampicillin, streptomycin, and gentamicin to further remove bacterial communities. Plates were maintained for one month in the same light and temperature conditions as described above, after which one colony was transferred to a new IMK plate supplemented with antibiotics and grown for one month. A single Symbiodiniaceae colony was then picked from the antibiotic agar plates and transferred to sterile 50 mL polypropylene culture flasks that contained 5 mL Daigo's IMK medium (0.5X concentration, prepared with fRSSW). This volume was then increased to 15 mL after two weeks and these cultures were then maintained (media changed fortnightly) for a year until the temperature stress experiment. Medium was diluted to 0.5X to increase reliance of the Symbiodiniaceae on their bacteria rather than receiving all their nutrients from the media itself. The resulting culture from this antibiotic treatment was named MMSF01-Ax.

Bacterial cultures

Twenty-three bacterial strains belonging to four genera of interest were selected based on potential beneficial functions reported in the literature (*Labrenzia, Muricauda, Marinobacter* and *Roseovarius*); these strains were previously isolated from *B. minutum* (Maire et al., 2021c) and were revived from glycerol stocks kept at -80°C as part of the culture collection at the Marine Microbial Symbiont Facility (University of Melbourne, VIC, Australia). These bacterial isolates were streaked onto marine agar (Difco™ Marine Agar 2216) or Reasoner's 2A (Oxoid R2A Agar CM0906B) agar plates, grown in an incubator at 26°C, and subcultured by re-streaking for use when required.

Qualitative DPPH assay

The 23 bacterial isolates mentioned earlier were assessed for their antioxidant capacity with a qualitative 2,2-diphenyl-1-picrylhydrazyl (DPPH) assay. DPPH is a free radical that appears purple when in solution, however antioxidant compounds present in solution cause a purple to yellow color change (Floegel et al., 2011). This qualitative assay was completed by streaking bacterial isolates onto marine agar or Reasoner's 2A agar plates which were then grown in a 26°C incubator for six days. Sterile Whatman #4 filter papers were placed on top of the streak plates with bacterial colonies, and the plates with filters were placed back into the incubator for approximately six hours to ensure bacteria were absorbed by the filter paper. In a fume hood, filter papers were removed using sterile forceps, and left to dry with the 'bacterial side' up for ~30 min, before 1 mL of 0.2 mM DPPH (Sigma-Aldrich) solution in methanol was applied with a pipette as per Dungan et al. (2021). Bacterial isolates were assessed for the formation of a white-yellow halo around the bacterial colonies following DPPH application. If a halo appeared within 1 min the isolate was deemed strongly positive. If a halo appeared between 1 and 3 min it was weakly positive, and negative readings occurred when no halos formed.

Flow cytometry for bacterial quantification

To count the number of bacteria present in *B. minutum* cultures, staining with SYBR green dye which binds to nucleic acids was carried out using a modified method by Lawson et al. (2020). SYBR green dye 10,000X (Sigma-Aldrich) was first diluted 1:500 using MilliQ water. Prior to sampling, flasks were shaken for 3 seconds to suspend *B. minutum* in solution. A sample of 250 µL was taken from each culture flask and diluted with 250 µL of 0.5X IMK media. Twenty-five µL of 1:500 SYBR green were applied to the samples and incubated for 15 min. An unstained sample was also processed as a control (receiving 25 µL of milliQ water). Before flow cytometry processing with a CytoFLEX LX flow cytometer (Beckman Coulter), samples were filtered through a 40 µm mesh-size strainer (pluriSelect) and vortexed to suspend cells and remove clumps. Violet SSC height was used as an acquisition trigger. Symbiodiniaceae cells were gated and counted by autofluorescence using a 405 nm violet laser (emission 763 ± 21.5 nm) (Figure S1). To differentiate SYBR green stained bacterial cells from debris and noise, 0.5X IMK media, MilliQ water and unstained samples were processed. Events measured in IMK-only samples (Figure S1A) were considered noise. Therefore, events from

Symbiodiniaceae samples falling in this part of the plot were also excluded (Figure S1D). Stained bacteria were analyzed *via* a bivariate plot of SYBR green fluorescence (488 nm excitation, emission 525 ± 20 nm) vs 405 nm side scatter (SSC) height. Singlet cells were gated and counted using a violet SSC area vs violet SSC height bivariate plot. At least 1000 Symbiodiniaceae cells were processed per sample. Bacterial count per Symbiodiniaceae cell was calculated by dividing bacterial cell count by Symbiodiniaceae cell count. These quantities were used to determine bacterial re-inoculation densities (see *Bacterial Re-inoculation* below).

Heat stress experiment

Symbiodiniaceae cultures

B. minutum cultures MMSF01 as well as MMSF01-Ax cultures treated with antibiotics were used for the heat stress experiment. These *B. minutum* cultures were subcultured into 20 experimental treatment culture flasks (Figure S2) at a starting density of ~5 x 10^5 cells mL^{-1}. Following bacterial inoculation (see below), cultures were maintained in the ambient incubator (26°C) for 24 hours before day 0 sampling. Each culture was then separated into two flasks, for ambient and elevated temperature treatments. Ambient culture flasks were kept in the 12h light:12h dark incubator (50–60 µmol photons m^{-2} s^{-1} of photosynthetically active radiation) at 26°C for the duration of the experiment. Elevated temperature treatment culture flasks were maintained in a 12h light:12h dark incubator under the same light conditions, at 32°C for the first 8 days of the experiment, with a subsequent temperature increase to 34°C on day 9 for seven days (Figure 1).

Bacterial re-inoculation

For each temperature treatment, cultures were subjected to four distinct treatments. The AB+ ROS+ (antibiotic treatment, bacterial inoculation with high antioxidant abilities) group aimed to assess the contribution of *Roseovarius* with putative antioxidant abilities to thermal tolerance. AB+ ROS- (antibiotic treatment, bacterial inoculation with low antioxidant abilities) was introduced to understand if *B. minutum* were exhibiting heterotrophic feeding whereby the bacteria would have acted as a food source (Jeong et al., 2012; Dungan et al., 2021). AB+ Control (antibiotic treatment, bacterial media inoculum) offered a comparison for the effect of *Roseovarius* inoculation, and the AB- Control (no antibiotic treatment, bacterial media inoculum) treatment group was included to understand the effect of the antibiotic treatment.

Bacterial isolate MMSF_3448 was chosen as the ROS+ bacterial treatment as it showed positive antioxidant properties in the DPPH assay and MMSF_3432 was chosen as ROS- as it was negative in the assay. Bacteria were streaked from frozen glycerol stocks onto marine agar plates and incubated at 26°C for 4 days. Using an inoculating loop, a single colony of each culture was transferred to

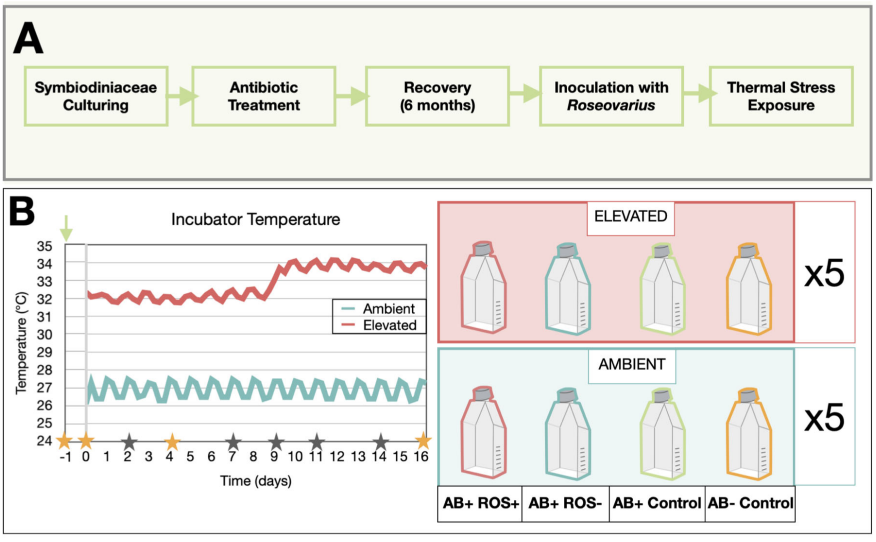

Symbiodiniaceae	Bacterial Inculum Added	Treatment Name
Antibiotic Treatment (AB+)	MMSF 3448 (ROS+)	AB+ ROS+
Antibiotic Treatment (AB+)	MMSF 3432 (ROS-)	AB+ ROS-
Antibiotic Treatment (AB+)	Marine Broth (Control)	AB+ Control
No Antibiotic Treatment (AB-)	Marine Broth (Control)	AB- Control

FIGURE 1
Experimental Design **(A)** Illustrates the sequence of experiments in this study. *B. minutum* were cultured and treated with antibiotics and maintained for one year until inoculation with *Roseovarius* and subsequent subjection to a heat stress. **(B)** The graph represents incubator temperature during the heat stress experiment obtained from data loggers (HOBO Pendant UA-001-08) in each incubator. Elevated incubator temperature was increased from 32°C to 34°C on day 9 of the experiment. Stars denote experiment sampling days, where orange stars show additional sampling for 16S rRNA gene metabarcoding. The green arrow indicates the day that *B. minutum* cultures were inoculated with bacteria. The right-hand side panel defines the four bacterial treatment groups (n = 5) exposed to ambient and elevated temperatures.

marine broth (Difco™ Micro Marine Broth 2216) (MB) and grown in an orbital incubator (Ratek orbital incubator) at 26°C and 300 rpm. Optical density (OD) readings were recorded at 600 nm using a plate reader (CLARIOstar Plus BGM Labtech). *Escherichia coli* approximations (OD_{600} of 0.5 is equal to 4 x 10^8 bacteria mL^{-1}) were used to calculate bacterial cell densities at measured ODs (Volkmer & Heinemann, 2011). Twelve hours prior to inoculation, broth cultures were diluted with MB to reach an OD_{600} of 0.1 and returned to the orbital incubator. Cultures with an OD_{600} of ~0.5 were vortexed and used to inoculate *B. minutum* a day prior to the temperature stress experiment, as per the following treatment groups listed in Figure 1.

As per bacterial abundance data obtained from 16S rRNA gene metabarcoding (Table 1), it was known that *Roseovarius* had 0.24% relative abundance prior to antibiotic treatment and was approximated to 0.5% for calculations. This, along with the bacterial cell counts per Symbiodiniaceae cell determined using SYBR green dye, was used to calculate the volume of inoculum required to deliver enough *Roseovarius* cells to restore its initial relative abundance. The number of *Roseovarius* cells to add through inoculation was determined by multiplying the Symbiodiniaceae cell density (5 x 10^6 cells mL^{-1}) by the number of bacteria present in the culture per cell (124 bacterial cells per Symbiodiniaceae cell for culture receiving ROS+ *Roseovarius* strain inoculum, 153 bacterial cells per Symbiodiniaceae cell for culture receiving ROS- *Roseovarius* strain inoculum). Of this value, 0.5% of these bacteria are *Roseovarius*, thus 309,584 cells mL^{-1} and 382,042 cells mL^{-1} for each treatment respectively. For 100 mL of culture, 30,958,350 and 38,204,200 *Roseovarius* cells were added. An inoculum with an optical density (OD_{600}) of 0.5 contains 4 x 10^8 cells mL^{-1} (*E. coli* approximation). The OD_{600} value for the ROS+ *Roseovarius* strain was determined to be 0.460 and 0.463 for ROS-, thus had bacterial densities of 3.8 x 10^8 cells mL^{-1} and 3.7 x 10^8 cells mL^{-1}. These densities divided by the number of *Roseovarius* cells determined earlier (30,958,350 and 38,204,200) calculated volumes of 84 µL for ROS+ and 103 µL ROS-. AB+ Control and AB- Control received a 90 µL (averaged value) of inoculum. These inoculum volumes were added to 100 mL Symbiodiniaceae cultures thus, the differences in inoculum volumes (80 uL – 100 uL) were deemed negligible due to the large final culture volume. To confirm inoculum viability, serial dilutions (10^{-1} to 10^{-8}) of each inoculum were plated onto MA plates with three replications per dilution. MA plates were incubated at 26°C for a week before colony forming units (CFUs) were counted (Table S2).

TABLE 1 Elimination of *Roseovarius* from *B. minutum* cultures.

Bacterial genus	Antibiotic Treatment	Mean Relative Abundance (%)
Labrenzia	AB-	12.15
	AB+	0.004
Marinobacter	AB -	0.48
	AB+	64.72
Muricauda	AB-	0.005
	AB+	0.15
Roseovarius	AB-	0.24
	AB+	0

Bacterial relative abundance in B. minutum of four genera of interest as determined by 16S rRNA gene metabarcoding, six months prior to inoculation and temperature exposure experiment where n = 3.

Symbiodiniaceae cell density

To quantify cell density over time, *B. minutum* cell density was obtained using a Countess II FL cell counter (Thermo Fisher scientific). Samples (100 µL) were taken from each replicate flask (five per treatment group). Of this, three 10 µL samples were processed to obtain cell density for each flask.

Microscopy PAM Fluorometry for Maximum Quantum Yield of PSII

To assess Symbiodiniaceae photosynthetic fitness, the maximum quantum yield of PSII (F_v/F_m of PSII) was measured using Pulse Amplitude Modulation (PAM) fluorometry. From each flask, 1 mL samples were briefly centrifuged (5 sec) to concentrate cells at the bottom of the tube, dark adapted for 15 min, and pipetted directly from the pellet onto a glass slide and covered with a cover slip for F_v/F_m estimations using microscopy-PAM (IMAGING-PAM *M-Series*, Walz, Germany) from 1300 hr. Samples belonging to a particular treatment group were processed at the same time on each sampling day to avoid variation in F_v/F_m due to the light variation across the day. Ten areas of interest containing three or more cells were focused simultaneously in each sample using a green colored neutral density filter (only allows green light to pass through) to avoid intense light exposure to samples, and imaged using blue measuring light. To obtain F_v/F_m, dark adapted samples were exposed to a measuring light intensity of 5 µmole quanta m^{-2} s^{-1} at 4 Hz frequency to record minimal fluorescence (F0) followed by an application of saturating pulse of 309 µmole quanta m^{-2} s^{-1} for 720 ms. The gain and damping were set to 7 and 15, respectively, to minimize noise.

16S rRNA gene metabarcoding

DNA extractions

DNA was extracted using a salting-out method as detailed by Wilson et al. (2002) with modifications as per Hartman et al. (2020) from 200 µL samples taken from *Breviolum minutum* cultures which included *B. minutum* cells and culture medium, six months prior to the thermal stress experiment (Figure S3). Four extraction blanks were included. The same method was used during the thermal stress experiment detailed below with 200 µL samples that were taken from each culture flask on days -1, 0, 4 and 16 of the experiment. Six DNA extraction blanks were included.

Metabarcoding library preparation

To amplify hypervariable regions V5-V6 of 16S rRNA genes, the primer pair 784F (5' GTGACCTATGAACTCAG GAGTCAGGATTAGATACCCTGGTA 3') and 1061R (' CTGAG

ACTTGCACATCGCAGCCRRCACGAGCTGACGAC 3') were used. Underlined are the Illumina adapters attached to the primers. 16S rRNA gene PCR amplification, library preparation, and sequencing were completed as per the method detailed by Maire et al. (2021b). Briefly, bacterial 16S rRNA genes were amplified with PCR using a Thermal Cycler (Applied Biosystems, ThermoFisher Scientific) as per the following conditions: denaturation at 95°C for 3 min, 18 cycles of: denaturation at 95°C for 15 sec, annealing at 55°C for 30 sec and extension at 72°C for 30 sec, ending with extension at 72°C for 7 min. Each reaction contained 1 μL of DNA (extracted from samples mentioned earlier), 1.5 μL of 10 uM each forward and reverse primers, 7.5 μL MyTaq HSRed MasterMix (BioLine) and 3.5 μL nuclease-free water (Thermofisher). Triplicates for each sample were conducted, and pooled following PCR. Preparation for library pooling was completed as per Maire et al. (2021c). Library preparation and MiSeq Illumina sequencing was performed at the Walter and Eliza Hall Institute (WEHI) in Melbourne, Victoria.

Data analyses

16S rRNA gene metabarcoding data analyses

16S rRNA gene metabarcoding data was processed using QIIME2 version 2021.8 (Bolyen et al., 2019). Metabarcoding data were obtained as paired-end, demultiplexed files with primers and adapters attached. The cutadapt plugin was used to remove primer and adapter sequences, with an error rate of 0.2. The quality of trimmed sequences was determined using the DADA2 plugin, which de-noises, filters, dereplicates, detects chimeras and merges paired-end reads (Callahan et al., 2016). Reads with low quality (Q-score < 30) were removed. To assign taxonomy, a SILVA classifier (version 138) was trained to classify bacterial 16S rRNA reads for hypervariable regions V5-V6. To construct a phylogenetic tree with mid-point rooting the alignment and phylogeny packages in QIIME2 were used (Caporaso et al., 2010). Reads that represented mitochondria and chloroplasts were filtered out. The metadata file, phylogenetic tree, and Amplicon Sequence Variant (ASV) tables were exported and analyzed in R studio.

The metadata file, phylogenetic tree, and Amplicon Sequence Variant (ASV) tables were imported into R studio for analyses, using the phyloseq package (McMurdie and Holmes, 2013). Rare ASVs (percentage abundance lower than 1.10^{-5}) were removed from the dataset. Samples with low read numbers (less than 400) were removed: 1 x ambient AB+ ROS-, 1 x ambient AB- Control and 3 x elevated AB+ ROS+, 1 x elevated AB- Control sampled on day 4, and 1 x ambient AB+ ROS+ from day 16. PCR and DNA blanks were analyzed to reveal contaminants using the decontam package (Table S3) for heat stress experiment data, as well as samples collected six months after antibiotic treatment (Table S4) (Davis et al., 2018). A Principal Coordinates Analysis (PCoA) plot was created using the Unifrac dissimilarity index, to visualize dissimilarities between bacterial communities in *B. minutum* cultures over time. One outlier (Ambient AB+ROS- collected on day 0) was removed from the plot, as well as the AB- Control samples. A 3-factor nonparametric permutational multivariate analysis of variance (PERMANOVA) using UniFrac distance matrix was conducted to inform the interactions between time, temperature and bacterial treatments. Number of permutations was 999. A second PERMANOVA was used to assess the factors of temperature and bacterial treatments on day 16. The indicator value analysis (De Cáceres and Legendre, 2009) was applied on Day 16 samples, in each of the four conditions independently (AB- Control, AB+ Control, AB+ ROS-, AB+ ROS-), to detect ASVs that were significantly associated with either ambient or elevated treatment using a significance threshold $\alpha = 0.05$, specificity = 0.9, and fidelity = 0.9. Four *Roseovarius* ASVs were detected in the metabarcoding data, however, only the major ASV present in the inocula was further analyzed, as the remaining ASVs had very low percentage abundance (i.e., 0.06%) in the inoculum samples, as well as experimental samples. Statistical test results were considered significant where $\alpha = 0.05$, unless otherwise stated. Graphs were generated using GraphPad Prism version 9.2.0.

Statistical analyses of phenotypic data in R Studio

Statistical analyses were conducted using R Studio version 1.3.1073. Shapiro-Wilk tests were used to confirm normality in distributions within groups (Ghasemi & Zahediasl, 2012). For cell density data log transformations were required to normalize distributions (Keene, 1995) and fulfil the underlying assumptions underpinning analysis of variance (ANOVA) use. Levene's tests confirmed homogeneity of variances (Gastwirth et al., 2009), thus 3 factor ANOVAs were used for statistical analyses of Symbiodiniaceae cell density and maximum quantum yield readings. Pairwise comparisons between groups were completed using Welch's t-tests (DeCoster, 2006) for the previously mentioned datasets.

Results

Roseovarius as ROS-scavenging bacteria

Of the 23 bacterial isolates tested for their ROS scavenging abilities, positive, or weakly positive readings were observed for only three isolates, with 20 appearing negative in the DPPH assay (Table S5). All three bacterial strains that recorded positive results belonged to the genus *Roseovarius*. Bacterial isolate MMSF_3448 was chosen as the ROS+ bacterial treatment and MMSF_3432 was chosen as ROS-. Analysis of previously obtained 16S rRNA gene sequences (Maire et al., 2021c) by BLAST showed that sequences for isolates MMSF_3448 and MMSF_3432 had 99% identity based on ~800 bp long fragments. Both isolates shared >99% identity with *Roseovarius confluentis, R. algicolus* and *R. atlanticus*. Thus, the species of MMSF_3448 and MMSF_3432 could not be determined, and are henceforth referred to as *Roseovarius* sp.

Effect of antibiotics and inoculation on Symbiodiniaceae bacterial community

Metabarcoding data collected six months after antibiotic treatment revealed changes in percentage abundances of bacteria belonging to the four genera of interest: *Labrenzia, Marinobacter, Muricauda* and *Roseovarius* prior to and post antibiotic treatment (Table 1). *Roseovarius* was entirely depleted in the antibiotic treatment cultures, with very low relative abundances of *Labrenzia* remaining (0.004%). Interestingly, *Muricauda* increased in relative abundance (0.005 to 0.15%) in the antibiotic treated *B. minutum*, while it was not detected in the non-treated culture, and *Marinobacter* showed greater relative abundance (0.5 to 65%) in antibiotic treated *B. minutum*. In addition to the four genera of interest, Phycisphaeraceae, Gammaproteobacteria, *Pseudohongiella*, and Leptospiraceae drastically diminished in relative abundance following antibiotic treatment whilst Micavibrionales and *Balneola* greatly increased (Figure S4). Thus, the antibiotic treatment was variably effective, but overall was successful in removing some bacterial species from *B. minutum* such as *Roseovarius*, which was then used for reinoculation.

The number of bacteria significantly increased following inoculation for all bacterial treatments with increases of greater magnitude observed for bacterial inocula compared to media alone (Figure 2; Table S6). AB+ ROS+, AB+ ROS- and AB- Control contained on average 130 bacterial cells per Symbiodiniaceae cell prior to inoculation (day -1) which increased variably depending on the treatment. Interestingly, AB+ Control had the highest number of bacterial cells on day -1 with an average of 194 bacterial cells per Symbiodiniaceae cell and AB- Control had the lowest with an average of 120. AB+ ROS- showed the highest post-inoculation count with an average of 250 cells mL^{-1}, with AB+ Control, AB+ ROS+ and AB- Control increasing to 242, 195 and 154, respectively. The ratio of the means of bacterial cell count before and after inoculation was approximately 1.6 for AB+ ROS+ and AB+ ROS- and 1.3 for AB+ Control and AB- Control. The greater increase observed for treatments receiving *Roseovarius* compared to bacterial media alone confirms the success of inoculation (Table S7).

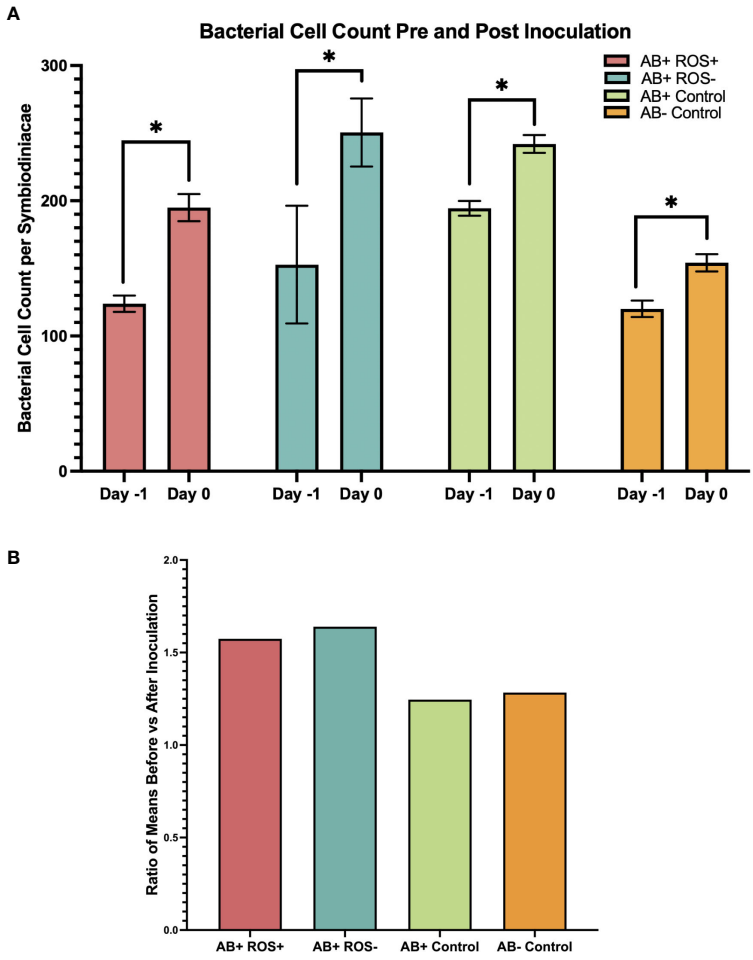

FIGURE 2
Bacterial cell counts increased following *Roseovarius* inoculation Bacterial cell count per Symbiodiniaceae cell, pre and post inoculation. Day -1 was measured prior to inoculation, and Day 0 one day after inoculation. **(A)** A significant increase in bacterial cell count was detected for all treatment groups by ANOVA. Bars represent the mean and error bars represent ± SD, where n = 5. Asterisk represents significant pairwise comparisons by Welch's t-tests where $p < 0.05$. **(B)** Ratio of the mean values of bacterial cell count before and after inoculation.

Inoculation with ROS-scavenging *Roseovarius* assisted with maintaining cell densities at elevated temperature

Symbiodiniaceae cell density was measured throughout the heat stress experiment (Figure 3A). A three-way ANOVA informed that all three factors (time, temperature, and bacterial treatment) (Table S8), as well as the two-way and three-way interactions between these factors, had a significant effect. Overall, cell density for all elevated treatments decreased over time, but it was found that AB+ ROS+ did not decrease as much as the other treatment groups (Figure 3A). On day 16, cell density was significantly lower for cultures in elevated temperature condition compared to ambient (Figure 3C; Table S9), confirming the negative effect of elevated temperature on cell density as well as signifying that the cells were under stress. Mean cell density at ambient temperatures were on average three times higher on day 16 compared to day 0 (Table S10): AB+ ROS-, AB+ Control and AB- Control treatments observed a 51%, 54% and 64% decrease in mean cell density, respectively, between day 0 and day 16. Conversely, AB+ ROS+ exposed to elevated temperature only observed a decrease of 7% in mean cell density over time. On day 16, cell density was significantly higher in elevated AB+ ROS+ compared to AB+ ROS-, and AB+ ROS+ compared to AB+ Control (Table S10). Additionally, Symbiodiniaceae cell density was significantly higher in AB+ Control vs AB- Control on day 16 (Table S10). Together these results suggest that *B. minutum* experienced thermal stress at elevated temperature which lessened cell density as time progressed, however the addition of *Roseovarius* through inoculation minimized the negative effect of temperature on cell fitness.

Inoculation with ROS-scavenging *Roseovarius* did not lead to detectable negative effects on photochemical efficiency of Symbiodiniaceae at elevated temperature

The maximum quantum yield (F_v/F_m) of the Symbiodiniaceae was measured as a proxy for photosynthetic fitness throughout the heat stress experiment (Figure 3B). A three-way ANOVA analysis

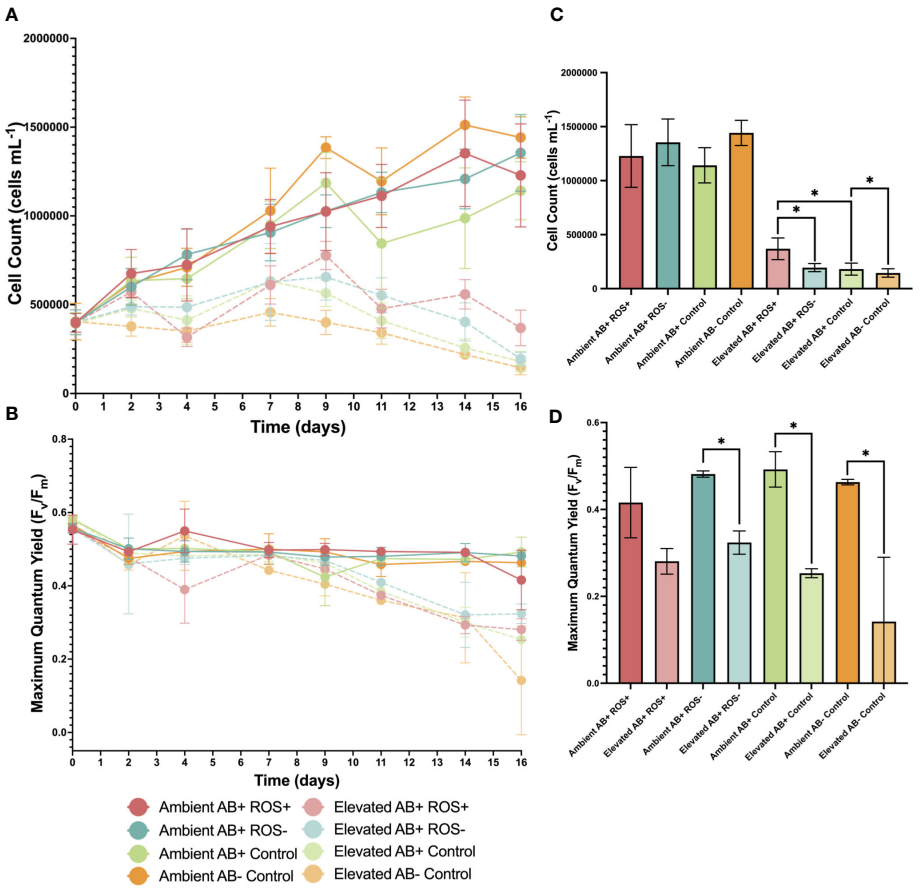

FIGURE 3
Roseovarius may assist in the maintenance of Symbiodiniaceae cell density and maximum quantum yield at elevated temperatures **(A)** Cell density of Symbiodiniaceae over time at ambient (26°C) (dark colors and solid lines) and heated (34°C) temperature (faded colors and dotted lines) for AB+ ROS+ bacteria (pink), AB+ ROS- (blue), AB+ Control (green) and AB- Control (orange). Each data point represents the mean and error bars are ± SD, where n = 5. **(B)** Maximum quantum yield of Symbiodiniaceae PSII over time. Each data point represents the mean and error bars are ± SD, where n = 3. **(C)** Symbiodiniaceae cell density on day 16. Bars represent the mean and error bars are ± SD, where n = 5. Asterisk denotes significant differences by Welch's t-tests where $p < 0.05$. **(D)** Maximum quantum yield of Symbiodiniaceae PSII on day 16. Each bar represents the mean and error bars are ± SD, where n = 3.

showed that the time and temperature, as well as their interaction, had a significant effect but bacterial treatment and all other interactions did not - at least not over the course of the experiment (Table S11). For all bacterial treatments, F_v/F_m was significantly lower on day 16 compared to day 0 at elevated temperature (Table S12), indicative of heat stress in these cultures. On day 16, however, pairwise t-tests confirmed that F_v/F_m was significantly lower in elevated AB+ ROS-, AB+ Control and AB- Control when compared to their ambient counterparts (Figure 3D; Table S13), suggesting there are greater disturbances to *B. minutum* maximum quantum yield when *Roseovarius* with antioxidant abilities are absent. Conversely, no significant differences were detected in F_v/F_m for ambient compared to elevated temperature treatments for AB+ ROS+ *B. minutum* on day 16 (Table S13), suggesting a role for *Roseovarius* for photochemical performance in *B. minutum* at heightened temperature. It is however possible that the lack of significant difference observed between AB+ROS+ on day 16 was due to the variability of samples that limited the power of statistical analyses. The greatest difference in F_v/F_m between day 0 and day 16 was observed for elevated AB- Control (75% decrease). Overall, F_v/F_m decreased for all treatment groups at elevated temperatures, suggesting that temperature strongly impacted the maximum quantum yield of *B. minutum* but the addition of *Roseovarius* minimized these effects.

Bacterial communities changed throughout exposure to elevated temperature

The bacterial community composition was highly similar among samples belonging to day -1, day 0, and day 4, regardless of the temperature or bacterial treatment (Figure 4A). However, on day 16, samples obtained from elevated temperature groups clustered away from those at ambient temperatures, suggesting a combined effect of time and temperature on bacterial community structure. PERMANOVA analysis confirmed these observations, as time and temperature, as well as their interaction, were significant in explaining the dissimilarity, but bacterial treatment was not (Table S14). However, the interaction between bacterial treatment and time was also found to be significant. In light of these interactions, further PERMANOVA analysis was conducted for day 16, which showed that bacterial communities were significantly different between ambient and elevated temperatures, and between bacterial treatments (Table S15). This pattern was also seen at the family level (Figure 4B). AB- Control was most different to AB+ ROS+, AB+ ROS- and AB+ Control on day 0, with the largest percentage abundance (20%) being bacteria of the family Bacteriovoracaceae. Major community composition changes over time were similar across the three treatments AB+ ROS+, AB+ ROS- and AB+ Control. Taxa such as Algiphilaceae and Balneolaceae showed a drastic decrease in relative abundance between day 0 and day 16, where Algiphilaceae decreased from an average of 35% to <1% and Balneolaceae decreased from 10% to 3%. Rickettsiales relative abundance increased variably, regardless of temperature, showing the impact of time alone on community composition. Other taxa, such as Terasakiellaceae and Oleiphilaceae, increased in relative abundance from an average of 3% to 10% in Terasakiellaceae and <1% to 6% on average in Oleiphilaceae only at elevated temperature, highlighting the effect of temperature over time on community composition. These changes were underpinned by differences in ASV abundances at ambient and elevated temperatures for each treatment group, which were investigated with an indicator analysis (Figure S5). For elevated treatments, ASV 15 UC Terasakiellaceae and ASV 16 *Oleiphilus* sp. were the most abundant indicator ASVs for AB+ Control, AB+ROS-, and AB+ROS+. For elevated AB- Control ASV 40 UC Saprospiraceae and ASV 31 *Pelagibius* sp. appeared in higher abundances. Ambient indicator species include ASV 03 UC Paracaedibacteraceae most prevalent in AB+ROS- and AB+ Control and ASV 01 UC Rickettsiales in AB- Control and AB +ROS+. *Labrenzia* were more abundant at elevated temperature with ASV 28 *Labrenzia* sp. and ASV 32 *Labrenzia marina* being abundant indicator ASVs at elevated temperatures. Altogether, these results suggest that bacterial community structure changed over time as a result of temperature exposure, with variable changes observed in different bacterial taxa.

Roseovarius inoculation was successful

To assess *Roseovarius* persistence following inoculation and thus the sustained success of inoculation over time, *Roseovarius* relative abundance was determined throughout the experiment using 16S rRNA gene metabarcoding. Following decontamination, three ASVs were found in the two inocula, all belonging to the genus *Roseovarius*, with one single ASV (*Roseovarius* sp. ASV01) making up 99% and 98% of the reads in the ROS+ and ROS- inocula, respectively which points to high inocula purity (Figure S6). The remaining 1-2% of reads were likely contaminants from library preparation, as well as the 1.9% ASV01 abundance which was observed in the control inoculum. Thus, the abundance of this major ASV that comprised the two *Roseovarius* inocula was further investigated. Prior to inoculation, *Roseovarius* sp. ASV01 relative abundances were ~4% for AB+ ROS+ and AB+ ROS-, 2% for AB+ Control and 0.6% for AB- Control, which contrasts with metabarcoding data that were obtained six months prior to the heat stress experiment where *Roseovarius* was not detected (Table 1). In fact, overall bacterial communities were quite different between the beginning of the heat stress experiment and the sampling conducted six months prior. Six months before the heat stress experiment, AB- cultures were dominated by Phycisphaeraceae, Stappiaceae, and Pseudohongiellaceae in comparison to AB+ cultures that mostly contained Marinobacteraceae as well as Balenoelaceae and Micavibrionales (Figure S4B). On day 0 of the heat stress experiment, Phycisphaeraceae were still highly abundant but Bacteriovoracaceae were most abundant for AB- cultures. At this time, Algiphilaceae, Balneolaceae, and Marinobacteraceae were observed in the highest abundance for AB+ cultures. *Roseovarius* relative abundance increased significantly over the course of the heat stress experiment (Figure 5; Table S16), particularly on day 16 for elevated treatment groups, with a 17% and 16% abundance observed

10.3389/fevo.2023.1079271

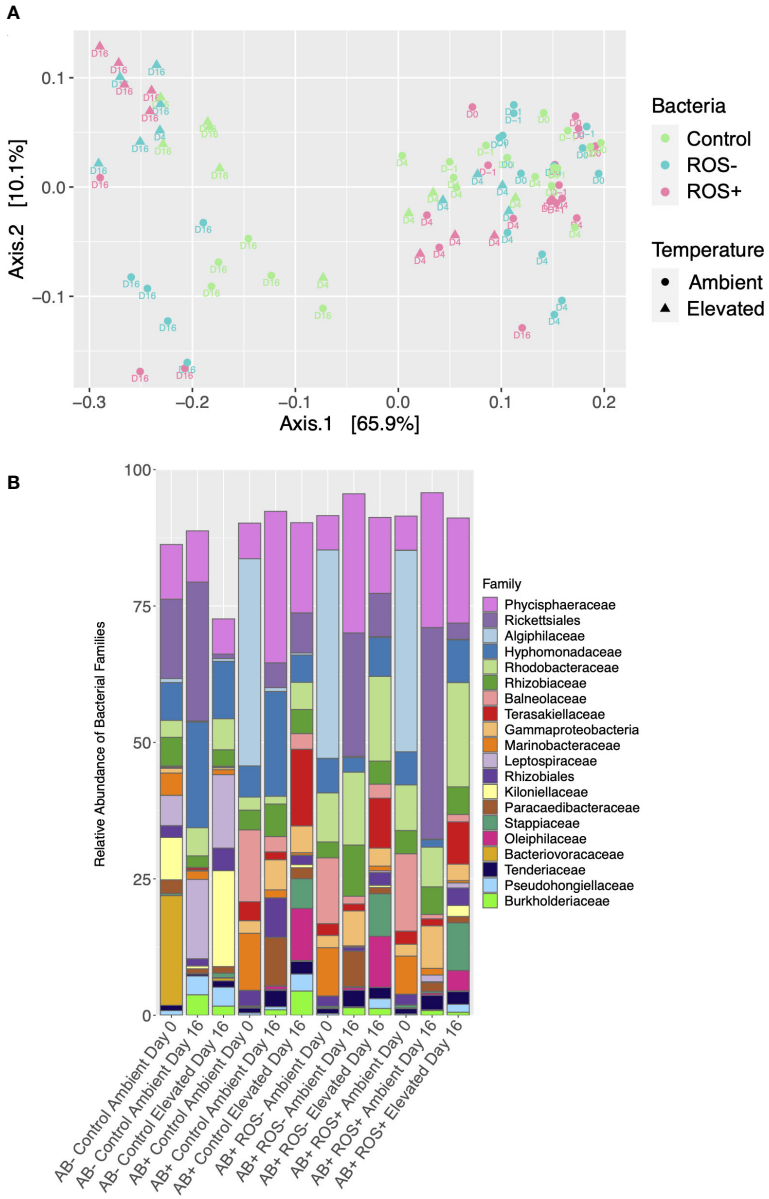

FIGURE 4
Bacterial communities changed throughout exposure to elevated temperature **(A)** PCoA plot where Axis 1 and Axis 2 are PC1 and PC2 respectively, representing the beta-diversity of bacterial communities of three of the bacterial treatments in antibiotic-treated cultures, AB+ ROS+ (Positive), AB+ ROS- (Negative) and AB+ Control (Media) at ambient and elevated temperatures. Each data point denotes a single sample, retrieved on a given sampling day: day -1, day 0, day 4 and day 16 (D-1, D0, D4 and D16, respectively) of the experiment. **(B)** Bar chart of percentage abundance of the top 20 bacterial families present in samples on day 0 and day 16, at ambient and elevated temperature.

for AB+ ROS+ and AB+ ROS- respectively at the conclusion of the experiment, compared to only 4% for AB+ Control and 1% for AB- Control, demonstrating that inoculated *Roseovarius* was able to establish itself in the *B. minutum* cultures. Further, on day 16, *Roseovarius* relative abundance was significantly higher at elevated temperature, compared to ambient, in the AB+ ROS+ and AB+ control treatments, but not for AB+ ROS- and AB- Control (Table S17). Overall, *Roseovarius* relative abundance showed greater increases over time after inoculation with *Roseovarius*, compared to negative controls confirming the successful establishment of inoculated *Roseovarius* into the *B. minutum* cultures.

Discussion

The relationship between Symbiodiniaceae and their bacteria is not extensively studied, and further inquiries are required to understand the functional contribution of bacteria to Symbiodiniaceae health and survival. Here, an antibiotic cocktail was administered to minimize *B. minutum*'s bacterial load and diversity, with subsequent inoculation with *Roseovarius* and exposure to elevated temperature. *B. minutum* inoculated with *Roseovarius* with high ROS-scavenging abilities showed greater cell density and smaller decreases in F_v/F_m at elevated temperatures, suggesting that *Roseovarius* may provide benefits to

10.3389/fevo.2023.1079271

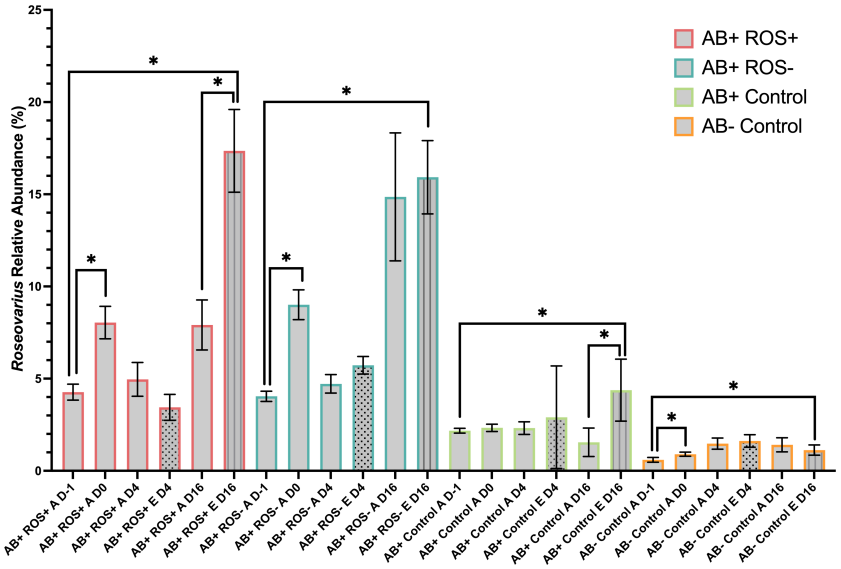

FIGURE 5
Roseovarius persisted in B. minutum culture following inoculation Relative abundance of *Roseovarius* sp ASV01 in each bacterial treatment over time (day-1 to day 16). A and E denote ambient and elevated temperatures, respectively. Bars represent the mean and error bars are ± SD, where n = 5. Asterisks denote significant differences by Welch's t-tests where $p < 0.05$. Significant differences were detected when comparing samples obtained prior to inoculation (day -1) and a day after inoculation (day 0), as well as comparisons between day -1 and day 16. Elevated treatment bars appear patterned on day 4 and day 16 to allow for clearer comparisons.

B. minutum under heat stress conditions. Analysis of Symbiodiniaceae bacterial communities through 16S rRNA gene metabarcoding revealed that *Roseovarius* relative abundance increased in *B. minutum* cultures following inoculation and increased with elevated temperature exposure, suggesting they may play a role in shielding *B. minutum* from the effects of thermal stress.

Antibiotic treatment was marginally effective at removing bacterial community members

The *B. minutum* cultures were not rendered axenic following antibiotic treatment. Of the four genera of interest (*Labrenzia, Marinobacter, Muricauda, Roseovarius)*, *Roseovarius* was no longer detected in antibiotic treated *B. minutum* cultures, with considerable decreases seen in *Labrenzia*. In contrast, *Muricauda* and *Marinobacter* showed an increase in relative abundance, in antibiotic treated *B. minutum*. Thus, the antibiotic treatment was successful in significantly reducing the abundance of certain genera, but not all. By estimating absolute bacterial load prior to inoculation, it was found that the cultures not treated with antibiotics had fewer bacteria present compared to all antibiotic treatment cultures. This pattern is opposite to expectations and suggests that the antibiotic treatment had limited effectiveness in removing bacteria associating with Symbiodiniaceae. Alternatively, the bacteria may have been able to grow back to pre-AB treatment levels during recovery, as the cultures were maintained for one year following antibiotic treatment. Additionally, while we observed an absence of *Roseovarius* six months after antibiotic treatment, samples taken approximately one year after antibiotic treatment during the heat stress experiment showed a resurgence of *Roseovarius*, which was accompanied by other major changes in bacterial community composition. This suggests that bacteria, including *Roseovarius*, may have been reintroduced following antibiotic treatment, or that undetectable levels of *Roseovarius* were still present which later resurfaced. Similar antibiotics durably depleted Flavobacteriia from Symbiodiniaceae in an earlier study, after two months of antibiotic treatment and three months of recovery, although absolute bacterial load was not measured (Motone et al., 2020). In contrast, Xiang et al. (2013) reported the complete elimination of bacterial associates in five Symbiodiniaceae cultures.

Interestingly, cultures that did not go through antibiotic treatment showed the greatest fitness decrease over time at elevated temperature, as reflected in the cell density and photochemical efficiency data. It is possible that some bacteria that resisted the antibiotic treatment were able to thrive following the removal of antibiotic-sensitive bacteria, and have functions that assist with thermal tolerance. The antibiotic treatment restructured the microbiome and it is possible that the microbiome modifications following antibiotic treatments rendered it more beneficial during thermal stress. Further studies with the *B. minutum* cultures without antibiotic treatment in addition to inoculation with ROS-scavenging bacteria (ROS+) and non-ROS-scavenging bacteria (ROS-) will help to understand these observed differences. The thermally tolerant photosymbiont genus *Durusdinium* has previously shown the greatest microbiome stability under experimental thermal stress, suggesting that stable microbiomes assist with thermal tolerance (Camp et al., 2020). Heat-evolved *Cladocopium*, exposed to elevated temperature (31°C)

for 6 years, housed less diverse but more stable bacterial communities than their wild type counterparts (Buerger et al., 2022), with differences in microbiome composition suspected to contribute to thermal tolerance. Thus, a heat-selected microbiome achieved through experimental evolution (Buerger et al., 2022) or inoculation with certain bacteria (Motone et al., 2020) may equip Symbiodiniaceae for elevated temperature conditions, however further functional studies are required.

Exposure to elevated temperature induced changes in bacterial communities of *B. minutum*

Changes in bacterial community structure were observed, with temperature being a significant factor influencing these changes, although those changes did not occur immediately. This suggests that the effects of bacterial treatment were delayed and coupled with extended exposure to thermal stress conditions. Therefore, other bacteria, beyond *Roseovarius*, may have played a role in thermal stress tolerance. This was also reflected in studies completed by Camp et al. (2020), whereby *B. minutum* experienced significant bacterial community changes when exposed to elevated temperatures. *B. minutum* was associated with both *Roseovarius* and *Labrenzia* at similar relative abundances under ambient and elevated temperature, with little *Hyphobacterium* observed at elevated temperature (Camp et al., 2020). Following Symbiodiniaceae experimental evolution, the genera *Labrenzia*, *Algiphilus*, *Hyphobacterium* and *Roseitalea* were more abundant in heat-evolved *Cladocopium* strains compared to wild type (Buerger et al., 2022). Interestingly, we observed higher *Algiphilus* (family Gammaproteobacteria) relative abundance following antibiotic treatment in *B. minutum*, although it decreased following exposure to elevated temperature. *Labrenzia* are found in high relative abundance across the majority of Symbiodiniaceae strains (Lawson et al., 2018; Camp et al., 2020; Maire et al., 2021c; Díaz-Almeyda et al., 2022). *Labrenzia* plays a role in the production of dimethylsulfoniopropionate (DMSP) in other dinoflagellates (Sunda et al., 2002) which is a compound that scavenges ROS, thus it may function as an antioxidant and assist with heat stress tolerance. In our analysis, *Labrenzia* were found in higher abundance at elevated temperature on day 16. The altered community following elevated temperature exposure in our study may have influenced thermal tolerance due to the presence of *Roseovarius*, *Labrenzia*, and bacterial species that provide a functional contribution to thermal stress mitigation.

Despite the antibiotic treatment's limited capacity to perturb the *B. minutum* microbiome and the resurgence of *Roseovarius* before the thermal stress experiment, *Roseovarius* established in the *B. minutum* cultures following inoculation. This suggests that treating Symbiodiniaceae with antibiotics may not be necessary in order to assess the contributions of inoculated bacteria. *Roseovarius* relative abundance had greater increases at elevated compared to ambient temperature, thus *Roseovarius* may be better at competing with other bacteria at elevated temperature.

Roseovarius may assist in the maintenance of Symbiodiniaceae cell density and maximum quantum yield at elevated temperatures

Re-inoculation with ROS-scavenging *Roseovarius* may have contributed to greater *B. minutum* cell density at elevated temperatures. At the conclusion of the temperature stress experiment, cell density at elevated temperatures were significantly higher for flasks inoculated with ROS-scavenging *Roseovarius*, compared to other elevated temperature bacterial treatment groups, albeit lower than in the ambient treatment. In addition, smaller reductions in maximum quantum yield were detected in flasks inoculated with ROS-scavenging *Roseovarius*, suggesting this treatment group maintained better photosynthetic fitness compared to controls at elevated temperatures. Statistical analyses may have been affected by sample variability, in turn contributing to the non-detectable differences in maximum quantum yield observed for ROS-scavenging *Roseovarius* inoculated flasks. Greater sample size in future studies would disentangle whether these observations were limited by the statistical analyses. In addition, since absolute bacterial load was not measured, observed *Roseovarius* increases only reflect the proportional change in bacterial communities, not whether *Roseovarius* cell abundance increased. Thus, future studies should measure absolute abundances to conclusively determine inoculation success and subsequent influence on inoculated species. The addition of a *Roseovarius* strain with low ROS-scavenging abilities was a useful control group as cultured Symbiodiniaceae can feed on bacteria (Jeong et al., 2012). If heterotrophic feeding was responsible for the observed fitness increases, the same effects would have been expected for the *Roseovarius* inoculation with the low ROS scavenging strain. Previous cnidarian probiotic studies have failed to include such treatment groups for comparison (Rosado et al., 2019; Doering et al., 2021; Santoro et al., 2021; Zhang et al., 2021), with few including an inoculum without the beneficial function under study (Dungan et al., 2021; Dungan et al., 2022), but it should become common practice in future investigations.

In a previous study by Maire et al. (2021c), species of *Roseovarius* appeared both closely and loosely associated to *B. minutum*. Relative abundances of *Roseovarius* were 1% for closely associated fractions and less than 0.01% for loosely associated fractions (Maire et al., 2021c), suggesting *Roseovarius* preferably closely associate with *Breviolum*. However, we cannot confirm the particular ASV assessed here closely associates with *B. minutum* as samples for DNA extraction were not washed and filtered upon collection. Thus, *Roseovarius* in our study may simply be free-living within the culture medium. Further, Maire et al. (2021c) suggest that bacteria appear on the external surface of Symbiodiniaceae cells

under culture conditions and are absent *in hospite*. As we cannot conclude the nature of the association of *Roseovarius* with *B. minutum* and there is a possibility that the bacteria exist within the culture medium, further research is required to determine whether *Roseovarius* closely associate with *B. minutum* and subsequently if this association confers any benefits *in hospite*.

Roseovarius was found to play a key role in sulfur cycling and the de-methylation of DMSP to dimethylsulfide (DMS) in the dinoflagellate *Pfiesteria piscicida* (Yoch, 2002; Miller and Belas, 2004). In species of *Roseovarius* isolated from seawater (González et al., 2003), DMS and DMSP were found to play a role in the DMSP antioxidant system and scavenge ROS (Sunda et al., 2002), which could contribute to the reduction of oxidative stress during thermal stress. Additionally, *Roseovarius* was detected in heat-stressed corals (Pootakham et al., 2019), and *Aliiroseovarius*, a closely related genus, increased in relative abundance during heat stress at high salinities in the sea anemone *Exaiptasia diaphana* (Randle et al., 2020), suggesting a functional contribution to thermal stress. Whole-genome sequencing of the two isolates used in our study should be undertaken to understand the mechanisms underlying the different effects they had on Symbiodiniaceae cultures, and whether it is indeed ROS-related or whether other biological processes are at play.

Microbiome manipulations such as those used in the present study are carried out to understand if Symbiodiniaceae-associated bacteria can enhance thermal tolerance. Targeted studies like our investigation as well as Motone et al. (2020) aim primarily to elucidate specific bacteria of interest that may confer beneficial functions and increase thermal tolerance of Symbiodiniaceae, and future investigations should assess the nature of the association of bacteria with Symbiodiniaceae *in hospite* in order to make concrete conclusions about their beneficial functions. It has been shown that bacterial communities of Symbiodiniaceae differ following experimental evolution (Buerger et al., 2022), and these changes may contribute to the increased Symbiodiniaceae heat tolerance. Further studies are required to assess if *Roseovarius* contribute to thermal tolerance of Symbiodiniaceae *in hospite* and whether there are potential implications in coral restoration. Insightful future investigations include inoculating Symbiodiniaceae, or corals experiencing thermal stress, to observe which bacterial community members are incorporated which could suggest beneficial functions.

Conclusion

This study begins to decipher the relationship between Symbiodiniaceae and their bacteria with a particular focus on the genus *Roseovarius*. The findings demonstrate the positive effect of *Roseovarius* inoculation on cultured Symbiodiniaceae exposed to thermal stress and suggest a potential functional role of *Roseovarius* in Symbiodiniaceae thermal tolerance. Further studies are required to explore whether bacterial inoculation with *Roseovarius* could be used to mitigate thermal stress in other Symbiodiniaceae species or in corals, and may give rise to new research avenues and coral restoration practices.

Data availability statement

The datasets presented in this study can be found in online repositories. The names of the repository/repositories and accession number(s) can be found below: https://www.ncbi.nlm.nih.gov/, PRJNA887911 https://www.ncbi.nlm.nih.gov/, PRJNA887545.

Author contributions

Conceptualization: KH, JM, and MO. Formal analysis: KH and JM. Funding acquisition: MO. Investigation: KH, JM, and PD. Methodology: KH, PD, and AP-G. Supervision: MO and JM. Visualization: KH. Writing – Original Draft Preparation: KH, JM, and MO. All authors contributed to manuscript revision, read, and approved the submitted version.

Funding

This study was funded by the Australian Research Council Laureate Fellowship FL180100036 to MO. PD was supported by Gordon Betty Moore foundation (grant number – 9351).

Acknowledgments

We are grateful to: Dr. Sanjida Topa for assisting with processing metabarcoding samples and Dr. Ashley Dungan for providing assistance with metabarcoding data analysis.

Conflict of interest

The authors declare that the research was conducted in the absence of any commercial or financial relationships that could be construed as a potential conflict of interest.

Publisher's note

Supplementary material

The Supplementary Material for this article can be found online at: https://www.frontiersin.org/articles/10.3389/fevo.2023.1079271/full#supplementary-material

References

Amin, S. A., Green, D. H., Waheeb, D. A., Gardes, A., and Carrano, C. J. (2012). Iron transport in the genus *Marinobacter*. *Biometals* 25, 135–147. doi: 10.1007/s10534-011-9491-9

Amin, S. A., Hmelo, L. R., van Tol, H. M., Furham, B. P., Carlson, L. T., Heal, K. R., et al. (2015). Interaction and signalling between a cosmopolitan phytoplankton and associated bacteria. *Nature* 522, 98–101. doi: 10.1038/nature14488

Barzilai, A., and Yamamoto, K. (2004). DNA damage responses to oxidative stress. *DNA Repair (Amst)* 3(8–9):1109–1115. doi: 10.1016/j.dnarep.2004.03.002

Bolyen, E., Rideout, J. R., Dillon, M. R., Bokulich, N. A., Abnet, C. C., Al-Ghalith, G. A., et al. (2019). Reproducible, interactive, scalable and extensible microbiome data science using QIIME 2. *Nat. Biotechnol.* 37, 852–857. doi: 10.1038/s41587-019-0209-9

Buerger, P., Vanstone, R. T., Maire, J., and van Oppen, M. J. H. (2022). Long-term heat selection of the coral Endosymbiont *Cladocopium* $C1^{acro}$ (Symbiodiniaceae) stabilizes associated bacterial communities. *Int. J. Mol. Sci.* 23 (9), 4913. doi: 10.3390/ijms23094913

Callahan, B. J., Mcmurdie, P. J., Rosen, M. J., Han, A. W., Johnson, A. J. A., and Holmes, S. P. (2016). DADA2: high-resolution sample inference from Illumina amplicon data. *Nat. Methods* 13, 581. doi: 10.1038/nmeth.3869

Camp, E. F., Kahlke, T., Nitschke, M. R., Varkey, D., Fisher, N. L., Fujise, L., et al. (2020). Revealing changes in the microbiome of Symbiodiniaceae under thermal stress. *Environ. Microbiol.* 22 (4), 1294–1309. doi: 10.1111/1462-2920.14935

Caporaso, J. G., Kuczynski, J., Stombaugh, J., Bittinger, K., Bushman, F. D., Costello, E. K., et al. (2010). QIIME allows analysis of high-throughput community sequencing data. *Nat. Methods* 7, 335–336. doi: 10.1038/nmeth.f.303

Cesar, H., Burke, L., and Pet-Soede, L. (2003). The economics of worldwide coral reef degradation, Cesar Environmental Economics Consulting, Arnhem.

Costa, R. M., Fidalgo, C., Cardenas, A., Frommlet, J. C., and Voolstra, C. R. (2019). Protocol for the generation of axenic/bacteria-depleted Symbiodiniaceae cultures. doi: 10.17504/protocols.io.87khzkw

Davis, N. M., Proctor, D. M., Holmes, S. P., Relman, D. A., and Callahan, B. J. (2018). Simple statistical identification and removal of contaminant sequences in marker-gene and metagenomics data. *Microbiome* 6, 226. doi: 10.1186/s40168-018-0605-2

De Cáceres, M., and Legendre, P. (2009). Associations between species and groups of sites: Indices and statistical inference. *Ecology* 90, 3566–3574. doi: 10.1890/08-1823.1

DeCoster, J. (2006) *Testing Group Differences using T-tests, ANOVA, and Nonparametric Measures*. Available at: http://www.stat-help.com/notes.html (Accessed 27/09/21).

Díaz-Almeyda, E. M., Ryba, T., Ohdera, A. H., Collins, S. M., Shafer, N., Link, C., et al. (2022). Thermal stress has minimal effects on bacterial communities of thermotolerant symbiodinium cultures. *Front. Ecol. Evol.* 10. doi: 10.3389/fevo.2022.764086

Doering, T., Maire, J., van Oppen, M. J. H., and Blackall, L. L. (2023). Advancing coral mirobiome manipulation to build long-term climate resilience. *Microbiol. Aust.* 44, 36–40. doi: 10.1071/MA23009

Doering, T., Wall, M., Putchim, L., Rattanawongwan, T., Schroeder, R., Hentschel, U., et al. (2021). Towards enhancing coral heat tolerance: a "microbiome transplantation" treatment using inoculations of homogenized coral tissues. *Microbiome* 9, 102. doi: 10.1186/s40168-021-01053-6

Dungan, A. M., Bulach, D., Lin, H., van Oppen, M. J. H., and Blackall, L. L. (2021). Development of a free radical scavenging bacterial consortium to mitigate oxidative stress in cnidarians. *Microbial Biotechnol.* 14 (5), 2025–2040. doi: 10.1111/1751-7915.13877

Dungan, A. M., Hartman, L. M., Lin, H., Blackall, L. L., and van Oppen, M. J. H. (2022). Exploring microbiome engineering as a strategy for improved thermal tolerance in *Exaiptasia diaphana*. *J. Appl. Microbiol.* 132 (4), 2940–2956. doi: 10.1111/jam.15465

Floegel, A., Dae-Ok, K., Chung, S. J., Koo, S. I., and Chun, O. K. (2011). Comparison of ABTS/DPPH assays to measure antioxidant capacity in popular antioxidant-rich US foods. *J. Food Composition Anal.* 24, 2043–1048. doi: 10.1016/j.jfca.2011.01.008

Fournier, A. (2013). The story of symbiosis with zooxanthellae, or how they enable their host to thrive in a nutrient poor environment. *Masters Biosci. Rev.*, 1–8.

Gastwirth, J. L., Gel, Y. R., and Miao, W. (2009). The impact of Levene's test of equality of variances on statistical theory and practice. *Stat. Sci.* 24 (3), 343–360. doi: 10.1214/09-STS301

Ghasemi, A., and Zahediasl, S. (2012). NorMality tests for statistical analysis: A guide for non-statisticians. *Int. J. Endocrinol. Metab.* 10 (2), 486–489. doi: 10.5812/ijem.3505

González, J. M., et al. (2003). Silicibacter pomeroyi sp. nov. and Roseovarius nubinhibens sp. nov., dimethylsulfoniopropionate-demethylating bacteria from marine environments. *Int. J. Syst. Evol. Microbiol.* 53 (5): 1261–1269. doi: 10.1099/ijs.0.02491-0

Hartman, L. M., van Oppen, M. J. H., and Blackall, L. L. (2020). Microbiota characterization of *Exaiptasia diaphana* from the Great Barrier Reef. *Anim. Microbiome* 2. doi: 10.1186/s42523-020-00029-5

Hughes, T. P., Barnes, M. L., Bellwood, D. R., Cinner, J. E., Cumming, G. S., Jackson, J. B. C., et al. (2017). Coral reefs in the anthropocene. *Nature* 546, 82–90. doi: 10.1038/nature22901

Jeong, H. J., Yoo, Y. D., Kang, N. S., Lim, A. S., Seong, K. A., Lee, S. Y., et al. (2012). Heterotrophic feeding as a newly identified survival strategy of the dinoflagellate. *Symbiodinium Proc. Natl. Acad. Sci.* 109 (31), 12604–12609. doi: 10.1073/pnas.1204302109

Keene, O. N. (1995). The log transformation is special. *Stat. Med.* 14:811–819. doi: 10.1002/sim.4780140810

LaJeunesse, T. C., Parkinson, J. E., Gabrielson, P. W., Jeong, H. J., Reimer, J. D., Voolstra, C. R., et al. (2018). Systematic revision of symbiodiniaceae highlights the antiquity and diversity of coral endosymbionts. *Curr. Biol.* 28 (16), 2570–2580. doi: 10.1016/j.cub.2018.07.008

Lawson, C. A., Seymour, J. R., Possell, M., Suggett, D. J., and Raina, J. B. (2020). The volatilomes of symbiodiniaceae-associated bacteria are influenced by chemical derived from their algal partner. *Front. Mar. Sci.* 7. doi: 10.3389/fmars.2020.00106

Lesser, M. P., Stochaj, W. R., Tapley, D. W., and Shick, J. M. (1990). Bleaching in coral reef anthozoans: effects of irradiance, ultraviolet radiation, and temperature on the activities of protective enzymes against active oxygen. *Coral Reefs* 8, 225–232. doi: 10.1007/BF00265015

Lesser, M. P. (1997). Oxidative stress causes coral bleaching during exposure to elevated temperatures. *Coral Reefs* 16, 187–192. doi: 10.1007/s003380050073

Maire, J., Blackall, L. L., and van Oppen, M. J. H. (2021a). Intracellular bacterial symbionts in corals: challenges and future directions. *Microorganisms* 9 (11), 2209. doi: 10.3390/microorganisms9112209

Maire, J., Blackall, L. L., and van Oppen, M. J. H. (2021b). Microbiome characterization of defensive tissues in the model anemone *Exaiptasia diaphana*. *BMC Microbiol.* 21, 152. doi: 10.1186/s12866-021-02211-4

Maire, J., Girvan, S. K., Barkla, S. E., Perez-Gonzalez, A., Suggett, D. J., Blackall, L. L., et al. (2021c). Intracellular bacteria are common and taxonomically diverse in cultured and in *hospite* algal endosymbionts of coral reefs. *ISME J.* 15, 2028–2042. doi: 10.1038/s41396-021-00902-4

Maire, J., and van Oppen, M. J. H. (2021). A role for bacterial experimental evolution in coral bleaching mitigation? *Trends Microbiol.* 30 (3), 217–228. doi: 10.1016/j.tim.2021.07.006

Matthews, J. L., Raina, J. B., Kahlke, T., Seymour, J. R., van Oppen, M. J. H., and Suggett, D. J. (2020). Symbiodiniaceae-bacteria interactions: rethinking metabolite exchange in reef-building corals as multi-partner metabolic networks. *Environ. Microbiol.* 22, 1675. doi: 10.1111/1462-2920.14918

McMurdie, P. J., and Holmes, S. (2013). phyloseq:An R package for reproducible interactive analysis and graphics of microbiome cencus data. *PLoS One* 8 (4), e61217. doi: 10.1371/journal.pone.0061217

Mehler, A. H. (1951). Studies on reactions of illuminated chloroplasts. I. Mechanism of the reduction of oxygen and other hill reagents. *Arch. Biochem. Biophysics* 33 (1), 65–77. doi: 10.1016/0003-9861(51)90082-3

Miller, T., and Belas, R. (2004). Dimethylsulfoniopropionate metabolism by Pfiesteria- associated *Roseobacter* spp. *Appl. Environ. Microbiol.* 70 (6), 3383–3391. doi: 10.1128/AEM.70.6.3383-3391.2004

Motone, K., Takagi, T., Aburaya, S., Miura, N., Aoki, W., and Ueda, M. (2020). A zeaxanthin- producing bacterium isolated from the algal phycosphere protects coral endosymbionts from environmental stress. *mBio* 11, e01019–e01019. doi: 10.1128/mBio.01019-19

Munday, P. L. (2004). Habitat loss, resource specialization, and extinction on coral reefs. *Global Change Biol.* 10 (10), 1642–1647. doi: 10.1111/j.1365-2486.2004.00839.x

Peixoto, R. S., Sweet, M., Villela, H. D. M., Cardoso, P., Thomas, T., Voolstra, C. R., et al. (2021). Coral probiotics: premise, promise, prospects. *Annu. Rev. Anim. Biosci.* 9, 265–288. doi: 10.1146/annurev-animal-090120-115444

Pootakham, W., Mhuantong, W., Yoocha, T., Putchim, L., Jomchai, N., Sonthirod, C., et al. (2019). Heat-induced shift in coral microbiome reveals several members of the Rhodobacteraceae family as indicator species for thermal stress in Porites lutea. *MicrobiologyOpen* 8 (12), e935. doi: 10.1002/mbo3.935

Randle, J. L., Cárdenas, A., Gegner, H. M., Ziegler, M., and Voolstra, C. R. (2020). Salinity-conveyed thermotolerance in the coral model Aiptasia is accompanied by distinct changes of the bacterial microbiome. *Front. Mar. Sci.* 7. doi: 10.3389/fmars.2020.573635

Richter, M., Ruhle, W., and Wild, A. (1990). Studies on the mechanism of photosystem II photoinhibition II. The involvement of toxic oxygen species. *Photosynthesis Res.* 24, 237–243. doi: 10.1007/BF00032311

Ritchie, K. B. (2012). "Bacterial symbionts of corals and *Symbiodinium*," in *Beneficial Microorganisms in Multicellular Life Forms*. Eds. E. Rosenberg and U. Gophna (Berlin, Heidelberg: Springer), 136–150.

Rosado, P. M., Leite, D. C. A., Duarte, G. A. S., Chaloub, R. M., Jospin, G., Nunes da Rocha, U., et al. (2019). Marine probiotics: increasing coral resistance to bleaching through microbiome manipulation. *ISME J.* 13 (4), 921–936. doi: 10.1038/s41396-018-0323-6

Santoro, E. P., Borges, R. M., Espinoza, J. L., Freire, M., Messias, C. S. M. A., Villela, H. D. M., et al. (2021). Coral microbiome manipulation elicits metabolic and genetic

restructuring to mitigate heat stress and evade mortality. *Sci. Adv.* 7 (33), eabg3088. doi: 10.1126/sciadv.abg308

Suggett, D. J., and Smith, D. J. (2019). Coral bleaching patterns are the outcome of complex biological and environmental networking. *Global Change Biol.* 26 (1), 68–79. doi: 10.1111/gcb.14871

Sunda, W., Kieber, D. J., Kiene, R. P., and Huntsman, S. (2002). An antioxidant function for DMSP and DMS in marine algae. *Nature* 418, 317–320. doi: 10.1038/nature00851

Szabó, M., Larkum, A. W. D., and Vass, I. (2020). "A review: the role of reactive oxygen species in mass coral bleaching," in *Photosynthesis in Algae: Biochemical and Physiological Mechanisms*, vol. 45 . Eds. A. Larkum, A. Grossman and J. Raven (Cham: Springer).

Tortorelli, G., Belderok, R., Davy, S. K., McFadden, G. I., and van Oppen, M. J. H. (2020). Host genotypic effect on algal symbiosis establishment in the coral model, the anemone *Exaiptasia diaphana*, from the great barrier reef. *Front. Mar. Sci.* 6. doi: 10.3389/fmars.2019.00833

van Oppen, M. J. H., and Blackall, L. L. (2019). Coral microbiome dynamics, functions and design in a changing world. *Nat. Rev. Microbiol.* 17, 557–567. doi: 10.1038/s41579-019-0223-4

van Oppen, M. J. H., Oliver, J. K., Putnam, H. M., and Gates, R. D. (2015). Building coral reef resilience through assisted evolution. *Proc. Natl. Acad. Sci.* 112 (8):2307–2313. doi: 10.1073/pnas.1422301112

Volkmer, B., and Heinemann, M. (2011). Condition-dependent cell volume and concentration of *Escherichia coli* to facilitate data conversion for systems biology modeling. *PLoS One* 6 (7):e23126. doi: 10.1371/journal.pone.0023126

Weis, V. M. (2008). Cellular mechanisms of Cnidarian bleaching: stress causes the collapse of symbiosis. *J. Exp. Biol.* 211, 3059–3066. doi: 10.1242/jeb.009597

Wilson, K., Li, Y., Whan, V., Lehnert, S., Byrne, K., Moore, S., et al. (2002). Genetic mapping of the black tiger shrimp *Penaeus monodon* with amplified fragment length polymorphism. *Aquaculture* 204, 297–309. doi: 10.1016/S0044-8486(01)00842-0

Xiang, T., Hambleton, E. A., DeNofrio, J. C., Pringle, J. R., and Grossman, A. R. (2013). Isolation of clonal axenic strains of the symbiotic dinoflagellate *Symbiodinium* and their growth and host specificity. *J. Phycol* 49 (3), 447–458. doi: 10.1111/jpy.12055

Yellowlees, D., Rees, T. A. V., and Leggat, W. (2008). Metabolic interactions between algal symbionts and invertebrate hosts. *Plant Cell Environ.* 31, 679–694. doi: 10.1111/j.1365-3040.2008.01802.x

Yoch, D. C. (2002). Dimethylsulfoniopropionate: its sources, role in the marine food web, and biological degradation to dimethylsulfide. *Appl. Environ. Microbiol.* 68, 5804–5815. doi: 10.1128/AEM.68.12.5804-5815.2002

Zhang, Y., Yang, Q., Ling, J., Long, L., Huang, H., Yin, J., et al. (2021). Shifting the microbiome of a coral holobiont and improving host physiology by inoculation with a potentially beneficial bacterial consortium. *BMC Microbiol.* 21, 130. doi: 10.1186/s12866-021-02167-5

frontiers | Frontiers in Ecology and Evolution

TYPE Original Research
PUBLISHED 20 October 2023
DOI 10.3389/fevo.2023.1194485

OPEN ACCESS

EDITED BY
Michael P. Doane,
Flinders University, Australia

REVIEWED BY
Thamasak Yeemin,
Ramkhamhaeng University, Thailand
Jesse Zaneveld,
University of Washington Bothell,
United States

*CORRESPONDENCE
Tess Moriarty
tess.moriarty@uon.edu.au

RECEIVED 27 March 2023
ACCEPTED 11 September 2023
PUBLISHED 20 October 2023

CITATION
Moriarty T, Ainsworth TD and Leggat W (2023) Identification of coral disease within the high-latitude reef, Lord Howe Island Marine Park.
Front. Ecol. Evol. 11:1194485.
doi: 10.3389/fevo.2023.1194485

Identification of coral disease within the high-latitude reef, Lord Howe Island Marine Park

Tess Moriarty[1]*, Tracy D. Ainsworth[2] and William Leggat[1]

[1]School of Environmental and Life Sciences, The University of Newcastle, Ourimbah, NSW, Australia, [2]School of Biological, Earth and Environmental Science, The University of New South Wales, Randwick, NSW, Australia

Coral disease prevalence has significantly increased under a changing climate, impacting coral community structure and functionality. The impacts and ecology of coral diseases are unclear in most high-latitude reefs (coral reefs above 28° north and below 28° south). High-latitude locations are vulnerable to climate change; therefore, identifying diseases and developing region-specific baselines are important for local management. We report the first coral disease findings at the UNESCO World Heritage listed Lord Howe Island Marine Park (31.5°S, 159°E), the southernmost coral reef system. This study assessed coral disease prevalence during November 2018, March 2019 and October 2019. Surveys from three lagoonal reefs identified four coral diseases: white syndrome, skeletal eroding band, growth anomalies and endolithic hypermycosis impacting six coral taxa (*Acropora, Isopora*, *Montipora, Pocillopora, Porites* and *Seriatopora*). Overall, disease prevalence was 5 ± 1% and significantly differed between time and site. Disease prevalence was highest in November 2018 (10 ± 1%) and significantly lower during March 2019 (5 ± 1%), coinciding with a bleaching event. White syndrome was the most prevalent disease (4 ± 1%) with 83 colonies of six taxa affected, predominately *Isopora*. Acroporids recorded the highest disease susceptibility, with three of the four diseases observed. Documenting baseline coral disease prevalence and monitoring throughout a bleaching event assists our understanding of disease ecology dynamics under current climate change impacts at high-latitude reefs.

KEYWORDS

coral disease, world heritage listed, high-latitude reef, coral bleaching, subtropical, Lord Howe Island

1 Introduction

The Anthropocene is characterised by a global degradation of coral reefs (Pratchett et al., 2014; Hughes et al., 2018). The widespread degradation of coral reefs is due to local-scale stressors such as water pollution, habitat degradation, invasive species domination and overfishing (Wilkinson, 2000; Carpenter et al., 2008) and global scale stressors resulting from climate change (Hoegh-Guldberg et al., 2007). Rising ocean temperatures

have led to a notable surge in both coral bleaching incidents (Sheppard, 2003; Hughes et al., 2017a; Hughes et al., 2017b; Frölicher and Laufkötter, 2018; Lough et al., 2018; Sully et al., 2019), and coral disease prevalence on coral reefs (Bruno et al., 2007; Harvell et al., 2007; Ruiz-Moreno et al., 2012; Maynard et al., 2015).

Coral disease outbreaks are projected to escalate on a global scale due to mounting local and global pressures. These pressures are expected to enhance pathogen virulence, expand the pathogen's range, and prolong its survival (Maynard et al., 2015). Moreover, these stressors contribute to heightened coral susceptibility to diseases, reduced immune function, and the emergence of previously unseen and opportunistic pathogens within the coral reef environment. Coral diseases are becoming increasingly widespread due to various non-biological stressors, such as elevated water temperatures (Aeby et al., 2020), sunlight light intensity (Muller and van Woesik, 2009), pollution (Redding et al., 2013; Page et al., 2023), sedimentation (Gintert et al., 2019), degraded water quality (Thompson et al., 2014; Yoshioka et al., 2016), plastic pollution (Lamb et al., 2018), in-water recreational activities (Lamb et al., 2014; Hein et al., 2015), proliferation of algae and their spatial distribution (Nugues et al., 2004; Smith et al., 2006; Sweet et al., 2013; Casey et al., 2014), and eutrophication (Bruno et al., 2003; Vega Thurber et al., 2014). These disease outbreaks and occurrences pose a significant threat to coral reefs, as they lead to a decline in coral fitness recorded as: reduced growth (Meesters et al., 1994; Nugues, 2002; Stimson, 2011), decreased fecundity (Weil et al., 2009; Stimson, 2011; Palmer and Baird, 2018), and increased mortality (Miller et al., 2009; Precht et al., 2016), consequently disrupting ecosystem function (Nugues, 2002; Haapkylä et al., 2013). Coral diseases have now gained recognition as one of the most critical environmental issues affecting the Indo-Pacific region, demanding urgent conservation attention (Sutherland et al., 2015). The preservation of coral reefs is of paramount importance to safeguard marine biodiversity and ecosystem health.

Coral disease was first recorded in the Caribbean in the 1970s (Antonius, 1976). New coral diseases have since been identified (Richardson, 1998; Rosenberg and Loya, 2013) with coral diseases recorded beyond the Caribbean and across all major coral reef ecosystems, including reefs of the Indo-Pacific (Willis et al., 2004; Myers and Raymundo, 2009; Page and Stoddart, 2010; Montano et al., 2012; Schleyer et al., 2018; Subhan et al., 2020). On the Great Barrier Reef (GBR), coral disease prevalence has been routinely monitored through the Long-Term Monitoring Program (LTMP) (Willis et al., 2004), with at least nine coral diseases identified, including the first description of "white syndrome" a term used to describe unidentified coral diseases showing signs of rapid tissue loss resulting in white regions of exposed coral skeleton. Other diseases include atramentous necrosis, black band disease, brown band disease, growth anomalies, pink spot, skeletal eroding band, ulcerative white spot syndrome, white syndrome, and white blotch disease (Jones et al., 2004; Willis et al., 2004; Bourne, 2005; Haapkylä et al., 2010). As such, studies on coral disease have expanded 50 years, but overall, coral diseases have remained poorly understood, with ambiguity in both disease identification and diagnostics (Richardson, 1998; Work and Aeby, 2006; Work et al., 2008c; Moriarty et al., 2020). Similarly, while coral disease records have become more common throughout tropical reef ecosystems, and recordings of coral diseases from subtropical high-latitude reefs (*coral reefs located below 28° south and above 28° north.*) (Dalton and Smith, 2006; Dalton et al., 2010; Schleyer et al., 2018), coral disease monitoring efforts have been patchy through time and space across Australia's high-latitude coral reefs.

The absence of comprehensive historical long-term data on disease identification, ecology and prevalence in high-latitude areas has made it difficult for researchers to interpret baseline surveys accurately representing disease prevalence in the area or potential outbreak numbers across high-latitude coral reefs. The reefs of Florida, USA are commonly referred to as high-latitude coral reefs and are where coral disease monitoring efforts have continued for over four decades (Richardson, 1998; Rosenberg and Loya, 2013). In 2014 a new disease, Stony Coral Tissue Loss Disease (SCTLD), was reported on the reefs of Florida (Precht et al., 2016), with the prevalence of the disease as high as 61%, causing significant mortalities to boulder coral morphologies reducing coral population densities to < 3% (Precht et al., 2016). STLD has spread across reefs in the region and is now prolific in the wider Caribbean (Alvarez-Filip et al., 2019; Weil et al., 2019). In comparison, other high-latitude reefs have had fewer extensive coral disease studies and report substantially less disease prevalence, for example, South Africa's Sodwana Bay 1.9–5.7% (Schleyer et al., 2018), the Northwestern Hawaiian Islands 0–7.09% (Aeby, 2006) and Eastern Australia's Solitary Islands 6.21–13.58% (Dalton and Smith, 2006). In 2003, the subtropical Solitary Islands experienced a concerning surge in the prevalence of a unique white syndrome, which had a significant impact on six common taxa of coral: *Pocillopora*, *Stylophora*, *Turbinaria*, *Acropora*, *Goniastrea* and *Porites* (Dalton and Smith, 2006; Dalton et al., 2010). The disease led to coral mortality, affecting approximately 27% of the colonies that were afflicted (Dalton and Smith, 2006). LHI's neighbouring high-latitude island, Norfolk Island is about 570 km north east of LHI, with similar coral taxa (Moriarty pers. obs.). In 2020, a serious outbreak of a white syndrome coral disease was triggered by heat stress and pollution events affecting the reef-building taxa *Montipora* spp. in the Norfolk Island lagoon (Page et al., 2023). During the outbreak, around 60% of the *Montipora* community had been impacted, and the disease severity increased by 54% during this period (Page et al., 2023). The spatial distribution of the disease suggested a strong association with exposure to poor water quality and the size class of coral colonies (Page et al., 2023). This highlights the vulnerability of coral reef ecosystem to the combined impacts of warming and pollution.

High-latitude reefs experience both lower water temperatures and light in comparison to their tropical coral reef counterparts. High-latitude coral reef ecosystems are widely reported as high-value ecosystems, and potentially protected from the most extreme impacts of climate change due to the reef's geographic location at the fringes of coral reef growth. These high-latitude coral reefs have been hypothesised as sites of refuge (Riegl, 2003), potentially providing resilience from warming ocean temperatures (Pandolfi et al., 2011). High-latitude reefs in Australia and Japan have also already experienced the expansion of tropical corals moving

poleward, suggesting these marginal reef locations are at risk of both loss of endemics and habitat expansion of tropical species (Yamano et al., 2011; Baird et al., 2012). In essence, high-latitude coral reefs are now recognised as at risk from local and global stressors, species invasions, and associated impacts to the coral populations, such as the emergence of coral disease. Here we surveyed the World Heritage Listed coral reef lagoon of Lord Howe Island (LHI) Marine Park from November 2018 to October 2019 to identify the occurrence and prevalence of coral disease at the world's southernmost coral reef system. We also report a disease outbreak and disease occurrence during a coral bleaching event, and in doing so, aim to provide a comprehensive description of coral disease ecology as a baseline for ongoing coral disease monitoring within the LHI Marine Park.

2 Methods

2.1 Study site

This study was undertaken under the Department of Primary Industries LHI Marine Park Research permit number: LHIMP/R/18015/12112018. The lagoonal coral reef of Lord Howe Island (31.5°S, 159°E, Figures 1A, B) was surveyed for benthic composition and disease prevalence in November 2018, March 2019, and October 2019, at three sites Coral Gardens, Erscotts and North Bay (Figure 1B). Lord Howe Island experiences tropical cyclones and thermal anomaly events (Steinberg et al., 2022; Moriarty et al., 2023). There have been four recorded mass bleaching events recorded since 1998, resulting in mass mortality and coral genera compositional changes (Harrison et al., 2011; Dalton et al., 2020; Steinberg et al., 2022). Environmental conditions vary across the reef sites, with Erscotts experiencing high wave action and tidal influence, which is also evident at Coral Gardens, whilst North Bay is a protected and sheltered bay (Figure 1B). The three sites are also situated in three different protection zones within the marine protected area (MPA), North Bay inside the fully protected sanctuary zone (SZ), Erscotts is located in the LHI lagoon SZ and Coral Gardens is situated inside of the habitat protection zone HPZ.

2.2 Belt transects

Transect tape was laid haphazardly parallel to shore at one depth interval of 0–5 m. Three 1 m × 20 m belt transects were conducted at each of the three sites, North Bay, Erscotts and Coral Gardens. Every hard coral colony within the three 1 m × 20 m belt transects were classified as categorical conditions as healthy or unhealthy based on typical disease signs. Unhealthy colonies were further assessed for the seven varying compromised health categories: diseased, bleached, injured, predation, dead, partially dead, and competition (Figure 2). The diseased coral colonies were further classified by disease and the characteristics

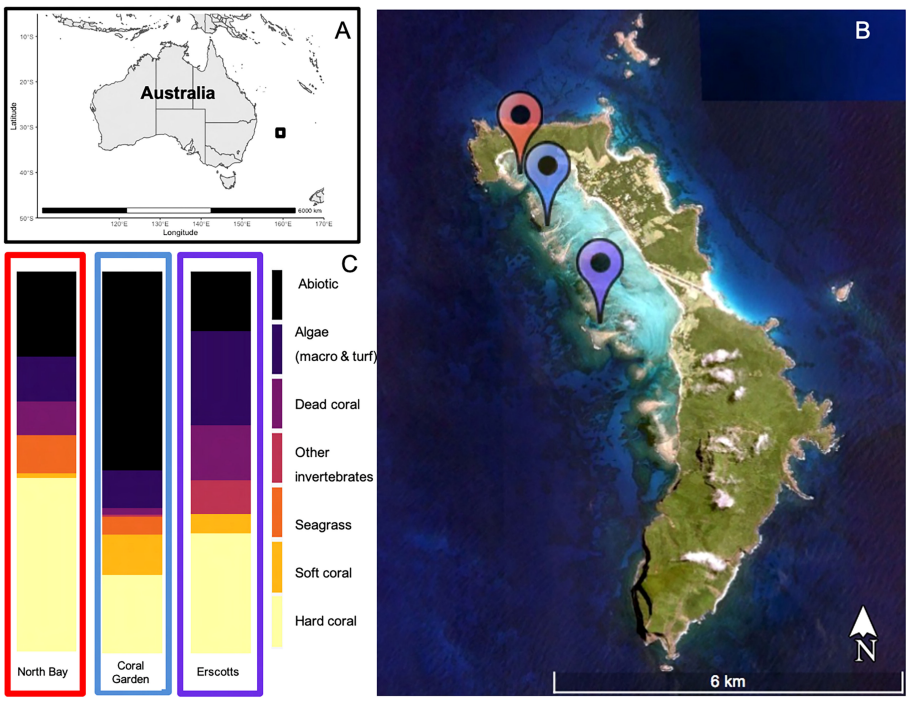

FIGURE 1
Lord Howe Island (black square) located ~600 km off the east coast of mainland Australia **(A)**. The three study sites were located in the LHI lagoon, North Bay (Red), Coral Gardens (Blue) and Erscotts Reef (Purple) **(B)** and their respective benthic compositions during November 2018 **(C)**.

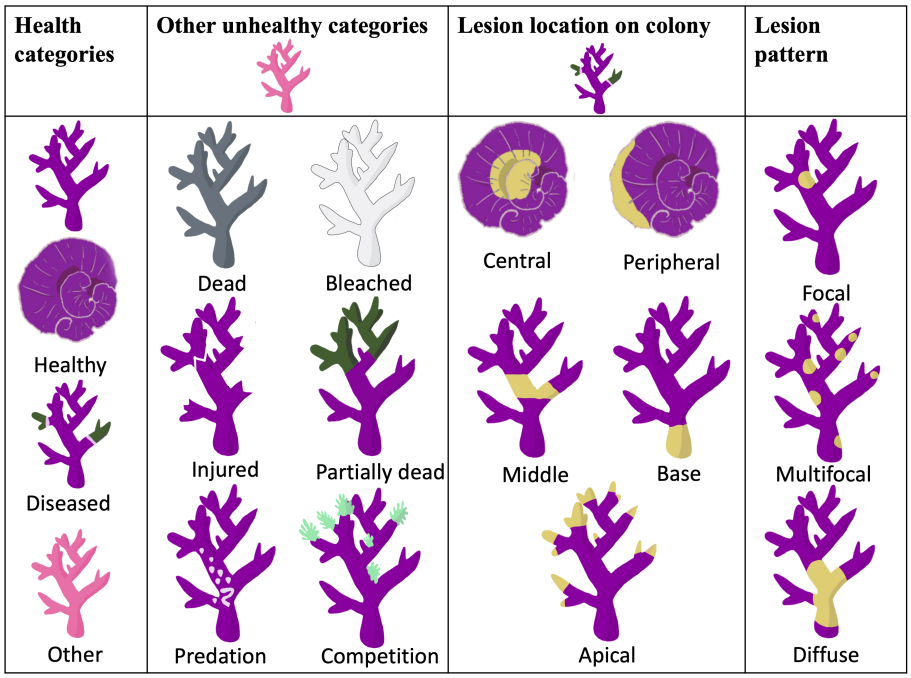

FIGURE 2
Health categories were assigned to the coral colonies surveyed within the belt transects at three distinct sites (see Figure 1). The classification of lesions on diseased corals was based on both the lesion's location on the colony and the specific pattern it exhibited. These criteria for lesion location and pattern have been adapted from the research conducted by Work and Aeby in 2006.

of the disease recorded, including the percentage of the coral colony affected, the location of the unhealthy section on the colony, shape of lesion, structure affected, lesion description (for example, discolouration, tissue loss, growth) (Figure 2). The coral colonies were identified to species level where possible along with their respective growth form (branching, sub-massive, encrusting, massive, tabular, staghorn and digitate). Coral diseases were identified using visual classification and samples taken for further disease examination later. Visual disease identification was made using distinguishing features as seen in Moriarty et al. (2020).

2.3 Benthic composition

Images were collected from the tape measure laid out for the belt transects using a Nikon COOLPIX W300 underwater camera. Three 1 m^2 photo quadrats were taken along each of the three transects per site at 4–5 m, 12–13 m and 16–17 m. The images were cropped to exhibit only the benthos within the quadrat and then uploaded to the web-based annotation program CoralNet (coralnet.ucsd.edu). Photographs were overlaid with 64 fixed points, which were analysed to species and functional groups (Table 1). Total live coral cover was recorded to genera and when possible species level.

2.4 Statistical analysis

Disease prevalence and health categories were determined by calculating the proportion of damaged/visually unhealthy colonies compared to the total number of coral colonies:

$$\text{Prevalence}\,(\%) = \frac{n\ of\ diseased\ or\ compromised\ health\ colonies}{N\ of\ coral\ colonies\ in\ transect} \times 100$$

Prevalence was calculated for each: monitored month, site, taxa, and coral disease. All statistical analysis was carried out in R version 3.6.2. Benthic composition was calculated by counting the number of each of the benthic categories observed and dividing it by the number of total counts per transect and then averaging the 3 transects to get the site benthic composition. The benthic composition was compared between sites (Sylph's Hole, North Bay and Coral Garden) using a one-way ANOVA and normality tests performed. To investigate significant effects a Tukey's *post hoc* analysis was conducted within each site and each benthic composition group. Disease prevalence was assessed using generalized linear mixed effects models (GLMM) in R using the package "glmmTMB" v1.0.1 for 1) health categories within sites, between months, and between sites within months and 2) within health categories for coral taxa within sites between months and between sites within months. Site and month were fixed variables,

10.3389/fevo.2023.1194485

TABLE 1 Benthic categories used during benthic community structure analysis.

Benthic group	Species code	Species description
Stony coral	Acr_arb	*Acropora* arborescent
	Acr_bra	*Acropora* branching
	Acr_dig	*Acropora* digitate
	Arc_tab	*Acropora* tabular
	Cypha	*Cyphastrea*
	Homo	*Homophyllia*
	Isopora	*Isopora cuneata*
	Para_austr	*Paragoniastrea australis*
	PocDam	*Pocillopora damicornis*
	Porites	*Porites*
	Seriatop	*Seriatopora hystrix*
	StPis	*Stylophora pistillata*
Soft coral	Soft	Soft coral
Other	Ascidian	Ascidian
Dead stony coral	D_coral	Dead coral
Algae	DeadAlg	Recently dead coral with algae
	Macro	Macro algae
	CCA	Crustose coralline algae
Seagrass	Seagrass	Seagrass
Other invertebrates	Sponge	Sponge
Abiotic	Silt	Silt
	Rock	Rock
	Sand	Sand

and transect was used as a random effect. A Poisson and binomial distribution were used, and best fit applied. Residual plots were visually inspected for appropriate fit with regards to dependency structure and deviations from homoscedasticity or normality. p-Values were calculated by likelihood-ratio tests and were considered significant using a confidence interval of 95% (alpha level = $p \leq 0.05$).

3 Results

3.1 Benthic composition

A total of 27 photo quadrats were collected from each site of the three monitoring months. The overall average hard coral cover at LHI was 33 ± 6%, average abiotic 30 ± 6%, average algae 16 ± 4%, average dead hard coral 8 ± 4%, average soft coral 6 ± 3%, seagrass 5 ± 4%. North Bay, Erscotts and Coral Gardens were dominated by hard coral (46 ± 13%, 31 ± 8% and 52 ± 11% respectively, Figure 1C), abiotic benthos (22 ± 9%, 16 ± 8% and 52 ± 11% respectively, Figure 1C) and algae (12 ± 8%, 25 ± 8% and 10 ± 5% respectively, Figure 1C). Soft coral contributed 11 ± 10% at Coral Gardens and only 1 ± 1% and 5 ± 3% at North Bay and Erscotts, respectively. The benthic composition was not significantly different between the sites ($p > 0.05$, Figure 1C).

3.2 Coral assemblage

Porites spp., *Pocillopora damicornis*, *Stylophora pistillata*, *Seriatopora hystrix* and *Isopora cuneata* were the most abundant corals between all sites and monitored months (Figure 3). Coral assemblages within site and taxa did not change significantly over time ($p > 0.05$; Figure 3A). Overall, the least abundant coral taxa at all three sites were *Acropora* spp. In comparison, *P. damicornis* had the highest individual number of coral colonies relative abundance of all coral taxa at Coral Gardens and Erscotts. *Porites* spp. was the highest relative abundant taxa at North Bay (Figure 3A). *Acropora* had the least amount of individual coral colonies between sites and months ranging from 1 ± 0.2% SE to 7 ± 3% relative abundance in comparison to *P. damicornis*, which had the highest relative abundance (17 ± 5% to 48 ± 7%; Figure 3A). *Acropora* spp. colonies recorded were mostly arborescent, staghorn and tabular and the largest in size of any other coral taxa (Sups 1). Absolute abundance of coral taxa did not differ statistically between sites and monitored months and within sites between months ($p > 0.05$; Figure 3B). Erscotts observed the most live coral colonies between the three monitored months (225 to 313 colonies; Figure 3B). *Acropora* spp. contributed to 20 ± 7% of the hard coral cover at LHI and was the highest overall taxa between all three sites (Table 2). *P. damicornis* contributed the second overall highest coral cover with 5 ± 2%, contributing to the second-highest coral taxa cover at North Bay (8 ± 5%, Table 2). The coral *I. cuneata* contributed to the second-highest percent cover at Coral Gardens and Erscotts (6 ± 5% and 5 ± 2% respectively, Table 2).

3.3 Coral disease surveys

Over the three monitoring months (November 2018, March 2019 and October 2019), a total of 1,751 coral colonies were observed from 17 genera (Table 3). Of these, 442 (26%) of the coral colonies showed signs of compromised health consistent with disease or bleaching (endosymbiosis breakdown) (Table 4, Figure 4). Coral disease accounted for 21% of the colonies observed with compromised health, and "other" signs accounted for 6% observed unhealthy colonies (Table 4, Figures 4, 5). During March 2019, a mass coral bleaching event was recorded at LHI (Steinberg et al., 2022; Moriarty et al., 2023) and was still evident in October 2019 (Figure 4), during which time bleached corals were the most frequently observed (73%) (including mortality, partial mortality and 100% bleached colonies; Table 4; Figure 4). Coral disease was highest in November 2018 (10 ± 1%) and not as

10.3389/fevo.2023.1194485

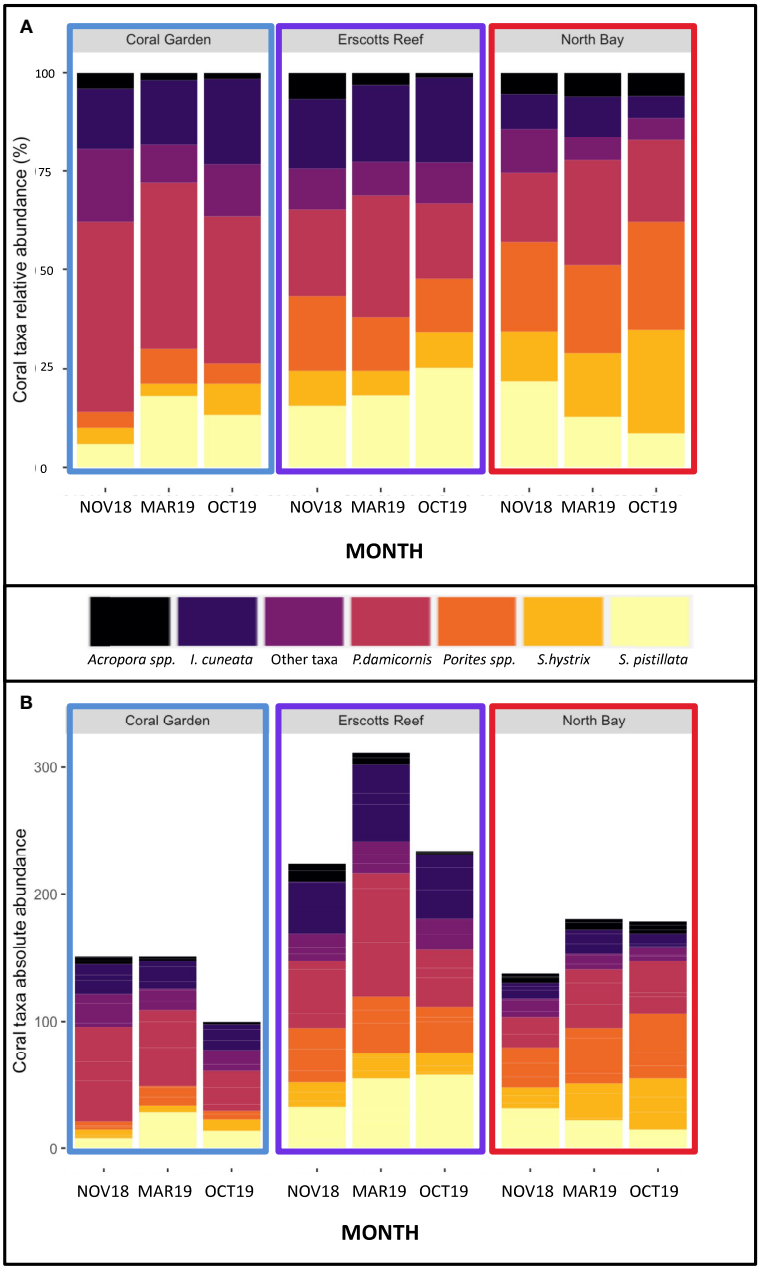

FIGURE 3
Coral taxa relative abundance **(A)** and absolute abundance **(B)** at Coral Garden (blue), Erscotts Reef (purple) and North Bay (Red) during November 2018 (NOV18), March 2019 (MAR19) and October 2019 (OCT19).

evident in March 2019 (5 ± 1%, GLM; $p = 0.0007$, Figure 4A, due to bleaching). Coral bleaching was not observed during the November 2018 surveys (GLM; $p = 0.0078$, Figure 4). Where disease was distinguishable from bleaching in March, Erscotts had the highest disease prevalence (9 ± 2%) compared to North Bay (3 ± 2%) and Coral Gardens (2 ± 1%), with Erscotts significantly higher than Coral Gardens (GLM; $p = 0.0084$; Figure 4B). No coral diseases were identified at Coral Gardens during October 2019 (Figure 4B). Erscotts highest coral disease prevalence was recorded during November (9 ± 2%) and March (9 ± 3%) before significant declines were recorded in disease prevalence in October (1 ± 1%; GLM; $p = 0.0067$ and GLM; $p = 0.0086$ respectively; Figure 4B). North Bay had significantly higher disease prevalence during November 2018 (10 ± 3%) than that recorded in March (3 ± 2%) and October (1 ± 1%; GLM; $p = 0.0023$; GLM; $p = 0.0049$ respectively; Figure 4B). At Coral Gardens, disease prevalence in November 2018 was 11 ± 3%, whereas coral disease was difficult to distinguish from bleached corals in March 2019 when prevalence was 2 ± 1% (GLM; $p = 0.0032$) and no disease was recorded in October 2019 (Figure 4B).

10.3389/fevo.2023.1194485

TABLE 2 Coral taxa percent cover at each of the three sites during November 2018.

Coral taxa	Coral Gardens		Erscott's		North Bay	
	Mean (%)	se	Mean (%)	se	Mean (%)	se
Acropora arborescent	0	0	0	0	31	15
Acropora branching	0	0	4	3	0	0
Acropora digitate	0	0	0	0	0	0
Acropora tabular	10	10	15	10	0	0
Acropora (total)	**10**	10	**19**	10	**31**	15
Cyphastrea	0	0	1	1	0	0
Goniopora	0	0	0	0	0	0
Isopora cuneata	**6**	5	**5**	2	1	1
Paragoniastrea australensis	0	0	0	0	0	0
Pocillopora damicornis	**5**	2	1	1	**8**	5
Porites	0	0	**3**	1	**2**	1
Seriatopora hystrix	0	0	0	0	1	0
Stylophora pistilatta	0	0	2	1	2	2

Data is from the photoquadrats and represent the average (mean) proportion of hard coral cover (%) with the three most common per site highlighted in bold.

TABLE 3 Abundance of white syndrome (WS), growth anomalies (GA) and skeletal eroding band (SEB) coral disease for each taxa.

Family	Taxa	n	WS	GA	SEB	Predation
Acroporidae	*Acropora*	64	7	2	6	5
	Isopora	261	53	2	0	12
	Montipora	10	1	0	0	0
Agariciidae	*Pavona*	6	0	0	0	0
Lobophylliidae	*Acanthastrea*	4	0	0	0	0
	Echinophyllia	1	0	0	0	0
	Homophyllia	15	0	0	0	0
Merulinidae	*Astrea*	21	0	0	0	0
	Cyphastrea	27	0	0	0	0
	Favites	10	0	0	0	0
	Paragoniastrea	17	0	0	0	0
	Platygyra	49	0	0	0	0
Pocilloporidae	*Pocillopora*	506	17	0	0	0
	Seriatopora	186	4	0	0	2
	Stylophora	276	0	0	0	0
Poritidae	*Goniopora*	8	0	0	0	0
	Porites	290	1	0	0	0
	Total	1751	83	4	4	19

10.3389/fevo.2023.1194485

TABLE 4 Total abundance and prevalence of observed compromised health in corals at LHI lagoon.

Condition	n	Total prevalence (%)	Compromised health prevalence (%)
Bleached	135	8	31
Disease	93	5	21
Recent whole colony mortality	83	5	19
Partial mortality	103	6	23
Predation	17	1	4
Competition	6	0.5	1
Injured	5	0.5	1
Total	442	26%	100%

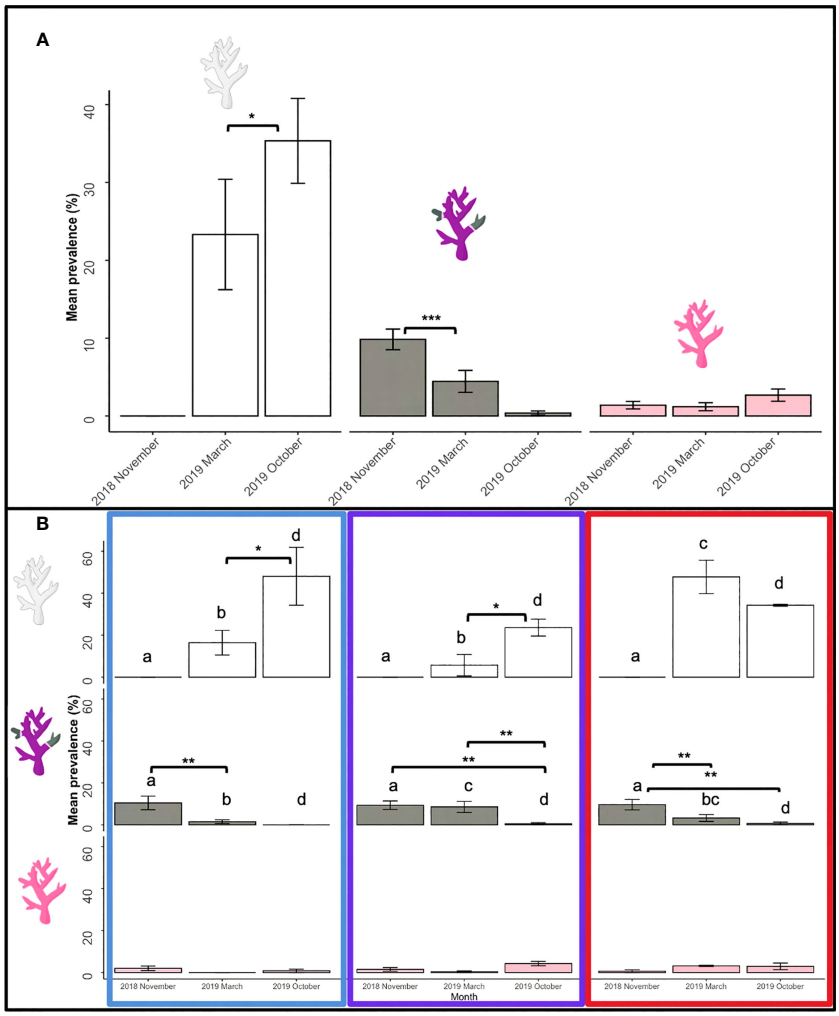

FIGURE 4
Unhealthy coral prevalence at LHI of bleached (white), diseased (grey) and other (pink) during November 2018, March 2019 and October 2019 **(A)**. Prevalence of coral bleaching (white), disease (grey) and other abnormalities (pink) between Coral Gardens (blue), Erscotts Reef (purple) and North Bay (red) **(B)**. Significant differences were determined using GLM analysis ($p < 0.05$). Asterisks indicate significant levels; * 0.05, ** 0.01, and *** 0.001.

3.4 Coral health conditions

Three distinct coral health conditions were identified in the LHI lagoon at Coral Gardens, North Bay and Erscotts and one off transect:

(1) white syndrome (WS) (Figures 6A–F),
(2) skeletal eroding band (SEB) (Figure 6G),
(3) growth anomalies (GA) (Table 3, Figures 6I–L) and
(4) endolithic hypermycosis (EH) (Figure 6H, off transect).

The overall coral disease prevalence for LHI lagoon was 5 ± 1%, and a total of 93 colonies were found with disease conditions (WS, SEB or GA) on all six coral genera, *Acropora, Isopora, Montipora, Pocillopora, Porites* and *Seriatopora* (Table 3, Figure 6) (three hard coral families, Acroporidae, Pocilloporidae, and Poritidae). The Acroporidae family accounted for 76% of the diseased colonies compared to Pocilloporidae and Poritidae, which only accounted for 23% and 1%, respectively (Table 3). Six coral species were found with coral disease, *Acropora* spp., *Isopora cuneata*, *Montipora* spp., *Pocillopora damicornis*, *Porites* spp. and *Seriatopora hystrix* (Table 3, Figure 7). *I. cuneata* was found to have the highest abundance of disease, 55 colonies impacted by white syndrome. In contrast, 21% of affected colonies were *Acropora* spp. (Table 3, Figure 7). In October 2019, only one *I. cuneata* colony was observed with a growth anomaly, found at Erscotts, one *Acropora* spp. colony with SEB and one *S. hystrix* colony with white syndrome (Table 3, Figure 6). White syndrome was recorded in all of the six taxa impacted by disease and was most prevalent in *Acropora* spp. (12 ± 6%) and *I. cuneata* (17 ± 5%; Table 3, Figure 7A). Growth anomalies were present only in *Acropora* spp. and *I. cuneata* colonies, and skeletal eroding band was only observed in *Acropora* spp. (Table 3, Figure 7A). White syndromes had the highest overall prevalence of 4 ± 1%, while growth anomalies and skeletal eroding band had similar prevalence's overall (0.3 ± 0.1% and 0.4 ± 0.3% respectively) (Figure 8). White syndrome prevalence was highest at Erscotts (6 ± 2%) in comparison to Coral Gardens (4 ± 2%) and North Bay (3 ± 1%) however, no significant differences were found between sites and month for any of the three observed diseases ($p > 0.05$). White

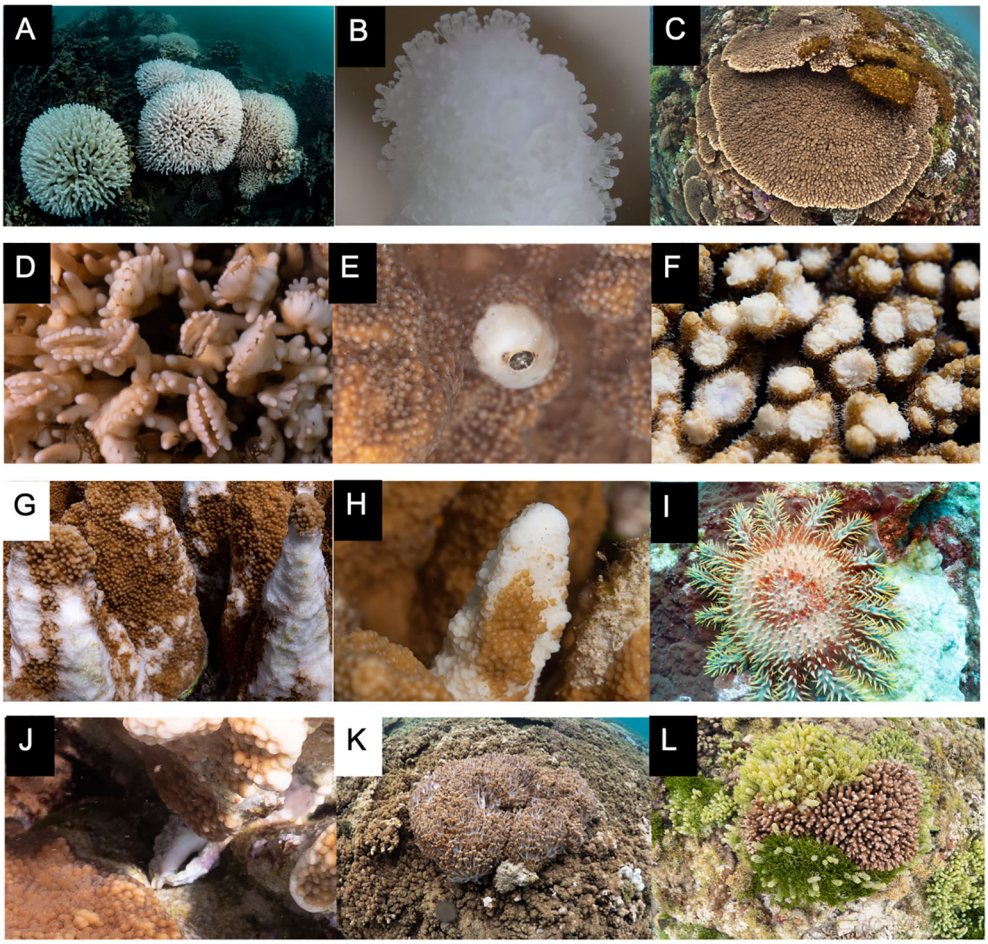

FIGURE 5
Other coral ailments found at LHI. **(A, B)** Coral bleaching of *P. damicornis* and *S. pistillata*, **(C)** algae cover in a tabular *Acropora* colony, **(D)** galls in *S. hystrix* from gall crabs, **(E)** invertebrate burrow in *I cuneata*, **(F)** predation of a tabular *Acropora* colony, **(G)** fish predation on *I cuneata*, **(H)** invertebrate predation on *I cuneata*, **(I)** COTS predation on *Turbinaria* colony, **(J)** Drupella predation, **(K)** soft coral competion on tabular *Acropora* colony, and **(L)** macro algae competition on a *P. damicornis* colony.

syndrome was recorded at all three monitored months compared to Coral Gardens and Erscotts, where no white syndrome was recorded within the belt transects during October 2019 (Figure 8). Growth anomalies were also found at all three sites with a similar overall prevalence between Coral Gardens, Erscotts and North Bay (0.3 ± 0.3%, 0.3 ± 0.2% and 0.3 ± 0.3% respectively; Figure 8). Skeletal eroding band was only observed in transects at North Bay (1 ± 1%) and was found at all three monitoring months (3 ± 2%, 0.5 ± 0.5% and 0.5 ± 0.5%; Figure 8). Endolithic hypermycosis was recorded off transect in the LHI lagoon. Endolithic hypermycosis was reported in a recently bleached *Porites* spp. colony (Figure 5H).

3.5 Disease descriptions

Three of the four coral diseases (GA, SEB and WS) was recorded in *Acropora* spp. colonies. *I. cuneata* and *Porites* spp. recorded two of the four diseases (GA and WS and WS and EH, respectively). The remaining taxa only recorded one disease (Table 3). White syndrome was the most prevalent disease at LHI, impacting 83 colonies (Table 3, Figures 7, 8). White syndrome had the highest taxa range (n = 6; Table 3, Figure 7). Lesion sizes for white syndrome ranged from 1–90% of the colony (Table 5).

- WS was characterised as a disease displaying white symptoms with a progression of tissue loss exposing the underlying coral skeleton. Tissue loss impacted both the polyps and coenosarc of colonies impacted by white syndrome, and lesion location on the colony was observed over the entire colony with a diffuse pattern (Table 5, Figures 9A, B).
- GAs were all located in the central regions of the coral colony, and colonies had focal and multifocal growth anomalies (Table 5). No damage or partial mortality or tissue loss was observed for colonies impacted by growth anomalies (Figures 9C, D).
- SEB impacted the apical regions of medium to large *Acropora* spp. colonies and was multifocal (Table 5) and was distinguished from white syndrome because small *Halofolliculina corallasia* (Figure 5F) were observed on the exposed skeleton, a characteristic of SEB (Willis et al., 2004) (Figures 9E, F).
- EH impacted the apical regions on the *Porites* spp. colony and was distinguished from normal pigmentation because pigmentation was under the bleached tissue (Figures 9G, H).

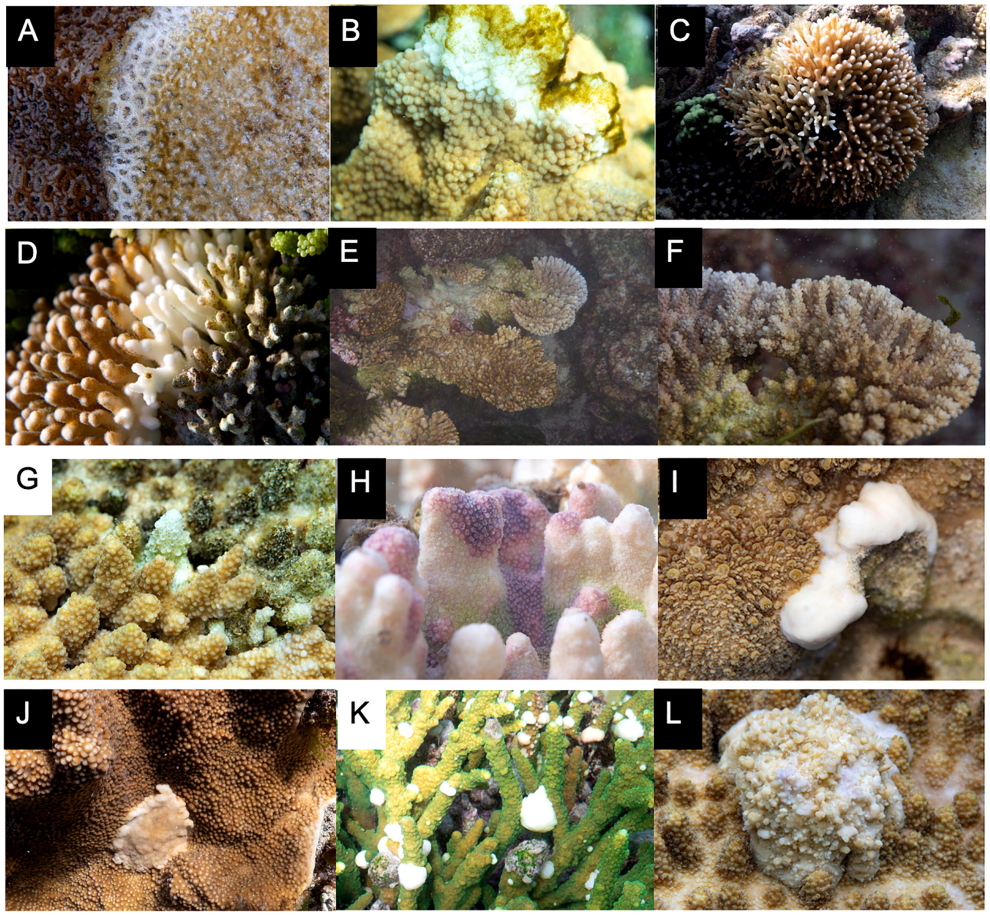

FIGURE 6
Coral diseases recorded within the LHI lagoon between November 2018 and October 2019. **(A–F)** White syndrome found in **(A)** Homophyllia, **(B)** *I cuneata*, and *S. pistillata*, **(C)** *S. hystrix*, **(D)** *P. damicornis*, **(E, F)** tabular *Acropora*, **(G)** skeletal eroding band in a tabular *Acropora*, **(H)** endolithic hypermycosis in *Porites*. **(I–L)** growth anomalies: **(I)** bosselated *Isopora* growth anomaly, **(J)** umbonate *Isopora* growth anomaly, **(K)** nodular *Acropora* growth anomaly and **(L)** exophytic *Acropora* growth anomaly.

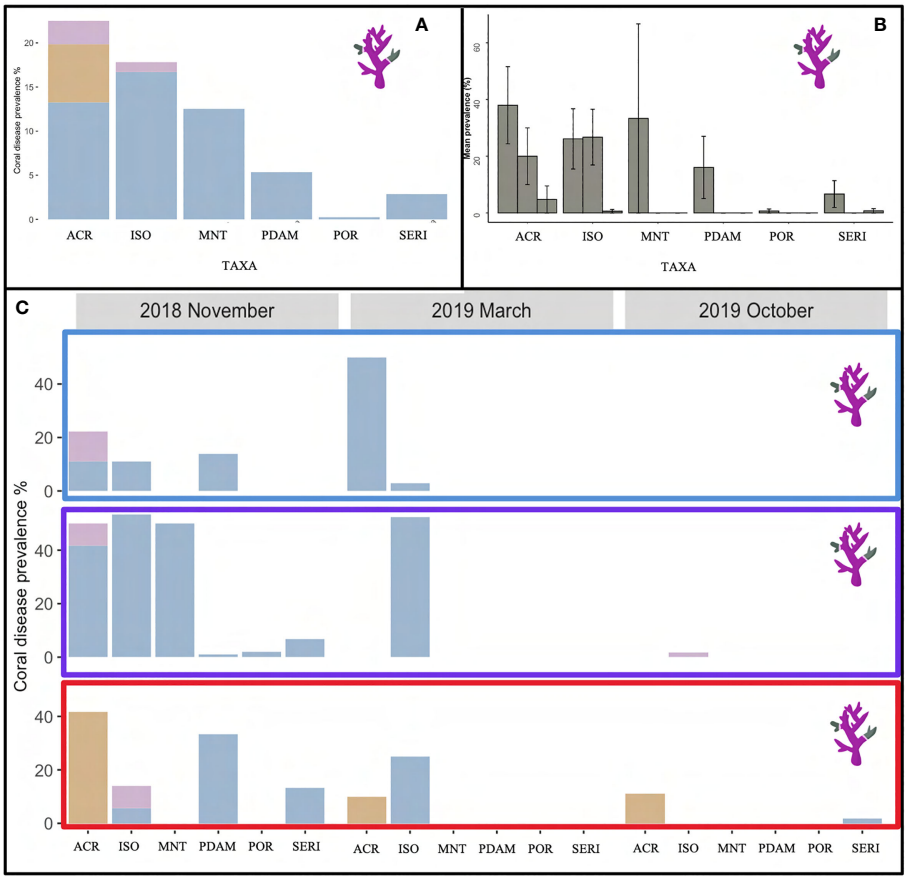

FIGURE 7
(A) Overall coral disease prevalence (%) found in the six impacted taxa, *Acropora* (ACR), *I cuneata* (ISO), *Montipora* (MNT), *P. damicornis* (PDAM), *Porites* (POR) and *S. hystrix* (Seri) within the LHI Marine Park lagoon for the three diseases found within the transects, growth anomalies (purple), skeletal eroding band (brown) and white syndrome (blue). **(B)** Coral disease prevalence in each of the six taxa during November 2018, March 2019 and October 2019 (respectively) and **(C)** between the three sites, Coral Gardens (blue rectangle), Erscotts Reef (purple rectangle) and North Bay (red rectangle) for growth anomalies (purple), skeletal eroding band (brown) and white syndrome (blue).

Both WS and SEB affected colonies were closely examined for corallivore snails, and crown-of-thorns starfish (COTS) as the predation lesions can appear similar to the WS and SEB disease lesions; however, none were found on or around surveyed colonies. There was a total of three *Drupella* found throughout the three monitored months in the LHI lagoon. COTS were observed at a close-by reef at depths greater than 16 m.

4 Discussion

Coral diseases contribute to global coral reef declines impacting the functionality and composition of reef systems (Bruno et al., 2007; Harvell et al., 2007; Thompson et al., 2014; Heres et al., 2021). Although coral disease studies and identification has been well established in the Caribbean reefs and the closer tropical reefs of the GBR, baseline studies at sites such as the UNESCO World Heritage-listed LHI Marine Park are lacking. Here we identify and describe four coral diseases, their prevalence and susceptible coral taxa within the lagoon of the LHI Marine Park. This study provides baseline coral disease data which is particularly important because of ongoing impacts resulting from climate change which has already caused detrimental impacts to the coral reef communities of LHI. Considering this reef holds high ecological importance, a resource such as this for managers would assist in identifying potential threats to the reef in the face of climate change. LHI Marine Park is the southernmost coral reef in the world, located approximately 600 km east of mainland Australia and over 1,000 km south of the GBR. The LHI Marine Park is regularly utilised for recreational fishing, SCUBA diving, snorkelling, surfing and commercial tourism (e.g., glass bottom boat tours, fishing and sightseeing), and the lagoon is subject to groundwater influxes, freshwater and sediment runoff. Two successive bleaching events were reported in 2010 and 2011 (Harrison et al., 2011; Dalton et al., 2020), with four individual coral bleaching events as a result of thermal stress between 1998 (Harrison et al., 2011; Dalton et al., 2020) and 2019 (Steinberg et al., 2022; Moriarty et al., 2023). Predation by the corallivore crown-of-thorns starfish has not been reported in the LHI lagoon, but these species have been commonly observed at depth around LHI (De Vantier and Deacon, 1990; Moriarty pers.

10.3389/fevo.2023.1194485

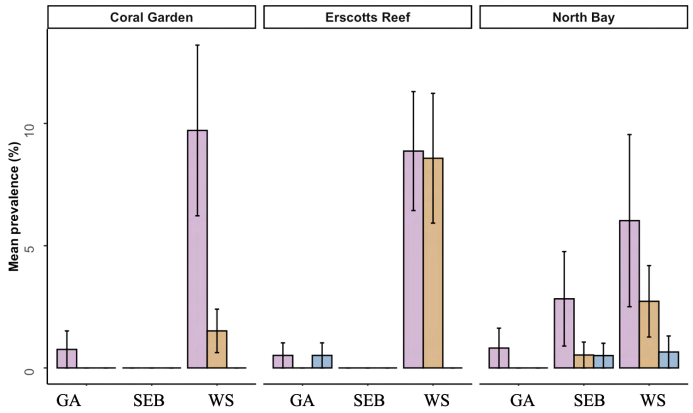

FIGURE 8
Mean prevalence of the three coral diseases recorded within the transects at the LHI lagoon, growth anomalies (GA), skeletal eroding band (SEB) and white syndrome (WS) at Coral Gardens, Erscotts Reef and North Bay in November 2018 (orange), March 2019 (maroon) and October 2019 (purple).

obs.). In 2008 an outbreak of the sea urchin *Tripneustes gratilla* was recorded at offshore locations around the island, impacting the densities of brown and red algae cover (Valentine and Edgar, 2010).

We surveyed three reefs within the LHI lagoon and found hard coral cover within the LHI lagoon contributes 33 ± 6% of the benthic composition (Coral Gardens, Erscotts and North Bay, Figure 1). The coral cover in the LHI lagoon is greater than other high-latitude reefs such as the Bahamas (28 ± 11%) (Weiler et al., 2019), South Africa (27%) (Schleyer et al., 2018), and lower than Japan's Tatsukushi reef on Shikoku Island (60%) (Denis et al., 2013) and Western Australia's Houtman Abrolhos Islands (> 70%) (Bridge et al., 2014). Algae cover is similar to the islands of Hawaii (Vroom and Braun, 2010) and the subtropical Solitary Islands (Dalton and Roff, 2013). Similar benthic compositions were recorded at LHI for hard coral, algae and soft coral in 1992–1993 (Harriott, 1999). In 1999 North Bay experienced high abundances of cyanobacteria and dead coral following the 1998 bleaching event (Harriott, 1999). However, our study found that hard coral cover was highest amongst the three sites at North Bay (46 ± 13%; Figure 1C), suggesting an increase in coral cover since 1999. The LHI reefs within the lagoon are dominated by colonies of *Porites* spp., *P. damicornis, S. pistillata, S. hystrix* and *I. cuneata* at all sites and between all monitored months (Figure 3A). *P. damicornis* being the most common species at Coral Gardens and Erscotts (17 ± 5%–48 ± 7%) with *Porites* spp. dominating the coral colony composition at North Bay (24 ± 3%) and apart from the individual taxa from the grouped "other taxa", *Acropora* spp. is the least common taxa in terms of colony abundance (1 ± 0.2%–7 ± 3%; Figure 3A). However, the large *Acropora* spp. colonies contribute a significant amount to the coral percent cover within the LHI lagoon (Table 2), contributing few but large colonies contributing to the reef composition. *Acropora* spp. is known to be susceptible to perturbations and, in particular, disease globally (Patterson et al., 2002; Williams and Miller, 2005; Ainsworth et al., 2007; Work et al., 2008a; Aeby et al., 2011; Irikawa et al., 2011; Roff et al., 2011; Wilson et al., 2012; Brodnicke et al., 2019).

Disease prevalence at LHI was found to be low during the survey period (5 ± 1%; Figure 4) and similar to disease prevalence previously reported on the southern GBR at Heron Island (August 2008; 4.22 ± 1.72%) (Haapkylä et al., 2010) and the subtropical Solitary Islands (Dalton and Smith, 2006). LHI's overall disease prevalence was also similar to the remote high-latitude Northwestern Hawaiian Islands, where overall prevalence ranged from 0.5% to 7.09% (Aeby, 2006). Three of the four diseases identified in LHI lagoon, white syndrome (WS), growth anomalies (GA) and skeletal eroding band (SEB), have previously been identified and described from Australia's Great Barrier Reef (Willis et al., 2004) with the exception of endolithic hypermycosis (EH). We found coral disease in six scleractinian coral genera over the 12-month period, with all three diseases present in *Acropora* spp.

4.1 Coral diseases at LHI

The four coral diseases recorded at LHI over the 12-month period is fewer in comparison to other Indo-Pacific reef systems. In

TABLE 5 Location and patterns of coral disease lesions of white syndrome, SEB and growth anomalies.

		Lesion location on colony					Lesion pattern		
Disease	n	Central	Peripheral	Apical	Middle	Base	Focal	Multifocal	Diffuse
White syndrome	83	14	13	16	37	8	0	0	83
SEB	6	0	0	6	0	0	0	6	0
Growth anomaly	4	4	0	0	0	0	2	2	0

comparison, six diseases have been recorded at Heron Island, GBR (Haapkylä et al., 2010), five at Mansuar Island, Raja Ampat Indonesia (Subhan et al., 2020), five at Wakatobi, southeast Sulawesi, Indonesia (Haapkylä et al., 2007), four at Koh Tao, Thailand (Lamb et al., 2014), five (possibly six) in the Maldives (Montano et al., 2012), six in the Philippines (Raymundo et al., 2018) and ten in the Northwestern Hawaiian Islands (Aeby, 2006).

All four diseases reported at LHI have been recorded in the Indo-Pacific. Growth anomalies have a global distribution (Raymundo et al., 2005; Aeby, 2006; Work et al., 2008a; Irikawa et al., 2011; Subhan et al., 2020; Aeby et al., 2021; Preston and Richards, 2021) and have been recorded in at least 14 coral taxa globally (Moriarty et al., 2020), here we recorded GAs in two taxa, *Acropora* a spp. and *I. cuneata* (Table 3). GAs have been recorded more commonly in *Acropora* species in Australia (Willis et al., 2004; Haapkylä et al., 2010), Japan (Irikawa et al., 2011), French Frigate Shoals, Johnston Atoll and American Samoa (Work et al., 2008a) and India (Rajasabapathy et al., 2020). *Isopora* growth anomalies were less commonly documented, with recordings only in Cocos Keeling Islands (Preston and Richards, 2021). The umbrella term for an unidentified disease that is experiencing white symptoms is called white syndrome. At LHI, we recorded white syndrome in five coral taxa: *Acropora* spp., *I. cuneata, Montipora* spp., *P. damicornis, Porites* spp., and *S. hystrix*. White syndrome has been recorded simultaneously in one or more of these species and taxa in the GBR (Willis et al., 2004; Haapkylä et al., 2010), Indonesia (Haapkylä et al., 2007), Maldives (Montano et al., 2012), Philippines (Raymundo et al., 2005), American Samoa (Wilson et al., 2012) and Norfolk Island (Page et al., 2023). Although white syndrome is found on coral reefs worldwide, it should be noted that individual species and regions could be experiencing varying region-specific diseases and have varying aetiologies. Skeletal eroding band was only recorded in *Acropora* spp. at LHI, and this disease has been recorded in *Acropora* spp., in the Maldives (Montano et al., 2012), the GBR (Haapkylä et al., 2010), and the Red Sea (Winkler et al., 2004). The one recorded off-transect endolithic hypermycosis was found in a *Porites* spp. colony which was currently 100% bleached. This was the only disease not reported in *Acropora* spp. and has been reported to impact massive boulder coral morphologies in the Pacific (Work et al., 2008b) and the Red Sea (Aeby et al., 2021).

Coral disease prevalence at LHI during the study period was potentially declining over time, although surveys in March 2109 were confounded by the occurrence of coral bleaching, making disease identification and distinguishing prior disease from bleaching more complex (Figure 4). In November 2018, all three sites were found to have similar disease prevalence. However, we found that North Bay and Erscotts disease prevalence had significantly declined in October 2019 compared to November 2018 (Figure 7). White syndrome was recorded at all three sites but not at all survey months. White syndrome was recorded in November 2018 and March 2019 at Coral Gardens and all three months at Erscotts and North Bay. North Bay was the only site at which all three diseases were recorded from the transects. Given the slow recovery from bleaching recorded (Moriarty et al., 2023), it is

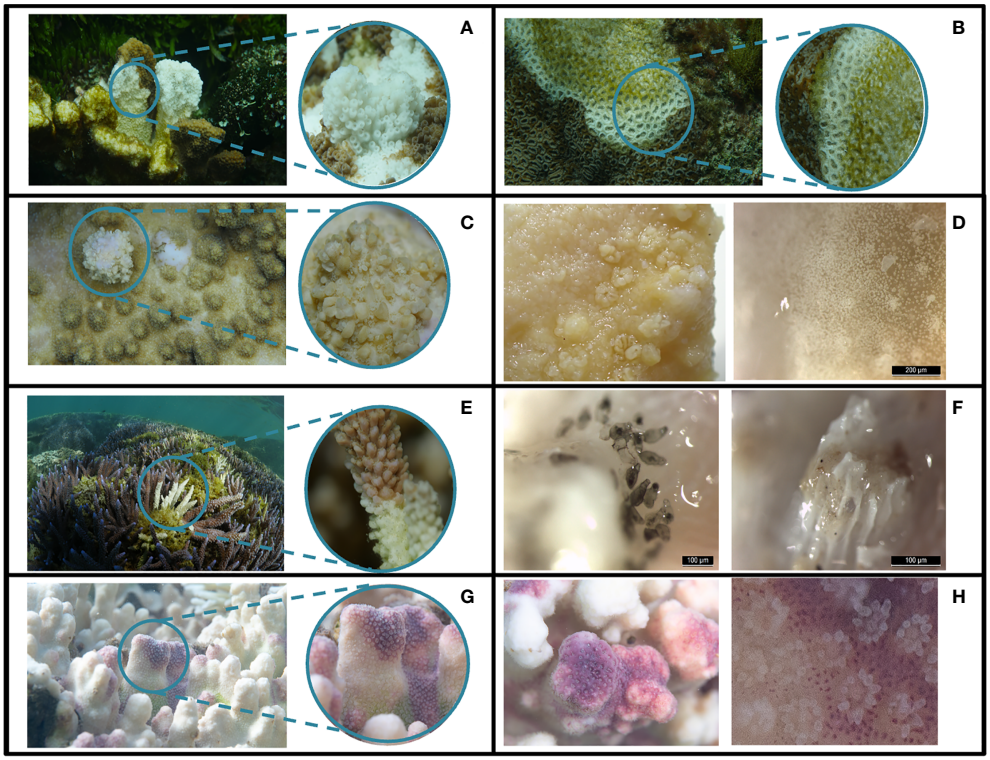

FIGURE 9
Coral diseases identified at LHI in 2018/2019. White syndrome **(A, B)**, growth anomaly **(C, D)**, skeletal eroding band **(E, F)**, and endolithic hypermycosis **(G, H)**.

also possible that post-stress disease emergence, if occurring, was not distinguishable from bleaching recovery in October 2019. A temporal offset between bleaching and post-bleaching disease emergence has been found in many studies. For example, a coral disease outbreak was reported in the US Virgin Islands nine months following a coral bleaching event in 2005 (Miller et al., 2009). White syndrome outbreaks have been reported in the winter of the year after bleaching, indicating a link between cold ocean temperatures up to two years after a bleaching event (Heron et al., 2010).

Interestingly, the *Acropora* spp. corals had the highest prevalence of disease, and all three disease states found within the transects were reported in *Acropora* spp. This pattern in disease occurrence in a species with low coral cover was also found in the GBR where pocilloporid species had the highest disease occurrence but the least cover on the reef (Willis et al., 2004). Skeletal eroding band was the first disease identified on the GBR and one of the most prevalent, with reports of the disease found on 90–100% of 18 reefs surveyed in 2004–2006, impacting about 82 hard coral species (Page and Willis, 2008). This study, however, reported SEB as the second most prevalent coral disease at LHI all of which were recorded on *Acropora* species (Figures 7, 8). Globally *Acropora* spp. have the highest number of disease reports in the literature (Ainsworth et al., 2007; Work et al., 2008a; Aeby et al., 2011; Irikawa et al., 2011; Roff et al., 2011; Muller et al., 2018; Rajasabapathy et al., 2020). *Acropora* spp. is thus considered to be susceptible to heat stress and disease (Brown, 1997; Madin et al., 2008; Aeby et al., 2011; Gilmour et al., 2013; Hobbs et al., 2015; Muller et al., 2018; Singh et al., 2019). *Acropora* spp. diseases have been recorded on most coral reefs, including on the Caribbean (Patterson et al., 2002; Sutherland and Ritchie, 2004; van Woesik and Randall, 2017), GBR (Willis et al., 2004; Haapkylä et al., 2010), Red Sea (Winkler et al., 2004; Mohamed and Sweet, 2019; Aeby et al., 2020; Aeby et al., 2021), and the Indo-Pacific Ocean (Aeby, 2006; Haapkylä et al., 2007; Montano et al., 2012). *Acropora* spp. dominated the reefs in the Maldives before the 1998 bleaching event comprising approximately 46% of the taxonomic composition reefs but now only contributes 1% of the coral cover (Edwards et al., 2001).

The most severely impacted coral taxa on LHI during the 2019 bleaching event were: *P.damicornis, S. pistillata, S. hystrix* and *Porites* spp (Moriarty et al., 2023). Furthermore, *Acropora* spp. and *I. cuneata*, two of the least susceptible to bleaching species at LHI in 2019 (Moriarty et al., 2023) where the only two species in which disease was observed during the bleaching event (Figure 7). Interestingly, in contrast to observations documented in the Great Barrier Reef where four diseases were identified (white syndrome, skeletal eroding band, black band and an unidentified disease) on *S. pistillata* (Willis et al., 2004), we found that although *S. pistillata* is one of the most prevalent coral taxa at LHI (n = 276), we recorded no signs of coral disease at any of the survey timepoints or at any of the reef sites (Table 3, Figure 7).

5 Conclusions

The occurrence and prevalence of coral diseases at the World Heritage Listed LHI could be the result of numerous factors such as, localised environmental parameters, host susceptibility and mode of transmission, and the normal disease occurrence expected within a population. To the best of our knowledge, this is the first coral disease publication from LHI, documenting disease identification and prevalence within the LHI lagoon. Importantly, coral disease was recorded in *Acropora* spp., a taxa which dominates the LHI lagoon benthos (Table 2) and had reported a higher thermal tolerance than some of the other reef building important taxa during the 2019 bleaching (Moriarty et al., 2023). Our observations suggest *Acropora* spp. colonies are also experiencing physiological perturbations, highlighting the need to identify disease causation within the LHI Marine Park. Coral and algae interactions have been linked with increased disease prevalence, and algae have been identified as a possible reservoir for coral disease pathogens (Nugues et al., 2004; Smith et al., 2006; Sweet et al., 2013; Casey et al., 2014) as well as increased water temperatures (Bruno et al., 2007; Ward et al., 2007; Heron et al., 2010; Ruiz-Moreno et al., 2012; van de Water et al., 2018; Aeby et al., 2020). Interestingly, algae composition is highest at Erscotts where coral disease was most prevalent and could be a contributing factor to disease prevalence (Figure 7C). In light of the bleaching event documented on the reef in 2019, it is imperative to conduct comprehensive and extended monitoring of the reef, including the tracking of localised disease occurrence and prevalence. Such efforts would provide management authorities with essential information in regards to the health of the reef post the 2019 bleaching event.

Data availability statement

The datasets presented in this study can be found in online repositories. A link to the data can be found below: https://github.com/tess-moriarty/LHI-coral-disease.

Ethics statement

The manuscript presents research on animals that do not require ethical approval for their study.

Author contributions

TM: Conceptualisation, Methodology, Validation, Formal Analysis, Investigation, Data curation, Writing – Original draft, Writing – Review and editing, Visualisation, Project administration, Funding acquisition. WL: Conceptualisation, Validation, Resources, Writing – Review and editing, Visualisation, Supervision, Project administration, Funding acquisition. TA: Conceptualisation, Validation, Resources, Writing – Review and editing, Visualisation, Supervision, Project administration, Funding acquisition. All authors contributed to the article and approved the submitted version.

Funding

This project was partially funded by a research grant from UNSW Scientia program awarded to TA 2018-2028, as well as funding from the Australian Research Council Discovery Project grant (DP180103199) awarded to TA and WL and the Women's Diving Hall of Fame – Marine Conservation Scholarship awarded to TM. The Lord Howe Island Marine Park, Environmental Tours Lord Howe and Pro Dive provided in-kind contributions providing boat support and access allowing the collection of data.

Acknowledgments

I would like to acknowledge the Darkinjung people the traditional owners on the land in which the write up of this research took place and pay my respects to the traditional owners of the land, past, present and emerging. The authors would like to thank New South Wales Department of Primary Industries (NSW DPI) – in particular Justin Gilligan, Emma Henry, Caitlin Woods, and Britt Anderson, for their knowledge and support during data collection. As well as NSW DPI's, Sallyann Gudge for going above and beyond with ongoing support and assistance throughout this project, we sincerely thank you. We thank all the LHI marine operators and in particular Dean Hiscox, Kayla Hiscox and family as well as Lisa and Aaron Ralph providing advice and access to sites. Rosie Steinberg (UNSW), Jesse Bergman (UNSW), Charlotte Page (UNSW) and Melissa Pappas (UNSW) for their assistance in the field with data collection. We would sincerely like to thank Blue Lagoon and Somerset Apartment Lord Howe Island for their generosity and support during our stays at LHI. And lastly, we thank the LHI Board for their support. The authors declare that they have no known conflicts of interest.

Conflict of interest

The authors declare that the research was conducted in the absence of any commercial or financial relationships that could be construed as a potential conflict of interest.

Publisher's note

References

Aeby, G. S. (2006). Baseline levels of coral disease in the Northwestern Hawaiian Islands. *Atoll Res Bull.* 543, 471–488.

Aeby, G. S., Howells, E., Work, T., Abrego, D., Williams, G. J., Wedding, L. M., et al. (2020). Localized outbreaks of coral disease on Arabian reefs are linked to extreme temperatures and environmental stressors. *Coral Reefs* 39 (3), 829–846. doi: 10.1007/s00338-020-01928-4

Aeby, G. S., Shore, A., Jensen, T., Ziegler, M., Work, T., and Voolstra, C. R. (2021). A comparative baseline of coral disease in three regions along the Saudi Arabian coast of the central Red Sea. *PloS One* 16 (7), e0246854. doi: 10.1371/journal.pone.0246854

Aeby, G. S., Williams, G. J., Franklin, E. C., Haapkyla, J., Harvell, C. D., Neale, S., et al. (2011). Growth anomalies on the coral genera acropora and porites are strongly associated with host density and human population size across the indo-pacific. *PloS One* 6 (2), e16887. doi: 10.1371/journal.pone.0016887

Ainsworth, T. D., Kvennefors, E. C., Blackall, L. L., Fine, M., and Hoegh-Guldberg, O. (2007). Disease and cell death in white syndrome of Acroporid corals on the Great Barrier Reef. *Mar. Biol.* 151 (1), 19–29. doi: 10.1007/s00227-006-0449-3

Alvarez-Filip, L., Estrada-Saldivar, N., Pérez-Cervantes, E., Molina-Hernández, A., and González-Barrios, F. J. (2019). A rapid spread of the stony coral tissue loss disease outbreak in the Mexican Caribbean. *PeerJ* 7, e8069. doi: 10.7717/peerj.8069

Antonius, A. (1976). New observations on coral destruction in reefs. *Mtg. Assoc. Isl. Mar. Lab. Carib.*, Mayaguez, Puerto Rico, 10, 3.

Baird, A. H., Sommer, B., and Madin, J. S. (2012). Pole-ward range expansion of Acropora spp. along the east coast of Australia. *Coral Reefs* 31 (4), 1063. doi: 10.1007/s00338-012-0928-6

Bourne, D. (2005). Microbiological assessment of a disease outbreak on corals from Magnetic Island (Great Barrier Reef, Australia). *Coral Reefs* 24 (2), 304–312. doi: 10.1007/s00338-005-0479-1

Bridge, T. C., Ferrari, R., Bryson, M., Hovey, R., Figueira, W. F., Williams, S. B., et al. (2014). Variable responses of benthic communities to anomalously warm sea temperatures on a high-latitude coral reef. *PloS One* 9 (11). doi: 10.1371/journal.pone.0113079

Brodnicke, O. B., Bourne, D. G., Heron, S. F., Pears, R. J., Stella, J. S., Smith, H. A., et al. (2019). Unravelling the links between heat stress, bleaching and disease: fate of tabular corals following a combined disease and bleaching event. *Coral Reefs* 38 (4), 591–603. doi: 10.1007/s00338-019-01813-9

Brown, B. E. (1997). Disturbances to reefs in recent times. In: C. Birkeland (ed) *Life Death coral reefs* (New York: Chapman & Hall), 354–379. doi: 10.1007/978-1-4615-5995-5_15

Bruno, J. F., Petes, L. E., Drew Harvell, C., and Hettinger, A. (2003). Nutrient enrichment can increase the severity of coral diseases. *Ecol. letters* 6 (12), 1056–1061. doi: 10.1046/j.1461-0248.2003.00544.x

Bruno, J. F., Selig, E. R., Casey, K. S., Page, C. A., Willis, B. L., Harvell, C. D., et al. (2007). Thermal stress and coral cover as drivers of coral disease outbreaks. *PloS Biol.* 5 (6), e124. doi: 10.1371/journal.pbio.0050124

Carpenter, K. E., Abrar, M., Aeby, G., Aronson, R. B., Banks, S., Bruckner, A., et al. (2008). One-third of reef-building corals face elevated extinction risk from climate change and local impacts. *Science* 321 (5888), 560–563. doi: 10.1126/science.1159196

Casey, J. M., Ainsworth, T. D., Choat, J. H., and Connolly, S. R. (2014). Farming behaviour of reef fishes increases the prevalence of coral disease associated microbes and black band disease. *Proc. R. Soc. B: Biol. Sci.* 281 (1788), 20141032. doi: 10.1098/rspb.2014.1032

Dalton, S. J., Carroll, A. G., Sampayo, E., Roff, G., Harrison, P. L., Entwistle, K., et al. (2020). Successive marine heatwaves cause disproportionate coral bleaching during a fast phase transition from El Niño to La Niña. *Sci. Total Environment* 715, 136951. doi: 10.1016/j.scitotenv.2020.136951

Dalton, S. J., Godwin, S., Smith, S., and Pereg, L. (2010). Australian subtropical white syndrome: a transmissible, temperature-dependent coral disease. *Mar. Freshw. Res.* 61 (3), 342–350. doi: 10.1071/MF09060

Dalton, S. J., and Roff, G. (2013). Spatial and temporal patterns of eastern Australia subtropical coral communities. *PloS One* 8 (9), e75873. doi: 10.1371/journal.pone.0075873

Dalton, S. J., and Smith, S. D. (2006). Coral disease dynamics at a subtropical location, Solitary Islands Marine Park, eastern Australia. *Coral Reefs* 25 (1), 37–45. doi: 10.1007/s00338-005-0039-8

Denis, V., Mezaki, T., Tanaka, K., Kuo, C.-Y., De Palmas, S., Keshavmurthy, S., et al. (2013). Coverage, diversity, and functionality of a high-latitude coral community (Tatsukushi, shikoku island, Japan). *PloS One* 8 (1), e54330. doi: 10.1371/journal.pone.0054330

De Vantier, L., and Deacon, G. (1990). Distribution of Acanthaster planci at Lord Howe Island, the southern-most Indo-Pacific reef. *Coral Reefs* 9 (3), 145–148. doi: 10.1007/BF00258226

Edwards, A. J., Clark, S., Zahir, H., Rajasuriya, A., Naseer, A., and Rubens, J. (2001). Coral bleaching and mortality on artificial and natural reefs in Maldives in 1998, sea

surface temperature anomalies and initial recovery. *Mar. pollut. Bulletin* 42 (1), 7–15. doi: 10.1016/S0025-326X(00)00200-9

Frölicher, T. L., and Laufkötter, C. (2018). Emerging risks from marine heat waves. *Nat. Commun.* 9 (1), 650. doi: 10.1038/s41467-018-03163-6

Gilmour, J. P., Smith, L. D., Heyward, A. J., Baird, A. H., and Pratchett, M. S. (2013). Recovery of an isolated coral reef system following severe disturbance. *Science* 340 (6128), 69–71. doi: 10.1126/science.1232310

Gintert, B. E., Precht, W. F., Fura, R., Rogers, K., Rice, M., Precht, L. L., et al. (2019). Regional coral disease outbreak overwhelms impacts from a local dredge project. *Environ. Monit. Assessment* 191 (10), 630. doi: 10.1007/s10661-019-7767-7

Haapkylä, J., Melbourne-Thomas, J., Flavell, M., and Willis, B. (2010). Spatiotemporal patterns of coral disease prevalence on Heron Island, Great Barrier Reef, Australia. *Coral Reefs* 29 (4), 1035–1045. doi: 10.1007/s00338-010-0660-z

Haapkylä, J., Melbourne-Thomas, J., Flavell, M., and Willis, B. (2013). Disease outbreaks, bleaching and a cyclone drive changes in coral assemblages on an inshore reef of the Great Barrier Reef. *J. Int. Soc. Reef Stud.* 32 (3), 815–824. doi: 10.1007/s00338-013-1029-x

Haapkylä, J., Seymour, A., Trebilco, J., and Smith, D. (2007). Coral disease prevalence and coral health in the Wakatobi Marine Park, south-east Sulawesi, Indonesia. *J. Mar. Biol. Assoc. united Kingdom* 87 (2), 403–414. doi: 10.1017/S0025315407055828

Harriott, V. (1999). Coral growth in subtropical eastern Australia. *Coral Reefs* 18 (3), 281–291. doi: 10.1007/s003380050195

Harrison, P. L., Dalton, S. J., and Carroll, A. G. (2011). Extensive coral bleaching on the world's southernmost coral reef at Lord Howe Island, Australia. *Coral Reefs* 30 (3), 775. doi: 10.1007/s00338-011-0778-7

Harvell, D., Jordán-Dahlgren, E., Merkel, S., Rosenberg, E., Raymundo, L., Smith, G., et al. (2007). Coral disease, environmental drivers, and the balance between coral and microbial associates. *Oceanography* 20, 172–195. doi: 10.5670/oceanog.2007.91

Hein, M. Y., Lamb, J. B., Scott, C., and Willis, B. L. (2015). Assessing baseline levels of coral health in a newly established marine protected area in a global scuba diving hotspot. *Mar. Environ. Res.* 103, 56–65. doi: 10.1016/j.marenvres.2014.11.008

Heres, M. M., Farmer, B. H., Elmer, F., and Hertler, H. (2021). Ecological consequences of stony coral tissue loss disease in the Turks and Caicos Islands. *Coral Reefs* 40 (2), 609–624. doi: 10.1007/s00338-021-02071-4

Heron, S. F., Willis, B. L., Skirving, W. J., Eakin, C. M., Page, C. A., and Miller, I. R. (2010). Summer hot snaps and winter conditions: modelling white syndrome outbreaks on great barrier reef corals. *PloS One* 5 (8), e12210. doi: 10.1371/journal.pone.0012210

Hobbs, J.-P. A., Frisch, A. J., Newman, S. J., and Wakefield, C. B. (2015). Selective impact of disease on coral communities: outbreak of white syndrome causes significant total mortality of acropora plate corals. *PloS One* 10 (7), e0132528. doi: 10.1371/journal.pone.0132528

Hoegh-Guldberg, O., Mumby, P. J., Hooten, A. J., Steneck, R. S., Greenfield, P., Gomez, E., et al. (2007). Coral reefs under rapid climate change and ocean acidification. *Science* 318 (5857), 1737–1742. doi: 10.1126/science.1152509

Hughes, T. P., Anderson, K. D., Connolly, S. R., Heron, S. F., Kerry, J. T., Lough, J. M., et al. (2018). Spatial and temporal patterns of mass bleaching of corals in the Anthropocene. *Science* 359 (6371), 80–83. doi: 10.1126/science.aan8048

Hughes, T. P., Barnes, M. L., Bellwood, D. R., Cinner, J. E., Cumming, G. S., Jackson, J. B. C., et al. (2017a). Coral reefs in the anthropocene. *Nature* 546 (7656), 82–90. doi: 10.1038/nature22901

Hughes, T. P., Kerry, J. T., Álvarez-Noriega, M., Álvarez-Romero, J. G., Anderson, K. D., Baird, A. H., et al. (2017b). Global warming and recurrent mass bleaching of corals. *Nature* 543 (7645), 373–377. doi: 10.1038/nature21707

Irikawa, A., Casareto, B. E., Suzuki, Y., Agostini, S., Hidaka, M., and van Woesik, R. (2011). Growth anomalies on Acropora cytherea corals. *Mar. pollut. Bulletin* 62 (8), 1702–1707. doi: 10.1016/j.marpolbul.2011.05.033

Jones, R. J., Bowyer, J., Hoegh-Guldberg, O., and Blackall, L. L. (2004). Dynamics of a temperature-related coral disease outbreak. *Mar. Ecol. Prog. Series* 281, 63–77. doi: 10.3354/meps281063

Lamb, J. B., True, J. D., Piromvaragorn, S., and Willis, B. L. (2014). Scuba diving damage and intensity of tourist activities increases coral disease prevalence. *Biol. Conserv.* 178, 88–96. doi: 10.1016/j.biocon.2014.06.027

Lamb, J. B., Willis, B. L., Fiorenza, E. A., Couch, C. S., Howard, R., Rader, D. N., et al. (2018). Plastic waste associated with disease on coral reefs. *Science* 359 (6374), 460–462. doi: 10.1126/science.aar3320

Lough, J. M., Anderson, K. D., and Hughes, T. P. (2018). Increasing thermal stress for tropical coral reefs: 1871–2017. *Sci. Rep.* 8 (1), 6079. doi: 10.1038/s41598-018-24530-9

Madin, J. S., O'Donnell, M. J., and Connolly, S. R. (2008). Climate-mediated mechanical changes to post-disturbance coral assemblages. *Biol. Letters* 4 (5), 490–493. doi: 10.1098/rsbl.2008.0249

Maynard, J., van Hooidonk, R., Eakin, C. M., Puotinen, M., Garren, M., Williams, G., et al. (2015). Projections of climate conditions that increase coral disease susceptibility and pathogen abundance and virulence. *Nat. Climate Change* 5 (7), 688–694. doi: 10.1038/nclimate2625

Meesters, E. H., Noordeloos, M., and Bak, R. P. M. (1994). Damage and regeneration: links to growth in the reef-building coral Montastrea annularis. *Mar. Ecol. Prog. Series* 112 (1/2), 119–128. Available at: https://www.jstor.org/stable/24847643

Miller, J., Muller, E., Rogers, C., Waara, R., Atkinson, A., Whelan, K., et al. (2009). Coral disease following massive bleaching in 2005 causes 60% decline in coral cover on reefs in the US Virgin Islands. *Coral Reefs* 28 (4), 925. doi: 10.1007/s00338-009-0531-7

Mohamed, A. R., and Sweet, M. (2019). "Current Knowledge of Coral Diseases Present Within the Red Sea," in *Oceanographic and Biological Aspects of the Red Sea*. Eds. N. M. A. Rasul and I. C. F. Stewart (Cham: Springer International Publishing), 387–400.

Montano, S., Strona, G., Seveso, D., and Galli, P. (2012). First report of coral diseases in the Republic of Maldives. *Dis. Aquat. Organisms* 101 (2), 159–165. doi: 10.3354/dao02515

Moriarty, T., Leggat, W., Heron, S. F., Steinberg, R., and Ainsworth, T. D. (2023). Bleaching, mortality and lengthy recovery on the coral reefs of Lord Howe Island. The 2019 marine heatwave suggests an uncertain future for high-latitude ecosystems. *PloS Climate* 2 (4), e0000080. doi: 10.1371/journal.pclm.0000080

Moriarty, T., Leggat, W., Huggett, M. J., and Ainsworth, T. D. (2020). Coral disease causes, consequences, and risk within coral restoration. *Trends Microbiol.* 28 (10), 793–807. doi: 10.1016/j.tim.2020.06.002

Muller, E. M., Bartels, E., and Baums, I. B. (2018). Bleaching causes loss of disease resistance within the threatened coral species Acropora cervicornis. *Elife* 7, e35066. doi: 10.7554/eLife.35066.028

Muller, E. M., and van Woesik, R. (2009). Shading reduces coral-disease progression. *Coral Reefs* 28 (3), 757–760. doi: 10.1007/s00338-009-0504-x

Myers, R. L., and Raymundo, L. J. (2009). Coral disease in Micronesian reefs: a link between disease prevalence and host abundance. *Dis. Aquat. Organisms* 87 (1-2), 97–104. doi: 10.3354/dao02139

Nugues, M. M. (2002). Impact of a coral disease outbreak on coral communities in St. Lucia: What and how much has been lost? *Mar. Ecol. Prog. Series* 229, 61–71. doi: 10.3354/meps229061

Nugues, M. M., Smith, G. W., van Hooidonk, R. J., Seabra, M. I., and Bak, R. P. M. (2004). Algal contact as a trigger for coral disease. *Ecol. Letters* 7 (10), 919–923. doi: 10.1111/j.1461-0248.2004.00651.x

Page, C. E., Leggat, W., Egan, S., and Ainsworth, T. D. (2023). A coral disease outbreak highlights vulnerability of remote high-latitude lagoons to global and local stressors. *iScience* 26 (3), 106205. doi: 10.1016/j.isci.2023.106205

Page, C. A., and Stoddart, J. A. (2010). New records of five coral diseases from the Pilbara Region of Western Australia. *Coral Reefs* 29 (4), 987. doi: 10.1007/s00338-010-0659-5

Page, C. A., and Willis, B. L. (2008). Epidemiology of skeletal eroding band on the Great Barrier Reef and the role of injury in the initiation of this widespread coral disease. *Coral Reefs* 27 (2), 257–272. doi: 10.1007/s00338-007-0317-8

Palmer, C. V., and Baird, A. H. (2018). Coral tumor-like growth anomalies induce an immune response and reduce fecundity. *Dis. Aquat. Organisms* 130 (1), 77–81. doi: 10.3354/dao03258

Pandolfi, J. M., Connolly, S. R., Marshall, D. J., and Cohen, A. L. (2011). Projecting coral reef futures under global warming and ocean acidification. *Science* 333 (6041), 418–422.

Patterson, K. L., Porter, J. W., Ritchie, K. B., Polson, S. W., Mueller, E., Peters, E. C., et al. (2002). The etiology of white pox, a lethal disease of the Caribbean elkhorn coral, Acropora palmata. *Proc. Natl. Acad. Sci.* 99 (13), 8725–8730. doi: 10.1073/pnas.092260099

Pratchett, M. S., Hoey, A. S., and Wilson, S. K. (2014). Reef degradation and the loss of critical ecosystem goods and services provided by coral reef fishes. *Curr. Opin. Environ. Sustainability* 7, 37–43. doi: 10.1016/j.cosust.2013.11.022

Precht, W. F., Gintert, B. E., Robbart, M. L., Fura, R., and Van Woesik, R. (2016). Unprecedented disease-related coral mortality in Southeastern Florida. *Sci. Rep.* 6 (1), 1–11. doi: 10.1038/srep31374

Preston, S., and Richards, Z. (2021). Biological consequences of an outbreak of growth anomalies on Isopora palifera at the Cocos (Keeling) Islands. *Coral Reefs* 40 (1), 97–109. doi: 10.1007/s00338-020-02019-0

Rajasabapathy, R., Ramasamy, K. P., Manikandan, B., Mohandass, C., and Arthur James, R. (2020). Bacterial communities associated with healthy and diseased (Skeletal growth anomaly) reef coral acropora cytherea from palk bay, India. *Front. Mar. Sci.* 7 (92). doi: 10.3389/fmars.2020.00092

Raymundo, L. J., Licuanan, W. L., and Kerr, A. M. (2018). Adding insult to injury: Ship groundings are associated with coral disease in a pristine reef. *PloS One* 13 (9), e0202939. doi: 10.1371/journal.pone.0202939

Raymundo, L. J., Rosell, K. B., Reboton, C. T., and Kaczmarsky, L. (2005). Coral diseases on Philippine reefs: genus Porites is a dominant host. *Dis. Aquat. organisms* 64 (3), 181–191. doi: 10.3354/dao064181

Redding, J. E., Myers-Miller, R. L., Baker, D. M., Fogel, M., Raymundo, L. J., and Kim, K. (2013). Link between sewage-derived nitrogen pollution and coral disease severity in Guam. *Mar. pollut. Bulletin* 73 (1), 57–63. doi: 10.1016/j.marpolbul.2013.06.002

Richardson, L. L. (1998). Coral diseases: what is really known? *Trends Ecol. Evol.* 13 (11), 438–443. doi: 10.1016/S0169-5347(98)01460-8

Riegl, B. (2003). Climate change and coral reefs: different effects in two high-latitude areas (Arabian Gulf, South Africa). *Coral reefs* 22 (4), 433–446. doi: 10.1007/s00338-003-0335-0

Roff, G., Kvennefors, E. C. E., Fine, M., Ortiz, J., Davy, J. E., and Hoegh-Guldberg, O. (2011). The ecology of 'Acroporid white syndrome', a coral disease from the southern great barrier reef. *PloS One* 6 (12), e26829. doi: 10.1371/journal.pone.0026829

Rosenberg, E., and Loya, Y. (2004). *Coral health and disease*. (Berlin, New York: Springer).

Ruiz-Moreno, D., Willis, B. L., Page, A. C., Weil, E., Cróquer, A., Vargas-Angel, B., et al. (2012). Global coral disease prevalence associated with sea temperature anomalies and local factors. *Dis. Aquat. Organisms* 100 (3), 249–261. doi: 10.3354/dao02488

Schleyer, M. H., Floros, C., Laing, S. C. S., Macdonald, A. H. H., Montoya-Maya, P. H., Morris, T., et al. (2018). What can South African reefs tell us about the future of high-latitude coral systems? *Mar. pollut. Bull.* 136, 491–507. doi: 10.1016/j.marpolbul.2018.09.014

Sheppard, C. R. C. (2003). Predicted recurrences of mass coral mortality in the Indian Ocean. *Nature* 425 (6955), 294–297. doi: 10.1038/nature01987

Singh, T., Iijima, M., Yasumoto, K., and Sakai, K. (2019). Effects of moderate thermal anomalies on Acropora corals around Sesoko Island, Okinawa. *PloS One* 14 (1), e0210795. doi: 10.1371/journal.pone.0210795

Smith, J. E., Shaw, M., Edwards, R. A., Obura, D., Pantos, O., Sala, E., et al. (2006). Indirect effects of algae on coral: algae-mediated, microbe-induced coral mortality. *Ecol. Letters* 9 (7), 835–845. doi: 10.1111/j.1461-0248.2006.00937.x

Steinberg, R. K., Ainsworth, T. D., Moriarty, T., Bednarek, T., Dafforn, K. A., and Johnston, E. L. (2022). Bleaching susceptibility and resistance of octocorals and anemones at the world's southern-most coral reef. *Front. Physiol.* 13. doi: 10.3389/fphys.2022.804193

Stimson, J. (2011). Ecological characterization of coral growth anomalies on Porites compressa in Hawai 'i. *Coral Reefs* 30 (1), 133–142. doi: 10.1007/s00338-010-0672-8

Subhan, B., Arafat, D., Rahmawati, F., Dasmasela, Y., Royhan, Q., Madduppa, H., et al. (2020). Coral disease at Mansuar Island, Raja Ampat, Indonesia. *Earth Environ. Sci.* 429 (1), 12027.

Sully, S., Burkepile, D. E., Donovan, M. K., Hodgson, G., and van Woesik, R. (2019). A global analysis of coral bleaching over the past two decades. *Nat. Commun.* 10 (1), 1264. doi: 10.1038/s41467-019-09238-2

Sutherland, W. J., Clout, M., Depledge, M., Dicks, L. V., Dinsdale, J., Entwistle, A. C., et al. (2015). A horizon scan of global conservation issues for 2015. *Trends Ecol. Evolution* 30 (1), 17–24. doi: 10.1016/j.tree.2014.11.002

Sutherland, K. P., and Ritchie, K. B. (2004). "White Pox Disease of the Caribbean Elkhorn Coral, Acropora palmata," in *Coral Health and Disease*. Eds. E. Rosenberg and Y. Loya (Berlin, Heidelberg: Springer Berlin Heidelberg), 289–300.

Sweet, M. J., Bythell, J. C., and Nugues, M. M. (2013). Algae as reservoirs for coral pathogens. *PloS One* 8 (7), e69717. doi: 10.1371/journal.pone.0069717

Thompson, A., Schroeder, T., Brando, V. E., and Schaffelke, B. (2014). Coral community responses to declining water quality: Whitsunday Islands, Great Barrier Reef, Australia. *Coral Reefs* 33 (4), 923–938. doi: 10.1007/s00338-014-1201-y

Valentine, J., and Edgar, G. (2010). Impacts of a population outbreak of the urchin Tripneustes gratilla amongst Lord Howe Island coral communities. *Coral Reefs* 29 (2), 399–410. doi: 10.1007/s00338-010-0610-9

van de Water, J. A. J. M., Chaib De Mares, M., Dixon, G. B., Raina, J.-B., Willis, B. L., Bourne, D. G., et al. (2018). Antimicrobial and stress responses to increased temperature and bacterial pathogen challenge in the holobiont of a reef-building coral. *Mol. Ecol.* 27 (4), 1065–1080. doi: 10.1111/mec.14489

van Woesik, R., and Randall, C. J. (2017). Coral disease hotspots in the Caribbean. *Ecosphere* 8 (5), e01814. doi: 10.1002/ecs2.1814

Vega Thurber, R. L., Burkepile, D. E., Fuchs, C., Shantz, A. A., McMinds, R., and Zaneveld, J. R. (2014). Chronic nutrient enrichment increases prevalence and severity of coral disease and bleaching. *Global Change Biol.* 20 (2), 544–554. doi: 10.1111/gcb.12450

Vroom, P. S., and Braun, C. L. (2010). Benthic composition of a healthy subtropical reef: baseline species-level cover, with an emphasis on algae, in the northwestern Hawaiian islands. *PloS One* 5 (3), e9733. doi: 10.1371/journal.pone.0009733

Ward, J. R., Kim, K., and Harvell, C. D. (2007). Temperature affects coral disease resistance and pathogen growth. *Mar. Ecol. Prog. Ser.* 329, 115–121. doi: 10.3354/meps329115

Weil, E., Cróquer, A., and Urreiztieta, I. (2009). Yellow band disease compromises the reproductive output of the Caribbean reef-building coral Montastraea faveolata (Anthozoa, Scleractinia). *Dis. Aquat. Organisms* 87 (1-2), 45–55. doi: 10.3354/dao02103

Weil, E., Hernández-Delgado, E., Gonzalez, M., Williams, S., Suleimán-Ramos, S., Figuerola, M., et al. (2019). Spread of the new coral disease "SCTLD" into the Caribbean: implications for Puerto Rico. *Reef Encounter* 34, 38–43.

Weiler, B. A., Van Leeuwen, T. E., and Stump, K. L. (2019). The extent of coral bleaching, disease and mortality for data-deficient reefs in Eleuthera, The Bahamas after the 2014–2017 global bleaching event. *Coral Reefs* 38 (4), 831–836. doi: 10.1007/s00338-019-01798-5

Wilkinson, C. ed. (2000). *Status of coral reefs of the world: 2000*. (Townsville/Dampier, Australia: Australia Institute Marine Science)

Williams, D. E., and Miller, M. W. (2005). Coral disease outbreak: pattern, prevalence and transmission in Acropora cervicornis. *Mar. Ecol. Prog. Series* 301, 119–128. doi: 10.3354/meps301119

Willis, B. L., Page, C. A., and Dinsdale, E. A. (2004). Coral disease on the Great Barrier Reef. In: E. Rosenberg and Y. Loya, editors. *Coral Health and Disease*. (Berlin: Springer-Verlag), pp. 69–104.

Wilson, B., Aeby, G. S., Work, T. M., and Bourne, D. G. (2012). Bacterial communities associated with healthy and Acropora white syndrome-affected corals from American Samoa. *FEMS Microbiol. Ecol.* 80 (2), 509–520. doi: 10.1111/j.1574-6941.2012.01319.x

Winkler, R., Antonius, A., and Abigail Renegar, D. (2004). The skeleton eroding band disease on coral reefs of Aqaba, Red Sea. *Mar. Ecol.* 25 (2), 129–144. doi: 10.1111/j.1439-0485.2004.00020.x

Work, T. M., and Aeby, G. S. (2006). Systematically describing gross lesions in corals. *Dis. Aquat. Organisms* 70 (1-2), 155–160. doi: 10.3354/dao070155

Work, T. M., Aeby, G. S., and Coles, S. L. (2008a). Distribution and morphology of growth anomalies in Acropora from the Indo-Pacific. *Dis. Aquat. Organisms* 78 (3), 255–264. doi: 10.3354/dao01881

Work, T. M., Aeby, G., Stanton, F., and Fenner, D. (2008b). Overgrowth of fungi (endolithic hypermycosis) associated with multifocal to diffuse distinct amorphous dark discoloration of corals in the Indo-Pacific. *Coral Reefs* 27 (3), 663. doi: 10.1007/s00338-008-0374-7

Work, T. M., Richardson, L. L., Reynolds, T. L., and Willis, B. L. (2008c). Biomedical and veterinary science can increase our understanding of coral disease. *J. Exp. Mar. Biol. Ecol.* 362 (2), 63–70. doi: 10.1016/j.jembe.2008.05.011

Yamano, H., Sugihara, K., and Nomura, K. (2011). Rapid poleward range expansion of tropical reef corals in response to rising sea surface temperatures. *Geophys. Res. Letters* 38 (4). doi: 10.1029/2010GL046474

Yoshioka, R. M., Kim, C. J., Tracy, A. M., Most, R., and Harvell, C. D. (2016). Linking sewage pollution and water quality to spatial patterns of Porites lobata growth anomalies in Puako, Hawaii. *Mar. pollut. Bull.* 104 (1-2), 313–321. doi: 10.1016/j.marpolbul.2016.01.002

frontiers | Frontiers in Ecology and Evolution

TYPE Review
PUBLISHED 18 December 2023
DOI 10.3389/fevo.2023.1190455

OPEN ACCESS

EDITED BY
Jennifer L. Matthews,
University of Technology Sydney, Australia

REVIEWED BY
Alexandra Dempsey,
Khaled bin Sultan Living Oceans Foundation, United States
Yvonne Sawall,
Bermuda Institute of Ocean Sciences, Bermuda

*CORRESPONDENCE
Jessica L. Bergman
j.bergman@unsw.edu.au

RECEIVED 20 March 2023
ACCEPTED 28 November 2023
PUBLISHED 18 December 2023

CITATION
Bergman JL, Richards ZT, Sawyers P and Ainsworth TD (2023) Environmental generalism, holobiont interactions, and Pocilloporid corals in the warming oceans of the eastern coast of Australia.
Front. Ecol. Evol. 11:1190455.
doi: 10.3389/fevo.2023.1190455

Environmental generalism, holobiont interactions, and Pocilloporid corals in the warming oceans of the eastern coast of Australia

Jessica L. Bergman[1]*, Zoe T. Richards[2,3], Paige Sawyers[4] and Tracy D. Ainsworth[1]

[1]Biological, Earth, and Environmental Sciences, University of New South Wales, Sydney, NSW, Australia, [2]Coral Conservation and Research Group, Trace and Environmental DNA Laboratory, School of Molecular and Life Sciences, Curtin University, Bentley, WA, Australia, [3]Collections and Research, Western Australian Museum, Welshpool, WA, Australia, [4]School of Environmental and Life Sciences, University of Newcastle, Callaghan, NSW, Australia

Ocean warming has been driving mortality events across the world's coral reef ecosystems and is resulting in multifaceted ecosystem restructuring. With the rapid shifts occurring across ecosystems, questions arise of which species, in which locations, have the capacity to persevere under climate change. Environmental generalism refers to species with the biological traits that support environmental flexibility, enabling the organism to occupy a broad range of environmental conditions. Some Scleractinia have been categorised as environmental generalists and proposed as likely winners under changing climate conditions, as environmental generalists have been considered less susceptible to environmental disturbance than specialist species. Given the complexity of the holobiont structure of corals, which includes photoendosymbiosis and diverse microbial consortia, understanding the complexity of the coral holobiont–environment interaction for the generalist corals will be an important factor in accurately predicting the success of these species into the future. Here we conduct a literature search to compile topics and concepts of environmental generalism for Australia's warming coral reef ecosystems and the breadth of holobiont responses to ecosystem restructuring. We synthesise these findings in the context of the latitudinal expanse of Australia's coral reefs to highlight how it is necessary to understand the biological underpinnings of generalist corals.

KEYWORDS

generalist, coral reefs, climate change, Pocilloporid, Australia

1 Introduction

Scleractinian, or hard (stony) corals are most widely known for their role as the trophic and structural foundation of coral reefs, particularly for reefs in warm, shallow, tropical waters (Hamylton et al., 2022). While corals dominate tropical reefs and provide the foundation for the most diverse ecosystems on the planet, corals are also found across a breadth of light and temperature regimes outside of reef forming structures, including within sandy bays, caves, coastal waterways, mangroves, seagrass beds, temperate waters and the deep sea (Perry and Larcombe, 2003; Cairns, 2007; Richards et al., 2016; Camp et al., 2019; Watanabe and Nakamura, 2019; Burt et al., 2020). In addition to being found across a range of marine ecosystems, this highly diverse group of organisms exhibits a wide variety of life history traits, growth forms, and adaptations to the array of environmental regimes in which they are found (Jackson, 1991; Connell et al., 2004; Todd, 2008; Zawada et al., 2019; Bairos-Novak et al., 2021). This diversity of coral life highlights the challenges that arise when forecasting the role this taxa will play in ecosystem restructuring under environmental change.

Global coral reef ecosystems, dominated by reef-forming scleractinia (Pandolfi et al., 2011; Vermeij et al., 2011; Hughes et al., 2018; Cornwall et al., 2021; Eddy et al., 2021), are undergoing significant changes due to anthropogenic climate change. Record warm temperatures and rates of warming are disrupting coral photoendosymbiosis and causing widespread whole organism heat-induced and bleaching-induced mortality across the world's coral reefs (Donovan et al., 2021; Hughes et al., 2021). As bleaching events increase in frequency, the impact of these disturbance events accumulates and affects the capacity of the ecosystem to recover (Dietzel et al., 2021). In one well-documented study undertaken between 1968 and 2004, comprising 6001 benthic surveys of 2,667 Indo-Pacific reefs, a 1–2% yearly decline in coral cover was demonstrated (Bruno and Selig, 2007). Similarly, in the Seychelles, a 17-year data set demonstrated mass bleaching events reduced live coral cover by > 90% in the reefs surveyed, leading to a shift towards a macroalgae-dominated ecosystem in nine out of 21 reefs (Graham et al., 2006; Graham et al., 2015). A time-series analysis of coral reefs in Moorea, French Polynesia found extensive coral loss and change in abundance of the major coral genera on the reef between 1979 and 2009 due to the cumulative impacts of *Acanthaster planci* outbreaks, cyclones, and bleaching (Pratchett et al., 2011). A similar trajectory has been reported for coral reefs in Okinawa, Japan, where net coral area declined 42–72% and changes in abundance of the dominant scleractinian taxa followed bleaching events, typhoons, and increased sedimentation (Harii et al., 2014). The recent coral cover report for the Great Barrier Reef by the Australian Institute of Marine Science (AIMS, 2022) also suggested that short-term gains in coral cover following severe bleaching and mortality events in 2021/2022 highlighted long-term impacts of shifting population structure to fast growing but thermally susceptible coral species. Fast-growing *Acropora* species, which drive recovery on damaged reefs, are also the most vulnerable to the common disturbances affecting the GBR (AIMS, 2022). These examples underscore widespread coral reef degradation from biological and anthropogenic stressors (Eddy et al., 2021). As such, coral reefs are now being altered in historically unprecedented ways (van Woesik et al., 2012).

The vast ecosystem restructure occurring in marine ecosystems has also been shown to include the replacement of historically dominant coral species with corals exhibiting more persistent, weedy, and opportunistic traits (Knowlton, 2001; McClanahan et al., 2007; de Bakker et al., 2016; Caballero Aragón et al., 2019; McWilliam et al., 2020; Cornwall et al., 2022). Generalist coral species, or those that thrive across a breadth of environmental conditions and are considered more tolerant of sub-optimal conditions than species within a narrow environmental niche (Richmond et al., 2005; Clavel et al., 2011; Darling et al., 2012), are hypothesised to play an important role in this population restructure (Courtney et al., 2020). In contrast, specialist species may be more susceptible to metapopulation dynamics under climate change, with potential extinction risks due to decreased effective population size and genetic variation in already small populations; this has been seen in butterflyfish (Lawton et al., 2011), marine teleosts (Smith and Fujio, 1982), and marine molluscs (Lavm and Nevo, 1981). Generalist coral species may be more successful than specialist coral species on reef ecosystems as the climate continues to change (Clavel et al., 2011; Chichorro et al., 2019), offering critical ecological opportunities for the reconfiguration of coral reefs. As such, addressing knowledge gaps in the potential for these species to expand into new habitats as ecosystem restructuring occurs is crucial for predicting both future reef structure and coral extinction risk (Bridge et al., 2020).

1.1 Terminology used in environmental generalism research for corals and coral reef ecosystems

Generalist species have been defined in ecology as those that exploit multiple habitat types or food sources, while a specialist is limited to only one or a few (van Tienderen, 1991). There are several ecological predictions that have been linked to both generalist and specialist species that hypothesise various uses of resources determine the range size of the species (Slatyer et al., 2013).This hypothesis states generalist species are more likely to have a higher tolerance towards habitat loss and climate change due to their adaptabilities and large range sizes through positive correlations between niche breadth and geographic range. Generalist species with a broad resource breadth are thought to be more persistent because they are less sensitive to stochastic fluctuations of any given resource. This concept is also the foundation of the generalism–specialism debate, where generalism in resource use and niche breadth has been suggested to create an ongoing cycle where the success of generalists drive speciation and species extinction (Dennis et al., 2011). However, there is clearly a wide range in how generalist species and their role in their environment is defined.

The terms "generalist species", "generalism" and "generalist coral" appear to be underutilized and inconsistently applied in coral reef research. For example, a search of primary research publications for the terms <*generalist AND coral*> between 2010 and 2022 identified 187 articles, of which only 72 studies related to specifically to Scleractinian coral species (opposed to other species within coral reef ecosystems). Of these studies, 2 species, *Montastrea cavernosa* and *Stylophora pistillata*, were the primary study species in the research conducted (Table 1). While definitions for generalist species and use of generalist terminology has varied in the primary literature, the research that has used these terms to-date has classified generalist species by the taxa within-reef distribution, with 68% of studies identified here referring to depth generalists (Figure 1). Generalist corals have also been defined through:

1) flexibility of their relationship with *Symbiodiniaceae* and the bacterial microbiome (16% of the identified studies),
2) variation in life history traits (11% of identified studies),
3) a broad environmental distribution (4% of identified studies), and
4) plastic morphology (1% of identified studies).

Two studies have conducted the most extensive categorisation of coral species within generalist and specialists groups:

Firstly, Darling et al. (2012) applied a trait-based classification approach for 143 species of coral, defining generalist species as those having life history traits of competitive, weedy, and stress-tolerant corals. Competitive species have traits that align with specialist species, such as efficiency in using resources and dominance in highly populated, ideal environments. Weedy corals have fast reproduction times and diverse species traits, which allows them to opportunistically colonise a variety of disturbed environments. Stress-tolerant corals are defined as those with slow growth, long generation times, large corallites, and high fecundity that help them to proliferate in chronically harsh environments. Generalist corals have overlapping traits with both weedy and stress tolerant corals, as defined by Darling et al. (2012), and we refer to corals with this set of traits as "generalists" from here on out. Sommer et al. (2014) also utilised trait-based filtering for corals along a latitudinal gradient in high-latitude eastern Australia, finding high-latitude coastal reefs to be mainly dominated by generalist coral species of massive morphologies, which persist in conditions of high environmental stress but also contribute to a low structural complexity and have limited recovery potential following disturbance due to slow-growing trait of massive morphotypes. However, consistent with Darling et al. (2012), the authors also found that species with similar functional characteristics have higher co-occurrence. This raises the question of how abiotic filtering (e.g. environmental parameters) will influence the structure of coral communities when corals with different life-history strategies (e.g. different growth rates or reproductive modes) share similar traits.

Table 2 summarises trait-based classifications used in the studies of Darling et al. (2012), Darling et al. (2019) and Sommer et al. (2014) to further elaborate on how generalist species can encompass a combination of various life history strategies or be composed of a subset of competitive taxa (as defined by Darling

TABLE 1 72 publications returned in a Google Scholar search for the terms <*generalist AND coral*> between 2010 and 2022, sorted into five primary categories used to define generalists in the literature: depth, environmental, life history, morphology, and symbiont.

Study	Taxa	Type
Bongaerts et al., 2010	Various or Review	Depth
van Oppen et al., 2011	*Seriatopora hystrix*	Depth
Bongaerts et al., 2013	*Acropora agaricites, Acropora lamarcki*	Depth
Serrano et al., 2014	*Montastraea cavernosa*	Depth
Bongaerts et al., 2015a	Various or Review	Depth
Bongaerts et al., 2015b	*Agaricia grahamae, Agaricia undata, Madracis pharensis*	Depth
Holstein et al., 2015	*Orbicella faveolata*	Depth
Thomas et al., 2015	*Stylophora pistillata, Seriotopora hystrix, Platygyra daedalea, Acropora humilis, Acropora valida*	Depth
Ziegler et al., 2015a	Various or Review	Depth
Brandtneris et al., 2016	*Orbicella faveolata, Agaricia lamarcki*	Depth
Holstein et al., 2016	*Orbicella faveolata, Porites astreoides*	Depth
Loya et al., 2016	*Orbicella faveolata, Porites astreoides*	Depth
Bollati et al., 2017	*Montastraea cavernosa*	Depth
Bongaerts et al., 2017	*Agaricia fragilis, Stephanocoenia intersepta, Montastrea cavernosa, Orbicella franksi*	Depth
Kahng et al., 2017	Various or Review	Depth
Silveira et al., 2017	*Stephanocoenia intersepta*	Depth
Feldman et al., 2018	*Paramontastraea peresi*	Depth
Garavelli et al., 2018	*Montastraea cavernosa*	Depth
Hernandez-Agreda et al., 2018	*Pachyseris speciosa, Mycedium elephantotus, Acropora aculeus*	Depth
Polinski and Voss 2018	*Montastraea cavernosa*	Depth
Shlesinger et al., 2018	*Acropora squarrosa, Acropora valida, Montipora verrucosa*	Depth
Soto et al., 2018	*Pocillopora verrucosa*	Depth
Studivan and Voss 2018a	*Montastraea cavernosa*	Depth

(Continued)

TABLE 1 Continued

Study	Taxa	Type
Studivan and Voss 2018b	*Montastraea cavernosa*	Depth
Polinski and Voss 2018	*Montastraea cavernosa*	Depth
Benayahu et al., 209	Octocorals	Depth
Bongaerts and Smith 2019	Various or Review	Depth
Eckert et al., 2019	*Montastrea cavernosa*	Depth
Eyal et al., 2019a	*Dipsastraea favus, Paramontastrea peresi, Porites lutea, Stylophora pistillata, Turbinaria reniformis*	Depth
Eyal et al., 2019b	*Montastraea cavernosa*	Depth
Kahng et al., 2019	Various or Review	Depth
Laverick et al., 2019	*Acropora lamarcki*	Depth
Lesser et al., 2019	Various or Review	Depth
Muir and Pichon 2019	*Mussidae* spp., *Fungiidae* spp., *Agariciidae* spp.	Depth
Shlesinger and Loya 2019	Various or Review	Depth
Smith et al., 2019	Various or Review	Depth
Studivan et al., 2019	*Montastraea cavernosa*	Depth
Tamir et al., 2019	*Stylophora pistillata*	Depth
Kramer et al., 2020	*Stylophora pistillata, Acropora squarrosa, Paramontastrea peresi, Porites lobata*	Depth
Martinez et al., 2020	*Stylophora pistillata*	Depth
Scucchia et al., 2020	*Stylophora pistillata*	Depth
Studivan and Voss 2020	*Montastraea cavernosa*	Depth
Tamir et al., 2020	*Acropora squarrosa, Montipora danae, Paramontastrea peresi, Porites lobata, Stylophora pistillata*	Depth
Bloomberg and Holstein 2021	*Montastraea cavernosa*	Depth
Eyal et al., 2021	*Stylophora pistillata*	Depth

(Continued)

TABLE 1 Continued

Study	Taxa	Type
Kramer et al., 2021a	*Stylophora pistillata*	Depth
Kramer et al., 2021b	*Stylophora pistillata, Acropora squarrosa, Paramontastrea peresi, Porites lobata*	Depth
Scucchia et al., 2021	*Stylophora pistillata*	Depth
Cacciapaglia and van Woesik 2015	Various, *Pocillopora* spp.	Environmental
Hernandez-Agreda et al., 2016	*Pachyseris speciosa*	Environmental
Bergman et al., 2021	*Pocillopora damicornis*	Environmental
Parasharya and Padate 2013	Various or Review	Life History
Guest et al., 2016	*Merulina, Pachyseris, Echinopora, Montipora*	Life History
Courtney et al., 2017	*Diploria labyrinthiformis, Porites astreoides, Pseudiploria strigosa, Favia fragum, Madracis decactis, Montastrea cacernosa, Orbicella franksi*	Life History
Grimsditch et al., 2017	*Echinopora* spp., *Pavona* spp., *Pocillopora* spp., *Montipora* spp.	Life History
Januchowski-Hartley et al., 2020	*Merulina* spp., *Pachyseris* spp., *Echinopora* spp.	Life History
Karisa et al., 2020	*Porites* spp., *Echinopora* spp.	Life History
Zweifler et al, 2021	*Merulina* spp.	Life History
Swain et al., 2021	Various or Review	Life History
Goodbody-Gringley and Waletich 2018	*Montastraea cavernosa*	Morphology
Fabina et al., 2012	Various or Review	Symbiont
Putnam et al., 2012	*Acropora* spp., *Leptastrea* spp., *Leptoseris* spp., *Montipora* spp., *Pavona* spp., *Pocillopora* spp.	Symbiont
Silverstein et al., 2012	Various or Review	Symbiont
Wang et al., 2012	*Isopora palifera, Stylophora pistillata*	Symbiont
Fabina et al., 2013	Various or Review	Symbiont
Ziegler et al., 2015b	*Pocillopora verrucosa, Porites lutea*	Symbiont
Claar et al., 2017	*Acropora* spp.	Symbiont

(Continued)

TABLE 1 Continued

Study	Taxa	Type
Ziegler et al., 2019	*Orbicella annularis, Orbicella faveolata*	Symbiont
Mies et al., 2020	*Mussismilia hispida, Mussismilia harttii, Favia gravida, Millepora alcicornis, Siderastrea* spp.	Symbiont
Wepfer et al., 2020	*Galaxea fascicularis*	Symbiont
Saad et al., 2021	*Acropora valida*	Symbiont
Varasteh et al., 2021	*Madracis decactis*	Symbiont

"Various or Review" refers to studies that didn't specify taxa or that contained mention of the terms <*generalist AND coral*> in a review, respectively. 50 studies refer to depth generalists, 3 studies refer to environmental generalists, 8 studies refer to life history generalists, 1 study refers to morphology generalists, and 12 studies refer to symbiont/microbiome generalists.

et al., 2012). The ambiguity in defining generalist species highlights a knowledge gap crucial for predicting and managing the form and function of future reefs and optimising conservation planning. Pocilloporid corals (Gray, 1840) are a widespread taxonomic group of scleractinian corals that have been reported on coral reef ecosystems worldwide across vast geographic, environmental, and depth ranges (Figure 2). Known to be a fast-growing and opportunistic genus (Brustolin et al., 2019), Pocilloporids serve as an example of generalist traits due to both high levels of phenotypic plasticity and a broad environmental distribution (Todd, 2008; Schmidt-Roach et al., 2014; Putnam et al., 2020; Burgess et al., 2021). The capacity for plasticity in the group contributes to the challenge of identifying species, species complexes and species ranges in addition to having substantial genetic variability amongst visually similar species (Todd, 2008). For example, *Pocillopora damicornis* has traditionally been described as four distinct ecomorphs – elongate, semi-disturbed, compact, and branching (Veron and Pichon, 1976). Recent studies have therefore used genetic and morphometric evidence to differentiate species within the Pocilloporids, with Schmidt-Roach et al. (2014) describing eight species within the *P. damicornis* species complex (including a novel taxon *Pocillopora bairdi*). Johnston et al. (2022) genetically identified 673 colonies in the *Pocillopora* species complex around Mo'orea, French Polynesia, and found that the 4 most abundant species were often visually indistinguishable yet exhibited clear physiological differences in response to light and water temperature variance. These studies indicate that while many Pocilloporid species are visually indistinguishable, genetic differences may be associated with distinct traits that affect their success in a changing environment. The misinterpretation of taxonomical units within species, e.g. for *Pocillopora damicornis* (Schmidt-Roach et al., 2012), contributes to challenges of disentangling morphological and life history variation with environment. This further highlights the complexity and plasticity of the *Pocilloporid* family. The wide variety of responses recorded between coral host, algal symbionts, bacterial microbiome ("holobiont"), and the holobiont–environment interaction, suggests that generalist corals such as the Pocilloporidae may have the breadth of plastic traits necessary to survive in a

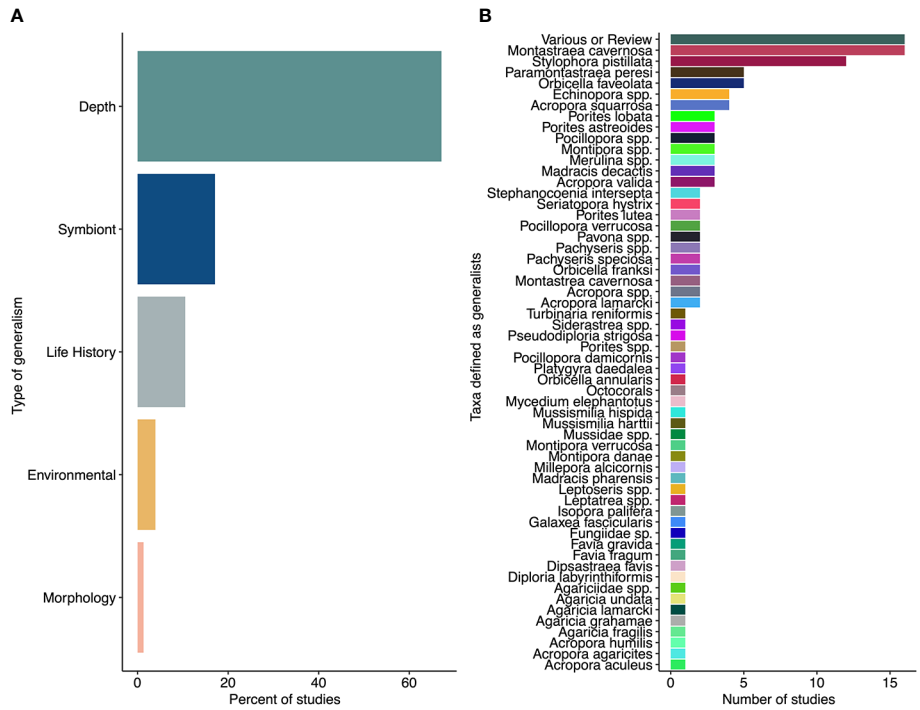

FIGURE 1
(A) Percentage of the 72 studies included in the present manuscript that are focused around each category of generalism. **(B)** Number of studies per taxa considered "generalists" in the 72 studies considered herein. "Various or Review" refers to studies that didn't specify taxa or that contained mention of the terms <*generalist AND coral*> in a review, respectively.

TABLE 2 A summary of trait-based classifications used by Darling et al. (2012), Darling et al. (2019), and Sommer et al. (2014) to define generalist species and three life-history forms contained within: weedy, stress-tolerant, and competitive.

		Generalist	Weedy	Stress-Tolerant	Competitive
Morphology	Massive/ Encrusting	Darling et al., 2012		Darling et al., 2012; Darling et al., 2019	
	Branching	Darling et al., 2012; Sommer et al., 2014	Darling et al., 2012; Sommer et al., 2014		Darling et al., 2012; Sommer et al., 2014; Darling et al., 2019
	Plating	Darling et al., 2012; Sommer et al., 2014			Darling et al., 2012; Darling et al., 2019
Reproductive Mode	Brooding	Darling et al., 2012	Darling et al., 2012		
	Broadcast			Darling et al., 2012	Darling et al., 2012
Colony Size	Small		Darling et al., 2012		
	Large	Darling et al., 2012		Darling et al., 2012, Darling et al., 2019	Darling et al., 2012
Growth Rate	Slow			Darling et al., 2019	
	Moderate	Darling et al., 2012			
	Fast		Darling et al., 2012; Darling et al., 2019		Darling et al., 2012; Darling et al., 2019
Fecundity	Low		Darling et al., 2012		
	High			Darling et al., 2012	
Framework-Building	Yes			Darling et al., 2019	Darling et al., 2019
	No	Darling et al., 2019	Darling et al., 2019		
Summary of Findings		Plating or laminar corals able to exist in a broad range of environments; may represent a subdominant group of deeper-water taxa	Fragile, low-profile colonies that contribute little to structural complexity and architectural structre of reefs	Large, slow-growing, hardy reef-building corals that can build complex reef structures to maintain coral-dominated reefs	Fast-growing, branching and plating reef-building corals that are vulnerable to multiple stressors
Pocilloporid species defined by Darling et al. (2019)		*Pocillopora aliciae, Pocillopora grandis, Pocillopora ligulata, Pocillopora meandrina, Pocillopora verrucosa, Pocillopora woodjonesi*	*Pocillopora damicornis*		

This table highlights the ambiguity and overlap between life history strategies and traits of reef corals, further highlighting a need to clearly define traits of generalist species.

changing world. Here we review (1) the traits of the Pocilloporid holobiont associated with environmental generalism; (2) the aspects of holobiont–environment interaction that would support the assumption of environmental generalism in this genera; and (3) the intersection of environmental generalism, holobiont structure, and the restructuring of a diverse range of coral habitats across Australia's east coast.

2 Generalist traits and the Pocilloporid holobiont

2.1 Morphological plasticity

Pocilloporid corals have a high degree of plasticity in overall skeletal morphology across environments (Todd, 2008; Johnston et al., 2017). Pocilloporids increase in compactness with increasing water motion (Kaandorp, 1999), vary in branch structure concurrent with degree of reef exposure (Lesser et al., 1994), and can appear elongate in subtropical regions while being robust in tropical regions (Schmidt-Roach et al., 2014). Furthermore, water flow and wave motion were found to systematically ordinate *Pocillopora* colony structure in Mo'orea, French Polynesia (Corso et al., 2022), due to physical forcing that likely aligns colonies with the dominant direction of the wave energy. Pocilloporids can also exhibit microstructural plasticity in response to light, water movement, and depth. Pocilloporid microstructure is influenced by environmental parameters, for example significant variation in 17 micro- and two macrostructural characteristics was observed in *Pocillopora verrucosa* colonies found between 7 and 38–45m depth (Gélin et al., 2018).

2.2 Tissue structure and within-colony symbiont distribution

Biological traits of tissue structure and its influence on symbiont distribution within a colony are believed to support vast

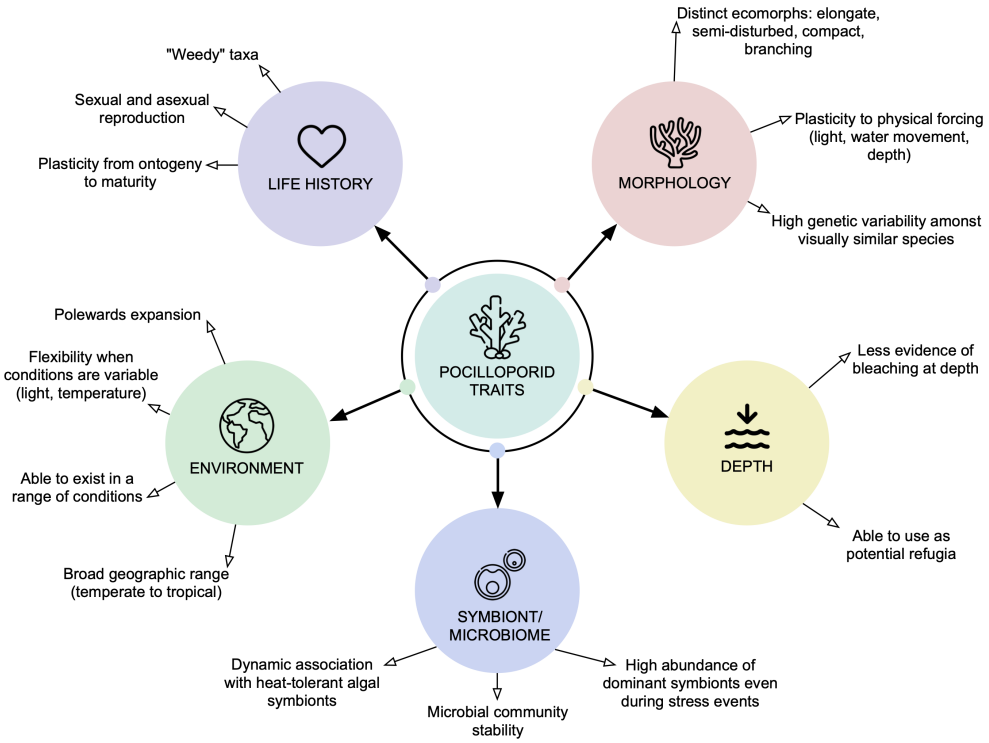

FIGURE 2
A schematic illustrating the five domains of generalist species defined in the literature search conducted herein, and how traits common to Pocilloporids apply to each domain. Black text arrows indicate how Pocilloporids may respond to influence their success when environmental pressures (e.g. increased light, rising temperatures, physical forcing) are applied.

environmental tolerance, including depth and light tolerance. In a study by Terraneo et al., examining symbiont types in shallow and mesophotic corals in the Red Sea, *Durusdinium* spp., known to assist with stress and thermal tolerance, was found predominately in shallow water corals compared to mesophotic corals (Terraneo et al., 2023). This suggests that symbiont distribution may be host and environment specific. Pocilloporids, characterised by an imperforate tissue structure that lacks intercalating tissues in a skeletal matrix (Yost et al., 2013), exhibit adaptability to diverse environmental conditions due to their shallow tissue depth. This tissue structure that predominantly extends across the surface of the skeleton contrasts with the tissue structure within the matrix of the colonial skeleton that is seen in perforate corals. Another potential contributing factor to the flexibility of Pocilloporids across different depths is their highly variable symbiont distribution related to light penetration and amplification within the colonies (Terán et al., 2010). Interestingly, Pocilloporids are the only genera that have been linked to polyp bail out responses (Fordyce et al., 2017; Chuang and Mitarai, 2020; Gösser et al., 2021), wherein individual polyps disassociate from a colony under stress and re-settle on the benthic substrate. It is important to note that to date the role of polyp bailout responses in Pocilloporid recovery of coral cover (Fordyce et al., 2017) following severe bleaching events has not been well investigated.

2.3 Bacterial microbiome stability

Several thousand microbes have been discovered within the coral microbiome (Rohwer et al., 2002). These are comprised of archaea, bacteria, viruses and Symbiodiniaceae (*Symbiodinium*) which inhabit the coral tissues, skeleton, mucus and gastrovascular cavity (Osman et al., 2018). These microbial interactions can either be mutualistic, parasitic or symbiotic interactions (Aranda et al., 2016). The ubiquitous distribution of Pocilloporid corals across environments have made them a well-studied target in coral bacterial microbiome research since 2018, characterising the *Pocillopora* microbiome across the Indo-Pacific and Red Sea. There also evidence that the coral microbial associations with *P. damicornis* may be a factor influencing bleaching response in these corals (Gilbert et al., 2012); namely, widely observed microbial patterns in response to bleaching may contribute to *Pocillopora*'s classification as a generalist. These include microbial stability during bleaching and across different environmental conditions (Ziegler et al., 2019; Brener-Raffalli et al., 2018; Pogoreutz et al., 2018; Epstein et al., 2019; Maher et al., 2020; Bergman et al., 2021). Some studies have found that despite severe bleaching in *P. damicornis* (e.g. loss of symbionts, but no mortality), bacterial communities did not increase in diversity, change, or become pathogen dominated; rather, the

community structure resembled that of healthy *P. damicornis* colonies (Bergman et al., 2021). Similar findings have been observed in *P. damicornis* larvae, where *Symbiodinium* cell densities of larvae decreased under high temperature conditions, but no reduced survivorship was observed (Haryanti et al., 2015). Bacterial shifts in response to bleaching have been observed, for example shifts in *Symbiodinium*-associated partner bacteria, such as *Lactococcus* and *Bacillus*, in *Pocillopora verrucosa* colonies during a natural bleaching event in the South China Sea (Yang et al., 2021). Interestingly, in a study of *P. acuta*, the microbiome was found to respond rapidly and flexibly to transplantation in Singapore, becoming similar to that of the local colonies at the transplanted reef within 1–2 days of transplantation (Deignan and McDougald, 2022). Even in stable communities, *Endozoicomonas* is a bacterial associate consistently found in the microbiome of Pocilloporid corals (Pogoreutz et al., 2018; Epstein et al., 2019; Voolstra and Ziegler, 2020; Ricci et al., 2022), with Maher et al. (2019) reporting *Endozoicomonas* dominate *Pocillopora* microbiomes that have declined in overall diversity. Microbial stability in *Pocillopora* in response to warming may contribute to its role as a generalist species on reefs.

2.4 Photoendosymbiont and holobiont bleaching responses

In Pocilloporid corals *Symbiodinium* are transferred maternally, leading to co-evolution with the host and species-specific associations of symbionts irrespective of geography (Pinzón and LaJeunesse, 2011; Schmidt-Roach et al., 2013a; Brener-Raffalli et al., 2018). Stability in patterns and composition of *P. damicornis*-associated Symbiodiniaceae has been found between adults and juveniles in the South China Sea irrespective of exposure to stress (i.e. ocean acidification), with a consistent dominance of the thermally tolerant endosymbiont *Durusdinium* spp. (Zhou et al., 2021). Endosymbiont population stability has also been observed in adult *Pocillopora*, with the stress-tolerant *Durusdinium* largely dominating the Symbiodiniaceae population in *P. acuta* throughout bleaching response of the host coral (Poquita-Du et al., 2020a; Poquita-Du et al., 2020b). In the Red Sea, where there are strong environmental gradients from north to south, *Symbiodinium microadriaticum* (type A1) has been found to dominate across a latitutinal gradient (Sawall et al., 2014). While the dominant resident *Symbiodinium* in *Pocillopora* corals often remain at a high abundance, even during stress events (e.g. cold-water bleaching, (McGinley et al., 2012), there is also some evidence of flexibility in host–symbiont combinations with variability across sites (Cunning et al., 2013) or environments (Ros et al., 2021; Botté et al., 2022). Observed interactions between physiological performance, host genotype, and symbiont communities in *P. damicornis*, as observed between flat or slope reef habitats of Australia's Heron Island in Marhoefer et al. (2021), emphasise that local adaptation of colonies as a product of environmental factors is also possible and should be accounted for.

3 The generalist holobiont–environment interaction and a changing climate

The largest influences on corals is the availability of photosynthetically available radiation (PAR), which causes variations in morphology, skeletal structures, photosynthetic traits, heterotrophic feeding, and Symbiondinaceae genera (Martinez et al., 2020). Generalist species are regarded as likely to be more successful than specialists as the climate continues to change (Clavel et al., 2011; Chichorro et al., 2019) due to their ability to adjust to these influences in their environment. Understanding the holobiont traits that contribute to environmental generalism is critical to predicting the structure of reefs under future scenarios. As global climate change continues to drive ecosystem change and novel environmental conditions become increasingly prevalent, the hypothesised increased role of environmental generalists in ecosystem stabilisation is evident (Graham et al., 2014; Williams and Graham, 2019). A recent study conducted on the reefs of French Polynesia investigating a 26-year monitoring database found that corals in the genus *Pocillopora* now make up 84% of the total recovery rate on the reef following disturbance (Pérez-Rosales et al., 2021). While the success of some genera on disturbed reefs is beneficial for overall coral coverage, a convergence towards post-disturbance communities less diverse and dominated by a single genera, morphology or phenotype (as shown by Pérez-Rosales et al. (2021) for 5 out of the 7 reefs) is also discussed as a key risk of sudden ecosystem declines under further disturbance events (Dalin et al., 2009; Palumbi et al., 2009; Lin, 2011). Palumbi et al. (2009) emphasise the importance of preserving biodiversity on reefs, as communities dominated by a single genus are likely have a more limited range of functions in response to disturbance than reefs composed of a diverse range of genera. Dominance of a single genera, especially one that is visually indistinguishable from other species within its genera, may be due to niche differences in co-occurring cryptic species. For example, Johnston et al. (2022) found greater differential abundances of *Pocilloporid* species across depths than amongst sites separated by several kilometers. The four most abundant species observed in this study were visibly indistinguishable at the gross colony level, yet exhibited differences in their associations and response to light irradiance and water temperature that may further promote their proliferation across reef environments with potentially varying degrees of generalism by species (Johnston et al., 2022).

Recent monitoring on the GBR following severe bleaching events of 2016–20 have also found an increase in dominance of *Pocillopora* species over the previously dominant specialist *Acropora* species (AIMS, 2021), noting that an increase in cover of a single genera had the potential to put the reefs at greater risk in future events. Therefore, the role of environmental generalist species (those with greater plasticity for a range of some conditions) will be uncertain in highly dynamic marine

environments, particularly those environments with severe and frequent extreme conditions (Munday, 2004; Camp et al., 2018).

As warming on temperate, subtropical, and tropical reefs continues to drive the emergence of novel ecosystems, efforts in conservation and ecosystem rehabilitation, repair, and restoration are now based around supporting (repair and rehabilitation) or actively undertaking (restoration) reconstruction of altered and degraded environments (Fox et al., 2019; Vardi et al., 2021; Shaver et al., 2022). Successful ecosystem repair, reconstruction or restoration involves identifying the target organisms that can acclimate and proliferate in both current and predicted future environmental conditions (Prober et al., 2015; van Oppen et al., 2017; Vardi et al., 2021; Shaver et al., 2022). Understanding the physiological range of the target organism in a dynamic environment for these types of conservation efforts will therefore be the cornerstone of the science of conservation ecology on coral reefs. Detailed understanding of the plasticity of the biological traits which underpin an organism's success across a range of environment parameters will be key for conservation efforts, particularly those focused on organisms that show resilience and environmental plasticity (Kimball et al., 2016; Boström-Einarsson et al., 2020; Shaver et al., 2022). The broad similarities amongst Pocilloporid species in the relationship between morphology, microbiome, and plasticity across sites or environmental conditions are therefore potentially key factors contributing to the success of this genera.

4 Australia as a case study: are there locations in eastern Australia where coral reefs are resistant to environmental change?

Australia's reefs have been subject to the impacts of climate change in recent years, and we focus specifically on several examples where reefs have been impacted by warming. We continue to build on the aforementioned point that generalist species may be better suited to acclimate to current environmental conditions (e.g. warming), but that it is critical to understand what role they will play in future reef conditions or in the highly dynamic marine environments mentioned herein. The majority of Australia's coral reef ecosystems extend across approximately 344,400 km^2 of the continent's east coast, which includes the ecosystems of tropical coral reefs, subtropical coral reefs, and high-latitude coral reefs (Great Barrier Reef Marine Park Authority, 2012; Figure 3). Most tropical corals are found 30–200 km offshore along the shallow inshore and lagoonal reefs, submerged reefs, mesophotic and deep-water coral reefs of the Great Barrier Reef/Coral Sea (Olsson et al., 2008). Subtropical continental shelf coral populations are also found along approximately 900 km of continental shelf from the southern Great Barrier Reef to the Solitary Islands, with temperate populations now being reported as far south as Sydney Harbour (Harriott and Banks, 1995; Harriott and Smith, 2002; Linklater et al., 2016; Roelfsema et al., 2016; Linklater et al., 2018; Linklater et al., 2019). Coral populations within the subtropical-to-temperate transition zone of Eastern Australia include marine habitats with unique assemblages of corals, sea grasses, kelps and turfs (Wilson and Harrison, 2003; Vergés et al., 2016; Sommer et al., 2017; Vergés et al., 2019). Further south, merging temperate and subtropical waters supports the development of new species, unique species interactions, and distinct habitats on the world's most southern coral reef, World Heritage-listed Lord Howe Island (Harriott et al., 1995; Noreen et al., 2009; Edgar et al., 2010).

Coral reefs within Australia's southern Great Barrier Reef and Great Southern Reef, particularly those at the convergence of sub-tropical and temperate zones, are as such experiencing climate mediated changes to species distribution and abundance, benthic habitat change, and the range extension of tropical species (Pandolfi et al., 2003; Brandl et al., 2019; Eddy et al., 2021). Warming oceans are driving high coral mortality, changes to population structure, emergence of new diseases, reduced growth, and reduced recruitment even on high-latitude reefs (generally outside of 30° N or S). Most evident of this problem is the severity and frequency of mass coral bleaching events now increasingly recorded in corals within Australia's understudied high-latitude reefs. For example, bleaching was recorded at Lord Howe Island in 1998, 2005, 2010, 2011 and 2019, one of the highest frequencies of coral bleaching events reported in Australia (Harrison et al., 2011; Dalton et al., 2020; Steinberg et al., 2022). Additionally, mass bleaching affected 22 high-latitude coral assemblages found south of the GBR in 2016 (Kim et al., 2019). Genetic evidence shows that connectivity to larger metapopulations is limited for corals growing at the southern edge of their species range (Noreen et al., 2015; Mizerek et al., 2021), resulting in high levels of evolutionary novelty (Miller and Ayre, 2008; Noreen et al., 2009; Schmidt-Roach et al., 2013a; Noreen et al., 2015) in these locations.

The observed species composition changes observed on temperate to subtropical reefs have the potential to profoundly alter temperate marine ecosystems within the coming decades. The question arises as to whether generalist corals will be a feature of Australia's changing east coast coral reef ecosystems as climate change continues to impact these regions. The response of generalist species, specifically Pocilloporids, to climate change and ocean warming in Australia has varied by region. For example, bleaching events occurring on the tropical reefs of the Great Barrier Reef have impacted almost all species (Stuart-Smith et al., 2018), with over 43% of reefs bleaching in 1998, 56% bleaching in 2002, and 85% in 2016 (Hughes et al., 2017) and region-wide coral bleaching occurring from February–April 2020 and December–March 2022 (Ainsworth et al., 2021, GBRMPA Reef Snapshot, 2022). *Pocillopora* spp. has been categorised as bleaching-sensitive on the GBR, showing declines in small colonies of up to 28% on the reef crest and 30.2% on the reef slope following mass coral bleaching in 2016/2017 (Dietzel et al., 2020). In the Keppel Island archipelago, situated on the southern inshore GBR, 21% of living corals were affected by bleaching, with *Pocillopora* and branching *Acropora* the most affected (Kennedy et al., 2017). Botté et al. (2022) also found a degree of mild, moderate, or severe bleaching in all *Pocillopora acuta* colonies sampled between 3.5–5.6°C-weeks on Pandora and Havannah Island reefs within the Palm Island group on the central GBR. However, in the Coral Sea, partial mortality was lower in

Pocillopora species during bleaching in 2020 than in 2018/2019 prior to bleaching, and overall incidence of partial mortality in all species surveyed remained below 5% (Burn et al., 2022). Outside of Australia, co-evolved mutualisms between *Pocillopora* corals and heat-tolerant symbionts have been found with few observable tradeoffs, suggesting that increased prevalence of these mutualisms will contribute to reef growth and the proliferation of *Pocillopora* spp. in warming environments (Mexico; Turnham et al., 2023). An additional study in Panama suggests that *Pocillopora* will be selected over other coral genera in warming regions, due to associations with thermotolerant symbionts, the potential acquisition of thermally tolerant symbionts during heat stress, and generalist traits such as a high growth rate and capacity for asexual reproduction through fragmentation (Palacio-Castro et al., 2023). However, in an Australian context, dominance of Pocilloporids on Australia's reefs will come with a reduction in non-Pocilloporid species in a formerly highly diverse region. This reduction in non-Pocilloporid species diversity may impact ecological functions and reef resilience to other stressors in highly variable, marginal environments.

In subtropical or marginal reefs, such as those around Norfolk Island and Lord Howe Island, the reefs are dominated by subtropical and temperate species and presumed to be isolated from surrounding bioregions. This creates a unique environment with a high presence of endemic fauna and peripheral populations vulnerable to extinction (van der Meer et al., 2015; Edgar et al., 2017). However, there has been limited research to date focused on coral populations in these subtropical environments, and how generalist species and the overall coral populations will be affected by warming oceans is largely unknown. At Lord Howe Island between 2005 and 2007 up to 95% of the coral community in the lagoon bleached, with 41% mortality occurring in *Pocillopora damicornis* as well as evidence of minor bleaching in Poritidae and Acroporidae (Dalton et al., 2011). In 2010, 2011 and 2019, bleaching was also observed in lagoonal sites at Lord Howe Island, with up to 99% of colonies bleached at shallow lagoon sites and *Pocillopora, Stylophora, Seriatopora*, and *Porites* as the most affected species (Dalton et al., 2020). The responses of Pocilloporids to warming are clearly variable across environments.

In temperate reefs, such as the continental coral reefs of the eastern extent of the Great Southern Reef (GSR) including the Solitary Islands Marine Park (SIMP) and the associated reefs of Australia's southeast coast, ocean warming is contributing to range contractions, habitat losses, changes in energy pathways, and the

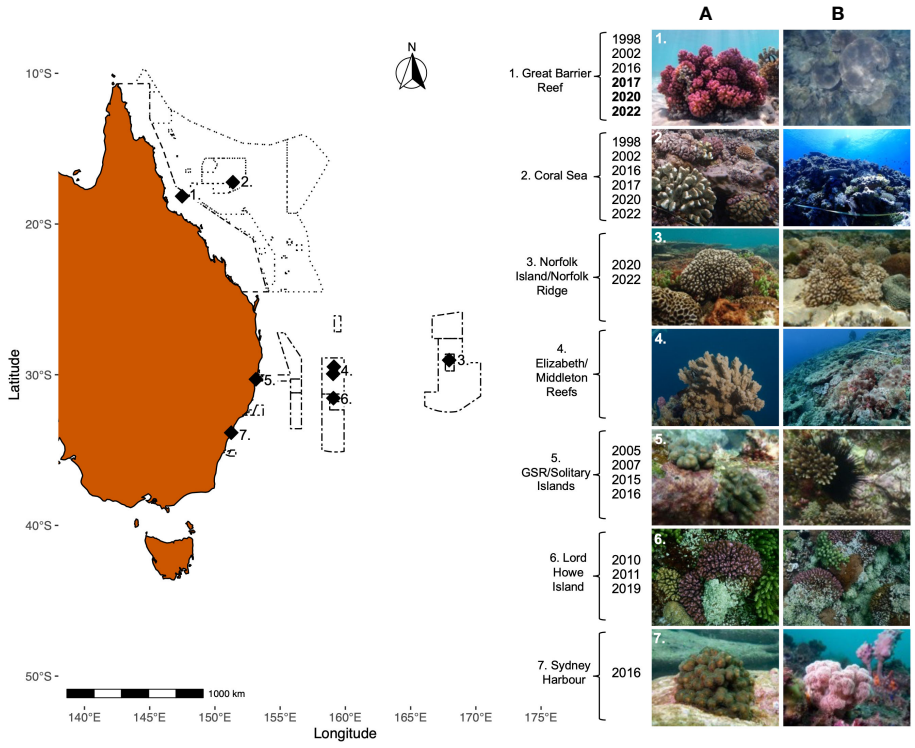

FIGURE 3
A map of reef locations included along Australia's east coast. Long dashes border the Great Barrier Reef Marine Park, dotted lines border the Coral Sea Marine Park, and dot-dash lines border the Temperate East Australian Marine Park Network. Sites are: 1). Great Barrier Reef, 2). Coral Sea, 3). Norfolk Island and Norfolk Ridge, 4). Elizabeth and Middleton Reefs, 5). Solitary Islands Marine Park, 6). The Lord Howe Seamount Chain, Lord Howe Island, and Ball's Pyramid, and 7). Sydney Harbour. For images on the right-hand side, numbers correspond to reef location and letters depict **(A)** an example of a Pocilloporid from each location and **(B)** a whole-reef image from each location. All pictures taken by Jessica Bergman, with the exception of images reproduced with permission: 2A, 2B: Parks Australia Coral Sea Marine Park Coral Reef Health Report; 4A, 4B: Antonia Cooper; 7A, 7B: John Turnbull. Bleaching events recorded at each location are listed along the left-hand side of the photos. For 1). Great Barrier Reef: Bolded dates are years when both the N. GBR and S. GBR bleached, and dates not in bold are years when only the N. GBR bleached.

facilitation of species (Wernberg et al., 2013; Vergés et al., 2014; Tuckett et al., 2017; Smith et al., 2021). In surveys of a bleaching event extending along the eastern coast of Australia from Flinders Reef to Southwest Rocks (including the SIMP), *Pocillopora* bleached more at sites where temperatures were historically cooler and overall, *Pocillopora* and *Porites* were more susceptible to bleaching than *Acropora, Goniastrea*, and *Turbinaria* (Kim et al., 2019). Bleaching severity also increased for *Pocillopora* spp. with latitude without a significant change in relative abundance (Kim et al., 2019). Abrupt changes to the size structure of the endemic *Pocillopora aliciae* were also noted following a bleaching event in 2016, demonstrating a strong association between heat stress and declining *P. aliciae* population density (Lachs et al., 2021). *P. aliciae* is a subtropical endemic branching coral (Schmidt-Roach et al., 2013a; Schmidt-Roach et al., 2013b; Schmidt-Roach et al., 2014), which is hypothesised to have extended its range into temperate (18.8–24.7°C 2012–2022 monthly average) habitats of Sydney NSW (Booth and Sear, 2018). Establishment of *P. aliciae* in temperate waterways has been suggested to accelerate tropicalization of coastal Sydney and facilitate benthic habitat complexity for fish communities, although further examination is needed to determine the limits of coral range extension into high-latitude regions (Abrego et al., 2021). However, despite generally exhibiting an enhanced stress tolerance characteristic of corals in a fluctuating environment (Oliver and Palumbi, 2011), *P. aliciae* has been deemed the least viable coral species under thermal stress at the SIMP (Cant et al., 2021) and is categorised as susceptible to thermal stress.

This is further evident with the 2016 El Niño and a corresponding increase in seawater temperatures of > 2°C above the long-term mean summer maxima causing bleaching in up to 60% of all corals in Sydney Harbour (Goyen et al., 2019). Incorporating the response of Pocilloporid species under thermal stress into the response of the benthic coral community as a whole, there is evidence of an overall decline in total coral cover at the SIMP between 1990 and 2014 (Mizerek et al., 2021). Taken together, these studies suggest that the response of Pocilloporid species to thermal stress within the reefs of eastern Australia are still equivocal and highly variable by region, and likely depend on location-specific adaptations.

5 Conclusion

Community reassembly, altered dispersal patterns, and novel species interactions, including novel holobiont–environment interactions, are hypothesised to be involved in the formation of entirely novel ecosystems (Spalding et al., 2007; Sommer et al., 2014; Sommer et al., 2017; Sommer et al., 2018). Ocean warming is hypothesised to warm regions considered marginal environments for coral growth and expand coral dominance in these locations (Beger et al., 2014; Tuckett et al., 2017; Booth and Sear, 2018; Nakabayashi et al., 2019; González-Pech et al., 2022). As such, recent studies have focused on how ocean warming may drive the development of novel coral ecosystems in high-latitude reef habitats, described as "changes in species configurations, interactions, and functions, within the parameter space of calcifying coral-dominated reefs" (Graham et al., 2014).

However, warming is also driving marine heatwaves and bleaching events, as seen in the past decades across Australia's subtropical and temperate reef systems and coral populations. In Australia alone, coral bleaching has been observed in high-latitude locations within the last two decades with a frequency and severity comparable to that of tropical locations. In Australia bleaching events have been reported at Lord Howe Island (Harrison et al., 2011; Dalton et al., 2020), Rottnest Island (Thomson et al., 2011; le Nohaïc et al., 2017), eastern New South Wales (Kim et al., 2019), Sydney Harbour (Goyen et al., 2019), and the Houtman Abrolhos Islands (Abdo et al., 2012; Smale et al., 2012). One of the most extreme examples of changing distribution is the expansion of the coral *Pocillopora aliciae* into temperate marine environments close to Sydney Harbour (González-Pech et al., 2022). It is therefore critical to understand which coral species, in which locations and by which means, are functioning as generalists as these species are predicted to be better able to withstand a changing environment. Generalist species may provide new ecological opportunities and play critical functional roles as coral reefs reconfigure under climate change. More research is warranted to define generalist traits and which species display them.

Author contributions

JB reviewed the literature and wrote the manuscript with contribution from TA, PS, and ZR. All authors contributed to the article and approved the submitted version.

Funding

This project was supported by a UNSW Scientia Scholarship, Australian Government Research Training Program Scholarship, and the American Australian Association's Graduate Education Fund Scholarship to JB. In addition, TA was supported by UNSW Scientia Funding and research conducted with Parks Australia.

Conflict of interest

The authors declare that the research was conducted in the absence of any commercial or financial relationships that could be construed as a potential conflict of interest.

Publisher's note

References

Abdo, D. A., Bellchambers, L. M., and Evans, S. N. (2012). Turning up the heat: increasing temperature and coral bleaching at the high latitude coral reefs of the Houtman Abrolhos Islands. *PloS One* 7, e43878. doi: 10.1371/journal.pone.0043878

Abrego, D., Howells, E. J., Smith, S. D. A., Madin, J. S., Sommer, B., Schmidt-Roach, S., et al. (2021). Factors limiting the range extension of corals into high-latitude reef regions. *Diversity* 13, 632. doi: 10.3390/d13120632

AIMS (2021). *Annual summary report of coral reef condition 2020/2021*. Townsville, QLD: Australian Institute of Marine Science.

AIMS (2022). *Annual summary report of coral reef condition 2021/2022*. Townsville, QLD: Australian Institute of Marine Science.

Ainsworth, T. D., Leggat, W., Silliman, B. R., Lantz, C. A., Bergman, J. L., Fordyce, A. J., et al. (2021). Rebuilding relationships on coral reefs: Coral bleaching knowledge-sharing to aid adaptation planning for reef users. *BioEssays* 43, 1–9. doi: 10.1002/bies.202100048

Aranda, M., Li, Y., Liew, Y. J., Baumgarten, S., Simakov, O., Wilson, M. C., et al. (2016). Genomes of coral dinoflagellate symbionts highlight evolutionary adaptations conducive to a symbiotic lifestyle. *Sci. Rep.* 6, 39734. doi: 10.1038/srep39734

Bairos-Novak, K. R., Hoogenboom, M. O., van Oppen, M. J. H., and Connolly, S. R. (2021). Coral adaptation to climate change: Meta-analysis reveals high heritability across multiple traits. *Glob Chang Biol.* 27, 5694–5710. doi: 10.1111/gcb.15829

Beger, M., Sommer, B., Harrison, P. L., Smith, S. D. A., and Pandolfi, J. M. (2014). Conserving potential coral reef refuges at high latitudes. *Divers. Distrib* 20, 245–257. doi: 10.1111/ddi.12140

Benayahu, Y., Bridge, T. C. L., Colin, P. L., Liberman, R., McFadden, C. S., Pizarro, O., et al. (2019). Octocorals of the Indo-Pacific. *Mesophotic Coral Ecosyst.*, 709–728. doi: 10.1007/978-3-319-92735-0_38

Bergman, J. L., Leggat, W., and Ainsworth, T. D. (2021). The meta-organism response of the environmental generalist Pocillopora damicornis exposed to differential accumulation of heat stress. *Front. Mar. Sci.* 8. doi: 10.3389/fmars.2021.664063/

Bloomberg, J., and Holstein, D. M. (2021). Mesophotic coral refuges following multiple disturbances. *Coral Reefs* 40, 821–834. doi: 10.1007/S00338-021-02087-W

Bollati, E., Plimmer, D., D'Angelo, C., and Wiedenmann, J. (2017). FRET-mediated long-range wavelength transformation by photoconvertible fluorescent proteins as an efficient mechanism to generate orange-red light in symbiotic deep water corals. *Int. J. Mol. Sci.* 18, 1174. doi: 10.3390/IJMS18071174

Bongaerts, P., Carmichael, M., Hay, K. B., Tonk, L., Frade, P. R., and Hoegh-Guldberg, O. (2015a). Prevalent endosymbiont zonation shapes the depth distributions of scleractinian coral species. *R Soc. Open Sci.* 2, 140297. doi: 10.1098/rsos.140297

Bongaerts, P., Frade, P. R., Hay, K. B., Englebert, N., Latijnhouwers, K. R. W., Bak, R. P. M., et al. (2015b). Deep down on a Caribbean reef: lower mesophotic depths harbor a specialized coral-endosymbiont community. *Sci. Rep.* 5, 1–9. doi: 10.1038/srep07652

Bongaerts, P., Frade, P. R., Ogier, J. J., Hay, K. B., van Bleijswijk, J., Englebert, N., et al. (2013). Sharing the slope: Depth partitioning of agariciid corals and associated Symbiodinium across shallow and mesophotic habitats (2-60 m) on a Caribbean reef. *BMC Evol. Biol.* 13, 1–15. doi: 10.1186/1471-2148-13-205

Bongaerts, P., Ridgway, T., Sampayo, E. M., and Hoegh-Guldberg, O. (2010). Assessing the "deep reef refugia" hypothesis: focus on Caribbean reefs. *Coral Reefs* 29, 309–327. doi: 10.1007/S00338-009-0581-X

Bongaerts, P., Riginos, C., Brunner, R., Englebert, N., Smith, S. R., and Hoegh-Guldberg, O. (2017). Deep reefs are not universal refuges: Reseeding potential varies among coral species. *Sci. Adv.* 3, e1602373. doi: 10.1126/sciadv.1602373

Bongaerts, P., and Smith, T. B. (2019). Beyond the "Deep Reef Refuge" hypothesis: a conceptual framework to characterize persistence at depth. *Coral Reefs World* 12, 881–895. doi: 10.1007/978-3-319-92735-0_45

Booth, D. J., and Sear, J. (2018). Coral expansion in Sydney and associated coral-reef. fishes. *Coral Reefs* 37, 995. doi: 10.1007/S00338-018-1727-5

Boström-Einarsson, L., Babcock, R. C., Bayraktarov, E., Ceccarelli, D., Cook, N., Ferse, S. C. A., et al. (2020). Coral restoration – A systematic review of current methods, successes, failures and future directions. *PloS One* 15, e0226631. doi: 10.1371/journal.pone.0226631

Botté, E. S., Cantin, N. E., Mocellin, V. J., O'Brien, P. A., Rocker, M. M., Frade, P. R., et al. (2022). Reef location has a greater impact than coral bleaching severity on the microbiome of Pocillopora acuta. *Coral Reefs* 41, 63–79. doi: 10.1007/s00338-021-02201-y

Brandl, S., Rasher, D., Côté, I., Casey, J., Darling, E., Lefcheck, J., et al. (2019). Coral reef ecosystem functioning: eight core processes and the role of biodiversity. *Front. Ecol. Environ.* 17, 445–454. doi: 10.1002/fee.2088

Brandtneris, V. W., Brandt, M. E., Glynn, P. W., Gyory, J., and Smith, T. B. (2016). Seasonal variability in calorimetric energy content of two caribbean mesophotic corals. *PloS One* 11, e0151953. doi: 10.1371/journal.pone.0151953

Brener-Raffalli, K., Clerissi, C., Vidal-Dupiol, J., Adjeroud, M., Bonhomme, F., Pratlong, M., et al. (2018). Thermal regime and host clade, rather than geography, drive Symbiodinium and bacterial assemblages in the scleractinian coral Pocillopora damicornis sensu lato. *Microbiome* 6, 39. doi: 10.1186/s40168-018-0423-6

Bridge, T. C. L., Luiz, O. J., Kuo, C. Y., Precoda, K., Madin, E. M. P., Madin, J. S., et al. (2020). Incongruence between life-history traits and conservation status in reef corals. *Coral Reefs* 39, 271–279. doi: 10.1007/S00338-019-01885-7

Bruno, J. F., and Selig, E. R. (2007). Regional decline of coral cover in the Indo-Pacific: Timing, extent, and subregional comparisons. *PloS One* 2, e711. doi: 10.1371/journal.pone.0000711

Brustolin, M. C., Nagelkerken, I., Ferreira, C. M., Goldenberg, S. U., Ullah, H., and Fonseca, G. (2019). Future ocean climate homogenizes communities across habitats through diversity loss and rise of generalist species. *Glob Chang Biol.* 25, 3539–3548. doi: 10.1111/gcb.14745

Burgess, S. C., Johnston, E. C., J Wyatt, A. S., Leichter, J. J., Edmunds, P. J., Johnston, E. C., et al. (2021). Response diversity in corals: hidden differences in bleaching mortality among cryptic Pocillopora species. *Ecology* 102, e03324. doi: 10.1002/ecy.3324

Burn, D., Matthews, S., Pisapia, C., Hoey, A., and Pratchett, M. (2022). Changes in the incidence of coral injuries during mass bleaching across Australia's Coral Sea Marine Park. *Mar. Ecol. Prog. Ser.* 682, 97–109. doi: 10.3354/meps13935

Burt, J. A., Camp, E. F., Enochs, I. C., Johansen, J. L., Morgan, K. M., Riegl, B., et al. (2020). Insights from extreme coral reefs in a changing world. *Coral Reefs* 39, 495–507. doi: 10.1007/S00338-020-01966-Y

Caballero Aragón, H., Armenteros, M., Perera Valderrama, S., Rey Villiers, N., Cobián Rojas, D., Campos Verdecia, K., et al. (2019). Ecological condition of coral reef assemblages in the Cuban Archipelago. *Mar. Biol. Rsrch* 15, 61–73. doi: 10.1080/17451000.2019.1577557

Cacciapaglia, C., and van Woesik, R. (2015). Reef-coral refugia in a rapidly changing ocean. *Glob Chang Biol.* 21, 2272–2282. doi: 10.1111/gcb.12851

Cairns, S. D. (2007). Deep-water corals: an overview with special reference to diversity and distribution of deep-water scleractinian corals. *B Mar. Sci.* 81, 311–322.

Camp, E., Edmondson, J., Doheny, A., Rumney, J., Grima, A., Huete, A., et al. (2019). Mangrove lagoons of the Great Barrier Reef support coral populations persisting under extreme environmental conditions. *Mar. Ecol. Prog. Ser.* 625, 1–14. doi: 10.3354/meps13073

Camp, E. F., Schoepf, V., Mumby, P. J., Hardtke, L. A., Rodolfo-Metalpa, R., Smith, D. J., et al. (2018). The future of coral reefs subject to rapid climate change: lessons from natural extreme environments. *Front. Mar. Sci.* 5. doi: 10.3389/fmars.2018.00004

Cant, J., Salguero-Gómez, R., Kim, S. W., Sims, C. A., Sommer, B., Brooks, M., et al. (2021). The projected degradation of subtropical coral assemblages by recurrent thermal stress. *J. Anim. Ecol.* 90, 233–247. doi: 10.1111/1365-2656.13340

Claar, D. C., Fabina, N. S., Putnam, H. M., Cunning, R., Sogin, E., Baum, J. K., et al. (2017). Embracing complexity in coral–algal symbioses. *Algal Cyanobacteria Symbioses*, 467–492. doi: 10.1142/9781786340580_0015

Chichorro, F., Juslén, A., and Cardoso, P. (2019). A review of the relation between species traits and extinction risk. *Biol. Conserv.* 237, 220–229. doi: 10.1016/j.biocon.2019.07.001

Chuang, P. S., and Mitarai, S. (2020). Signaling pathways in the coral polyp bail-out response. *Coral Reefs* 39, 1535–1548. doi: 10.1007/S00338-020-01983-X

Clavel, J., Julliard, R., and Devictor, V. (2011). Worldwide decline of specialist species: toward a global functional homogenization? *Front. Ecol. Environ.* 9, 222–228. doi: 10.1890/080216

Connell, J. H., Hughes, T. P., Wallace, C. C., Tanner, J. E., Harms, K. E., and Kerr, A. M. (2004). A long-term study of competition and diversity of corals. *Ecol. Monogr.* 74, 179–210. doi: 10.1890/02-4043

Cornwall, C. E., Comeau, S., Kornder, N. A., Perry, C. T., van Hooidonk, R., DeCarlo, T. M., et al. (2021). Global declines in coral reef calcium carbonate production under ocean acidification and warming. *P Natl. Acad. Sci.* 118, e2015265118. doi: 10.1073/pnas.2015265118

Cornwall, C. E., Comeau, S., Putnam, H., and Schoepf, V. (2022). Impacts of ocean warming and acidification on calcifying coral reef taxa: mechanisms responsible and adaptive capacity. *Emerg. Top. Life Sci.* 6, 1–9. doi: 10.1042/etls20210226

Corso, J., French, B., Edwards, C., Pedersen, N., Zgliczynski, B., Planes, S., et al. (2022). Non-random orientation of Pocillopora colonies on forereefs of Moorea, French Polynesia. *Mar. Ecol. Prog. Ser.* 693, 177-182. doi: 10.3354/meps14078

Courtney, T. A., Barnes, B. B., Chollett, I., Elahi, R., Gross, K., Guest, J. R., et al. (2020). Disturbances drive changes in coral community assemblages and coral calcification capacity. *Ecosphere* 11, e03066. doi: 10.1002/ecs2.3066

Courtney, T. A., Lebrato, M., Bates, N. R., Collins, A., de Putron, S. J., Garley, R., et al. (2017). Environmental controls on modern scleractinian coral and reef-scale calcification. *Sci. Adv.* 3. doi: 10.1126/sciadv.1701356

Cunning, R., Glynn, P. W., and Baker, A. C. (2013). Flexible associations between Pocillopora corals and Symbiodinium limit utility of symbiosis ecology in defining species. *Coral Reefs* 32, 795–801. doi: 10.1007/S00338-013-1036-Y

Dalin, P., Kindvall, O., and Björkman, C. (2009). Reduced population control of an insect pest in managed willow monocultures. *PloS One* 4, e5487. doi: 10.1371/journal.pone.0005487

Dalton, S. J., Carroll, A. G., Dalton, S. J., and Carroll, A. G. (2011). Monitoring coral health to determine coral bleaching response at high latitude eastern Australian reefs: an applied model for a changing climate. *Diversity* 3, 592–610. doi: 10.3390/d3040592

Dalton, S. J., Carroll, A. G., Sampayo, E., Roff, G., Harrison, P. L., Entwistle, K., et al. (2020). Successive marine heatwaves cause disproportionate coral bleaching during a fast phase transition from El Niño to La Niña. *Sci. Total Environ.* 715, 136951. doi: 10.1016/j.scitotenv.2020.136951

Darling, E. S., Alvarez-Filip, L., Oliver, T. A., McClanahan, T. R., and Côté, I. M. (2012). Evaluating life-history strategies of reef corals from species traits. *Ecol. Lett.* 15, 1378–1386. doi: 10.1111/j.1461-0248.2012.01861.x

Darling, E. S., McClanahan, T. R., Maina, J., Gurney, G. G., Graham, N. A. J., Januchowski-Hartley, F., et al. (2019). Social–environmental drivers inform strategic management of coral reefs in the Anthropocene. *Nat. Ecol. Evo.* 3, 1341–1350. doi: 10.1038/s41559-019-0953-8

de Bakker, D. M., Meesters, E. H., Bak, R. P. M., Nieuwland, G., and van Duyl, F. C. (2016). Long-term shifts in coral communities on shallow to deep reef slopes of Curaçao and Bonaire: Are there any winners? *Front. Mar. Sci.* 3. doi: 10.3389/fmars.2016.00247

Deignan, L. K., and McDougald, D. (2022). Differential response of the microbiome of Pocillopora acuta to reciprocal transplantation within Singapore. *Microb. Ecol.* 83, 608–618. doi: 10.1007/s00248-021-01793-w

Dennis, R. L. H., Dapporto, L., Fattorini, S., and Cook, L. M. (2011). The generalism–specialism debate: the role of generalists in the life and death of species. *Biol. J. Linn Soc.* 104, 725–737. doi: 10.1111/J.1095-8312.2011.01789.X

Dietzel, A., Bode, M., Connolly, S. R., and Hughes, T. P. (2020). Long-term shifts in the colony size structure of coral populations along the Great Barrier Reef. *P Roy Soc. B-Biol Sci.* 287, 20201432. doi: 10.1098/rspb.2020.1432

Dietzel, A., Connolly, S. R., Hughes, T. P., and Bode, M. (2021). The spatial footprint and patchiness of large-scale disturbances on coral reefs. *Glob Chang Biol.* 27, 4825–4838. doi: 10.1111/gcb.15805

Donovan, M. K., Burkepile, D. E., Kratochwill, C., Shlesinger, T., Sully, S., Oliver, T. A., et al. (2021). Local conditions magnify coral loss after marine heatwaves. *Science* 372, 977–980. doi: 10.1126/science.abd9464

Eckert, R. J., Studivan, M. S., and Voss, J. D. (2019). Populations of the coral species Montastraea cavernosa on the Belize Barrier Reef lack vertical connectivity. *Sci. Rep.* 9, 1–11. doi: 10.1038/s41598-019-43479-x

Eddy, T. D., Lam, V. W. Y., Reygondeau, G., Cisneros-Montemayor, A. M., Greer, K., Palomares, M. L. D., et al. (2021). Global decline in capacity of coral reefs to provide ecosystem services. *One Earth* 4, 1278–1285. doi: 10.1016/j.oneear.2021.08.016

Edgar, C. J., Ceccarelli, G. J., Stuart-Smith, D. D., and Cooper, R. D. (2017). Biodiversity survey of the temperate east coast commonwealth marine reserve network: Elizabeth & Middleton reefs, Lord Howe island & Norfolk island. *Reef Life Survey Foundation Incorporated*.

Edgar, G. J., Davey, A., Kelly, G., Mawbey, R. B., and Parsons, K. (2010). Biogeographical and ecological context for managing threats to coral and rocky reef communities in the Lord Howe Island Marine Park, South-Western Pacific. *Aquat Conserv.* 20, 378–396. doi: 10.1002/aqc.1075

Epstein, H. E., Torda, G., and van Oppen, M. J. H. (2019). Relative stability of the Pocillopora acuta microbiome throughout a thermal stress event. *Coral Reefs* 38, 373–386. doi: 10.1007/S00338-019-01783-Y

Eyal, G., Cohen, I., Eyal-Shaham, L., Ben-Zvi, O., Tikochinski, Y., and Loya, Y. (2019a). Photoacclimation and induction of light-enhanced calcification in the mesophotic coral Euphyllia paradivisa. *R Soc. Open Sci.* 6. doi: 10.1098/rsos.180527

Eyal, G., Eyal-Shaham, L., and Loya, Y. (2021). Symbiodiniaceae conduct under natural bleaching stress during advanced gametogenesis stages of a mesophotic coral. *Coral Reefs* 40, 959–964. doi: 10.1007/S00338-021-02082-1

Eyal, G., Tamir, R., Kramer, N., Eyal-Shaham, L., and Loya, Y. (2019b). The Red Sea: Israel. *Coral Reefs World* 12, 199–214. doi: 10.1007/978-3-319-92735-0_11

Fabina, N. S., Putnam, H. M., Franklin, E. C., Stat, M., and Gates, R. D. (2012). Transmission mode predicts specificity and interaction patterns in coral-symbiodinium networks. *PloS One* 7, e44970. doi: 10.1371/journal.pone.0044970

Fabina, N. S., Putnam, H. M., Franklin, E. C., Stat, M., and Gates, R. D. (2013). Symbiotic specificity, association patterns, and function determine community responses to global changes: defining critical research areas for coral-Symbiodinium symbioses. *Glob Chang Biol.* 19, 3306–3316. doi: 10.1111/gcb.12320

Feldman, B., Shlesinger, T., and Loya, Y. (2018). Mesophotic coral-reef environments depress the reproduction of the coral Paramontastraea peresi in the Red Sea. *Coral Reefs* 37, 201–214. doi: 10.1007/S00338-017-1648-8

Fordyce, A., Camp, E., and Ainsworth, T. D. (2017). Polyp bailout in Pocillopora damicornis following thermal stress. *F1000 Res.* 6, 687. doi: 10.12688/f1000research.11522.2

Fox, H. E., Harris, J. L., Darling, E. S., Ahmadia, G. N., Estradivari, and Razak, T. B. (2019). Rebuilding coral reefs: success (and failure) 16 years after low-cost, low-tech restoration. *Restor. Ecol.* 27, 862–869. doi: 10.1111/rec.12935

GBRMPA. (2017). *Final report: 2016 coral bleaching event on the Great Barrier Reef.* Townsville, QLD: Great Barrier Reef Marine Park Authority.

Garavelli, L., Studivan, M. S., Voss, J. D., Kuba, A., Figueiredo, J., and Chérubin, L. M. (2018). Assessment of mesophotic coral ecosystem connectivity for proposed expansion of a marine sanctuary in the Northwest Gulf of Mexico: Larval dynamics. *Front. Mar. Sci.* 5. doi: 10.3389/fmars.2018.00174

Gray, J. E. (1840). Pocilloporidae. *Synopsis of the Contents of the British Museum* 41, 54–84.

Gélin, P., Fauvelot, C., Bigot, L., Baly, J., and Magalon, H. (2018). From population connectivity to the art of striping Russian dolls: the lessons from Pocillopora corals. *Ecol. Evol.* 8, 1411–1426. doi: 10.1002/ece3.3747

Gilbert, J. A., Hill, R., Doblin, M. A., and Ralph, P. J. (2012). Microbial consortia increase thermal tolerance of corals. *Mar. Biol.* 159, 1763–1771. doi: 10.1007/S00227-012-1967-9

González-Pech, R., Hughes, D., Strudwick, P., Lewis, B., Booth, D., Figueira, W., et al. (2022). Physiological factors facilitating the persistence of Pocillopora aliciae and Plesiastrea versipora in temperate reefs of south-eastern Australia under ocean warming. *Coral Reefs* 41, 1239–1253. doi: 10.1007/S00338-022-02277-0

Gösser, F., Raulf, A., Mosig, A., Tollrian, R., and Schweinsberg, M. (2021). Signaling pathways of heat- and hypersalinity-induced polyp bailout in Pocillopora acuta. *Coral Reefs* 40, 1713–1728. doi: 10.1007/S00338-021-02191-X

Goodbody-Gringley, G., and Waletich, J. (2018). Morphological plasticity of the depth generalist coral, Montastraea cavernosa, on mesophotic reefs in Bermuda. *Ecology* 99, 1688–1690. Available at: https://www.jstor.org/stable/26625782.

Goyen, S., Camp, E. F., Fujise, L., Lloyd, A., Nitschke, M. R., LaJeunensse, T., et al. (2019). Mass coral bleaching of P. versipora in Sydney Harbour driven by the 2015–2016 heatwave. *Coral Reefs* 38, 815–830. doi: 10.1007/S00338-019-01797-6

Graham, N. A., Cinner, J. E., Norström, A. V., and Nyström, M. (2014). Coral reefs as novel ecosystems: embracing new futures. *Curr. Opin. Environ. Sustain* 7, 9–14. doi: 10.1016/j.cosust.2013.11.023

Graham, N. A. J., Jennings, S., MacNeil, M. A., Mouillot, D., and Wilson, S. K. (2015). Predicting climate-driven regime shifts versus rebound potential in coral reefs. *Nature* 518, 94–97. doi: 10.1038/nature14140

Graham, N. A. J., Wilson, S. K., Jennings, S., Polunin, N. V. C., Bijoux, J. P., and Robinson, J. (2006). Dynamic fragility of oceanic coral reef ecosystems. *P Natl. Acad. Sci.* 103, 8425–8429. doi: 10.1073/pnas.0600693103

Great Barrier Reef Marine Park Authority. (2012). *Great Barrier Reef general reference map*. Available at: http://hdl.handle.net/11017/869.

Grimsditch, G., Pisapia, C., Huck, M., Karisa, J., Obura, D., and Sweet, M. (2017). Variation in size frequency distribution of coral populations under different fishing pressures in two contrasting locations in the Indian Ocean. *Mar. Environ. Res.* 131, 146–155. doi: 10.1016/j.marenvres.2017.09.017

Guest, J. R., Tun, K., Low, J., Vergés, A., Marzinelli, E. M., Campbell, A. H., et al. (2016). 27 years of benthic and coral community dynamics on turbid, highly urbanised reefs off Singapore. *Sci. Rep.* 6, 1–10. doi: 10.1038/srep36260

S. M. Hamylton, P. Hutchings and Hoegh-Guldberg, (Eds.) (2022). *Coral reefs of Australia: perspectives from beyond the water's edge.* (Australia: CSIRO Publishing).

Harii, S., Hongo, C., Ishihara, M., Ide, Y., Kayanne, H., and Kayanne, H. (2014). Impacts of multiple disturbances on coral communities at Ishigaki Island, Okinawa, Japan, during a 15 year survey. *Mar. Ecol. Prog. Ser.* 509, 171–180. doi: 10.3354/meps10890

Harriott, V. J., and Banks, S. A. (1995). Recruitment of scleractinian corals in the Solitary Islands Marine Reserve, a high latitude coral-dominated community in Eastern Australia. *Mar. Ecol. Prog. Ser.* 123, 155–161. doi: 10.3354/meps123155

Harriott, V. J., Harrison, P. L., and Banks, S. A. (1995). The coral communities of Lord Howe Island. *Mar. Freshw. Res.* 46, 457–465. doi: 10.1071/mf9950457

Harriott, V., and Smith, S. (2002). Coral population dynamics in a subtropical coral community, Solitary Islands Marine Park, Australia. *Proc. 9th Int. Coral Reef Symposium* 1, 573–581.

Harrison, P., Dalton, S., and Carroll, A. (2011). Extensive coral bleaching on the world's southernmost coral reef at Lord Howe Island, Australia. *Coral Reefs* 30, 775. doi: 10.1007/s00338-011-0778-7

Haryanti, D., Yasuda, N., Harii, S., and Hidaka, M. (2015). High tolerance of symbiotic larvae of Pocillopora damicornis to thermal stress. *Zool Stud.* 54, 52. doi: 10.1186/s40555-015-0134-7

Hernandez-Agreda, A., Leggat, W., and Ainsworth, T. D. (2018). A comparative analysis of microbial DNA preparation methods for use with massive and branching coral growth forms. *Front. Microbiol.* 9. doi: 10.3389/fmicb.2018.02146

Hernandez-Agreda, A., Leggat, W., Bongaerts, P., and Ainsworth, T. D. (2016). The microbial signature provides insight into the mechanistic basis of coral success across reef habitats. *MBio* 4, e00560–e00516. doi: 10.1128/mBio.00560-16

Holstein, D. M., Paris, C. B., Vaz, A. C., and Smith, T. B. (2016). Modeling vertical coral connectivity and mesophotic refugia. *Coral Reefs* 35, 23–37. doi: 10.1007/S00338-015-1339-2

Holstein, D. M., Smith, T. B., Gyory, J., and Paris, C. B. (2015). Fertile fathoms: Deep reproductive refugia for threatened shallow corals. *Sci. Rep.* 5, 1–12. doi: 10.1038/srep12407

Hughes, T. P., Kerry, J. T., Álvarez-Noriega, M., Álvarez-Romero, J. G., Anderson, K. D., Baird, A. H., et al. (2017). Global warming and recurrent mass bleaching of corals. *Nature* 543, 373–377. doi: 10.1038/nature21707

Hughes, T. P., Kerry, J. T., Baird, A. H., Connolly, S. R., Dietzel, A., Eakin, C. M., et al. (2018). Global warming transforms coral reef assemblages. *Nature* 556, 492–496. doi: 10.1038/s41586-018-0041-2

Hughes, T., Kerry, J., Connolly, S., and Álvarez-Romero, J. (2021). Emergent properties in the responses of tropical corals to recurrent climate extremes. *Curr. Biol.* 23, 5393–5399. doi: 10.1016/j.cub.2021.10.046

Januchowski-Hartley, F. A., Bauman, A. G., Morgan, K. M., Seah, J. C. L., Huang, D., and Todd, P. A. (anda2020a). Accreting coral reefs in a highly urbanized environment. *Coral Reefs* 39, 717–731. doi: 10.1007/S00338-020-01953-3/

Jackson, J. B. C. (1991). Adaptation and diversity of reef corals. *Bioscience* 41, 475–482. doi: 10.2307/1311805

Johnston, E. C., Forsman, Z. H., Flot, J. F., Schmidt-Roach, S., Pinzón, J. H., Knapp, I. S. S., et al. (2017). A genomic glance through the fog of plasticity and diversification in Pocillopora. *Sci. Rep.* 7, 1–11. doi: 10.1038/s41598-017-06085-3

Johnston, E. C., Wyatt, A. S. J., Leichter, J. J., and Burgess, S. C. (2022). Niche differences in co-occurring cryptic coral species (*Pocillopora* spp.). *Coral Reefs* 41, 767–778. doi: 10.1007/S00338-021-02107-9

Kaandorp, J. A. (1999). Morphological analysis of growth forms of branching marine sessile organisms along environmental gradients. *Mar. Biol.* 134, 295–306. doi: 10.1007/S002270050547

Kahng, S. E., Akkaynak, D., Shlesinger, T., Hochberg, E. J., Wiedenmann, J., Tamir, R., et al. (2019). Light, temperature, photosynthesis, heterotrophy, and the lower depth limits of mesophotic coral ecosystems. *Mesophotic Coral Ecosyst.* (Cham), 801–828. doi: 10.1007/978-3-319-92735-0_42

Kahng, S., Copus, J., and Wagner, D. (2017). Mesophotic coral ecosystems. *Mar. Anim. Forests* 10, 978. doi: 10.1007/978-3-319-17001-5_4-1

Karisa, J. F., Obura, D. O., and Chen, C. A. (2020). Spatial heterogeneity of coral reef benthic communities in Kenya. *PloS One* 15, e0237397. doi: 10.1371/journal.pone.0237397

Kennedy, E., Ordoñez, A., and Diaz-Pulido, G. (2017). Coral bleaching in the southern inshore Great Barrier Reef: a case study from the Keppel Islands. *Mar. Freshw. Res.* 69, 191–197. doi: 10.1071/MF16317

Kim, S. W., Sampayo, E. M., Sommer, B., Sims, C. A., Gómez-Cabrera, M., del, C., et al. (2019). Refugia under threat: Mass bleaching of coral assemblages in high-latitude eastern Australia. *Glob Chang Biol.* 25, 3918–3931. doi: 10.1111/gcb.14772

Kimball, S., Funk, J. L., Sandquist, D. R., and Ehleringer, J. R. (2016). "Ecophysiological considerations for restoration," in *Foundations of restoration ecology* (Washington, DC: Island Press/Center for Resource Economics), 153–181. doi: 10.5822/978-1-61091-698-16

Knowlton, N. (2001). The future of coral reefs. *Proc. Natl. Acad. Sci. U.S.A.* 98, 5419–5425. doi: 10.1073/pnas.091092998

Kramer, N., Guan, J., Chen, S., Wangpraseurt, D., and Loya, Y. (2021a). Characterization of morpho-functional traits in mesophotic corals reveals optimized light capture and photosynthesis. *bioRxiv*. doi: 10.1101/2021.09.29.462347

Kramer, N., Tamir, R., Ben-Zvi, O., Jacques, S. L., Loya, Y., and Wangpraseurt, D. (2021b). Efficient light-harvesting of mesophotic corals is facilitated by coral optical traits. *Funct. Ecol.* 36, 406–418. doi: 10.1111/1365-2435.13948

Kramer, N., Tamir, R., Eyal, G., and Loya, Y. (2020). Coral morphology portrays the spatial distribution and population size-structure along a 5–100 m depth gradient. *Front. Mar. Sci.* 7. doi: 10.3389/fmars.2020.00615

Lachs, L., Sommer, B., Cant, J., Hodge, J. M., Malcolm, H. A., Pandolfi, J. M., et al. (2021). Linking population size structure, heat stress and bleaching responses in a subtropical endemic coral. *Coral Reefs* 40, 777–790. doi: 10.1007/S00338-021-02081-2

Lavm, B., and Nevo, E. (1981). Genetic diversity in marine molluscs: a test of the niche-width variation hypothesis. *Mar. Ecol.* 2, 335–342. doi: 10.1111/J.1439-0485.1981.TB00275.X

Lawton, R. J., Messmer, V., Pratchett, M. S., and Bay, L. K. (2011). High gene flow across large geographic scales reduces extinction risk for a highly specialised coral feeding butterflyfish. *Mol. Ecol.* 20, 3584–3598. doi: 10.1111/J.1365-294X.2011.05207.X

Laverick, J. H., Green, T. K., Burdett, H. L., Newton, J., and Rogers, A. D. (2019). Depth alone is an inappropriate proxy for physiological change in the mesophotic coral Agaricia lamarcki. *J. Mar. Biol. Assoc. United Kingdom* 99, 1535–1546. doi: 10.1017/S0025315419000547

le Nohaïc, M., Ross, C. L., Cornwall, C. E., Comeau, S., Lowe, R., McCulloch, M. T., et al. (2017). Marine heatwave causes unprecedented regional mass bleaching of thermally resistant corals in northwestern Australia. *Sci. Rep.* 7, 1–11. doi: 10.1038/s41598-017-14794-y

Lesser, M., Weis, V., Patterson, M., and Jokiel, P. (1994). Effects of morphology and water motion on carbon delivery and productivity in the reef coral, Pocillopora damicornis (Linnaeus): diffusion barriers, inorganic carbon. *J. Exp. Mar. Biol. Ecol.* 178, 153–179. doi: 10.1016/0022-0981(94)90034-5

Lesser, M. P., Slattery, M., Laverick, J. H., Macartney, K. J., and Bridge, T. C. (2019). Global community breaks at 60 m on mesophotic coral reefs. *Global Ecol. Biogeography* 28, 1403–1416. doi: 10.1111/geb.12940

Lin, B. (2011). Resilience in agriculture through crop diversification: adaptive management for environmental change. *Bioscience* 61, 183–193. doi: 10.1525/bio.2011.61.3.4

Linklater, M., Carroll, A. G., Hamylton, S. M., Jordan, A. R., Brooke, B. P., Nichol, S. L., et al. (2016). High coral cover on a mesophotic, subtropical island platform at the limits of coral reef growth. *Cont Shelf Res.* 130, 34–46. doi: 10.1016/j.csr.2016.10.003

Linklater, M., Ingleton, T. C., Kinsela, M. A., Morris, B. D., Allen, K. M., Sutherland, M. D., et al. (2019). Techniques for classifying seabed morphology and composition on a subtropical-temperate continental shelf. *Geosci J.* 9, 141. doi: 10.3390/geosciences9030141

Linklater, M., Jordan B, A. R., Carroll, A. G., Neilson, J., Gudge B, S., Brooke, B. P., et al. (2018). Mesophotic corals on the subtropical shelves of Lord Howe Island and Balls Pyramid, south-western Pacific Ocean. *Mar. Freshw. Res.* 70, 43–61. doi: 10.1071/mf18151

Loya, Y., Eyal, G., Treibitz, T., Lesser, M. P., and Appeldoorn, R. (2016). Theme section on mesophotic coral ecosystems: advances in knowledge and future perspectives. *Coral Reefs* 35, 1–9. doi: 10.1007/S00338-016-1410-7

Mies, M., Francini-Filho, R. B., Zilberberg, C., Garrido, A. G., Longo, G. O., Laurentino, E., et al. (2020). South Atlantic coral reefs are major global warming refugia and less susceptible to bleaching. *Front. Mar. Sci.* 7. doi: 10.3389/fmars.2020.00514

Maher, R. L., Rice, M. M., McMinds, R., Burkepile, D. E., and Vega Thurber, R. (2019). Multiple stressors interact primarily through antagonism to drive changes in the coral microbiome. *Sci. Rep.* 9, 1–12. doi: 10.1038/s41598-019-43274-8

Maher, R. L., Schmeltzer, E. R., Meiling, S., McMinds, R., Ezzat, L., Shantz, A. A., et al. (2020). Coral microbiomes demonstrate flexibility and resilience through a reduction in community diversity following a thermal stress event. *Front. Ecol. Evol.* 8. doi: 10.3389/fevo.2020.555698

Marhoefer, S. R., Zenger, K. R., Strugnell, J. M., Logan, M., van Oppen, M. J., Kenkel, C. D., et al. (2021). Signatures of adaptation and acclimatization to reef flat and slope habitats in the coral *Pocillopora damicornis*. *Front. Mar. Sci.* 8. doi: 10.3389/fmars.2021.704709

Martinez, S., Kolodny, Y., Shemesh, E., Scucchia, F., Nevo, R., Levin-Zaidman, S., et al. (2020). Energy sources of the depth-generalist mixotrophic coral Stylophora pistillata. *Front. Mar. Sci.* 7, 566663. doi: 10.3389/fmars.2020.566663

McClanahan, T. R., Ateweberhan, M., Graham, N. A. J., Wilson, S. K., Sebastián, C. R., Guillaume, M. M., et al. (2007). Western Indian Ocean coral communities: bleaching responses and susceptibility to extinction. *Mar. Ecol. Prog. Ser.* 337, 1–13. doi: 10.3354/meps337001

McGinley, M., Aschaffenburg, M., Pettay, D., Smith, R., LaJeunesse, T., and Warner, M. (2012). *Symbiodinium* spp. in colonies of eastern Pacific *Pocillopora* spp. are highly stable despite the prevalence of low-abundance background populations. *Mar. Ecol. Prog. Ser.* 462, 1–7. doi: 10.3354/meps09914

McWilliam, M., Pratchett, M. S., Hoogenboom, M. O., and Hughes, T. P. (2020). Deficits in functional trait diversity following recovery on coral reefs. *P Roy Soc. B-Biol Sci.* 287, 20192628. doi: 10.1098/rspb.2019.2628

Miller, K., and Ayre, D. (2008). Protection of genetic diversity and maintenance of connectivity among reef corals within marine protected areas. *Conserv. Biol.* 22, 1245–1254. doi: 10.1111/j.1523-1739.2008.00985.x

Mizerek, T. L., Madin, J. S., Benzoni, F., Huang, D., Luiz, O. J., Mera, H., et al. (2021). No evidence for tropicalization of coral assemblages in a subtropical climate change hot spot. *Coral Reefs* 40, 1451–1461. doi: 10.1007/S00338-021-02167-X

Muir, P. R., and Pichon, M. (2019). Biodiversity of reef-building, scleractinian corals. *Coral Reefs World* (Cham), 589–620. doi: 10.1007/978-3-319-92735-0_33

Munday, P. (2004). Habitat loss, resource specialization, and extinction on coral reefs. *Glob Chang Biol.* 10, 1642–1647. doi: 10.1111/j.1365-2486.2004.00839.x

Nakabayashi, A., Yamakita, T., Nakamura, T., Aizawa, H., Kitano, Y. F., Iguchi, A., et al. (2019). The potential role of temperate Japanese regions as refugia for the coral Acropora hyacinthus in the face of climate change. *Sci. Rep.* 9, 1–12. doi: 10.1038/s41598-018-38333-5

Noreen, A. M. E., Harrison, P. L., and van Oppen, M. J. H. (2009). Genetic diversity and connectivity in a brooding reef coral at the limit of its distribution. *P Roy Soc. B-Biol Sci.* 276, 3927–3935. doi: 10.1098/RSPB.2009.1050

Noreen, A. M. E., Schmidt-Roach, S., Harrison, P. L., and van Oppen, M. J. H. (2015). Diverse associations among coral host haplotypes and algal endosymbionts may drive adaptation at geographically peripheral and ecologically marginal locations. *J. Biogeogr* 42, 1639–1650. doi: 10.1111/jbi.12536

Oliver, T. A., and Palumbi, S. R. (2011). Do fluctuating temperature environments elevate coral thermal tolerance? *Coral Reefs* 30, 429–440. doi: 10.1007/s00338-011-0721-y

Olsson, P., Folke, C., and Hughes, T. P. (2008). Navigating the transition to ecosystem-based management of the Great Barrier Reef, Australia. *P Natl. Acad. Sci.* 105, 9489–9494. doi: 10.1073/PNAS.0706905105

Osman, E. O., Smith, D. J., Ziegler, M., Kürten, B., Conrad, C., El-Haddad, K. M., et al. (2018). Thermal refugia against coral bleaching throughout the northern Red Sea. *Global Change Biol.* 24, e474–e484. doi: 10.1111/gcb.13895

Palacio-Castro, A. M., Smith, T. B., Brandtneris, V., and Baker, A. C. (2023). Increased dominance of heat-tolerant symbionts creates resilient coral reefs in near-term ocean warming. *Proc Natl Acad Sci* 120, e2202388120. doi: 10.1073/pnas.2202388120

Palumbi, S., Sandifer, P., Allan, J., Beck, M., Fautin, D., Fogarty, M., et al. (2009). Managing for ocean biodiversity to sustain marine ecosystem services. *Front. Ecol. Environ.* 7, 204–211. doi: 10.1890/070135

Pandolfi, J. M., Bradbury, R. H., Sala, E., Hughes, T. P., Bjorndal, K. A., Cooke, R. G., et al. (2003). Global trajectories of the long-term decline of coral reef ecosystems. *Science* 301, 955–958. doi: 10.1126/science.1085706

Pandolfi, J. M., Connolly, S. R., Marshall, D. J., and Cohen, A. L. (2011). Projecting coral reef futures under global warming and ocean acidification. *Science* 333, 418–422. doi: 10.1126/science.1204794

Parasharya, D., and Padate, G. (2013). Status of scleractinian corals of Narara reef in the Gulf of Kachchh, western India. *Jalplavit* 4, 49–59.

Pérez-Rosales, G., Brandl, S. J., Chancerelle, Y., Siu, G., Martinez, E., Parravicini, V., et al. (2021). Documenting decadal disturbance dynamics reveals archipelago-specific recovery and compositional change on Polynesian reefs. *Mar. pollut. Bull.* 170, 112659. doi: 10.1016/j.marpolbul.2021.112659

Perry, C. T., and Larcombe, P. (2003). Marginal and non-reef-building coral environments. *Coral Reefs* 22, 427–432. doi: 10.1007/S00338-003-0330-5

Pinzón, J. H., and LaJeunesse, T. C. (2011). Species delimitation of common reef corals in the genus Pocillopora using nucleotide sequence phylogenies, population genetics and symbiosis ecology. *Mol. Ecol.* 20, 311–325. doi: 10.1111/j.1365-294X.2010.04939.x

Pogoreutz, C., Rädecker, N., Cárdenas, A., Gärdes, A., Wild, C., and Voolstra, C. R. (2018). Dominance of Endozoicomonas bacteria throughout coral bleaching and mortality suggests structural inflexibility of the Pocillopora verrucosa microbiome. *Ecol. Evol.* 8, 2240–2252. doi: 10.1002/ece3.3830

Polinski, J. M., and Voss, J. D. (2018). Evidence of photoacclimatization at mesophotic depths in the coral-Symbiodinium symbiosis at Flower Garden Banks National Marine Sanctuary and McGrail Bank. *Coral Reefs* 37, 779–789. doi: 10.1007/S00338-018-1701-2

Poquita-Du, R., Goh, Y., Huang, D., Chou, L., and Todd, P. (2020a). Gene expression and photophysiological changes in Pocillopora acuta coral holobiont following heat stress and recovery. *Microorganisms* 8, 1227. doi: 10.3390/microorganisms8081227

Poquita-Du, R., Huang, D., Chou, L., and Todd, P. (2020b). The contribution of stress-tolerant endosymbiotic dinoflagellate Durusdinium to Pocillopora acuta survival in a highly urbanized reef system. *Coral Reefs* 39, 745–755. doi: 10.1007/s00338-020-01902-0

Pratchett, M. S., Trapon, M., Berumen, M. L., and Chong-Seng, K. (2011). Recent disturbances augment community shifts in coral assemblages in Moorea, French Polynesia. *Coral Reefs* 30, 183–193. doi: 10.1007/s00338-010-0678-2

Prober, S. M., Byrne, M., McLean, E. H., Steane, D. A., Potts, B. M., Vaillancourt, R. E., et al. (2015). Climate-adjusted provenancing: a strategy for climate-resilient ecological restoration. *Front. Ecol. Evol.* 3. doi: 10.3389/fevo.2015.00065

Putnam, H. M., Ritson-Williams, R., Cruz, J. A., Davidson, J. M., and Gates, R. D. (2020). Environmentally-induced parental or developmental conditioning influences coral offspring ecological performance. *Sci. Rep.* 10, 1–14. doi: 10.1038/s41598-020-70605-x

Putnam, H. M., Stat, M., Pochon, X., and Gates, R. D. (2012). Endosymbiotic flexibility associates with environmental sensitivity in scleractinian corals. *P Roy Soc. B-Biol Sci.* 279, 4352–4361. doi: 10.1098/rspb.2012.1454

Ricci, F., Tandon, K., Black, J. R., Cao, K.-A. L., Blackall, L. L., and Verbruggen, H. (2022). Host traits and phylogeny contribute to shaping coral-bacterial symbioses. *mSystems* 7, e00044–e00022. doi: 10.1128/msystems.00044-22

Richards, Z., Kirkendale, L., Moore, G., Hosie, A., Huisman, J., Bryce, M., et al. (2016). Marine biodiversity in temperate Western Australia: multi-taxon surveys of Minden and Roe reefs. *Diversity* 8, 7. doi: 10.3390/D8020007

Richmond, C. E., Breitburg, D. L., and Rose, K. A. (2005). The role of environmental generalist species in ecosystem function. *Ecol. Modell* 188, 279–295. doi: 10.1016/j.ecolmodel.2005.03.002

Roelfsema, C., Thurstan, R., Beger, M., Dudgeon, C., Loder, J., Kovacs, E., et al. (2016). A citizen science approach: A detailed ecological assessment of subtropical reefs at point lookout, Australia. *PloS One* 11, e0163407. doi: 10.1371/journal.pone.0163407

Rohwer, F., Seguritan, V., Azam, F., and Knowlton, N. (2002). Diversity and distribution of coral-associated bacteria. *Mar. Ecol. Prog. Ser.* 243, 1–10. doi: 10.3354/meps243001

Ros, M., Suggett, D. J., Edmondson, J., Haydon, T., Hughes, D. J., Kim, M., et al. (2021). Symbiont shuffling across environmental gradients aligns with changes in carbon uptake and translocation in the reef-building coral Pocillopora acuta. *Coral Reefs* 40, 595–607. doi: 10.1007/S00338-021-02066-1

Saad, O. S., Lin, X., Ng, T. Y., Li, L., Ang, P., and Lin, S. (2022). Species richness and generalists–specialists mosaicism of symbiodiniacean symbionts in corals from Hong Kong revealed by high-throughput ITS sequencing. *Coral Reefs* 41, 1–12. doi: 10.1007/S00338-021-02196-6

Sawall, Y., Al-Sofyani, A., Banguera-Hinestroza, E., and Voolstra, C. R. (2014). Spatio-temporal analyses of Symbiodinium physiology of the coral Pocillopora verrucosa along large-scale nutrient and temperature gradients in the Red Sea. *PloS One* 9, e103179. doi: 10.1371/journal.pone.0103179

Schmidt-Roach, S., Lundgren, P., Miller, K. J., Gerlach, G., Noreen, A. M. E., and Andreakis, N. (2012). Assessing hidden species diversity in the coral Pocillopora damicornis from Eastern Australia. *Coral Reefs* 32, 161–172. doi: 10.1007/s00338-012-0959-z

Schmidt-Roach, S., Lundgren, P., Miller, K. J., Gerlach, G., Noreen, A. M. E., and Andreakis, N. (2013a). Assessing hidden species diversity in the coral Pocillopora damicornis from Eastern Australia. *Coral Reefs* 32, 161–172. doi: 10.1007/s00338-012-0959-z

Schmidt-Roach, S., Miller, K., and Andreakis, N. (2013b). Pocillopora aliciae: A new species of scleractinian coral (Scleractinia, Pocilloporidae) from subtropical Eastern Australia. *Zootaxa* 3626, 576–582. doi: 10.11646/zootaxa.3626.4.11

Schmidt-Roach, S., Miller, K. J., Lundgren, P., and Andreakis, N. (2014). With eyes wide open: a revision of species within and closely related to the Pocillopora damicornis species complex (Scleractinia; Pocilloporidae) using morphology and genetics. *Zoo J. Linn Soc.* 170, 1–33. doi: 10.1111/zoj12092

Scucchia, F., Malik, A., Putnam, H. M., and Mass, T. (2021). Genetic and physiological traits conferring tolerance to ocean acidification in mesophotic corals. *Glob Chang Biol.* 27, 5276–5294. doi: 10.1111/gcb.15812

Scucchia, F., Nativ, H., Neder, M., Goodbody-Gringley, G., and Mass, T. (2020). Physiological characteristics of Stylophora pistillata larvae across a depth gradient. *Front. Mar. Sci.* 7. doi: 10.3389/fmars.2020.00013

Serrano, X. M., Baums, I. B., O'Reilly, K., Smith, T. B., Jones, R. J., Shearer, T. L., et al. (2014). Geographic differences in vertical connectivity in the Caribbean coral Montastraea cavernosa despite high levels of horizontal connectivity at shallow depths. *Mol. Ecol.* 23, 4226–4240. doi: 10.1111/mec.12861

Shaver, E. C., McLeod, E., Hein, M. Y., Palumbi, S. R., Quigley, K., Vardi, T., et al. (2022). A roadmap to integrating resilience into the practice of coral reef restoration. *Glob Chang Biol.* 28, 4752–4764. doi: 10.1111/gcb.16212

Shlesinger, T., Grinblat, M., Rapuano, H., Amit, T., and Loya, Y. (2018). Can mesophotic reefs replenish shallow reefs? Reduced coral reproductive performance casts a doubt. *Ecology* 99, 421–437. doi: 10.1002/ecy.2098

Shlesinger, T., and Loya, Y. (2019). Sexual reproduction of scleractinian corals in mesophotic coral ecosystems vs. shallow reefs. *Coral Reefs World* (Cham), 653–666. doi: 10.1007/978-3-319-92735-0_35

Silveira, C. B., Gregoracci, G. B., Coutinho, F. H., Silva, G. G. Z., Haggerty, J. M., de Oliveira, L. S., et al. (2017). Bacterial community associated with the reef coral *Mussismilia braziliensis*'s momentum boundary layer over a diel cycle. *Front. Microbiol.* 8. doi: 10.3389/fmicb.2017.00784

Silverstein, R. N., Correa, A. M. S., and Baker, A. C. (2012). Specificity is rarely absolute in coral–algal symbiosis: implications for coral response to climate change. *P Roy Soc. B-Biol Sci.* 279, 2609–2618. doi: 10.1098/rspb.2012.0055

Slatyer, R. A., Hirst, M., and Sexton, J. P. (2013). Niche breadth predicts geographical range size: a general ecological pattern. *Ecol. Lett.* 16, 1104–1114. doi: 10.1111/ele.12140

Smale, D., and Reefs, T. W.-C. (2012). Ecological observations associated with an anomalous warming event at the Houtman Abrolhos Islands, Western Australia. *Coral Reefs* 31, 441. doi: 10.1007/s00338-012-0873-4. 2012, Undefined.

Smith, P. J., and Fujio, Y. (1982). Genetic variation in marine teleosts: High variability in habitat specialists and low variability in habitat generalists. *Mar. Biol.* 69, 7–20. doi: 10.1007/BF003969551 69,

Smith, S. M., Malcolm, H. A., Marzinelli, E. M., Schultz, A. L., Steinberg, P. D., and Vergés, A. (2021). Tropicalization and kelp loss shift trophic composition and lead to more winners than losers in fish communities. *Glob Chang Biol.* 27, 2537–2548. doi: 10.1111/gcb.15592

Smith, T. B., Holstein, D. M., and Ennis, R. S. (2019). Disturbance in mesophotic coral ecosystems and linkages to conservation and management. *Coral Reefs World* 12, 911–929. doi: 10.1007/978-3-319-92735-0_47

Sommer, B., Beger, M., Harrison, P. L., Babcock, R. C., and Pandolfi, J. M. (2018). Differential response to abiotic stress controls species distributions at biogeographic transition zones. *Ecography* 41, 478–490. doi: 10.1111/ecog.02986

Sommer, B., Harrison, P. L., Beger, M., and Pandolfi, J. M. (2014). Trait-mediated environmental filtering drives assembly at biogeographic transition zones. *Ecology* 95, 1000–1009. doi: 10.1890/13-1445.1

Sommer, B., Sampayo, E. M., Beger, M., Harrison, P. L., Babcock, R. C., and Pandolfi, J. M. (2017). Local and regional controls of phylogenetic structure at the high-latitude range limits of corals. *P Roy Soc. B-Biol Sci.* 284, 20170915. doi: 10.1098/rspb.2017.0915

Soto, D., de Palmas, S., Ho, M. J., Denis, V., and Chen, C. A. (2018). Spatial variation in the morphological traits of Pocillopora verrucosa along a depth gradient in Taiwan. *PloS One* 13, e0202586. doi: 10.1371/journal.pone.0202586

Spalding, M., Fox, H., Allen, G., Davidson, N., Ferdaña, Z., Finlayson, M., et al. (2007). Marine ecoregions of the world: a bioregionalization of coastal and shelf areas. *Bioscience* 57, 573–583. doi: 10.1641/B570707

Steinberg, R. K., Ainsworth, T. D., Moriarty, T., Bednarek, T., Dafforn, K. A., and Johnston, E. L. (2022). Bleaching susceptibility and resistance of octocorals and anemones at the world's southern-most coral reef. *Front. Physiol.* 13. doi: 10.3389/fphys.2022.804193

Stuart-Smith, R. D., Brown, C. J., Ceccarelli, D. M., and Edgar, G. J. (2018). Ecosystem restructuring along the Great Barrier Reef following mass coral bleaching. *Nature* 560, 92–96. doi: 10.1038/s41586-018-0359-9

Studivan, M. S., Milstein, G., and Voss, J. D. (2019). Montastraea cavernosa corallite structure demonstrates distinct morphotypes across shallow and mesophotic depth zones in the Gulf of Mexico. *PloS One* 14, e0203732. doi: 10.1371/journal.pone.0203732

Studivan, M. S., and Voss, J. D. (2018a). Assessment of mesophotic coral ecosystem connectivity for proposed expansion of a Marine sanctuary in the Northwest gulf of Mexico: Population genetics. *Front. Mar. Sci.* 5. doi: 10.3389/fmars.2018.00152

Studivan, M. S., and Voss, J. D. (2018b). Population connectivity among shallow and mesophotic Montastraea cavernosa corals in the Gulf of Mexico identifies potential for refugia. *Coral Reefs* 37, 1183–1196. doi: 10.1007/S00338-018-1733-7

Studivan, M. S., and Voss, J. D. (2020). Transcriptomic plasticity of mesophotic corals among natural populations and transplants of Montastraea cavernosa in the Gulf of Mexico and Belize. *Mol. Ecol.* 29, 2399–2415. doi: 10.1111/mec.15495

Swain, T. D., Lax, S., Gilbert, J., Backman, V., and Marcelino, L. A. (2021).). A phylogeny-informed analysis of the global coral-symbiodiniaceae interaction network reveals that traits correlated with thermal bleaching are specific to symbiont transmission mode. *mSystems* 6. doi: 10.1128/msystems.00266-21

Tamir, R., Ben-Zvi, O., Eyal, G., Kramer, N., and Loya, Y. (2020). Reciprocal-transplantation between shallow and mesophotic stony corals. *Mar. Environ. Res.* 161, 105035. doi: 10.1016/j.marenvres.2020.105035

Tamir, R., Eyal, G., Kramer, N., Laverick, J. H., and Loya, Y. (2019). Light environment drives the shallow-to-mesophotic coral community transition. *Ecosphere* 10, e02839. doi: 10.1002/ecs2.2839

Thomas, C. J., Bridge, T. C. L., Figueiredo, J., Deleersnijder, E., and Hanert, E. (2015). Connectivity between submerged and near-sea-surface coral reefs: can submerged reef populations act as refuges? *Divers. Distrib* 21, 1254–1266. doi: 10.1111/ddi.12360

Terán, E., Méndez, E. R., Enríquez, S., and Iglesias-Prieto, R. (2010). Multiple light scattering and absorption in reef-building corals. *Appl. Opt* 49, 5032–5042. doi: 10.1364/AO.49.005032

Terraneo, T. I., Ouhssain, M., Castano, C. B., Aranda, M., Hume, B. C., Marchese, F., et al. (2023). From the shallow to the mesophotic: a characterization of Symbiodiniaceae diversity in the Red Sea NEOM region. *Front. Mar. Sci.* 10, 1077805. doi: 10.3389/fmars.2023.1077805

Thomson, D. P., Bearham, D., Graham, F., and Eagle, J. V. (2011). High latitude, deeper water coral bleaching at Rottnest Island, Western Australia. *Coral Reefs* 30, 1107. doi: 10.1007/S00338-011-0811-X

Todd, P. A. (2008). Morphological plasticity in scleractinian corals. *Biol. Rev.* 83, 315–337. doi: 10.1111/j.1469-185X.2008.00045.x

Tuckett, C. A., de Bettignies, T., Fromont, J., and Wernberg, T. (2017). Expansion of corals on temperate reefs: direct and indirect effects of marine heatwaves. *Coral Reefs* 36, 947–956. doi: 10.1007/s00338-017-1586-5

Turnham, K. E., Aschaffenburg, D. M., Tye Pettay, D., Paz-García, D. A., Reyes-Bonilla, H., Pinzón, J., et al. (2023). High physiological function for corals with thermally tolerant, host-adapted symbionts. *P Roy Soc. B-Biol Sci.* 290, 20231021. doi: 10.1098/rspb.2023.1021

van der Meer, M. H., Berumen, M. L., Hobbs, J. P. A., and van Herwerden, L. (2015). Population connectivity and the effectiveness of marine protected areas to protect vulnerable, exploited and endemic coral reef fishes at an endemic hotspot. *Coral Reefs* 34, 393–402. doi: 10.1007/S00338-014-1242-2

van Oppen, M. J. H., Gates, R. D., Blackall, L. L., Cantin, N., Chakravarti, L. J., Chan, W. Y., et al. (2017). Shifting paradigms in restoration of the world's coral reefs. *Glob Chang Biol.* 23, 3437–3448. doi: 10.1111/gcb.13647

van Oppen, M. J. H., Bongaerts, P., Underwood, J. N., Peplow, L. M., and Cooper, T. F. (2011). The role of deep reefs in shallow reef recovery: an assessment of vertical connectivity in a brooding coral from west and east Australia. *Mol. Ecol.* 20, 1647–1660. doi: 10.1111/J.1365-294X.2011.05050.X

van Tienderen, P. H. (1991). Evolution of generalists and specialists in spatially heterogeneous environments. *Evolution* 45, 1317–1331. doi: 10.1111/J.1558-5646.1991.TB02638.X

van Woesik, R., Franklin, E. C., O'Leary, J., McClanahan, T. R., Klaus, J. S., and Budd, A. F. (2012). Hosts of the plio-pleistocene past reflect modern-day coral vulnerability. *P Roy Soc. B-Biol Sci.* 279, 2448–2456. doi: 10.1098/rspb.2011.2621

Vardi, T., Hoot, W. C., Levy, J., Shaver, E., Winters, R. S., Banaszak, A. T., et al. (2021). Six priorities to advance the science and practice of coral reef restoration worldwide. *Restor. Ecol.* 29, e13498. doi: 10.1111/REC.13498

Varasteh, T., Salazar, V., Tschoeke, D., Francini-Filho, R. B., Swings, J., Garcia, G., et al. (2021). Breviolum and Cladocopium are dominant among Symbiodiniaceae of the coral holobiont Madracis decactis. *Microb. Ecol.* 84, 325–335. doi: 10.1007/S00248-021-01868-8

Vergés, A., Doropoulos, C., Malcolm, H. A., Skye, M., Garcia-Pizá, M., Marzinelli, E. M., et al. (2016). Long-term empirical evidence of ocean warming leading to tropicalization of fish communities, increased herbivory, and loss of kelp. *Proc. Natl. Acad. Sci.* 113, 13791–13796. doi: 10.1073/pnas.1610725113

Vergés, A., Mccosker, E., Mayer-Pinto, M., Coleman, M. A., Wernberg, T., Ainsworth, T., et al. (2019). Tropicalisation of temperate reefs: Implications for ecosystem functions and management actions. *Funct. Ecol.*, 1–14. doi: 10.1111/1365-2435.13310

Vergés, A., Steinberg, P. D., Hay, M. E., Poore, A. G. B., Campbell, A. H., Ballesteros, E., et al. (2014). The tropicalization of temperate marine ecosystems: climate-mediated changes in herbivory and community phase shifts. *P Roy Soc. B-Biol Sci.* 281, 1–10. doi: 10.1098/rspb.2014.0846

Vermeij, M., Bakker, J., van der Hal, N., and Bak, R. (2011). Juvenile coral abundance has decreased by more than 50% in only three decades on a small Caribbean island. *Diversity* 3, 296–307. doi: 10.3390/d3030296

Veron, J., and Pichon, M. (1976). "Scleractinia of eastern Australia. Part I: families thamnasteriidae, astrocoeniidae, pocilloporidae," in *Corals of the world* (Canberra, Australia: Australian Institute of Marine Science & Australian National University Press).

Voolstra, C. R., and Ziegler, M. (2020). Adapting with microbial help: microbiome flexibility facilitates rapid responses to environmental change. *BioEssays* 42, 2000004. doi: 10.1002/bies.202000004

Watanabe, A., and Nakamura, T. (2019). Carbon dynamics in coral reefs. *Blue Carbon Shallow Coast. Ecosyst.*, 273–293. doi: 10.1007/978-981-13-1295-3_10

Wang, J. T., Chen, Y. Y., Tew, K. S., Meng, P. J., and Chen, C. A. (2012). Physiological and biochemical performances of menthol-induced aposymbiotic corals. *PloS One* 7, e46406. doi: 10.1371/journal.pone.0046406

Wernberg, T., Smale, D., Tuya, F., Thomsen, M., Langlois, T., de Bettignies, T., et al. (2013). An extreme climatic event alters marine ecosystem structure in a global biodiversity hotspot. *Nat. Clim Chang* 3, 78–82. doi: 10.1038/nclimate1627

Wepfer, P. H., Nakajima, Y., Hui, F. K. C., Mitarai, S., and Economo, E. P. (2020). Metacommunity ecology of Symbiodiniaceae hosted by the coral Galaxea fascicularis. *Mar. Ecol. Prog. Ser.* 633, 71–87. doi: 10.3354/meps13177

Williams, G. J., and Graham, N. A. J. (2019). Rethinking coral reef functional futures. *Funct. Ecol.* 33, 942–947. doi: 10.1111/1365-2435.13374

Wilson, J., and Harrison, P. (2003). Spawning patterns of scleractinian corals at the Solitary Islands - a high latitude coral community in eastern Australia. *Mar. Ecol. Prog. Ser.* 260, 115–123. doi: 10.3354/meps260115

Yang, Q., Zhang, Y., Ahmad, M., Ling, J., Zhou, W., Zhang, Y., et al. (2021). Microbial community structure shifts and potential Symbiodinium partner bacterial groups of bleaching coral Pocillopora verrucosa in South China Sea. *Ecotoxicology* 30, 966–974. doi: 10.1007/S10646-021-02380-Y/

Yost, D. M., Wang, L.-H., Fan, T.-Y., Chen, C.-S., Lee, R. W., Sogin, E., et al. (2013). Diversity in skeletal architecture influences biological heterogeneity and Symbiodinium habitat in corals. *Zoology* 116, 262–269. doi: 10.1016/j.zool.2013.06.001

Zawada, K. J. A., Madin, J. S., Baird, A. H., Bridge, T. C. L., and Dornelas, M. (2019). Morphological traits can track coral reef responses to the Anthropocene. *Funct. Ecol.* 33, 962–975. doi: 10.1111/1365-2435.13358

Zhou, G., Tong, H., Cai, L., and Huang, H. (2021). Transgenerational effects on the coral Pocillopora damicornis microbiome under ocean acidification. *Microb. Ecol.* 82, 572–580. doi: 10.1007/S00248-021-01690-2

Ziegler, M., Grupstra, C. G. B., Barreto, M. M., Eaton, M., BaOmar, J., Zubier, K., et al. (2019). Coral bacterial community structure responds to environmental change in a host-specific manner. *Nat. Commun.* 10, 1–11. doi: 10.1038/s41467-019-10969-5

Ziegler, M., Roder, C., Bchel, C., and Voolstra, C. R. (2015A). Niche acclimatization in Red Sea corals is dependent on flexibility of host-symbiont association. *Mar. Ecol. Prog. Ser.* 533, 149–161. doi: 10.3354/meps11365

Ziegler, M., Roder, C. M., Büchel, C., and Voolstra, C. R. (2015B). Mesophotic coral depth acclimatization is a function of host-specific symbiont physiology. *Front. Mar. Sci.* 2. doi: 10.3389/fmars.2015.00004

Zweifler, A., O'leary, M., Morgan, K., and Browne, N. K. (2021). Turbid coral reefs: past, present and future – a review. *Diversity* 13, 251. doi: 10.3390/D13060251

Frontiers in
Ecology and Evolution

Ecological and evolutionary research into our natural and anthropogenic world

This multidisciplinary journal covers the spectrum of ecological and evolutionary inquiry. It provides insights into our natural and anthropogenic world, and how it can best be managed.

Discover the latest Research Topics

See more →

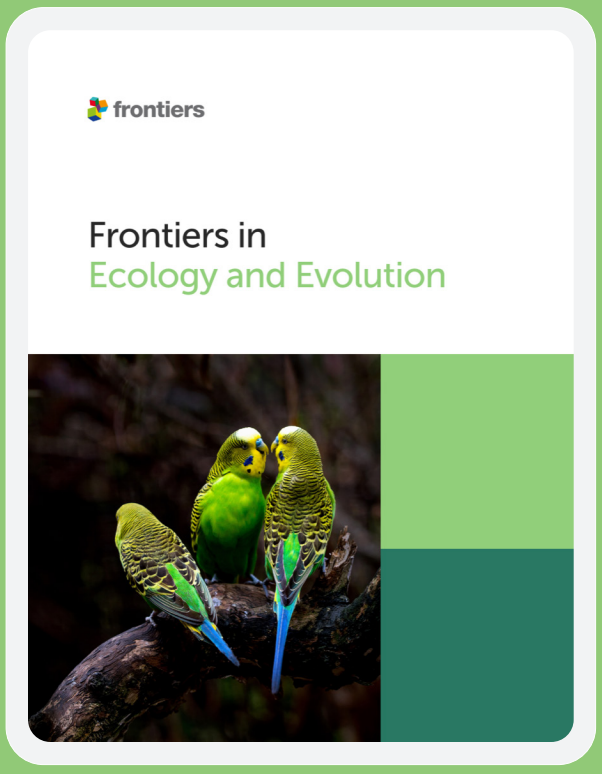

Frontiers

Avenue du Tribunal-Fédéral 34
1005 Lausanne, Switzerland
frontiersin.org

Contact us

+41 (0)21 510 17 00
frontiersin.org/about/contact